



UNIVERSIDAD NACIONAL AUTÓNOMA DE MÉXICO

POSGRADO EN CIENCIAS BIOLÓGICAS

Instituto de Biología

DIVERSIFICACIÓN ADAPTATIVA EN
LAS PLANTAS LEÑOSAS: SOSTÉN,
ALMACENAMIENTO Y CONDUCCIÓN
EN TALLOS DEL CLADO *SIMARUBA*
(*Bursera*, BURSERACEAE)

TESIS

QUE PARA OBTENER EL GRADO ACADÉMICO DE

DOCTORA EN CIENCIAS

P R E S E N T A

JULIETA ALEJANDRA ROSELL GARCÍA

TUTOR PRINCIPAL DE TESIS: DR. MARK EARL OLSON

COMITÉ TUTOR: DR. CÉSAR AUGUSTO DOMÍNGUEZ
PEREZ-TEJADA
DR. FRANCISCO JOSÉ SÁNCHEZ SESMA

MÉXICO, D.F.

OCTUBRE, 2010



Universidad Nacional
Autónoma de México

Dirección General de Bibliotecas de la UNAM

Biblioteca Central



UNAM – Dirección General de Bibliotecas
Tesis Digitales
Restricciones de uso

DERECHOS RESERVADOS ©
PROHIBIDA SU REPRODUCCIÓN TOTAL O PARCIAL

Todo el material contenido en esta tesis esta protegido por la Ley Federal del Derecho de Autor (LFDA) de los Estados Unidos Mexicanos (México).

El uso de imágenes, fragmentos de videos, y demás material que sea objeto de protección de los derechos de autor, será exclusivamente para fines educativos e informativos y deberá citar la fuente donde la obtuvo mencionando el autor o autores. Cualquier uso distinto como el lucro, reproducción, edición o modificación, será perseguido y sancionado por el respectivo titular de los Derechos de Autor.

Dr. Isidro Ávila Martínez
Director General de Administración Escolar, UNAM

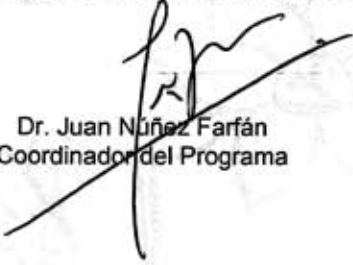
Presente

Me permito informar a usted que en la reunión ordinaria del Comité Académico del Posgrado en Ciencias Biológicas, celebrada el día 23 de agosto de 2010, se aprobó el siguiente jurado para el examen de grado de **DOCTORA EN CIENCIAS** de la alumna **ROSELL GARCÍA JULIETA ALEJANDRA** con número de cuenta **95503798** con la tesis titulada: "**Diversificación adaptativa en las plantas leñosas: sostén, almacenamiento y conducción en tallos del clado *simaruba* (*Bursera*, *Burseraceae*)**", realizada bajo la dirección del **DR. MARK EARL OLSON**:

Presidente:	DR. CÉSAR AUGUSTO DOMÍNGUEZ PÉREZ TEJADA
Vocal:	DR. JUAN ENRIQUE FORNONI AGNELLI
Vocal:	DR. HORACIO ARMANDO PAZ HERNÁNDEZ
Vocal:	DR. GUILLERMO PEDRO ÁNGELES ÁLVAREZ
Secretario:	DR. MARK EARL OLSON
Suplente:	DR. LUIS ENRIQUE EGUIARTE FRUNS
Suplente:	DR. FRANCISCO JOSÉ SÁNCHEZ SESMA

Sin otro particular, me es grato enviarle un cordial saludo.

Atentamente
"POR MI RAZA HABLARA EL ESPIRITU"
Cd. Universitaria, D.F. a 27 de septiembre de 2010.


Dr. Juan Núñez Farfán
Coordinador del Programa

c.c.p. Expediente del (la) interesado (a).

AGRADECIMIENTOS

Al Posgrado en Ciencias Biológicas de la Universidad Nacional Autónoma de México por el apoyo recibido durante mis estudios doctorales.

Al CONACYT por la beca doctoral #172233 y por el financiamiento recibido a través del proyecto #46475. De igual manera, quisiera agradecer al PAPIIT por el financiamiento a través del proyecto #IN228207 y a la American Society of Plant Taxonomists por el financiamiento recibido.

A los miembros del comité tutorial, Dr. Mark E. Olson, Dr. César A. Domínguez Pérez-Tejada y Dr. Francisco J. Sánchez-Sesma, por la orientación, la asesoría, y las discusiones que le han dado forma a esta tesis. Sus sugerencias críticas a mi trabajo han sido una parte fundamental de mi formación. Gracias por el apoyo y la confianza en todas las fases de este trabajo y en el ámbito personal.

A los revisores de la tesis y miembros del sínodo, Dr. Guillermo Ángeles Álvarez, Dr. Luis Eguiarte Fruns, Dr. Juan Fornoni Agnelli y Dr. Horacio Paz Hernández, por sus comentarios y sugerencias que enriquecieron enormemente este texto. Gracias también por su muy generosa orientación y apoyo en las diferentes etapas de esta investigación.

Al Instituto de Biología, UNAM, por el apoyo recibido durante mis estudios doctorales.

Al Dr. Luis Eguiarte por su apoyo académico constante y también por el apoyo administrativo como responsable del proyecto que financió una parte importante de esta investigación.

A la M. en C. Rosalinda Medina Lemos por su generosa orientación con todo lo relacionado con las especies del clado de *Bursera simaruba*.

A la Dra. Rebeca Aguirre y al M. en C. Salvador Zamora por su paciente asesoría en todo lo relacionado con la estadística de esta tesis.

Al Dr. Guillermo Ángeles Álvarez, a la Dra. Claudia Paredes, al Dr. Jorge López Portillo, y al Dr. Frank Ewers por su orientación en la implementación de los métodos de medición de vulnerabilidad a la cavitación.

Al Dr. Jerzy Rzedowski y a la Maestra Graciela Calderón por su amable orientación y las estimulantes discusiones sobre la sistemática de las especies del clado *simaruba*.

A la M. en C. Laura Márquez por su paciente enseñanza de las técnicas moleculares, su constante asesoría y por la ayuda con la secuenciación.

A la Dra. Andrea Weeks y el Dr. Arturo De Nova por su ayuda y orientación con la reconstrucción filogenética del clado *simaruba*.

A la Dra. Hilda Flores, a la M. en C. Verónica Juárez y al resto del personal del Herbario Nacional (MEXU) por su apoyo durante la medición de variables morfométricas del clado *simaruba*. De igual manera, al Dr. Sergio Zamudio, al Dr. Víctor Steinmann, a la Biol. Yocupitzia Ramírez y al resto del personal del Herbario Regional del Bajío (IEB) por su apoyo durante la medición de los ejemplares de su maravillosa colección.

A la Dra. Patricia Feria, al M. en C. Leonardo Alvarado y al Dr. Norberto Martínez por la extracción de los datos climáticos usados en este trabajo.

Al Dr. Juan Fornoni y al Dr. Mariano Ordano por la orientación en la implementación de los métodos para la comparación de matrices.

Al Dr. Calixto León Gómez por su paciente ayuda con diversas técnicas relacionadas con la madera.

A Rocío González por su constante apoyo e infinita paciencia.

A José Luis Díaz por su ayuda con todo tipo de cotizaciones, compras, envíos y salidas a campo.

Al Dr. Juan Núñez Farfán por su apoyo como Coordinador del Posgrado en Ciencias Biológicas y por su asesoría académica. Gracias también a todo el personal de la Coordinación de este programa.

A la Dra. María de los Ángeles Herrera y al Dr. Fausto Méndez por su apoyo durante su gestión como representantes del Programa de Posgrado en Ciencias Biológicas en el IBUNAM.

A los queridos compañeros del laboratorio, Angélica Cervantes, Gabriela Montes, Jacqueline Pérez, Laura Trejo, Leonardo Alvarado, Norberto Martínez, Roberto Gómez y Vanessa Rojas, por su apoyo, solidaridad y buen humor durante todos estos años de convivencia. Gracias por sus atinados comentarios en versiones preliminares de este y otros manuscritos.

Al Dr. Jorge Vega, la Dra. Katherine Renton, el M. en C. Enrique Ramírez, la M. en C. Beatriz Hernández y al resto del personal de la Estación de Biología Tropical de Chamela por su apoyo durante las interminables mediciones en sus instalaciones. De igual manera a la Biol. Rosamond Coates y al personal de la Estación de Biología Tropical Los Tuxtlas por las facilidades para la medición de la población veracruzana de *B. simaruba*.

A Mark Olson, Martha García y Angélica Cervantes por su invaluable ayuda en la colecta y medición de miles de tallos de *Bursera*.

Al personal de la biblioteca del Instituto de Biología por su apoyo siempre que he necesitado algún servicio de la biblioteca.

A mi madre por su ayuda con trabajo de campo y mediciones, pero sobre todo por su ánimo y cariño en todas las etapas de este trabajo.

A mi familia y mis amigos por su presencia y apoyo constante.

A todos aquellos mencionados en los agradecimientos de cada capítulo y no incluidos en esta lista, gracias nuevamente.

ÍNDICE

RESUMEN	1
INTRODUCCIÓN	7
 CAPÍTULO 1	
RELACIONES FILOGENÉTICAS DEL COMPLEJO	
DE ESPECIES <i>BURSERA SIMARUBA</i>	
Resumen	12
Introducción	13
Materiales y métodos	16
Resultados	18
Discusión	22
Conclusiones	23
Apéndice A	24
Literatura citada	25
Apéndice B	27
Apéndice C	31
Figura suplementaria	32
 CAPÍTULO 2	
FORMA, TAMAÑO Y BIOMECÁNICA, LA TRÍADA INSEPARABLE DE LA	
EVOLUCIÓN MORFOLÓGICA ADAPTATIVA, EN TALLOS DEL	
CLADO <i>BURSERA SIMARUBA</i> DE ÁRBOLES TROPICALES	
Resumen	33
Introducción	34
Materiales y métodos	38
Resultados	43
Discusión	45
Conclusiones	50
Literatura citada	52

Tablas	57
Figuras	60
Apéndice 1	65
Apéndice 2	66
Apéndice 3	66

CAPÍTULO 3

INTEGRACIÓN FUNCIONAL Y DIVERSIFICACIÓN ADAPTATIVA EN

LOS TALLOS DEL CLADO <i>BURSERIA SIMARUBA</i>	67
Resumen	68
Introducción	70
Materiales y métodos	80
Resultados	92
Discusión	108
Conclusiones	120
Literatura citada	122
Apéndice A	128
Apéndice B	131
Apéndice C	134

CONCLUSIONES GENERALES	138
-------------------------------------	-----

ANEXO A

Probando supuestos implícitos sobre la dependencia en la edad o en el tamaño por parte de la biomecánica de los tallos usando <i>Pittocaulon praecox</i> (Asteraceae)	141
---	-----

ANEXO B

Regresión logística en la anatomía comparada de la madera: tipos de traqueidas, terminología anatómica, y nuevas inferencias del conjunto de datos de Carlquist y Hoekman del sur de California	154
---	-----

RESUMEN

Las estructuras biológicas usualmente desempeñan más de una función de manera simultánea. Esto se traduce en una fuerte integración entre las funciones y las partes de los organismos. Cuando las funciones involucradas son antagonistas, surgen patrones de covariación negativa o trade-offs. Estos patrones tienen implicaciones muy importantes para la adaptación, pues pueden frenar a la selección natural y en consecuencia limitar los fenotipos que observamos. El efecto de los trade-offs ha sido estudiado a niveles poblacionales o interespecíficos, pero son muy escasos los trabajos que ligan estos dos niveles. Por ello, son necesarios más estudios que validen las generalizaciones que usualmente se hacen del nivel estudiado hacia el otro nivel. Para abordar el efecto de los trade-offs en la diversificación morfológica, ligando los niveles poblacionales e interespecíficos, se estudiaron los tallos leñosos de las plantas. Los tallos son sistemas ideales por desempeñar básicamente tres funciones: sostén mecánico, almacenamiento y conducción. Tomando como sistema de estudio los tallos leñosos de un grupo muy diverso de plantas, el complejo *simaruba* dentro del género *Bursera* (Burseraceae), se estudiaron los trade-offs entre las funciones principales de los tallos para entender la integración de las estructuras multifuncionales y su efecto en la diversificación morfológica entre niveles evolutivos.

El primer paso para abordar las preguntas de este estudio fue reconstruir las relaciones filogenéticas del sistema de estudio y aclarar los límites entre las especies del complejo de *B. simaruba*. Este complejo, uno de los más complicados dentro del género, incluye especies con gran parecido morfológico entre ellas y con *B. simaruba*, la especie de más amplia distribución dentro del género. Con base en el gran parecido y el traslape parcial de su distribución con la de *B. simaruba* se había propuesto que estas especies podrían haber surgido a partir de poblaciones de *B. simaruba*, por lo que se habían denominado especies “satélite”. Secuenciando cinco marcadores moleculares (*psbA-trnH*, *PEPC*, *ETS*, *ITS* y *NIAi3*) para más de 70 muestras, y realizando análisis de máxima parsimonia y análisis bayesianos, fue posible determinar que el complejo constituye un clado, que las especies satélite no se derivan de *B. simaruba*, y que al menos parte de su parecido se debe a convergencia o paralelismo. Además de permitir poner a prueba el origen de los satélites, la reconstrucción filogenética también contribuyó a la delimitación

taxonómica de estas especies. Con base en muestras de México, Centroamérica y las Antillas se validó el estatus de *B. simaruba* como especie y se concluyó que las diferencias morfológicas son producto de la plasticidad. Para la discusión de los límites entre especies también se utilizaron caracteres ecológicos, mismos que apoyaron lo sugerido por la reconstrucción filogenética. Finalmente, se discutió la utilidad de los caracteres morfológicos tradicionales tomando la filogenia como marco de referencia.

El gran parecido morfológico y convergente a nivel de las hojas causante de las complicaciones taxonómicas en el clado *simaruba* contrasta con la gran diversidad de ambientes que ocupan las especies y las diferencias en tamaño, arquitectura y grado de succulencia que se observan en sus tallos. Esta gran diversidad estructural asociada estrechamente con las condiciones ambientales permitió poner a prueba hipótesis adaptativas relacionadas con la diversificación morfológica y biomecánica de los tallos, que es el tema del capítulo dos. Aunque la evolución del tamaño y la forma de los organismos está relacionada con las características mecánicas de sus tejidos, se sabe poco sobre las diferencias en las relaciones entre el tamaño, la forma y la mecánica en distintos ambientes. Estudiando nueve especies del clado *simaruba*, que ocupan desde bosques tropicales caducifolios muy secos hasta perennifolios, y las relaciones entre el tamaño de los árboles, la alometría de las ramas y las propiedades mecánicas de éstas, se encontró que la disponibilidad de agua está asociada positivamente con la rigidez a la flexión del tallo, la madera y la corteza. Así, las especies en las localidades más lluviosas tienen un mayor desempeño mecánico, en contraste con las especies de zonas secas, donde la selección natural probablemente favorece el almacenamiento de agua y almidón a costa de la reducción en el soporte mecánico. Las propiedades mecánicas están a su vez asociadas con las relaciones alométricas de las ramas, de forma que ramas más largas para su ancho están presentes en los árboles con mayor resistencia a la flexión. Se detectaron algunas desviaciones a estas relaciones que estuvieron asociadas a plantas con hábitos de crecimiento marcadamente diferentes. *Bursera instabilis*, un árbol con ramas lianescentes, presentó ramas más largas para su ancho y su resistencia mecánica. En contraste, *B. standleyana*, un árbol hemiepífita, presentó valores mecánicos más altos dadas sus relaciones alométricas, posiblemente como resultado de las necesidades hidráulicas. Estas desviaciones ilustran el impacto de las relaciones tamaño-forma-mecánica en la evolución

morfológica. Esta tríada define un morfoespacio accesible ontogenéticamente, pero contiene zonas que no parecen ser favorecidas por la selección natural.

Una vez explorada la naturaleza adaptativa de los cambios mecánicos en el grupo, fue posible incrementar el número de funciones en el análisis de la integración de los tallos en el capítulo tres. Analizando 20 variables funcionales relacionadas con la conductividad, el sostén mecánico y el almacenamiento, y muestreando a nivel de poblaciones ($n=8$) y de especies ($n=9$), se encontró una fuerte integración entre las funciones del tallo. En general, los patrones de integración se conservaron tanto entre poblaciones (excepto en dos casos), como entre especies, implicando efectos en la diversificación morfológica de los tallos. Los trade-offs se ubicaron principalmente entre variables relacionadas con el sostén mecánico y aquellas que reflejaron almacenamiento. La conductividad no presentó covariación con otras funciones, pero se detectó un trade-off entre la seguridad y la eficiencia conductiva. Si bien los patrones de covariación se conservaron entre especies, hay cambios importantes en los valores medios de desempeño de las diferentes funciones que se asocian con condiciones ambientales, sugiriendo que la selección natural es responsable de los cambios de desempeño en la función que se optimiza, además de ser el agente causal que mantiene los patrones de covariación observados. La integración funcional que afecta los patrones de diversificación en el clado *simaruba* podría estar impactando la diversificación de los tallos leñosos en general, dado el reporte reiterado de ciertos trade-offs en la madera de diversos sistemas.

ABSTRACT

Most biological structures multitask, which translates into strong functional integration between the parts of a structure. When functions are antagonistic, patterns of negative covariation emerge, suggesting trade-offs between functions. Covariation patterns in general, and trade-offs in particular, have strong implications for adaptation studies, given that they can impose limits to natural selection and the observable phenotypes. Trade-off studies have focused on the population or interspecific level and generalize their results to their unstudied level. For this reason, more studies are necessary to validate this generalization. To study the effect of trade-offs in morphological diversification, linking population and interspecific levels, we studied woody stems. These structures are ideal simple systems performing three main functions: mechanical support, storage and water conduction. Using a highly diverse group of tropical trees, the *simaruba* complex of *Bursera* (Burseraceae), we studied trade-offs between the main functions of the stem to understand integration in multitasking structures and its effect in morphological diversification.

The first step in answering these questions was reconstructing the phylogenetic relationships of the study system and clarifying species limits within the *simaruba* complex. This group of species is one of the most complicated within *Bursera*. Main complications in the complex arise from the strong morphological similarity between some of its species and *B. simaruba*, the most widely distributed species within the complex and also the genus. Based on the strong resemblance and the partial overlap of their geographic distribution with that of *B. simaruba*, it had been proposed that these species could have originated from *B. simaruba*, and thus their being designated “satellite” species. Sequencing five molecular markers (*psbA-trnH*, *PEPC*, *ETS*, *ITS* y *NIAi3*) in more than 70 samples and performing maximum parsimony and Bayesian analyses, we showed the monophyletic nature of the complex, that most satellites were not derived from *B. simaruba*, and that much of the similarity between these species is likely due to convergence or parallelism. In addition to testing the origin of satellites, the phylogenetic reconstruction contributed to the taxonomic delimitation of the species in the complex, suggesting a potential synonymies and recommending the inclusion of two of the species under the same name. Based on samples from Mexico, Central America and the Antilles,

the status of *B. simaruba* as a valid species was supported and morphological differences between populations were considered the result of plasticity. The ecological characters, which were also used to discuss species limits, were congruent with phylogenetic results. Finally, the phylogeny was used as a framework to assess the usefulness of traditional morphological characters.

The strong similarity in leaf, flower and fruit morphology causing taxonomic complications in the *simaruba* clade contrasts strongly with the high environmental diversity and high disparity in size, architecture and succulence of its stems. This strong structural diversity, closely related to environmental conditions, allowed testing adaptive hypotheses regarding stem morphological and biomechanical diversification, which is the topic of chapter two of this thesis. Although the evolution of organismal size and shape is closely related to mechanical properties of tissues, little is known about differences in the size-shape-mechanics relationship in different environments. We approached this question by studying nine species of the *simaruba* clade living in a wide variety of environments, from very dry tropical deciduous forests to rainforests. Studying relationships between tree size, branch allometry and mechanics, we found that water availability in the habitat is positively associated to stem, wood and bark flexural stiffness. Species in the rainiest localities have higher mechanical resistance, contrasting with species of dry habitats, where natural selection has likely favored water and starch storage at the expense of mechanical support. Mechanical properties are in turn associated with branch allometry, with branches that are longer for a given diameter occurring in trees with stiffer wood. Some deviations were detected and were associated with markedly differing growth habits. *Bursera instabilis*, a dry forest tree with lianescent branches had longer branches for their diameter and their mechanical properties. In contrast, *B. standleyana*, a hemiepiphyte of Costa Rican rainforests had mechanical values "too high" for its branch allometry, likely as a result of hydraulic needs. These deviations illustrate the impact of the size-shape-mechanics triad in morphological evolution. this chapter ends discussing morphospace regions that are occupied by observed diversity, and those that are ontogenetically accesible, but seem to be maladaptive.

Once the adaptive nature of biomechanical changes in the group was explored, we increased the number of stem functions analyzed and approached trade-offs between

functions from a phenotypic integration perspective. Analyzing 20 functional variables related to conductivity, mechanical support, and storage, and sampling eight populations and nine species, we found strong functional integration in woody stems. In general, integration patterns were conserved between populations (except for two) and also between species, suggesting an effect of functional integration in stem morphological diversification. Trade-offs emerged mainly between variables related to mechanical support and storage. Conductivity did not covary with other functions, but showed a trade-off between safety and efficiency. Patterns of covariation were conserved between species, but strong changes in mean performance values for each function were detected, and were associated with environmental conditions, suggesting that natural selection was responsible for these changes, in addition to being the causal agent maintaining the observed covariation patterns between functions. Functional integration affecting diversification in the *simaruba* clade could be representative of woody stems in general, given the pervasive nature of trade-offs in wood.

INTRODUCCIÓN

Cualquier estructura biológica suele realizar varias funciones de manera simultánea. Cuando estas funciones son antagónicas pueden generarse asociaciones muy estrechas entre las partes, que se manifiestan a través de fuertes patrones de covariación negativa (Reznick y Travis, 1996). En estos casos, el cambio en una de las partes acarrea cambios de tipo compensatorio en otra(s) parte(s) de la estructura. A esta clase de fenómenos se le ha denominado trade-offs en áreas de la biología como la genética cuantitativa o el estudio de las historias de vida. En este último campo suele hacerse hincapié en que el cambio inicial resultará en un incremento de la adecuación, mientras que el cambio compensatorio implicará un decremento (Roff, 2002; Roff y Fairbairn, 2007).

La presencia de relaciones tipo trade-off, y en general cualquier correlación entre partes o caracteres, tiene implicaciones fuertes para los estudios de adaptación (Ordano et al., 2008). En primer lugar, su presencia dificulta distinguir aquellos caracteres que son sujetos principales de la selección natural de aquellos que se alteran como consecuencia del cambio en los primeros (Lewontin, 1977). Los trade-offs también podrían implicar una especie de “freno” para la acción de la selección natural (Cheverud, 1984; Ghalambor et al., 2003), y por lo tanto, para las posibilidades de adaptación de los organismos. Por ejemplo, la acción de la selección natural para aumentar el nivel de almacenamiento de almidón en los tallos leñosos demanda un volumen mayor de parénquima, un tejido mecánicamente pobre. En consecuencia, cuando la selección natural aumenta el grado de almacenamiento, hay una reducción inevitable en las capacidades de sostén mecánico de un tallo, y en la talla máxima que un árbol puede alcanzar. Como puede apreciarse, los trade-offs y la adaptación están íntimamente ligados: el estudio de trade-offs involucra directamente el de la adaptación, y en cualquier estudio adaptativo estaremos frente al fenómeno omnipresente de correlación entre caracteres, en muchos casos correspondiente a un trade-off.

Los trade-offs se han abordado en un nivel poblacional, a partir del cual se generaliza hacia el nivel interespecífico (p.e. Roff y Gélinas, 2003), o en un nivel interespecífico (p.e. Badyaev y Ghalambor, 2001; Shiota y Kimura, 2007), pero son muy pocos los trabajos que reúnen ambos enfoques. En consecuencia, no tenemos la certeza de que una relación tipo trade-off esté presente de la misma manera entre poblaciones y entre especies. Comprobar que este supuesto es cierto es indispensable para fundamentar las

generalizaciones entre niveles. Este trabajo contribuye a revisar este supuesto considerando diferentes niveles para determinar si estas negociaciones entre funciones se presentan de la misma manera entre poblaciones y entre especies, o si existen diferencias cualitativas entre niveles.

Dada su sencillez estructural y sus pocas restricciones ontogenéticas (Rosell et al., 2007), los tallos de las plantas son modelos ideales para el estudio de trade-offs y de la integración funcional en general. Estas estructuras están compuestas por una cantidad reducida de tipos celulares (aproximadamente 15, en comparación con los más de 200 en los mamíferos), y solamente desempeñan tres funciones principales: almacenamiento de productos fotosintéticos y agua, sostén mecánico y conducción de agua. Todas las células de la madera se derivan de las mismas células meristemáticas cambiales (Carlquist, 2001). Por ello, cada célula cambial se enfrenta al dilema de producir una célula especializada en una u otra función, mostrando la disyuntiva a nivel celular que luego se traducirá en una disyuntiva a nivel funcional, dada la naturaleza antagónica de las funciones del tallo, p.e. entre el sostén mecánico y el almacenamiento, ejemplo que se discutió con anterioridad. Los reportes de covariación negativa entre las funciones del tallo son numerosos y dan idea de la fuerte integración que debe ocurrir en los tallos leñosos (Gartner, 2001; Pratt et al., 2007; Sperry et al., 2008; Chave et al., 2009), y de su potencial como modelos para el estudio de la integración funcional en un contexto adaptativo.

Para un estudio de trade-offs como el que aquí se propone, es necesario un modelo de estudio con alta diversidad morfológica y ambiental a nivel interpoblacional e interespecífico. El clado *simaruba* de *Bursera* reúne justamente estas características. Contiene un número razonable de especies de muy alta diversidad para el enfoque interespecífico, además de especies de muy amplia distribución, como *Bursera simaruba* y *B. grandifolia*, en ambientes muy contrastantes generando diversidad también entre poblaciones. La gran diversidad morfológica y estructural de las aproximadamente 15 especies del clado se asocia estrechamente a una alta variación en hábitat (del bosque tropical muy seco a selva alta perennifolia). Las especies son muy diferentes en cuanto a su tamaño (árboles de 3 a 25 m), arquitectura (ramas erectas, curvadas, lianescentes e incluso una epífita), proporción de tejidos (áreas porcentuales de médula, corteza y madera variables) y anatomía. Estas características de disparidad convierten al clado en el sistema

con el nivel de diversidad ideal para someter a prueba las hipótesis de este trabajo, incluyendo la naturaleza adaptativa de la diversificación dentro del grupo.

Tomando como sistema de estudio estructuras sencillas de un clado muy diverso de plantas -tallos de los árboles del clado *simaruba*-, en este trabajo se estudiaron las negociaciones entre las principales funciones de los tallos (sostén mecánico, conducción y almacenamiento de agua y productos fotosintéticos) para entender más sobre la integración funcional y morfológica de las estructuras biológicas multifuncionales. Como primer paso para abordar estas preguntas fue necesario reconstruir las relaciones filogenéticas del clado *simaruba*, que es el tema central del primer capítulo de esta tesis. Este grupo de árboles tropicales constituye un complejo de especies, uno de los más complicados dentro del género *Bursera*, dado el fuerte traslape entre la morfología de las especies (Rzedowski et al., 2007). Los recientes cambios taxonómicos y la descripción de nuevas especies (Rzedowski y Calderón, 2000) hicieron necesaria la reconstrucción de la filogenia del grupo para contribuir a aclarar cuántas especies pertenecen al grupo y los límites entre ellas. Además de estos resultados, la reconstrucción filogenética permitió poner a prueba el origen de especies y evaluar los caracteres tradicionales usados en la taxonomía del grupo. Contar con una hipótesis filogenética nos permitió también implementar métodos comparativos filogenéticos para poner a prueba hipótesis adaptativas.

La filogenia de las especies del clado *simaruba* dio un marco histórico para poner a prueba la naturaleza adaptativa de la diversificación morfológica de los tallos del grupo, que es el tema que se discute en el capítulo dos de esta tesis. A pesar de que es evidente la importancia del tamaño, la forma y las propiedades mecánicas de las estructuras orgánicas en el proceso adaptativo, son muy escasos los estudios que abordan las relaciones de esta tríada en un contexto adaptativo. La gran diversidad en hábito, tamaño y forma de los tallos del clado *simaruba*, que se asocia estrechamente con condiciones ambientales, convierte al grupo en un sistema ideal para abordar el efecto de estas relaciones en la diversificación morfológica adaptativa.

La importancia de la integración funcional en la diversificación morfológica de los tallos fue clara al considerar el sostén mecánico y el almacenamiento de agua y productos fotosintéticos discutido en el capítulo dos. Sin embargo, los tallos realizan una tercera función principal, la conductividad hidráulica, que debe ser analizada para un

entendimiento global de las disyuntivas de asignación de recursos en el tallo. Además, para entender la fuerza de estas disyuntivas en la diversificación, es necesario comparar si los patrones de integración funcional emergen de igual forma entre niveles, es decir, si las mismas disyuntivas que se observan a niveles poblacionales son las que están guiando la diversificación a niveles mayores. El tercer y último capítulo de este trabajo aborda las disyuntivas entre las tres funciones y compara los patrones de covariación entre niveles con el objetivo de entender más sobre la integración funcional y morfológica de las estructuras biológicas multifuncionales en un contexto adaptativo.

El capítulo relacionado con la filogenia del clado se encuentra en proceso de publicación, por lo que se incluyen las pruebas de galeras directamente en el Capítulo 1. El siguiente capítulo relacionado con la tríada tamaño-forma-mecánica se presenta a manera de artículo. Este manuscrito será sometido próximamente a revisión en una revista de biología evolutiva. El tercer capítulo tiene un formato monográfico estándar. Finalmente, se anexan dos publicaciones que generé durante mis estudios doctorales, que fueron de gran importancia para lo que aquí se presenta. El primero de ellos compara el uso de la edad o el tamaño como factor para explicar la variación de las propiedades mecánicas (Anexo A). El otro artículo aborda el uso de la regresión logística en la anatomía comparada de la madera y discute las ventajas del uso de los tallos leñosos como modelo en estudios adaptativos (Anexo B).

LITERATURA CITADA

- Badyaev, A. V. y C. K. Ghalambor. 2001. Evolution of life histories along elevational gradients: trade-off between parental care and fecundity. *Ecology* 82: 2948-2960.
- Carlquist, S. 2001. *Comparative Wood Anatomy*. Springer, Heidelberg, Alemania. 2a edición.
- Chave, J., Coomes, D., Jansen, S., Lewis, S. L., Swenson, N. G. y A. E. Zanne. 2009. Towards a worldwide wood economics spectrum. *Ecology Letters* 12: 351-366.
- Cheverud, J. M. 1984. Quantitative genetics and developmental constraints on evolution by selection. *Journal of Theoretical Biology* 110: 155-171.
- Gartner, B. L. 2001. Multitasking and tradeoffs in stems, and the costly dominion of domatia. *New Phytologist* 151: 311-313.
- Ghalambor, C. K., Walker, J. A. y D. N. Reznick. 2003. Multi-trait selection, adaptation, and constraints on the evolution of burst swimming performance. *Integrative Comparative Biology* 43: 431-438.
- Lewontin, R. 1977. Adattamento. En Einaudi, G. (Ed.). *Enciclopedia Einaudi*, vol. 1, Turin, Italia. Reimpreso en inglés en Levins, R. y R. Lewontin. 1985 *The Dialectical Biologist*. Harvard University Press, Cambridge, Massachusetts.

- Ordano, M., Fornoni, J., Boege, K., y C. A. Domínguez. 2008. The adaptive value of phenotypic floral integration. *New Phytologist* 179: 1883-1192.
- Pratt, R. B., Jacobsen, A. L., Ewers, F. W. y S. D. Davis. 2007. Relationships among xylem transport, biomechanics and storage in stems and roots of nine Rhamnaceae species of the California chaparral. *New Phytologist*. 174: 787-798.
- Reznick, D. N. y J. Travis. 1996. The empirical study of adaptation in natural populations. En Rose, M. R. y G. V. Lauder (eds.). *Adaptation*. Academic Press, San Diego: 243-289.
- Roff, D. A. 2002. *Life history evolution*. Sinauer Associates, Sunderland, Massachusetts.
- Roff, D. A. y D. J. Fairbairn. 2007. The evolution of trade-offs: where are we? *Journal of Evolutionary Biology* 20: 433-447.
- Roff, D. A. y M. B. Gélinas. 2003. Phenotypic plasticity and the evolution of trade-offs: the quantitative genetics of resource allocation in the wing dimorphic cricket, *Gryllus firmus*. *Journal of Evolutionary Biology* 16: 55-63.
- Rosell, J. A., Olson, M. E., Aguirre-Hernández, R. y S. Carlquist. 2007. Logistic regression in comparative wood anatomy: tracheid types, wood anatomical terminology, and new inferences from the Carlquist and Hoekman southern Californian data set. *Botanical Journal of the Linnean Society* 154: 331-351.
- Rzedowski, J. y G. Calderón. 2000. Una nueva especie de *Bursera* (Burseraceae) del estado de Oaxaca (México). *Acta Botánica Mexicana* 52: 75-81.
- Rzedowski, J., Medina, R. y G. Calderón. 2007. Segunda restauración de *Bursera ovalifolia* y nombre nuevo para otro componente del complejo de *B. simaruba* (Burseraceae). *Acta Botánica Mexicana* 81: 45-70.
- Shiota, H. y M. T. Kimura. 2007. Evolutionary trade-offs between thermal tolerance and locomotor and developmental performance in drosophilid flies. *Biological Journal of the Linnean Society* 90:375-380.
- Sperry, J. S., Meinzer, F. C., y K. A. McCulloh. 2008. Safety and efficiency conflicts in hydraulic architecture: scaling from tissues to trees. *Plant, Cell and Environment* 31: 632-645.

CAPÍTULO 1.

RELACIONES FILOGENÉTICAS DEL COMPLEJO DE ESPECIES *BURSER*

***SIMARUBA*. MANUSCRITO EN PRENSA EN MOLECULAR PHYLOGENETICS AND
EVOLUTION.**



Contents lists available at ScienceDirect

Molecular Phylogenetics and Evolution

journal homepage: www.elsevier.com/locate/ympev

Diversification in species complexes: Tests of species origin and delimitation in the *Bursera simaruba* clade of tropical trees (Burseraceae)

Julieta A. Rosell^a, Mark E. Olson^a, Andrea Weeks^b, J. Arturo De-Nova^a, Rosalinda Medina Lemos^a, Jacqueline Pérez Camacho^{c,1}, Teresa P. Feria^d, Roberto Gómez-Bermejo^a, Juan C. Montero^e, Luis E. Eguiarte^c

^a Instituto de Biología, Universidad Nacional Autónoma de México, Tercer Circuito sn de Cd. Universitaria, México D.F., C.P. 04510, Mexico

^b Department of Environmental Science and Policy, George Mason University, MSN 5F2, Fairfax, VA 22030, USA

^c Instituto de Ecología, Universidad Nacional Autónoma de México, Tercer Circuito sn de Cd. Universitaria, México D.F., C.P. 04510, Mexico

^d Laboratory of Landscape Ecology, Department of Biology, University of Texas-Pan American, 1201 W. University Drive, Edinburg, TX 78541, USA

^e Facultad de Biología, Universidad Michoacana de San Nicolás de Hidalgo, Av. Fco. J. Mújica sn, Col. Felicitas del Río, C.P. 58030, Morelia, Michoacán, Mexico

ARTICLE INFO

Article history:

Received 1 April 2010

Revised 4 August 2010

Accepted 9 August 2010

Available online xxxxx

Keywords:

Antilles

Convergence

Mexico

Parallelism

Paraphyletic species

Plasticity

ABSTRACT

Molecular phylogenies are invaluable for testing morphology-based species delimitation in species complexes, as well as for examining hypotheses regarding the origination of species in these groups. Using five nucleotide markers, we reconstructed the phylogeny of the *Bursera simaruba* species complex of neotropical trees to test the notion that four “satellite” species originated from populations of the most widely distributed member of the genus, *B. simaruba*, which the satellites strongly resemble. In addition to molecular phylogenetic reconstruction, we tested species delimitation of *B. simaruba* and the satellites using multivariate analyses of morphological and ecological characters. The analyses evaluated the taxonomic value of these traditional characters and pinpointed those in need of further study, such as the expression of pubescence. Phylogenetic data rejected the origin of three satellite species from their purported ancestor, *B. simaruba*, and we ascribe their morphological similarity to convergence or parallelism. The fourth satellite species likely represents one end of a spectrum of inflorescence length variation within *B. simaruba* and is conspecific. Despite its marked morphological variability, we recovered *B. simaruba* as a single valid species, which implies that it maintains genetic cohesion among distant populations throughout its vast range.

© 2010 Elsevier Inc. All rights reserved.

1. Introduction

Species are the working units in most of biology, yet delimiting species is fraught with complexity (Barraclough and Nee, 2001; Sites and Marshall, 2003, 2004). In a phylogenetic framework, the species of traditional taxonomy can be viewed as hypotheses tested by recovering either non-polyphyletic or polyphyletic groupings. Most species concepts view monophyly as congruent with a species hypothesis (e.g. Baum and Shaw, 1995; Shaw, 1998), and some also recognize the possibility of paraphyletic species (Coyne and Orr, 2004; Crisp and Chandler, 1996; Harrison, 1998; Templeton, 1989). However, virtually all concepts view polyphyly as a rejection of a species hypothesis. Because molecular phylogenetic hypotheses can readily identify polyphyletic taxa, they are an excellent aid in delimiting species (Knowles and

Carstens, 2007; Wiens and Penkrot, 2002), especially in the case of species complexes, whose continuously varying morphological characters often confound morphology-based taxonomies (e.g. Campbell et al., 2004; Leliaert et al., 2009). In this work, we test species hypotheses in the *Bursera simaruba* complex, a group of neotropical trees with a knotty taxonomic history resulting from the strong morphological similarity and overlapping geographic distributions of its species (Rzedowski et al., 2007).

The history of species delimitation in the *simaruba* complex exemplifies central issues in species complex systematics. Species complexes may contain widespread, morphologically variable species, as in the painted turtle (Starkey et al., 2003), or multiple ecologically distinct species that are morphologically similar, as in the *Rana pipiens* complex (Hillis, 1988). Both the single and the multiple species scenarios have been proposed by taxonomists for entities of the *simaruba* complex (Bullock, 1936; McVaugh and Rzedowski, 1965; Rzedowski et al., 2007; Standley, 1923), especially for *B. simaruba*, the species from which the complex derives its name (Fig. 1A). Commonly known as the gumbo-limbo tree or palo mulato, *B. simaruba* is a conspicuous element in virtually all

Corresponding author. Fax: +52 55 55501760.

E-mail address: julietarosell@hotmail.com (J.A. Rosell).

¹ Present address: Instituto de Ecología y Sistemática, Carr. de Varona km. 3½, Capdevila, Boyeros, C.P. 10800, Ciudad de La Habana, Cuba.

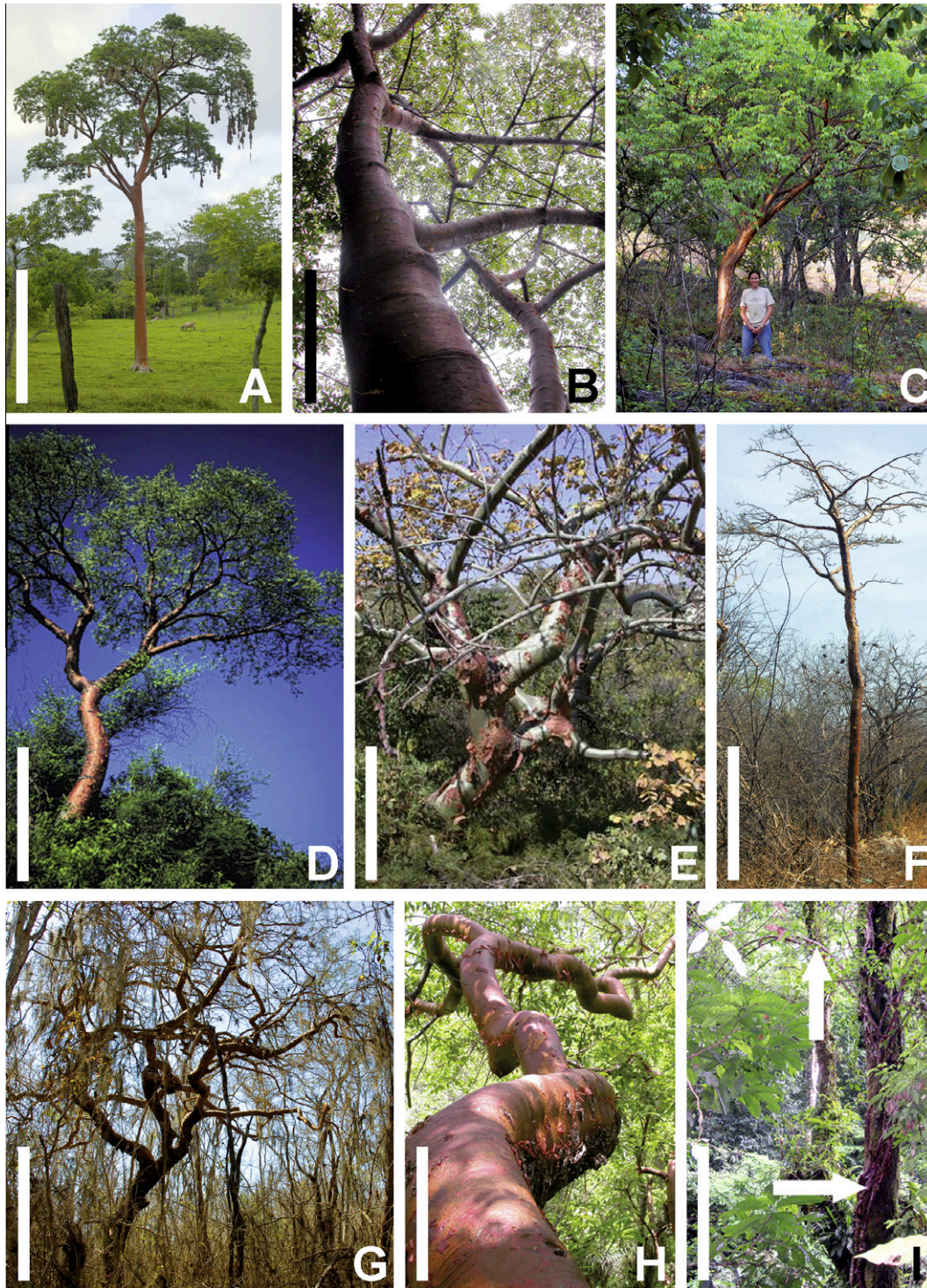


Fig. 1. Habit diversity in the *Bursera simaruba* species complex. This figure shows the red to copper colored peeling outer bark that characterizes the group, and that, for its size, the clade spans an exceptional array of life forms. (A–C) *Bursera simaruba* and “satellites.” (A) *B. simaruba* remnant in a pasture cut from lowland rainforest. Scale = 10 m. (B) *B. attenuata* in a subdeciduous tropical forest canyon. Scale = 1.5 m. (C) *B. ovalifolia* resembles a smaller, intricately branched *B. simaruba*. Person = 1.90 m. (D–H) Representatives of the *simaruba* complex from tropical deciduous forests. (D) *B. longipes*, one of the smallest members of the clade, growing in very dry tropical deciduous forest. Scale = 2.5 m. (E) *B. grandifolia* is a widespread dryland shrub to medium tree, distinguished by its waxy green trunk shedding ragged copper sheets of outer bark. Scale = 6 m. (F) *B. laurihuertae* is endemic to the low, dense woods of the southern Isthmus of Tehuantepec. Scale = 1.5 m. (G) *B. instabilis* is unique for its long, slender branches, which in large individuals become lianescent. Scale = 1.5 m. (H) *B. cinerea*, a water-storing tree from tropical deciduous forest canyons. Scale = 0.75 m. (I) *B. standleyana*, the hemiepiphytic member of the genus, growing at 20 m above the floor of the rainforest. The lower arrow indicates the long lianescent roots that bring water from the soil; the upper arrow singles out arching branches. Scale = 1.5 m.

tropical forests below 1400 m from Mexico to northern South America, Florida, and the West Indies (Fig. 2). It varies from small trees of subdeciduous forest to towering rainforest emergents, and

in the amount and distribution of leaf pubescence, leaflet shape and number, and bark color (Rzedowski et al., 2007; Rzedowski and Kruse, 1979). Although this variation has often been inter-



Fig. 2. Distribution of *B. simaruba* (in gray) and its satellite species *B. attenuata*, *B. itzae*, *B. ovalifolia*, and *B. roseana*.

preted as phenotypic plasticity, it could also indicate that what is now recognized as a single polymorphic species in fact includes several, one of the central questions of species complex taxonomy.

In addition to allowing us to examine the issue of species delimitation, species complexes are also natural model systems for understanding how new species arise (Kopp and Barmina, 2005; Kornfield and Smith, 2000; Losos, 1994). Scattered within the vast distribution of *B. simaruba* are four species (Fig. 2), which are so similar in habit, habitat, and leaflet number, shape, size, and pubescence that they have been termed “satellite” species (Rzedowski et al., 2007). These species, *B. attenuata*, *B. itzae*, *B. roseana*, and *B. ovalifolia* (Fig. 1A–C), could have originated from isolated populations of *B. simaruba*. In phylogenetic terms this hypothesis would translate into each satellite appearing nested within a paraphyletic *B. simaruba* (Crisp and Chandler, 1996; Funk and Omland, 2003; Graybeal, 1995; Hedin, 1997; Omland et al., 2000; Patton and Smith, 1994; Slade and Moritz, 1998; Talbot and Shields, 1996). Alternatively, if sufficient time has elapsed and genetic loci have attained reciprocal monophyly (Avice and Ball, 1990; Funk and Omland, 2003; Omland et al., 2006; Rieseberg and Brouillet, 1994; Shaw, 1998), the paraphyletic pattern of *B. simaruba* could be erased, leaving the set of satellites as a clade sister to *B. simaruba* or a grade basal to it. Finding that satellites are more closely related to other species and not *B. simaruba* would reject the hypothesis that they are derived from the gumbo-limbo and would make the satellites likely examples of morphological convergence or parallelism.

1.1. Species delimitation in the *simaruba* complex: genetics, phenetics, and ecology

The *simaruba* complex is part of an abundant, species-rich American genus of trees and shrubs whose center of diversity is Mexico. The complex comprises 15 species spanning a remarkable array of life form and ecology (Fig. 1, Table 1). They are distinguished from other *Bursera* by their reddish peeling phellem (outer bark), compound leaves without wings on the rachis, ovate to

broadly elliptic entire leaflets with mostly acuminate apices and brochidodromous venation, and three-valved fruits with reddish pseudarils covering the endocarp completely. Although the complex has long been recognized as distinct (McVaugh and Rzedowski, 1965; Rzedowski and Kruse, 1979), and is well supported in molecular phylogenies (Becerra, 2003; Becerra and Venable, 1999), species limits and relationships within the group have always been regarded as problematic (Daly, 1993; Rzedowski et al., 2005, 2007). Molecular phylogenies have included only a few species of the complex and provide little resolution within the group (Becerra, 2003; Becerra and Venable, 1999).

As in many plant groups, the taxonomy of the *simaruba* complex employs combinations of plastic and potentially evolutionarily labile characters, rather than unique synapomorphies (Daly, 1993; Appendix B, Supplementary material). Years of taxonomic confusion have resulted, reaching a zenith in the satellite species, in which barely diagnostic combinations of leaflet number, pubescence patterns, and fruit size are used to delimit species, with taxonomic realignments continuing to the present day (Bullock, 1936; McVaugh and Rzedowski, 1965; Rzedowski et al., 2007; Standley, 1923). To test morphologically-based species delimitations, we include in our phylogenetic reconstruction two or more samples of eight of the species in the complex, including the four satellite species. In addition, we performed the first phenetic study of the morphological characters used in the *simaruba* complex taxonomy and compare it to our molecular phylogeny, an approach that we use to rank a wide array of traditional characters in their diagnostic effectiveness.

In addition to morphological and molecular characters, ecology can also help delimit species (Ruiz-Sanchez and Sosa, 2010). Therefore, we test for ecological differentiation between *B. simaruba* and its satellites through multivariate analyses of environmental variables (Stockman and Bond, 2007). We assume that different niches between species would reject the hypothesis of ecological exchangeability, which, along with genetic exchangeability, is one of two main aspects of the cohesion species concept, which we follow here (Templeton, 1989).

Table 1

Habitat and distribution of the 15 species in the *B. simaruba* species complex and its nine related Antillean species, plus an undescribed Cuban endemic. Elevation is included for *B. simaruba* and its satellite species. TDF: tropical deciduous forest, TSDF: tropical subdeciduous forest, TRF: tropical rainforest.

<i>Simaruba</i> complex species	Habitat and distribution
<i>B. arborea</i> (Rose) L. Riley ^c	TDF, Mexican Pacific coast and Durango
<i>B. attenuata</i> (Rose) L. Riley ^{a,c}	TDF and TSDF, 600–1000 m, western Mexican Pacific coast and Durango
<i>B. cinerea</i> Engl. ^c	TDF, Mexico: upper Papaloapan river basin
<i>B. grandifolia</i> (Schltdl.) Engl. ^c	TDF, western and central Mexico, Balsas Depression
<i>B. instabilis</i> McVaugh & Rzed. ^c	TDF, Mexican Pacific coast
<i>B. inversa</i> Daly	TRF, Panama, Colombia and Venezuela
<i>B. itzae</i> Lundell ^{a,b}	TRF, N shore of Lake Petén Itzá, Guatemala
<i>B. krusei</i> Rzed. ^{b,c}	TDF, Mexico: Guerrero and Oaxaca
<i>B. laurihuertae</i> Rzed. & Calderón ^{b,c}	TDF, Mexico: southeastern Oaxaca
<i>B. longipes</i> (Rose) Standl. ^c	TDF, Mexico: eastern Balsas Depression
<i>B. ovalifolia</i> (Schltdl.) Engl. ^{a,b,c}	TDF and TSDF, 0–1500 (1850) m, Pacific coast from Mexico to Costa Rica
<i>B. permollis</i> Standl. & Steyerl. ^b	TDF, El Salvador, Guatemala, Honduras, Nicaragua
<i>B. roseana</i> Rzed., Calderón & Medina ^{a,c}	TDF and TSDF, 1200–1900 m, Western and southern Mexican Pacific coast, western central Mexico
<i>B. simaruba</i> (L.) Sarg. ^c	TSDF and TRF, <1400 m, southern Florida to northern Brazil, including both Mexican coasts, the Caribbean, and Central America
<i>B. standleyana</i> L. O. Williams & Cuatrec. ^b	TRF, hemiepiphytic tree, Costa Rica (San José and Puntarenas Provinces)
Antillean species	
<i>B. aromatica</i> Proctor	TDF on limestone, northwestern Jamaica
<i>B. frenningae</i> Correll	TDF, Bahamas (Great Exhuma, Cat Island, Long Island)
<i>B. hollickii</i> Fawc. & Rendle	TDF on limestone, southern central coast of Jamaica
<i>B. inaguensis</i> Britton	TDF on limestone, Bahamas (Little Inagua) and Cuba
<i>B. nashii</i> Urb.	TDF on limestone, Haiti and the Dominican Republic
<i>B. spinescens</i> (Urb.) Urb. & Ekman	TDF on limestone, Haiti and the Dominican Republic
<i>B. shaferi</i> Urb. ^b	TDF on limestone, western Cuba
<i>B. sp. nov.</i> ^b	TDF on limestone, eastern Cuba
<i>Commiphora angustata</i> (Grieseb.) Moncada ^b	TSDF, western and central Cuba
<i>C. glauca</i> (Grieseb.) Moncada ^b	TDF on limestone, eastern Cuba

^a Hypothesized “satellite” species.

^b Species in this paper not included in previous *Bursera* phylogenies.

^c Species included in morphometric analyses.

Finally, we test the membership in the *simaruba* complex of some six species from Mexico and Central America, which have never been included in prior phylogenetic analyses (Table 1). In our phylogenetic reconstruction, we also include eight mostly narrow endemic Antillean species. These species are closely related to the *simaruba* complex, with which they share the tree habit, reddish peeling outer bark, and compound leaves with entire leaflets, but differ in having tougher, smaller leaflets with a thicker waxy cuticle (Daly, 1993). However, it is not clear whether these species form a clade, perhaps sister to or within the *simaruba* complex (Weeks and Simpson, 2004), or, for example, a polyphyletic group derived from repeated invasions of the Antilles from the mainland. In summary, our phylogenetic reconstruction of the complex and the Antillean group includes DNA sequence data from five chloroplast and nuclear markers for 71 samples; 50% of the sampled species and over 90% of the DNA sequences are new contributions to *Bursera* phylogeny reconstructions (Appendix A).

2. Materials and methods

2.1. Taxon sampling

We sampled all known species in the *simaruba* complex except for *B. inversa* (Table 1). From the related Antillean group, we included all species except *B. hollickii* and *B. aromatica*. Sampling for *B. simaruba* included morphologically and environmentally contrasting individuals from Mexico, Central America, and Cuba (Appendix A), along with published sequences from the Dominican Republic and Florida (Weeks and Simpson, 2004). The samples we collected at the type locality of *B. itzae* were sterile, so they could not be assigned to species with certainty and are thus referred to as *B. “itzae”*. Of the Antillean species group, we included an undescribed Cuban species, three poorly known Cuban endemics, which

had been transferred to *Commiphora* based on pollen morphology (Moncada-Ferrara, 1989), and four previously sequenced Caribbean species (Weeks and Simpson, 2004; Appendix A). Our outgroup sampling included species of the two subgenera of *Bursera*, *Bursera* and *Elaphrium*, as well as three species of *Commiphora*, the sister taxon to *Bursera* subg. *Bursera* (Weeks et al., 2005) or perhaps to all of *Bursera* (Becerra, 2003). We downloaded outgroup sequences from GenBank and sequenced missing markers from our collections. GenBank accession numbers are listed in Appendix A.

2.2. DNA extraction, PCR amplification, sequencing, and alignment

We extracted DNA with DNeasy Plant Mini Kits (Qiagen, Valencia, CA) from living and herbarium material (Appendix A). We sequenced five markers, two low-copy nuclear regions (the fourth intron of the phosphoenolpyruvate carboxylase gene, *PEPC*, and the third intron of the nuclear nitrate reductase gene, *NIAi3*), two multiple-copy regions (the internal and external transcribed spacer regions of the nuclear ribosomal DNA, *ITS* and *ETS*), and one from the chloroplast (the *psbA-trnH* intergenic spacer).

We used published primers and protocols to amplify *psbA-trnH* (Sang et al., 1997; Weeks and Simpson, 2004), *PEPC* (Olson, 2002), and *ETS* (Baldwin and Markos, 1998; Weeks and Simpson, 2004). We increased specificity for *PEPC* by raising the annealing temperature to 62 °C for eight samples. We amplified *ITS* with the external and internal primers of Fine et al. (2005), with the following protocol: 97 °C/3 min; nine cycles of 97 °C/1 min, with a touchdown starting at 56 °C/1 min and decreasing 1 °C every cycle, 72 °C/45 s + 4 s/cycle; 30 additional cycles with 48 °C as annealing temperature and a final extension at 72 °C/7 min. Finally, the protocol for *NIAi3* (Howarth and Baum, 2002) started at 94 °C/3 min; 14 cycles of 94 °C/1 min, with a touchdown starting at 62 °C/2 min and decreasing 1 °C each cycle, 72 °C/3 min; 21 additional cycles with

48 °C as annealing temperature and a final extension at 72 °C/7 min. PCR volumes of 25 µL included 10–100 ng of template DNA, 2.5 µL of 10× PCR buffer, 0.5 µL of 10 µM dNTPs in an equimolar ratio, 0.75 µL of 50 µM MgCl₂, 0.63 µL of each of the 10 µM primers, 5 µL of Q solution (Qiagen), and 1 U of *Taq* polymerase added after the initial denaturation step.

When necessary, we cloned PCR products by ligation into pGEM-T vector (Promega, Madison, WI) and transformation of competent *Escherichia coli* (JM109). We sequenced three positively transformed colonies for each sample cloned. Due to the presence of more than one product, we cloned the *NIAi3* PCR products of six samples, one of *B. permollis* (J. Linares 7326), two samples of *B. grandifolia* (Rosell 50 and Olson 1026) and three of *B. simaruba* (Rosell 46, Rosell 51, and Olson 1063). The other nuclear markers *ETS*, *ITS*, and *PEPC* were not cloned due to the observed congruence between their tree topologies; previous studies have shown coalescence within samples in closely related species for *ETS* (Weeks and Simpson, 2004).

PCR products were purified with QIAquick PCR purification kit (Qiagen), and sequenced bidirectionally using the BigDye Terminator cycle sequencing kit (Applied Biosystems, Foster City, CA) in final volumes of 10 µL. Sequencing products were cleaned with Sephadex G-50 (GE Healthcare Bio-Sciences, Piscataway, NJ) and run on an ABI 3100 automated DNA sequencer (Applied Biosystems). Sequences were edited using Sequencher v.4.6 (Gene Codes, Ann Arbor, MI) and aligned using Se-Al v.2.0a11 Carbon (Rambaut, 2002).

2.3. Maximum parsimony analyses (MP)

We analyzed data matrices by marker, in combined analyses with congruent markers as assessed by the incongruence length difference test (ILD, Farris et al., 1995), and also the five loci together. We included potentially informative characters only, which were unordered and weighted equally. We treated gaps as missing data and performed analyses in NONA 2.0 (Goloboff, 1999) using the parsimony ratchet (Nixon, 1999) with WinClada v.1.00.08 (Nixon, 2002) as a shell program. We conducted three searches with different starting seeds using 300 iterations (100 trees held per iteration). We sampled 10% of the characters for reweighting during the parsimony ratchet and calculated a strict consensus from most parsimonious trees. To evaluate support, we used TNT (Goloboff et al., 2008) running 1000 replicates with the “traditional search” approach with TBR set to 100 replications holding 50 trees, and saving the consensus of each resampling matrix. We assessed congruence between each marker using ILD tests as implemented in WinClada v.1.00.08, running 1000 replicates.

2.4. Bayesian analyses (BA)

We used ModelTest v.3.7 (Posada and Crandall, 1998) to determine the model of evolution that best fit each of the five markers and, as for parsimony, performed Bayesian analyses of each mar-

ker, combined data of congruent markers, and finally of the five loci combined. We used MrBayes v.3.2 (Huelsenbeck and Ronquist, 2001) run on the CIPRES portal v.2.2 (Miller et al., 2009). For combined datasets, we performed partitioned analyses, applying a different model of evolution to each marker (Table 2), and ran four Markov chains simultaneously for 15 million generations, starting with a random tree, setting the heating parameter to 0.01 to improve the probability of exchange between chains, which was very low with the default value of 0.2, and sampling trees every 200 generations. After 15 million generations, average split deviations were <0.01 and the plot of the likelihood score vs. MCMC generation suggested that stationarity had been reached after 3.75 million generations. Majority-rule consensus trees were derived from 56,250 trees after a 25% burn-in. Analyses by marker were run for five million generations under the same conditions as combined analyses, reaching average split deviations <0.007.

2.5. Species delimitation using molecular characters

Using combined analyses and analyses by marker derived from MP and BA, we assessed whether species were mono-, para-, or polyphyletic, or whether monophyly or paraphyly could not be rejected because of polytomies in the phylogenetic tree. In assessing the poly-, para-, or mono-phyletic status of a species, we considered nodes with parsimony bootstrap values (PB) ≥70% (Hillis and Bull, 1993) or posterior probabilities (PP) ≥0.95 to be strongly supported.

2.6. Species delimitation using morphological characters

We measured 476 herbarium specimens of eleven Mexican species of the *simaruba* complex, including all satellites except *B. itzae*, for which material was not available (Table 1). We measured 24 morphological variables of taxonomic importance (Table 3) on specimens deposited in the National Herbarium of Mexico (MEXU) and the Herbarium of the Centro Regional del Bajío (IEB). We included minimum and maximum values per specimen for continuous variables to reflect intraspecific variation. To evaluate the effectiveness and relative importance of these variables in separating species, we performed discriminant analyses in R v.2.9.2 (R Development Core Team, 2009). We log-transformed some variables to achieve normality and assessed homoscedasticity graphically; no variables had correlations >0.9. We centered and scaled all variables and there were no missing data. We repeated the discriminant analysis including only *B. simaruba* and its satellites to assess which variables were useful in discriminating these four morphologically similar species.

2.7. Species delimitation using ecological characters

To evaluate ecological differentiation between all satellites, except for *B. itzae*, and *B. simaruba*, we performed a principal

Table 2

Summary of parsimony analyses for each marker and combined markers (congruent markers *PEPC* + *ETS* + *ITS* and all five markers), and models of sequence evolution used for Bayesian analyses.

	No. maximum parsimonious trees (length)	Aligned length (bp)	No. parsimony informative characters (%)	CI	RI	RC	Model of sequence evolution
<i>psbA-trnH</i>	336 (84)	564	61 (11)	0.82	0.96	0.787	TVM+Γ
<i>PEPC</i>	71,174 (137)	588	88 (15)	0.77	0.93	0.716	HKY+Γ
<i>ETS</i>	49,090 (210)	389	84 (22)	0.56	0.86	0.482	TVM+I+Γ
<i>ITS</i>	58,220 (539)	754	164 (22)	0.48	0.76	0.365	GTR+I+Γ
<i>NIAi3</i>	645 (216)	679	135 (20)	0.81	0.95	0.770	TVM+I
<i>PEPC+ETS+ITS</i>	57,690 (993)	1731	336 (19)	0.48	0.78	0.374	–
Five markers	58,737 (1309)	2974	532 (18)	0.55	0.83	0.457	–

Table 3

Characters and results of morphometric analysis including all species and that including only *B. simaruba* and satellites. Only the first two discriminant functions (DF) are presented. *L*, length; min, minimum; max, maximum; *W*, width. Variables with high contribution to the DF in bold.

	All species		<i>B. simaruba</i> + satellites	
	DF1	DF2	DF1	DF2
Leaf <i>L</i> min	-0.048	0.26	-0.096	-0.556
Leaf <i>L</i> max	-0.131	-0.138	0.235	0.296
Leaf <i>W</i> min	0.172	-0.242	-0.238	0.041
Leaf <i>W</i> max	-0.234	0.176	-0.049	0.365
Petiole base pubescence ^a	-0.075	-0.691	0.654	-0.019
Petiole shaft pubescence ^a	-0.014	0.349	-0.027	-0.083
Petiole <i>L</i> min	-0.116	-0.135	0.09	0.463
Petiole <i>L</i> max	0.197	0.225	-0.334	-0.297
Petiolute <i>L</i> terminal leaflet min	0.133	-0.134	0.208	0.019
Petiolute <i>L</i> terminal leaflet max	0.041	0.122	-0.444	0.112
Petiolute <i>L</i> lateral leaflet min	0.089	-0.231	0.182	-0.618
Petiolute <i>L</i> lateral leaflet max	-0.048	-0.308	0.015	-0.255
Petiolute pubescence ^a	-0.206	-0.424	0.277	-0.682
Leaflet number min	-0.097	-1.172	0.722	0.73
Leaflet number max	0.507	-0.557	-0.124	-0.179
Leaflet upper surface pubescence ^b	-1.474	0.005	0.342	-0.912
Leaflet lower surface pubescence ^c	0.193	0.56	-0.75	1.293
Infructescence <i>L</i> min	0.103	-0.118	-0.218	0.082
Infructescence <i>L</i> max	0.11	0.226	0.016	-0.207
Infructescence robustness ^d	-0.037	-0.628	0.953	0.131
Fruit <i>L</i> min	-0.092	-0.339	0.037	0.234
Fruit <i>L</i> max	0.126	0.039	0.583	-0.03
Fruit apex ^e	0.103	0.19	0.095	0.332
Fruit pubescence ^f	-2.663	-0.717		

All characters were continuous, except ^aabsent, scarce, abundant; ^babsent, present only on midvein, scarce on main veins, abundant on main veins; ^cabsent, present only on midvein, present in two basal tufts, scarce on main veins, abundant on main veins; ^dslender, medium, robust; ^eobtuse, acute, acuminate; ^fpresent, absent; * excluded character.

components analysis (PCA) on 19 climatic variables extracted from WorldClim 1.4 (Table 4; Hijmans et al., 2005) based on 462 locality data from specimens at MEXU and IEB. Following Stockman and Bond (2007), we performed a multiple analysis of variance (MANOVA) on PC scores to assess differences between those species appearing as sister taxa according to our phylogenetic results. We assessed homoscedasticity of dependent variables before applying the MANOVA, and when this assumption was violated, we performed a non-parametric MANOVA (Anderson, 2001). To assess which PC accounted for the overall difference detected by the parametric and non-parametric MANOVAs, we performed *t*- or Mann–Whitney tests per species pairs, adjusting alpha levels to account for multiple tests. We performed these analyses with R.

Table 4

Results for the PCA of climatic variables. *T*, temperature; qtr, quarter; ppt, precipitation; Max, maximum; Min, minimum. Variables with high loadings in bold.

Variable	PC1	PC2	PC3
Annual mean <i>T</i>	0.366	-0.025	-0.039
Mean diurnal range	-0.174	0.228	0.075
Isothermality	0.167	0.194	0.402
<i>T</i> seasonality	-0.194	-0.118	-0.481
Max <i>T</i> warmest month	0.254	0.026	-0.243
Min <i>T</i> coldest month	0.359	-0.074	0.063
<i>T</i> annual range	-0.278	0.102	-0.212
Mean <i>T</i> wettest qtr	0.332	-0.04	-0.173
Mean <i>T</i> driest qtr	0.352	-0.044	0.04
Mean <i>T</i> warmest qtr	0.331	-0.064	-0.205
Mean <i>T</i> coldest qtr	0.362	0.024	0.139
Annual ppt	-0.045	-0.37	0.188
Ppt wettest month	-0.078	-0.317	0.277
Ppt driest month	-0.008	-0.368	-0.115
Ppt seasonality	-0.037	0.282	0.288
Ppt wettest qtr	-0.086	-0.305	0.309
Ppt driest qtr	-0.004	-0.374	-0.104
Ppt warmest qtr	-0.091	-0.222	0.289
Ppt coldest qtr	-0.004	-0.369	-0.031

3. Results

Alignment was unambiguous, except for a portion of *PEPC*, which we excluded from the analyses (positions 836–886 of the matrix with concatenated markers). Alignments are available from TreeBASE (<http://purl.org/phylo/treebase/phylo/study/TB2:S10354>).

3.1. Analyses of single markers and ILD tests

The clones of *ETS* downloaded from GenBank (Appendix A), and the clones of *NIAi3* of *B. permollis* (J. Linares 7326), and two of the three samples of *B. simaruba* (Rosell 46 and Olson 1063) coalesced per sample under MP, so consensus sequences were used for terminal taxa. The remaining three samples for which we cloned *NIAi3* did not coalesce. Two sequences of *NIAi3*, differing in five nucleotides, were present in two samples of *B. grandifolia* (Rosell 50 and Olson 1026) and grouped with other *B. grandifolia* collections but not with each other. To streamline combined analyses, whose main purpose was to identify relationships among *simaruba* complex members rather than within *B. grandifolia*, we generated a consensus sequence. One sample of *B. simaruba* (Rosell 51) had two different sequences differing mainly in a 26 bp deletion and 14 nucleotides. The other 27 *B. simaruba* samples had only one or the other of these two sequences. Stop codons in the coding portion (the third exon), which would indicate loss of function, were absent in both sequences, so we decided to include the two *NIAi3* sequences of *B. simaruba* as separate terminal taxa (* in Figs. 3 and 4) duplicating all the other markers.

We include the lengths of the datasets and results from MP by marker in Table 2. Each marker separately recovered only certain groups of species. Fig. 3 includes the results of *psbA-trnH* and *NIAi3* in isolation, and of the combined analyses of the other nuclear markers, which were congruent according to ILD tests. Pairwise ILD tests showed that significant incongruence was mostly restricted to *psbA-trnH* and *NIAi3* with respect to all the other markers. No significant incongruence was found between *PEPC*

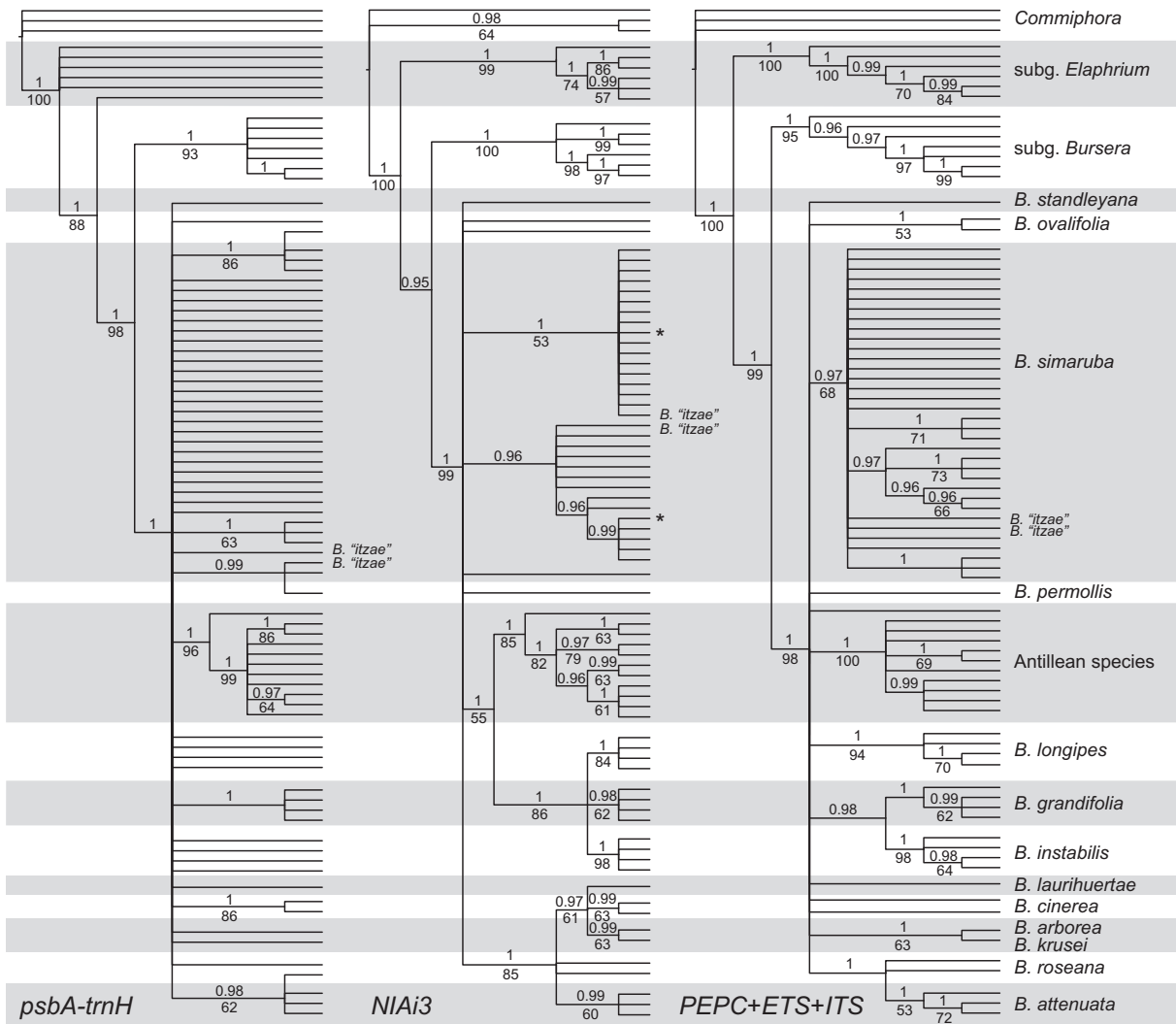


Fig. 3. Congruence between markers in the phylogenetic reconstruction of the *simaruba* complex and its related Antillean species. Bayesian 95% majority-rule consensus cladograms based on *psbA-trnH*, *NIAi3*, and the combined analysis of *PEPC*, *ETS*, *ITS*. Posterior probabilities are shown above branches, and parsimony bootstrap values >50 below branches; *: clones of the *B. simaruba* sample with two different versions of *NIAi3*.

and *ETS* ($p = 0.393$), *PEPC* and *ITS* ($p = 0.114$), *ETS* and *ITS* ($p = 0.173$), and between *psbA-trnH* and *ITS* ($p = 0.06$).

The chloroplast marker mostly informed regarding the deepest relationships, poorly resolving the complex itself (Fig. 3). All markers showed maximum phylogenetic support (PP = 1.0, PB = 100) for the genus *Bursera* and most recovered clades of its two subgenera. A well-supported clade including the *simaruba* complex species and the Antillean species was recovered by all markers with BA (PP ≥ 0.98) and by *PEPC*, *ETS* and *NIAi3* under MP (PB ≥ 82). All markers recovered a well-supported clade including all Antillean species (PP = 1.0, PB ≥ 85), but with *ETS* and *PEPC* the clade excluded *B. spinescens*. With most markers, this Antillean clade appeared in a polytomy with clades of the *simaruba* complex, but with *NIAi3* it was recovered well within the *simaruba* complex as sister to the *grandifolia*-*longipes* clade with strong Bayesian support (Fig. 3). Two well-supported clades of *B. simaruba* samples were recovered by *NIAi3*, each composed of one of the two different sequences found in the cloned *B. simaruba* sample (Fig. 3).

3.2. Analyses from combined-marker datasets

The aligned combined dataset had a length of 2974 bp. In combination, the five loci strongly supported a clade including

the species of the *B. simaruba* complex and also of the Antillean group (Fig. 4). Although major clades in the phylogeny had good support, deeper relationships were not fully resolved. The Antillean clade was maximally supported, but its position was unresolved, as was the case also for *B. permollis* and *B. standleyana* (Fig. 4). Satellite species *B. attenuata* and *B. roseana* grouped in a clade that did not include *B. simaruba*, whereas *B. "itzae"* samples appeared intercalated among *B. simaruba* samples. Finally, *B. ovalifolia* appeared as sister of *B. permollis*, but this relationship had low support (Fig. 4).

3.3. Species delimitation using molecular characters

In the five-marker analyses, *B. simaruba* samples formed a clade with strong support, which also included *B. "itzae"* samples (Fig. 4). Well-supported groups with geographic affinity were recovered within the clade, including a Costa Rican Pacific coast group, a Caribbean group (with collections from the Dominican Republic, and most of those from the Yucatan and Cuba), and the Mexican Pacific coast group (Nayarit, Colima, and all but one Jalisco sample; Fig. 4). *NIAi3* recovered two well-supported clades of *B. simaruba*, but left out one sample (Fig. 3). A clade with all but one sample of *B. simaruba* and *B. "itzae"* was recovered by *ITS* (PP = 0.94) and

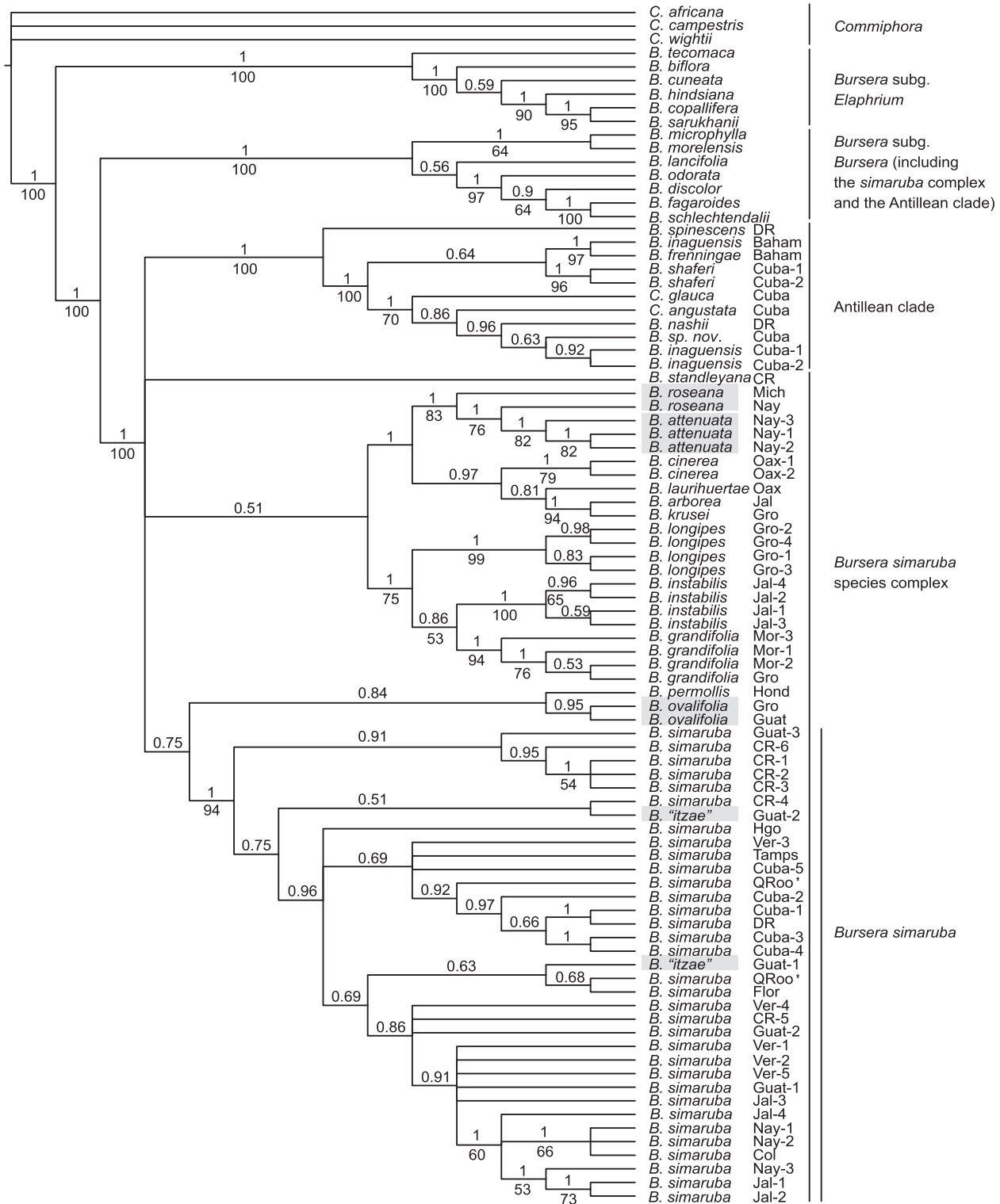


Fig. 4. Phylogeny of the *Bursera simaruba* species complex and its related Antillean species based on five markers. Bayesian 50% majority-rule consensus cladogram is shown with posterior probabilities above branches, and parsimony bootstrap values > 50 below branches. Labels on terminals indicate voucher locality (Appendix A); gray boxes highlight *simaruba* satellite species; *: clones of the *B. simaruba* sample with two different versions of *NIAi3*.

also with *ETS* (PP = 0.98) but included *B. arborea* and *B. krusei*. When *ITS*, *PEPC*, and *ETS* were combined, a well-supported clade of *B. simaruba* samples was recovered (Fig. 3).

Two of the four satellites were non-mono-phyletic, while the other two were recovered as strongly supported clades. In the five-marker analyses, *B. roseana* was paraphyletic in a clade that also

included a strongly-supported group of *B. attenuata* samples (Fig. 4). The *B. attenuata* group was recovered by *ITS* (PP ≥ 0.97, PB = 54) and *NIAi3* (Fig. 3), but included also a *B. roseana* accession in the case of *PEPC* and *psbA-trnH* (Fig. 3). The other *B. roseana* collection usually appeared in a polytomy at the next highest level in the tree. The two *B. ovalifolia* samples were recovered as a clade with

strong support in the combined analyses (Fig. 4) and by *ITS* (PP = 1.0, PB = 70). The other markers did not reject its monophyly, except for *psbA-trnH*, which recovered a *B. ovalifolia* sample in a strongly supported clade with *B. simaruba* samples (Fig. 3). In contrast, the two samples from the type locality of *B. itzae* were recovered as polyphyletic within the clade of *B. simaruba* samples in the combined analyses and with *NIAi3* and *psbA-trnH* (Fig. 3), and in a polytomy including these samples with all other individual markers.

Finally, *B. inaguensis* appeared polyphyletic, with Cuban samples included with other Cuban species and *B. nashii*, whereas *B. inaguensis* from the Bahamas was sister to *B. frenningae* (Fig. 4). Under BA, *ETS*, *ITS*, and *NIAi3* also supported the polyphyletic status of *B. inaguensis*, but its potential monophyly was not rejected under MP or by the remaining markers. All other species represented by two or more samples appeared monophyletic in the combined analysis (Fig. 4) or their monophyly could not be rejected by individual markers (Fig. 3).

3.4. Species delimitation using morphological characters

The first two discriminant functions (DF) of the analysis including all species explained 69% of the observed variance (DF1 = 55%, DF2 = 14%). DF1 indicated that fruit and upper leaflet surface pubescence and the maximum number of leaflets are the most important characters for discriminating between species, followed by the minimum number of leaflets, petiole base and lower leaflet surface pubescence, and infructescence robustness, characters with high coefficients for DF2 (Table 3). A plot of these two DFs shows *B. grandifolia* and *B. krusei* close to one another due to their pubescent fruits and leaflets (Fig. 5A), but because of its more numerous leaflets, *B. grandifolia* was lower on the vertical axis. Specimens of *B. cinerea*, a species with pubescent leaflets but glabrous fruits, appeared to the right and close to *B. arborea*, which has pubescent to glabrous leaflets. Another cluster was formed by *B. instabilis* and *B. laurihuertae*, which share the glabrous one to three-foliolate condition, although some specimens of *B. instabilis* showed scant pubescence and are higher on the vertical axis. A large group formed by *B. simaruba* and its satellites fell to the right because of their glabrous fruits and upper leaflet surfaces, and higher maximum leaflet number. *Bursera longipes* overlapped with

this group, but is readily distinguished by its bluish waxy upper cuticle and small habit. Some specimens fell far from the species they belong to, e.g. the pubescent-fruited specimens of *B. simaruba* (Fig. 5A). Leave-one-out classification tables revealed that species were classified correctly >92% of the time except for *B. simaruba*, which was misclassified 10% of the time, *B. attenuata* 12%, *B. ovalifolia* 12%, *B. roseana* 28%, *B. arborea* 18%, and *B. instabilis* 38% (Appendix C, Supplementary material). Misclassifications of *B. simaruba* and its satellites were mostly due to assignment to another of these four taxonomically difficult species. Specimens of *B. instabilis* were often misclassified as *B. laurihuertae*, a situation that could be avoided by including leaflet apex and shape, which readily distinguish these species.

In the discriminant analysis of *B. simaruba* and its satellites, fruit pubescence was removed because it was present in only four specimens. The first two DF explained 93% (DF = 72%, DF2 = 21%) of total observed variance. To discriminate between *B. simaruba* and its satellites, infructescence robustness, leaflet lower surface and petiole base pubescence, minimum number of leaflets, and maximum fruit length were useful characters, followed by leaflet upper surface and petiolule pubescence, minimum lateral leaflet petiolule length, and minimum leaf length (Table 3). Although these characters tended to separate satellites, some specimens overlapped, highlighting the continuous ranges of some of these characters (Fig. 5B). DF1 separated *B. simaruba* with its robust infructescences, more numerous leaflets, large fruits, and pubescent petiole bases. On the left side of the graph, *B. attenuata* has the opposite characteristics. The other two satellites, *B. ovalifolia* and *B. roseana*, could not be separated on the basis of DF1 alone because of their wide ranges in leaflet lower surface pubescence and infructescence robustness (Appendix B). In contrast, DF2 helped separate *B. ovalifolia* because of its long lateral leaflet petiolules. Classification of *B. simaruba* and *B. ovalifolia* tended to be correct (>92%), but not of *B. attenuata* (88%) and *B. roseana* (62%, Appendix C).

3.5. Satellite species delimitation using ecological characters

The first three PCs of environmental variables accounted for 82% of the variability (PC1 = 38%, PC2 = 33%, PC3 = 11%). Six temperature variables had high loadings on PC1, six precipitation variables on

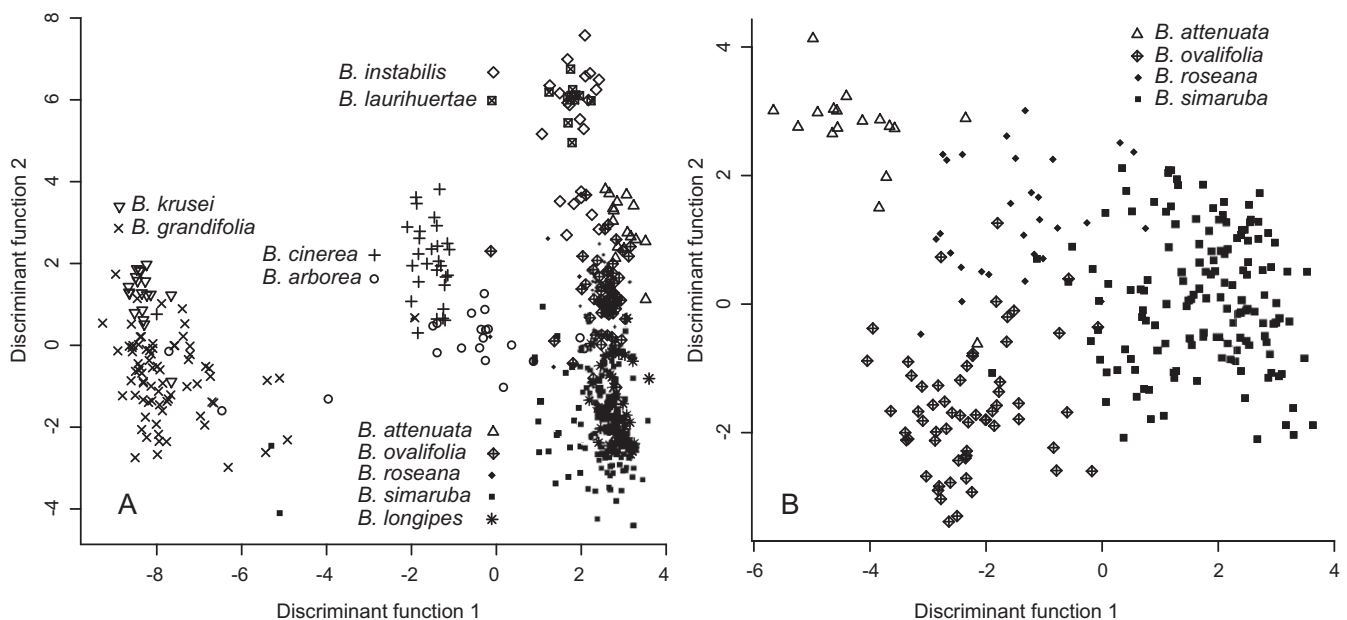


Fig. 5. Morphological phenetic analysis of the Mexican members of the *simaruba* complex. Distribution of specimens according to the first two discriminant functions including all *simaruba* complex species (A) and only *B. simaruba* and its satellite species (B), showing marked overlap between species, especially the satellites.

PC2, and isothermality and temperature seasonality on PC3 (Table 4). We compared ecologically *B. attenuata* and *B. roseana*, which appeared as sister taxa in our phylogeny, and also *B. simaruba* and *B. ovalifolia*, a relationship resulting from one of the possible locations of *B. ovalifolia*, given its unresolved position in the phylogeny, but the only one that would be of interest for this comparison given our goal of using ecological information to delimit satellite species from *B. simaruba*. The MANOVA of the first three PCs rejected the null hypothesis of no ecological differences between *B. attenuata* and *B. roseana* ($F_{3,78} = 11.07$, $p < 0.001$), but only PC2, which was related to precipitation, showed significant differences ($t = -4.717$, $p < 0.001$). A non-parametric MANOVA of the first three PCs rejected the hypothesis of no differences between *B. ovalifolia* and *B. simaruba* ($F_{1,378} = 52.17$, $p < 0.001$). Mann–Whitney tests found differences between these two species regarding temperature (PC1: $W = 18360.5$, $p < 0.001$), precipitation (PC2: $W = 22111.5$, $p < 0.001$), and seasonality (PC3: $W = 19012.5$, $p < 0.001$).

4. Discussion

4.1. Species delimitation and the taxonomy of the *simaruba* complex

We recovered the two most widespread species of the complex as monophyletic. Given its morphological variability and wide range, along with the confusing taxonomy of the complex, we fully expected to recover a paraphyletic *B. simaruba*. However, not only was the species monophyletic but the apparently weak geographic structuring of its populations (Fig. 4) implies genetic cohesion between distant populations via pollen and seed dispersal (Dunphy and Hamrick, 2007; Greenberg et al., 1995; Sousa, 1969). *Bursera simaruba* monophyly is based on considering *B. itzae* a likely synonym of *B. simaruba*, an issue discussed below. Like *B. simaruba*, and despite a long history of nomenclatural changes and wide distribution (Rzedowski et al., 2007; Table 1, Fig. 2), *B. ovalifolia* collections from distant localities formed a single clade. Although one of the possible positions of *B. ovalifolia* is as sister to *B. simaruba* and their ranges overlap (Fig. 2), their ecological conditions differ in temperature, precipitation, and seasonality, suggesting they are not ecologically interchangeable and supporting the validity of *B. ovalifolia* as a separate species.

The three species recovered as non-monophyletic highlight the need for taxonomic revision of these taxa. The paraphyletic pattern of *B. roseana* could suggest that *B. attenuata* is derived from this species and reciprocal monophyly has not been attained, or that both species are in fact the same taxon. *Bursera attenuata* is conceived of as a lowland entity and *B. roseana* its highland counterpart, so we expected their environmental conditions to differ strongly. Surprisingly, only precipitation differed (PC2). Given that their pubescence patterns overlap considerably, and to a lesser extent their distributions (Fig. 2), it may be that the two species are a single entity that varies with elevation (McVaugh and Rzedowski, 1965). With regard to *B. itzae*, it was polyphyletically embedded within *B. simaruba* (Fig. 4). *Bursera itzae* is distinguished from *B. simaruba* by its relatively long inflorescences (15–20 cm; Lundell, 1968). Not known when *B. itzae* was described, however, is that this characteristic varies considerably within *B. simaruba*, especially in Guatemala (M. Véliz, pers. comm.) and adjacent Mexico, where we have observed inflorescences up to 22 cm long. Although our results await confirmation based on unequivocally identified fertile material, we suspect that *B. itzae* simply represents a variant of *B. simaruba* with long inflorescences. Finally, Cuban and Bahamian collections of *B. inaguensis* appeared in two different places in the phylogeny (Fig. 4). Our Cuban collections differ markedly from Bahamian material in leaf and inflorescence features, making it likely that Cuban *B. inaguensis* represents a distinct species.

As was the case with molecular characters, species of the *simaruba* complex could for the most part be reliably distinguished in discriminant analyses of morphological characters (Fig. 5, Appendix C), despite their pronounced morphological plasticity (Appendix B). Although pubescence patterns were crucial for discriminating species (Table 3), the ranges and patterns of expression of indumentum are poorly understood in the complex. Bewilderingly, pubescence may vary between populations, individuals, and even leaflets of the same leaf. In addition, the expression of pubescence in one part of the leaf may not be independent of its production in other parts. For example, the development of trichomes on the lower surface of leaflets seems necessary for production on the upper surface. Ascertaining the independence or lack thereof of pubescence states will determine how they can be coded and interpreted in future analyses. Because of high levels of variation, accurate identification of some species in the clade, particularly the satellites, would seem to require extensive collections from different parts of individual trees, as well as from numerous individuals of the same population. In cases of unusual combinations of morphological characters, identification via molecular characters may be the only alternative at present.

4.2. The origin of satellite species

Our results do not support the origin of the satellites *B. attenuata*, *B. ovalifolia*, and *B. roseana* from *B. simaruba*, suggesting instead that their similarity is due to convergence or parallelism. Distant *B. attenuata* and *B. roseana* are clearly not derived from *B. simaruba* (Fig. 4). As for *B. ovalifolia*, support for its position as sister to *B. permollis* in the analyses with all markers was low, so one of its possible positions is as sister to *B. simaruba* (Fig. 4), making the origin of *B. ovalifolia* from *B. simaruba* a possibility. Nevertheless, support for a *ovalifolia*-*permollis* clade becomes strong in the absence of the chloroplast marker (see Section 4.3 and Fig. 7, Supplementary material), a topology that would translate into rejecting the origin of *B. ovalifolia* from *B. simaruba*. The similarity between *B. simaruba* and the satellites is in a suite of features, many of which occur in other species but all of which tend to be found together only in these four species (Fig. 6, Appendix B). Given that most species in the genus are trees of tropical deciduous forests or shrubs of xerophytic scrubs, it is likely that the massive size of some populations of *B. simaruba* and its satellites derives from their repeated invasions of moister forests (Fig. 6).

4.3. Congruence and testing membership in the *simaruba* complex

Although the recovery of some species as members of the *simaruba* complex clade reaffirmed previous results (Becerra, 2003), the placement of others was heretofore uncertain. This was the case of the unifoliolate Oaxacan endemic *B. laurihuertae* (Rzedowski and Calderón, 2000), whose position among species with several leaflets makes it another example of the changes in leaflet number widespread in the genus (Rzedowski and Kruse, 1979). Likewise, the Central American *B. standleyana* and *B. permollis* were confirmed as belonging to the complex. Although unresolved, the distant placement of *B. permollis* from *B. grandifolia* suggests that the synonymy proposed for these two species (Daly, 1993; Porter and Pool, 2001) is unnecessary.

Although we recovered a single clade including all Antillean species (Figs. 3 and 4), its position as sister to or part of the *simaruba* complex could not be resolved. Based on our five marker reconstruction, the placement of the Antillean clade as sister to the whole *simaruba* complex (Weeks and Simpson, 2004) or to the *grandifolia*-*longipes* clade, as suggested by *NI*Ai3, results in a tree with the same number of steps. Because of the numerous synapomorphies supporting the Antillean clade itself, it seems

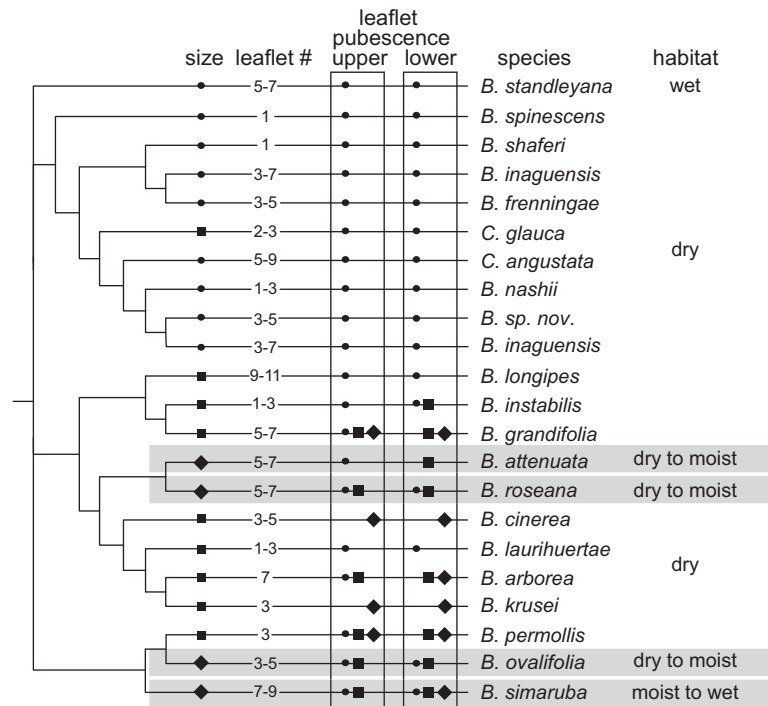


Fig. 6. Convergence/parallelism in the *simaruba* complex. Similarity between *B. simaruba* and its satellites mapped on the phylogeny of the *simaruba* complex and its related Antillean clade, illustrating the similarity between satellites and *B. simaruba* in a suite of features. Size: circle = small tree or shrub (<8 m), square = small to medium tree (<16 m), diamond = small to large tree (>16 m); Pubescence: circle = glabrous, square = sparsely pubescent, diamond = pubescent; Habitat: dry = tropical deciduous forest, moist = tropical subdeciduous forest; wet = tropical rainforest.

unlikely that its ambiguous placement is due to hybridization or lineage sorting, but rather that more characters are needed. This lack of information could also explain the unresolved position of *B. standleyana*, whose molecular changes were also mostly autapomorphic. The position of *B. permollis* within a strongly supported clade of *B. simaruba* samples in the analyses of *psbA-trnH* contrasts with its unresolved position in the analyses by other markers (Fig. 3), and also with its strongly supported location as sister to *B. ovalifolia* when *psbA-trnH* is excluded from analysis (Fig. 7, Supplementary material). This incongruence between the chloroplast and nuclear markers could suggest genetic influence of *B. simaruba* in this sample.

The two main clades within *B. simaruba* reflect two *NIAi3* sequence variants that differ mainly in a characteristic deletion. In general, each *B. simaruba* sample had one or the other of these variants, but both occurred together in one sample. These two sequence types may represent different alleles or paralogues. Differences between the sequences are comparable to those found between alleles in *Scaevola* (Howarth and Baum, 2005), which, together with the absence of stop codons, would suggest that the versions are alleles rather than pseudogenes. At the same time, duplications of *NIAi3* have been found in the tribe Canarieae within Burseraceae (Weeks, 2009), and in other families (Hamman-Khalifa et al., 2007; Yi et al., 2008), although the sequences found in *B. simaruba* did not correspond to those in Canarieae. Whether they represent alleles or paralogues with potential associated lineage sorting, in the genus these sequences seem to be restricted to *B. simaruba* (J.A. De-Nova, unpublished results), and they would not affect the phylogenetic reconstruction of the *simaruba* complex.

5. Conclusion

As in many species complexes, molecular tools proved invaluable in our analysis of the *simaruba* clade, in which high levels of

intraspecific morphological plasticity coexist with marked overlap between species. Results pinpointed priority species that require further sampling for molecular and morphological work, and also characters that need to be reexamined to refine the taxonomy of the group. The molecular phylogeny of the *simaruba* complex allowed us to reject the origin of three satellite species from their purported ancestor, *B. simaruba*, and to ascribe their morphological similarity as likely being due to convergence or parallelism. Distinguishing the effects of similarity due to common ancestry, convergence, or parallelism, if they can in fact be separated, is a major challenge of species complex biology, especially as evolutionary developmental biology blurs some of these distinctions (Abouheif, 2008; Kim et al., 2003). The *simaruba* complex appears to provide excellent examples for studies of adaptive divergence, convergence, or parallelism, and our phylogeny offers an essential framework for any such effort using the *simaruba* complex as a model system.

Acknowledgments

This project was supported by grants from CONACYT (46475), PAPIIT/DGAPA (IN228207), US NSF (0919179) and the Cactus and Succulent Society of America. J.A.R. acknowledges the support of CONACYT through a graduate scholarship, the Programa de Posgrado en Ciencias Biológicas, UNAM, and the Graduate Student Grant from the American Society of Plant Taxonomists. We thank Drs. Jerzy Rzedowski and Graciela Calderón for their kind and generous orientation; Laura Márquez for her help with sequencing of the samples; Cristina Martínez for samples of Cuban species; Hilda Flores, Verónica Juárez, Sergio Zamudio, Victor Steinmann, Yocupitzia Ramírez and the rest of the staff of MEXU and IEB for facilitating the measurement of specimens; Katherine Renton for samples; René Cerritos and Martín García Varela for their help with cloning; Erika Aguirre, Laura Espinosa, and Calixto León for their help in the

laboratory; Wayne Pfeiffer, Lucie Chan, and Mark Miller, members of the Cipres Portal staff, for their help running Bayesian analyses; Salvador Zamora for statistical advice; Brad Boyle, the Organization for Tropical Studies, and Francisco Morales for their help during fieldwork in Costa Rica; David Gernandt, Mario García Paris, César Domínguez, Leonardo Alvarado, Angélica Cervantes, Laura Trejo, and Susana Magallón for critical discussions; Barbara Whitlock and the anonymous reviewers, whose thoughtful suggestions greatly improved this paper.

Appendix A.

Voucher information, sample labels and GenBank accession numbers (*psbA-trnH*, *PEPC*, *ETS*, *ITS*, *NIAi3*) for the species sampled. All vouchers are deposited in MEXU, unless otherwise stated. Mx: Mexico; NA: not available. GenBank accession numbers of previously published sequences are designated by a superscript corresponding to the following publications: ^aBecerra (2003), ^bWeeks and Simpson (2004), ^cWeeks et al. (2005), ^dWeeks and Simpson (2007).

B. arborea: **Jal** = Chamela, Jalisco, Mx (Rosell 16), GQ377870, GQ377934, GQ378006, GQ378070, GQ378140.

B. attenuata: **Nay-1** = Tepic, Nayarit, Mx (R. Medina 3412), GQ377871, GQ377935, GQ378007, GQ378071, GQ378141; **Nay-2** = Santa Ma. Del Oro, Nayarit, Mx (R. Medina 3417), GQ377872, GQ377936, GQ378008, GQ378072, GQ378142; **Nay-3** = Santa Ma. Del Oro, Nayarit, Mx (R. Medina 3423), GQ377873, GQ377937, GQ378009, GQ378073, GQ378143.

B. cinerea: **Oax-1** = Jayacatlán, Oaxaca, Mx (Rosell 40), GQ377874, GQ377938, GQ378010, GQ378074, GQ378144; **Oax-2** = Teotitlán, Oaxaca, Mx (R. Medina 1281), GQ377875, GQ377939, GQ378011, GQ378075, GQ378145.

B. frenningae: **Baham** = Fairchild Tropical Garden, Bahamas (79410F, TEX), AY309392^b, AY309366^b, AY309311–AY309313^b, GQ378076, GQ378152.

B. grandifolia: **Mor-1** = Alpuyecá, Morelos, Mx (Rosell 50), GQ377876, GQ377940, GQ378012, GQ378077, GQ378146–GQ378147; **Mor-2** = Atlacholoaya, Morelos, Mx (Rosell 5), GQ377877, GQ377941, GQ378013, GQ378078, GQ378148; **Mor-3** = Atlacholoaya, Morelos, Mx (Olson 1026), GQ377878, GQ377942, GQ378014, GQ378079, GQ378149–GQ378150; **Gro** = Taxco, Guerrero, Mx (R. Medina 3977), GQ377879, GQ377943, GQ378015, GQ378080, GQ378151.

B. inaguensis: **Cuba-1** = Rafael Freyre, Holguín, Cuba (42572, HAC), GQ377880, GQ377944, GQ378016, GQ378081, GQ378153; **Cuba-2** = Bahía de Naranjos, Holguín, Cuba (42569, HAC), GQ377881, GQ377945, GQ378017, GQ378082, GQ378154; **Baham** = Inagua, Fairchild Tropical Garden (64269M, TEX), AY309393^b, AY309367^b, AY309314–AY309316^b, GQ378083, GQ378155.

B. instabilis: **Jal-1** = Chamela, Jalisco, Mx (Rosell 11), GQ377882, GQ377946, GQ378018, GQ378084, GQ378156; **Jal-2** = Chamela, Jalisco, Mx (Rosell 12), GQ377883, GQ377947, GQ378019, GQ378085, GQ378157; **Jal-3** = Chamela, Jalisco, Mx (Rosell 13), GQ377884, GQ377948, GQ378020, GQ378086, GQ378158; **Jal-4** = Chamela, Jalisco, Mx (J.C. Montero 923), GQ377885, GQ377949, GQ378021, GQ378087, GQ378159.

B. "itzae": **Guat-1** = Lake Petén Itzá, Guatemala (J.C. Montero 1029), GQ377886, GQ377950, GQ378022, GQ378088, GQ378160; **Guat-2** = Lake Petén Itzá, Guatemala (J.C. Montero 1030), GQ377887, GQ377951, GQ378023, GQ378089, GQ378161.

B. krusei: **Gro** = Río Papagayo, Guerrero, Mx (R. Medina 4045), GQ377888, GQ377952, GQ378024, GQ378090, GQ378162.

B. laurihuertae: **Oax** = Tehuantepec, Oaxaca, Mx (Olson 1119), GQ377889, GQ377953, GQ378025, GQ378091, GQ378163.

B. longipes: **Gro-1** = La Organera, Guerrero, Mx (Olson 1029), GQ377890, GQ377954, GQ378026, GQ378092, GQ378164; **Gro-2** = Xalitla, Guerrero, Mx (Cervantes 5), GQ377891, GQ377955, GQ378027, GQ378093, GQ378165; **Gro-3** = Xochipala, Guerrero, Mx (Olson 1028), GQ377892, GQ377956, GQ378028, GQ378094, GQ378166; **Gro-4** = Xochipala, Guerrero, Mx (R. Medina P-6), GQ377893, GQ377957, GQ378029, GQ378095, GQ378167.

B. nashii: **DR** = Dominican Republic (Weeks 01–VIII–22–1, TEX), AY309389^b, AY309363^b, AY309302–AY309304^b, NA, GQ378168.

B. ovalifolia: **Gro** = Río Papagayo, Guerrero, Mx (Olson 1128), GQ377894, GQ377958, GQ378030, GQ378096, GQ378169; **Guat** = La Antigua, Sacatepéquez, Guatemala (Olson 1133), GQ377895, GQ377959, GQ378031, GQ378097, GQ378170.

B. permollis: **Hond** = Maraita, Francisco Morazán, Honduras (J. Linares 7326), GQ377896, GQ377960, GQ378032, GQ378098, GQ378171–GQ378172.

B. roseana: **Mich** = Río Cupatitzio, Michoacán, Mx (Rosell 25), GQ377899, GQ377963, GQ378035, GQ378101, GQ378175; **Nay** = El Cuarenteño, Nayarit, Mx (R. Medina 3406), GQ377900, GQ377964, GQ378036, GQ378102, GQ378176.

B. simaruba: **Col** = Tecmán, Colima, Mx (J. C. Montero 938), GQ377897, GQ377961, GQ378033, GQ378099, GQ378173; **Hgo** = Tolantongo, Hidalgo, Mx (R. Medina 4430), GQ377901, GQ377965, GQ378037, GQ378103, GQ378177; **Jal-1** = Chamela, Jalisco, Mx (Olson 1078), GQ377902, GQ377966, GQ378038, GQ378104, GQ378178; **Jal-2** = Chamela, Jalisco, Mx (Olson 1079), GQ377903, GQ377967, GQ378039, GQ378105, GQ378179; **Jal-3** = Chamela, Jalisco, Mx (Olson 1080), GQ377904, GQ377968, GQ378040, GQ378106, GQ378180; **Jal-4** = Tomatlán, Jalisco, Mx (J.C. Montero 932), GQ377898, GQ377962, GQ378034, GQ378100, GQ378174; **Nay-1** = Tepic, Nayarit, Mx (R. Medina 3413), GQ377924, GQ377989, GQ378061, GQ378127, GQ378204; **Nay-2** = Tepic, Nayarit, Mx (R. Medina 3414), GQ377925, GQ377990, GQ378062, GQ378128, GQ378205; **Nay-3** = Tepic, Nayarit, Mx (Olson 1072), GQ377905, GQ377969, GQ378041, GQ378107, GQ378181; **QRoo** = Cozumel, Quintana Roo, Mx (Rosell 51), GQ377906, GQ377970, GQ378042, GQ378108, GQ378182–GQ378183; **Tamps** = Ciudad Mante, Tamaulipas, Mx (Olson 1040), GQ377907, GQ377971, GQ378043, GQ378109, GQ378184; **Ver-1** = Los Tuxtlas, Veracruz, Mx (Rosell sn), GQ377908, GQ377972, GQ378044, GQ378110, GQ378185; **Ver-2** = Los Tuxtlas, Veracruz, Mx (Rosell 44), GQ377909, GQ377973, GQ378045, GQ378111, GQ378186; **Ver-3** = Los Tuxtlas, Veracruz, Mx (Rosell 46), GQ377910, GQ377974, GQ378046, GQ378112, GQ378187–GQ378189; **Ver-4** = Los Tuxtlas, Veracruz, Mx (Rosell 45), GQ377911, GQ377975, GQ378047, GQ378113, GQ378190; **Ver-5** = Isla, Veracruz, Mx (Olson 1034), GQ377912, GQ377976, GQ378048, GQ378114, GQ378191; **CR-1** = Palo Verde, Guanacaste, Costa Rica (A. Fernández & C. Hood 1128, MO), GQ377913, GQ377977, GQ378049, GQ378115, GQ378192; **CR-2** = Palo Verde, Guanacaste, Costa Rica (M.F. Quigley 856, MO), GQ377914, GQ377978, GQ378050, GQ378116, GQ378193; **CR-3** = Palo Verde, Guanacaste, Costa Rica (Olson 1046, INB), GQ377915, GQ377979, GQ378051, GQ378117, GQ378194; **CR-4** = La Selva, Heredia, Costa Rica (Whitson 343, MO), GQ377916, GQ377980, GQ378052, GQ378118, GQ378195; **CR-5** = Cahuita, Limón, Costa Rica (Olson 1063), GQ377917, GQ377981, GQ378053, GQ378119, GQ378196–GQ378197; **CR-6** = La Cangreja, San José, Costa Rica (Olson 1061, INB), GQ377918, GQ377982, GQ378054, GQ378120, GQ378198; **Cuba-1** = Bahía de Naranjos, Holguín, Cuba (42570, HAC), GQ377919, GQ377983, GQ378055, GQ378121, GQ378199; **Cuba-2** = Gibara, Holguín, Cuba (C. Martínez et al., 2284, RAS), GQ377920, GQ377984, GQ378056, GQ378122, NA; **Cuba-3** = Gibara, Holguín, Cuba (C. Martínez et al., 2285, RAS), GQ377921, GQ377985, GQ378057, GQ378123, GQ378200; **Cuba-4** = Gibara, Holguín, Cuba (42573, HAC), GQ377922, GQ377986,

GQ378058, GQ378124, GQ378201; **Cuba-5** = Havana-Pinar del Río hwy, Pinar del Río, Cuba (42563, HAC), NA, GQ377987, GQ378059, GQ378125, GQ378202; **Guat-1** = Ceibal, Guatemala (J.C. Montero 1028), GQ377926, GQ377991, GQ378063, GQ378129, GQ378206; **Guat-2** = Ciudad Vieja, Guatemala (J.C. Montero 1005), GQ377923, GQ377988, GQ378060, GQ378126, GQ378203; **Guat-3** = Lake Petén Itzá, Guatemala (J.C. Montero 1032), GQ377927, GQ377992, GQ378064, GQ378130, GQ378207; **DR** = Dominican Republic, AY309401^b, AY309379^b, AY309344–AY309346^b, NA, NA; **Flor** = Florida, AY309402^b, AY309378^b, AY309341–AY309343^b, NA, NA.

B. shaferi: Cuba-1 = Viñales, Pinar del Río, Cuba (42561, HAC), GQ377929, GQ377993, NA, GQ378131, GQ378208; **Cuba-2** = Viñales, Pinar del Río, Cuba (42562, HAC), GQ377928, GQ377994, GQ378065, NA, GQ378209.

B. sp. nov.: Cuba = Gibara, Holguín, Cuba (42557, HAC), GQ377930, GQ377995, GQ378066, GQ378132, GQ378210.

B. spinescens: DR = Dominican Republic (Weeks 01–VIII–23–1, TEX), AY309403^b, AY309388^b, AY309356–AY309358^b, NA, GQ378211.

B. standleyana: CR = La Cangreja, San José, Costa Rica (J.F. Morales 1944, MO), GQ377931, GQ377996, GQ378067, GQ378133, GQ378212.

Commiphora angustata: Cuba = Trinidad, Sancti Spiritus, Cuba (42575, HAC), GQ377932, NA, GQ378068, GQ378134, GQ378213.

C. glauca: Cuba = Yateritas, Guantánamo, Cuba (42577, HAC), GQ377933, GQ377997, GQ378069, GQ378135, GQ378214.

Outgroup species: B. biflora: UNAM Botanical Garden, Mx (J.C. Montero sn), AY831896^d, GQ377998, AY315039–AY315041^c, AF445807^a, GQ378215.

B. copallifera: Taxco, Guerrero, Mx (R. Medina 3975), AY831897^d, GQ377999, AY315042–AY315044^c, AF445833^a, GQ378216.

B. cuneata: La Pera, Morelos, Mx (J.C. Montero 808), AY831898^d, GQ378000, AY315045–AY315047^c, AF445825^a, GQ378217.

B. discolor: Chilpancingo, Guerrero, Mx (R. Medina 4028), AY309390^b, AY309364^b, AY309305–AY309307^b, AF445846^a, GQ378218.

B. fagaroides: Chiranganguo, Michoacán, Mx (R. Medina 4227), AY309391^b, AY309365^b, AY309308–AY309310^b, AF445843^a, GQ378219.

B. hindsiana: Sonora, Mx (J. Núñez-Farfán sn), AY831899^d, GQ378001, AY315048–AY315050^c, GQ378136, GQ378220.

B. lancifolia: Casa Verde, Guerrero, Mx (R. Medina 4007), AY309394^b, AY309368^b, AY309317–AY309319^b, AF445857^a, GQ378221.

B. microphylla: Sonora, Mx (J. Núñez-Farfán sn), AY309396^b, AY309370^b, AY309326–AY309328^b, AF445855^a, GQ378222.

B. morelensis: Cuicatlán, Oaxaca, Mx (R. Medina 3971), AY309397^b, AY309371^b, AY309329–AY309331^b, AF445852^a, GQ378223.

B. odorata: Mexico, AY309398^b, AY309372^b, AY309332–AY309334^b, AF445850^a, NA.

B. sarukhanii: San Jerónimo, Michoacán, Mx (R. Medina 4246), AY831900^d, GQ378002, AY315051–AY315053^c, AF445820^a, GQ378224.

B. schlehtendalii: Palo Verde, Guanacaste, Costa Rica (Olson 1050, INB), AY309400^b, AY309377^b, AY309323–AY309325^b, AF445847^a, GQ378225.

B. tecomaca: Guerrero, Mx (R. Medina 4512), AY309409^b, AY309362^b, AY309359–AY309361^b, AF445838^a, GQ378226.

Commiphora africana: South Africa (Weeks 02–XII–09–03, TEX), AY831901^d, GQ378003, AY831869^d, GQ378137, GQ378227.

C. campestris: Zimbabwe (Weeks 00–VI–24–3, TEX), AY831906^d, GQ378004, AY831873^d, GQ378138, GQ378228.

C. wightii: India (Weeks 00–VIII–18–3, TEX), AY831936^d, GQ378005, AY315081–AY315083^c, GQ378139, GQ378229.

Appendix B. Supplementary data

Supplementary data associated with this article can be found, in the online version, at doi:10.1016/j.ympbev.2010.08.004.

References

- Abouheif, E., 2008. Parallelism as the pattern and process of mesoevolution. *Evol. Dev.* 10, 3–5.
- Anderson, M.J., 2001. A new method for non-parametric multivariate analysis of variance. *Austral Ecol.* 26, 32–46.
- Avise, J.C., Ball, R.M., 1990. Principles of genealogical concordance in species concepts and biological taxonomy. *Oxf. Surv. Evol. Biol.* 7, 45–67.
- Baldwin, B.G., Markos, S., 1998. Phylogenetic utility of the external transcribed spacer (ETS) of 18S–26S rDNA: congruence of ETS and its trees of *Calycadenia* (Compositae). *Mol. Phylogenet. Evol.* 10, 449–463.
- Barracough, T.G., Nee, S., 2001. Phylogenetics and speciation. *Trends Ecol. Evol.* 16, 391–399.
- Baum, D., Shaw, K.L., 1995. Genealogical perspectives on the species problem. In: Hoch, P.C., Stephenson, A.G. (Eds.), *Experimental and Molecular Approaches to Plant Biosystematics*. Missouri Botanical Garden, St. Louis, pp. 289–303.
- Becerra, J.X., 2003. Evolution of Mexican *Bursera* (Burseraceae) inferred from ITS, ETS, and 5S nuclear ribosomal DNA sequences. *Mol. Phylogenet. Evol.* 26, 300–309.
- Becerra, J.X., Venable, D.L., 1999. Nuclear ribosomal DNA phylogeny and its implications for evolutionary trends in Mexican *Bursera* (Burseraceae). *Am. J. Bot.* 86, 1047–1057.
- Bullock, A.A., 1936. Notes on the Mexican species of the genus *Bursera*. *Bull. Misc. Inf. Kew* 1936, 346–387.
- Campbell, P., Schneider, C.J., Adnan, A.M., Zubaid, A., Kunz, T.H., 2004. Phylogeny and phylogeography of Old World fruit bats in the *Cynopterus brachyotis* complex. *Mol. Phylogenet. Evol.* 33, 764–781.
- Coyne, J.A., Orr, H.A., 2004. *Speciation*. Sinauer, Sunderland.
- Crisp, M.D., Chandler, G.T., 1996. Paraphyletic species. *Telopea* 6, 813–844.
- Daly, C.D., 1993. Notes on *Bursera* in South America, including a new species. *Studies in Neotropical Burseraceae VII*. *Brittonia* 45, 240–246.
- Dunphy, B.K., Hamrick, J.L., 2007. Estimation of gene flow into fragmented populations of *Bursera simaruba* (Burseraceae) in the dry-forest life zone of Puerto Rico. *Am. J. Bot.* 94, 1786–1794.
- Farris, J.S., Källersjö, M., Kluge, A.G., Bult, C., 1995. Testing significance of incongruence. *Cladistics* 10, 315–319.
- Fine, P.V.A., Daly, D.C., Villa, G., Mesones, I., Cameron, K.M., 2005. The contribution of edaphic heterogeneity to the evolution and diversity of Burseraceae trees in the Western Amazon. *Evolution* 59, 1464–1478.
- Funk, D.F., Omland, K.E., 2003. Species-level paraphyly and polyphyly: frequency, causes, and consequences, with insights from animal mitochondrial DNA. *Annu. Rev. Ecol. Syst.* 34, 397–423.
- Goloboff, P., 1999. NONA (NO NAME) ver. 2. Published by the author, Tucumán, Argentina. Available from: <<http://www.cladistics.com/aboutNona>> (accessed 2009).
- Goloboff, P.A., Farris, J.S., Nixon, K.C., 2008. TNT, a free program for phylogenetic analysis. *Cladistics* 24, 774–786.
- Graybeal, A., 1995. Naming species. *Syst. Biol.* 44, 237–250.
- Greenberg, R., Foster, M.S., Márquez-Valdelamar, L., 1995. The role of the white-eyed vireo in the dispersal of *Bursera* fruit on the Yucatan Peninsula. *J. Trop. Ecol.* 11, 619–639.
- Hamman-Khalifa, A.M., Navajas-Pérez, R., De la Herrán, R., Ruiz Rejón, M., Garrido-Ramos, M.A., Ruiz Rejón, C., Rosúa, J.L., 2007. Establishing the genetic relationships between wild and cultivated olives using a nuclear intron from nitrate reductase (*nia-i3*). *Plant Syst. Evol.* 269, 63–73.
- Harrison, R.G., 1998. Linking evolutionary pattern and process. The relevance of species concepts for the study of speciation. In: Howard, D.J., Berlocher, S.H. (Eds.), *Endless Forms. Species and Speciation*. Oxford University Press, New York, pp. 19–31.
- Hedin, M.C., 1997. Speciation history in a diverse clade of habitat-specialized spiders (Araneae: Nesticidae: *Nesticus*). *Evolution* 51, 1929–1945.
- Hijmans, R.J., Cameron, S.E., Parra, J.L., Jones, P.G., Jarvis, A., 2005. Very high resolution interpolated climate surfaces for global land areas. *Int. J. Climatol.* 25, 1965–1978.
- Hillis, D.M., 1988. Systematics of the *Rana pipiens* complex: puzzle and paradigm. *Annu. Rev. Ecol. Syst.* 19, 39–63.
- Hillis, D.M., Bull, J.J., 1993. An empirical test of bootstrapping as a method for assessing confidence in phylogenetic analyses. *Syst. Biol.* 42, 182–192.
- Howarth, D.G., Baum, D.A., 2002. Phylogenetic utility of a nuclear intron from nitrate reductase for the study of closely related plant species. *Mol. Phylogenet. Evol.* 23, 525–528.
- Howarth, D.G., Baum, D.A., 2005. Genealogical evidence of homoploid hybrid speciation in an adaptive radiation of *Scaevola* (Goodeniaceae) in the Hawaiian Islands. *Evolution* 59, 948–961.

- Huelsenbeck, J.P., Ronquist, F., 2001. MrBayes: Bayesian inference of phylogenetic trees. *Bioinformatics* 17, 754–755.
- Kim, M., McCormick, S., Timmermans, M., Sinha, N., 2003. The expression domain of PHANTASTICA determines leaflet placement in compound leaves. *Nature* 424, 438–443.
- Knowles, L.L., Carstens, B.C., 2007. Delimiting species without monophyletic trees. *Syst. Biol.* 56, 887–895.
- Kopp, A., Barmina, O., 2005. Evolutionary history of the *Drosophila bipectinata* species complex. *Genet. Res.* 85, 23–46.
- Kornfield, I., Smith, P.F., 2000. African cichlid fishes: model systems for evolutionary biology. *Annu. Rev. Ecol. Syst.* 31, 163–196.
- Leliaert, F., Verbruggen, H., Wysor, B., De Clerck, O., 2009. DNA taxonomy in morphologically plastic taxa: algorithmic species delimitation in the *Boodlea* complex (Chlorophyta: Cladophorales). *Mol. Phylogenet. Evol.* 53, 122–133.
- Losos, J.B., 1994. Integrative approaches to evolutionary ecology: *Anolis* lizards as model systems. *Annu. Rev. Ecol. Syst.* 25, 467–493.
- Lundell, C.L., 1968. Studies of tropical American plants-V. *Wrightia* 4, 79–96.
- McVaugh, R., Rzedowski, J., 1965. Synopsis of the genus *Bursera* L. in western Mexico, with notes on the material of *Bursera* collected by Sessé & Mocino. *Kew Bull.* 18, 317–346.
- Miller, M.A., Holder, M.T., Vos, R., Midford, P.E., Liebowitz, T., Chan, L., Hoover, P., Warnow, T., 2009. The CIPRES Portals. CIPRES. Available from: <http://www.phylo.org/sub_sections/portal/> (accessed 2009).
- Moncada-Ferrara, M., 1989. Reporte del género *Commiphora* Jacq. (Burseraceae) para Cuba. *Rev. Jard. Bot. Nac.* 10, 3–9.
- Nixon, K.C., 1999. The parsimony ratchet, a new method for rapid parsimony analysis. *Cladistics* 15, 407–414.
- Nixon, K.C., 2002. WinClada ver. 1.00.08. Published by the author, Ithaca, New York. Available from: <<http://www.cladistics.com/aboutWinc>> (accessed 2008).
- Olson, M.E., 2002. Combining data from DNA sequences and morphology for a phylogeny of Moringaceae (Brassicales). *Syst. Bot.* 27, 55–73.
- Omland, K.E., Tarr, C.L., Boarman, W.I., Marzluff, J.M., Fleischer, R.C., 2000. Cryptic genetic variation and parapatry in ravens. *Proc. R. Soc. Lond. B* 267, 2475–2482.
- Omland, K.E., Baker, J.M., Peters, J.L., 2006. Genetic signatures of intermediate divergence: population history of Old and New World Holarctic ravens (*Corvus corax*). *Mol. Ecol.* 15, 795–808.
- Patton, J.L., Smith, M.F., 1994. Parapatry, polyphyly, and the nature of species boundaries in pocket gophers (genus *Thomomys*). *Syst. Biol.* 43, 11–26.
- Porter, D.M., Pool, A., 2001. Burseraceae. In: Stevens, W.D., Ulloa, C., Pool, A., Montiel, O.M. (Eds.), *Flora de Nicaragua. Monographs in Systematic Botany from the Missouri Botanical Garden*. Missouri Botanical Garden, St. Louis, pp. 500–503.
- Posada, D., Crandall, K.A., 1998. ModelTest: testing the model of DNA substitution. *Bioinformatics* 14, 817–818.
- R Development Core Team, 2009. R: A language and environment for statistical computing, v.2.9.2. Available from: <<http://www.R-project.org/>> (accessed 2009).
- Rambaut, A., 2002. SE-AL v.2.0a11: sequence alignment editor. Available from: <<http://tree.bio.ed.ac.uk/software/seal/>> (accessed 2008).
- Rieseberg, L.H., Brouillet, L., 1994. Are many plant species paraphyletic? *Taxon* 43, 21–32.
- Ruiz-Sanchez, E., Sosa, V., 2010. Delimiting species boundaries within the Neotropical bamboo *Otatea* (Poaceae: Bambusoideae) using molecular, morphological and ecological data. *Mol. Phylogenet. Evol.* 54, 344–356.
- Rzedowski, J., Calderón, G., 2000. Una nueva especie de *Bursera* (Burseraceae) del estado de Oaxaca (México). *Acta Bot. Mex.* 52, 75–81.
- Rzedowski, J., Kruse, H., 1979. Algunas tendencias evolutivas en *Bursera* (Burseraceae). *Taxon* 28, 103–116.
- Rzedowski, J., Medina, R., Calderón, G., 2005. Inventario del conocimiento taxonómico, así como de la diversidad y del endemismo regionales de las especies mexicanas de *Bursera* (Burseraceae). *Acta Bot. Mex.* 70, 85–111.
- Rzedowski, J., Medina, R., Calderón, G., 2007. Segunda restauración de *Bursera ovalifolia* y nombre nuevo para otro componente del complejo de *B. simaruba* (Burseraceae). *Acta Bot. Mex.* 81, 45–70.
- Sang, T., Crawford, D.J., Stuessy, T.F., 1997. Chloroplast DNA phylogeny, reticulate evolution, and biogeography of *Paonia* (Paeoniaceae). *Am. J. Bot.* 84, 1120–1136.
- Shaw, K.L., 1998. Species and the diversity of natural groups. In: Howard, D.J., Berlocher, S.H. (Eds.), *Endless Forms. Species and Speciation*. Oxford University Press, New York, pp. 44–56.
- Sites Jr., J.W., Marshall, J.C., 2003. Delimiting species: a Renaissance issue in systematic biology. *Trends Ecol. Evol.* 18, 462–470.
- Sites Jr., J.W., Marshall, J.C., 2004. Operational criteria for delimiting species. *Annu. Rev. Ecol. Evol. Syst.* 35, 199–227.
- Slade, R.W., Moritz, C., 1998. Phylogeography of *Bufo marinus* from its natural and introduced ranges. *Proc. R. Soc. Lond. B* 265, 769–777.
- Sousa, M., 1969. Influencia de las aves en la vegetación de la Laguna del Majahual en Los Tuxtlas. *Ver. Bol. Soc. Bot. Mex.* 30, 97–112.
- Standley, P.C., 1923. Burseraceae. Trees and shrubs of Mexico. *Contr. US Natl. Herb.* 23, 542–552.
- Starkey, D.E., Shaffer, B., Burke, R.L., Forstner, R.J., Iverson, J.B., Janzen, F.J., Rhodin, A.G.J., Ultsch, G.R., 2003. Molecular systematics, phylogeography and the effects of Pleistocene glaciation in the painted turtle (*Chrysemys picta*) complex. *Evolution* 57, 119–128.
- Stockman, A.K., Bond, J.E., 2007. Delimiting cohesion species: extreme population structuring and the role of ecological interchangeability. *Mol. Ecol.* 16, 3374–3392.
- Talbot, S.L., Shields, G.F., 1996. Phylogeography of brown bears (*Ursus arctos*) of Alaska and parapatry within the Ursidae. *Mol. Phylogenet. Evol.* 5, 477–494.
- Templeton, A.R., 1989. The meaning of species and speciation: a genetic perspective. In: Otte, D., Endler, J.A. (Eds.), *Speciation and Its Consequences*. Sinauer Associates, Sunderland, pp. 3–27.
- Weeks, A., 2009. Evolution of the pili nut genus (*Canarium* L., Burseraceae) and its cultivated species. *Genet. Resour. Crop Evol.* 56, 765–781.
- Weeks, A., Simpson, B.B., 2004. Molecular genetic evidence for interspecific hybridization among endemic Hispaniolan *Bursera* (Burseraceae). *Am. J. Bot.* 91, 976–984.
- Weeks, A., Daly, D.C., Simpson, B.B., 2005. The phylogenetic history and biogeography of the frankincense and myrrh family (Burseraceae) based on nuclear and chloroplast sequence data. *Mol. Phylogenet. Evol.* 35, 85–101.
- Weeks, A., Simpson, B.B., 2007. Molecular phylogenetic analysis of *Commiphora* (Burseraceae) yields insight on the evolution and historical biogeography of an “impossible” genus. *Mol. Phylogenet. Evol.* 42, 62–79.
- Wiens, J.J., Penkrot, T.A., 2002. Delimiting species using DNA and morphological variation and discordant species limits in spiny lizards (*Sceloporus*). *Syst. Biol.* 51, 69–91.
- Yi, T., Wen, J., Golan-Goldhirsch, A., Palfitt, D.E., 2008. Phylogenetics and reticulate evolution in *Pistacia* (Anacardiaceae). *Am. J. Bot.* 95, 241–251.

Appendix B. Characters of taxonomic importance in 13 of the 15 known members of the *B. simaruba* complex, and in 4 of the 9 closely related Antillean species, as well as an undescribed Cuban species. Data were measurements of herbarium specimens and living individuals in the field. Median values and ranges in parentheses are reported for species included in morphometric analyses; for the other species, only mean values or ranges are reported. All measurements in cm. Information on *B. inaguensis* is from Cuban specimens. NA: not available.

Character	<i>B. arborea</i>	<i>B. attenuata</i>	<i>B. cinerea</i>	<i>B. grandifolia</i>	<i>B. inaguensis</i>	<i>B. instabilis</i>
leaf size (length x width)	19.5 (12.0-30.0) x 14.0 (11.0-18.0)	24.5 (18.0-38.0) x 15.0 (11.0-24.0)	17.5 (3.5-36.0) x 13.0 (3.0-27.0)	23.0 (9.0-50.0) x 14.0 (4.0-26.0)	6.5 x 5.3	9.0 (2.2-25.0) x 6.0 (1.0-16.0)
swollen petiole	absent	absent	absent	usually absent	absent	absent
petiole length	5.5 (3.0-11.0)	8.0 (6.0-13.5)	6.5 (2.0-12.0)	7.5 (2.5-16.0)	0.4-3.1	2.7 (0.5-15.0)
petiole indumentum	pubescent	glabrous	pubescent	pubescent	glabrous	usually glabrous
petiolule length: lateral (LL) and terminal leaflets (TL)	0.4 (0.1-1.2) LL; 1.2 (0.7-2.2) TL	0.3 (0.1-1.2) LL; 1.7 (0.6-3.6) TL	0.4 (0.1-3.0) LL; 1.5 (1.0-7.5) TL	0.2 (0.1-0.6) LL; 1.5 (1.0-6.5) TL	0.2-0.7 LL; 0.1-0.8 TL	0.2 (0.1-1.3) LL; 0.8 (0.2-2.5) TL
leaflet number	(5) 7 (-11)	(3) 5-7 (-11)	(1) 3-5	(3) 5-7 (9)	3-7	1-3 (5)
leaflet apex	acuminate to short caudate	acuminate-caudate	caudate-acuminate	caudate	acute-obtuse, mucronate	acute to short acuminate
leaflet base	cuneate and oblique	cuneate to rounded and oblique	cuneate to subcordate and oblique	cuneate	acute-obtuse	cordate and oblique
leaflet indumentum: upper surface (U), lower surface (L)	U: glabrous to sparse on veins; L: sparse on veins to pubescent	U: glabrous; L: glabrous or two tufts on leaflet base	U, L: densely pubescent	U: glabrous to densely pubescent; L: sparse to densely pubescent	U, L: glabrous	U: glabrous; L: glabrous to sparsely pubescent on leaflet base
leaflet texture	membranaceous	membranaceous	membranaceous	membranaceous	coriaceous	chartaceous
leaflet luster	dull	dull	shiny	dull	dull	shiny
color contrast between upper and lower surface of leaflet	present	absent	absent	absent	absent	present

Robustness of peduncles and pedicels of infructescence	slender	slender	slender to intermediate	slender to robust	slender	slender
Infructescence length	3.0 (1.6-7.0)	6.5 (4.0-14.0)	3.5 (1.4-13.0)	2.5 (1.0-13.0)	6.0	2.3 (0.8-5.0)
Fruit size	0.7 (0.5-1.0)	0.8 (0.6-1.0)	0.8 (0.5-1.0)	0.8 (0.5-1.4)	0.7	0.7 (0.5-1.2)
Fruit apex	obtuse	acute	usually acute	obtuse	acute	acute
Fruit pubescence	usually glabrous	glabrous	usually glabrous	pubescent	glabrous	glabrous

Character	<i>B. krusei</i>	<i>B. laurihuertae</i>	<i>B. longipes</i>	<i>B. ovalifolia</i>	<i>B. permollis</i>	<i>B. roseana</i>
leaf size (length x width)	22.0 (12.0-30.0) x 18.0 (12.0-27.0)	6.0 (2.5-12.0) x 3.0 (1.0-11.5)	19.0 (10.0-30.0) x 9.0 (3.5-18.0)	20.0 (11.5-35.0) x 14.5 (8.0-25.0)	20.0 x 15.0	25.0 (13.0-40.0) x 17.5 (10.0-27.0)
swollen petiole	absent	absent	absent	absent	absent	absent
petiole length	8.5 (4.0-12.5)	1.2 (0.3-4.5)	6.0 (2.0-11.0)	6.5 (3.0-14.0)	4.0-8.0	8.0 (3.0-15.0)
petiole indumentum	pubescent	glabrous	usually glabrous	glabrous to pubescent	glabrous to pubescent	glabrous to pubescent
petiolule length: lateral (LL) and terminal leaflets (TL)	0.4 (0.2-1.5) LL; 2.5 (0.7-5.0) TL	0.1 (0.1-0.3) LL; 0.7 (0.4-1.4) TL	0.9 (0.1-2.5) LL; 1.3 (0.3-3.0) TL	0.8 (0.1-2.5) LL; 2.1 (0.8-5.0) TL	0.3-0.8 LL; 1.0-2.0 TL	0.2 (0.1-1.2) LL; 1.8 (0.5-4.2) TL
leaflet number	(1) 3 (5)	1-3 (5)	(3-) 9-11 (13)	3-5 (-9)	3 (5)	(3) 5-7 (9)
leaflet apex	caudate	truncate, rounded, cuspidate, retuse	acuminate to abruptly acuminate	abruptly acuminate	abruptly acuminate to caudate	abruptly long acuminate
leaflet base	rounded and oblique	cuneate to rounded or truncated	cuneate and oblique	cordate and oblique	cordate	cuneate to truncate
leaflet indumentum: upper surface (U), lower surface (L)	U: pubescent; L: densely pubescent	U, L: glabrous	U, L: glabrous	U: glabrous to sparse on veins; L: glabrous to sparse or pubescent on veins	U: glabrous to densely pubescent; L: sparse to densely pubescent	U: glabrous to sparse on veins; L: glabrous to pubescent on veins

leaflet texture	membranaceous	chartaceous to coriaceous	chartaceous	membranaceous	membranaceous	membranaceous to chartaceous
leaflet luster	dull	shiny	dull	dull	dull	shiny
color contrast between upper and lower surface of leaflet	absent	present	present	absent	absent	absent
Robustness of peduncules and pedicels of infructescence	slender	slender	slender to intermediate	usually slender	slender to intermediate	slender to robust
Infructescence length	4.0 (2.0-11.0)	1.7 (1.0-3.0)	4.0 (0.5-10.0)	5.5 (2.5-13.5)	2.0-4.0	4.5 (2.0-10.0)
Fruit size	0.6 (0.5-0.8)	0.8 (0.6-1.0)	1.0 (0.5-1.3)	0.8 (0.6-1.0)	0.7-0.9	0.9 (0.6-1.1)
Fruit apex	usually acute	acute to very acute	usually obtuse	usually acute	acute to very acute	obtuse to very acute
Fruit pubescence	pubescent	glabrous	glabrous	glabrous	glabrous to pubescent	glabrous

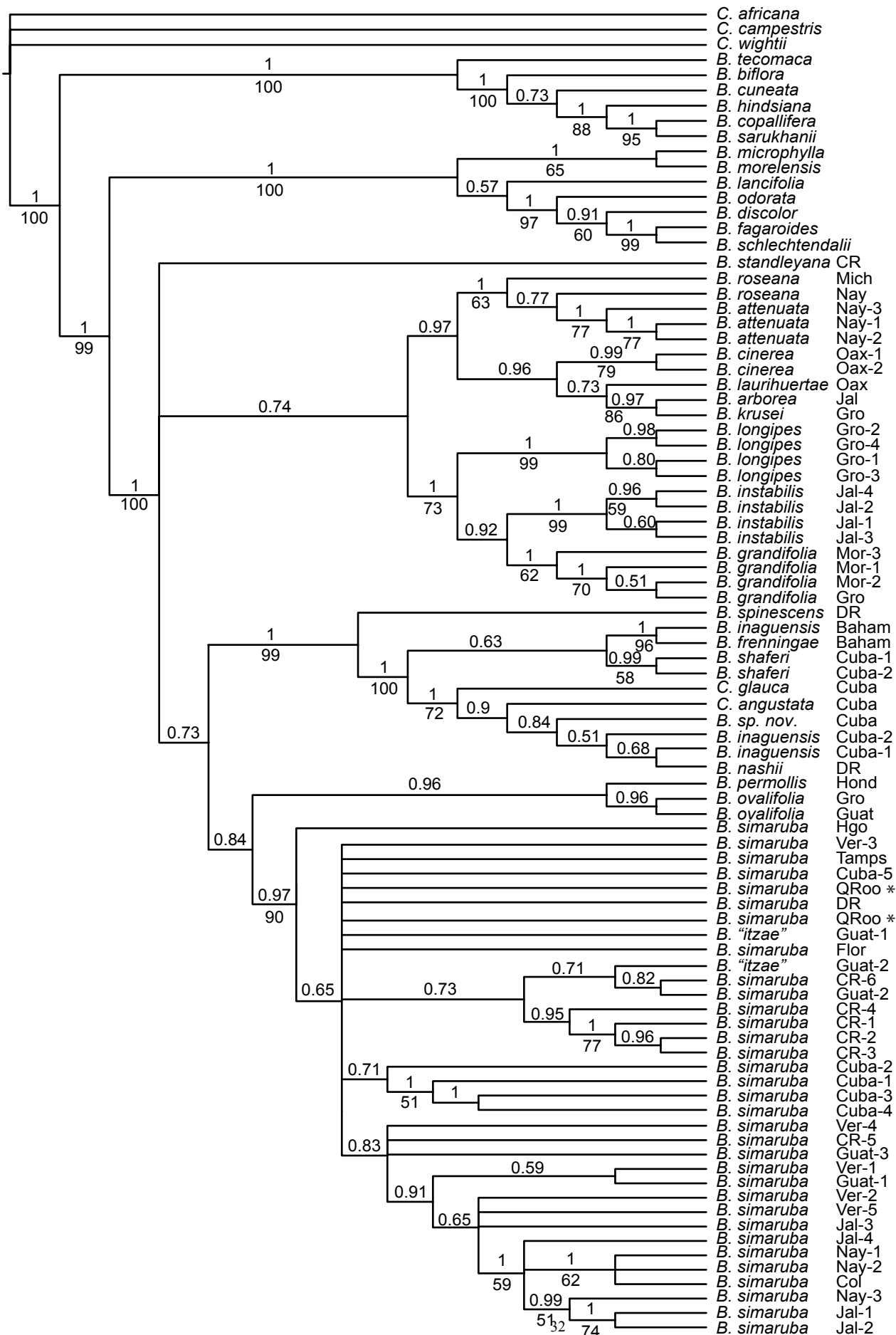
Character	<i>B. shaferi</i>	<i>B. simaruba</i>	<i>B. sp. nov.</i>	<i>B. standleyana</i>	<i>C. angustata</i>	<i>C. glauca</i>
leaf size (length x width)	6.0 x 5.0	23.0 (10.0-45.0) x 13.5 (8.0-25.0)	3.0 x 0.5	38.0 x 26.0	16.0 x 8.0	5.0 x 1.4
swollen petiole	absent	usually present	absent	absent	absent	absent
petiole length	1.3-2.3	6.5 (2.5-14.0)	0.7-0.8	10.0-12.0	1.5-4.7	0.4-1.8
petiole indumentum	glabrous	usually glabrous with pubescent base	glabrous	glabrous	glabrous	glabrous
petiolule length: lateral (LL) and terminal leaflets (TL)	1.0-1.5	0.5 (0.1-1.8) LL; 1.4 (0.2-4.0) TL	0.1-0.3 LL; 0.2 TL	1.6-2.0 LL; 2.5-4.0 TL	0.3-0.8 LL; 0.1-0.3 TL	0.4-0.5 LL; 0.4-0.5 TL
leaflet number	1 (2-3)	(3-) 7-9 (-15)	3-5	5-7	5-9	(1) 2-3 (5)
leaflet apex	acute	acuminate	acute and mucronate	abruptly acuminate to acuminate	acute-obtuse and mucronate	acute-obtuse and mucronate
leaflet base	obtuse	cuneate and oblique	acute	cordate and oblique	acute	acute-obtuse

leaflet indumentum: upper surface (U), lower surface (L)	U, L: glabrous	U: glabrous to sparse on veins; L: glabrous to pubescent	U, L: glabrous	U, L: glabrous	U, L: glabrous	U, L: glabrous
leaflet texture	coriaceous	membranaceous, chartaceous, or coriaceous	very coriaceous	membranaceous	coriaceous	very coriaceous
leaflet luster	upper surface shiny	shiny	shiny	shiny	dull	upper surface shiny
color contrast between upper and lower surface of leaflet	present	absent	absent	absent	present	absent
Robustness of peduncules and pedicels of infructescence	slender	intermediate to robust	slender	slender	slender	slender
Infructescence length	1.0-1.5	5.5 (2.0-22.0)	NA	5.0-9.0	10.0	NA
Fruit size	0.9	1.0 (0.7-1.3)	0.8	0.5-0.7	0.6	0.6
Fruit apex	acute	acute to very acute	acute	very acute	acute	acute
Fruit pubescence	glabrous	usually glabrous	glabrous	glabrous	glabrous	glabrous

Appendix C. Classification using cross-validation of specimens included in the morphometric analysis that included all species and that including *B. simaruba* and satellites only. Species names in columns indicate empirical identification of specimens; species names in rows indicate the predicted identification based on discriminant functions. arbo: *B. arborea*, atte: *B. attenuata*, cine: *B. cinerea*, gran: *B. grandifolia*, inst: *B. instabilis*, krus: *B. krusei*, laur: *B. laurihuertae*, long: *B. longipes*, oval: *B. ovalifolia*, rose: *B. roseana*, sima: *B. simaruba*.

		Empirical identification														
		All species											<i>B. simaruba</i> + satellites			
		arbo	atte	cine	gran	inst	krus	laur	long	oval	rose	sima	atte	oval	rose	sima
Predicted identification	arbo	18	0	0	0	0	0	0	0	0	0	1	-	-	-	-
	atte	0	15	0	0	2	0	0	0	1	1	0	15	1	1	0
	cine	0	0	28	1	0	0	0	0	1	1	0	-	-	-	-
	gran	3	0	1	74	0	0	0	0	0	0	2	-	-	-	-
	inst	0	0	0	0	13	0	1	0	0	0	0	-	-	-	-
	krus	0	0	0	0	0	19	0	0	0	0	0	-	-	-	-
	laur	0	0	0	0	6	0	11	0	0	0	0	-	-	-	-
	long	0	0	0	0	0	0	0	46	0	0	0	-	-	-	-
	oval	0	1	0	0	0	0	0	1	53	5	4	1	55	6	4
	rose	0	1	0	0	0	0	0	0	2	21	7	1	1	18	5
	sima	1	0	0	0	0	0	0	0	3	1	131	0	3	4	136
Total	22	17	29	75	21	19	12	47	60	29	145	17	60	29	145	
% correct	82	88	97	99	62	100	92	98	88	72	90	88	92	62	94	

Figure 7. Phylogeny of the *Bursera simaruba* species complex and its related Antillean species based on four nuclear markers (*PEPC*, *ETS*, *ITS* and *NIAi3*). Bayesian 50% majority-rule consensus cladogram is shown with posterior probabilities above branches, and parsimony bootstrap values >50 below branches. Labels on terminals indicate voucher locality (Appendix A); * : clones of the *B. simaruba* sample with two different versions of *NIAi3*.



CAPÍTULO 2.

DIVERSIFICACIÓN MORFOLÓGICA Y LA RELACIÓN ENTRE TAMAÑO, FORMA Y MECÁNICA EN LOS TALLOS DEL CLADO *SIMARUBA* (*BURSER*A, BURSERACEAE).

ABSTRACT

Adaptive evolution of organismal size and shape necessarily involves tissue mechanical characteristics, yet how the size-shape-mechanics triad changes across environments is little documented. We studied nine species from ten populations of trees in the *Bursera simaruba* clade (Burseraceae) and found that across habitats water availability was positively associated with stem, wood, and bark tissue stiffness (elastic modulus E), likely the result of selection favoring water and starch storage at the expense of support in dry areas. In most species, all with a conventional tree habit, stiffer stems and wood were associated with longer, more slender stems. Deviations from this relationship implied marked habit differences in the form of *B. instabilis*, a tree with lianescent branches, and *B. standleyana*, a rigid-stemmed hemiepiphyte, illustrating the necessary relationship between size, shape, and mechanics in morphological evolution. E_{wood} and E_{bark} covaried positively across environments; ontogenetic modulation of the mechanical contribution of bark occurred through variation in bark quantity, whereas wood varied ontogenetically both in amount and E . In plants in general, some parts of the stem length-diameter-mechanics morphospace are occupied whereas empty regions, e.g. very short and wide stems with high density wood, are likely ontogenetically possible but not favored by selection.

Key words: adaptation, allometry, convergence, morphological evolution, morphospace, ontogeny

INTRODUCTION

The vast array of organismal shape and size is inextricably linked to tissue mechanical properties (Niklas 1992, 1994; Vogel 2003). Ontogenetic or interspecific differences in shape, size, or mechanics will necessarily give rise to differences in the emergent functional behavior of the structure involved (Rowe & Speck 2005; Swartz & Middleton 2008). For example, although larger birds have larger flight feathers, their feathers are made up of material that is less rigid for their body size than those of smaller birds (Worcester 1996). Relatively more flexible feathers may be favored in larger birds as a sort of aerial shock absorber, a marked functional difference associated with small modulations in the relationship between tissue mechanical properties and organ size and shape. Despite the

importance of understanding the interplay between size, proportions, and biomechanics in the adaptive diversification of organisms, few studies show how this relationship varies continuously across environments (Day & Jayne 2007; Habib 2010). This is a crucial consideration, because identifying predictable relationships between environmental selective factors and the mechanical behavior of biological structures would provide a keystone for inferences of adaptive associations between mechanics, size, and shape.

With their simple structure and near ubiquity, tree stems provide a convenient study system for testing hypotheses concerning the ways that organismal proportions should vary with mechanics across selective regimes (Niklas 1992; Sterck et al. 2006). Here we test the expectation that more rigid stem materials should be associated with longer branches for a given diameter, an expectation that can be explained in terms of the modulus of elasticity E and the second moment of area I . The modulus of elasticity describes how resistant a given material is to bending, and refers to a material in the abstract, so hard-to-bend "steel" has high E whereas bendable "rubber" has low E (Gere 2002). The second moment of area I describes the size and shape of a beam in cross section in terms of how well placed its material is to resist bending (Pisarenko et al. 1979). The product of E and I expresses the resistance to bending of a particular beam and is known as flexural stiffness.

How much a beam attached at one end bends (its deflection δ) can be approximated as $qL^4/8EI$, where q is a weight distributed along the beam, such as the weight of the beam itself, and L is its length (Gere 2002). Thinking of tree branches as beams, this equation illustrates how evolutionary changes in E should affect stem proportions. In self-supporting trees, natural selection should favor branches that maintain their position in the canopy without excessive support costs (Niklas 1993). Assuming for the moment that this means that δ will remain constant between species, then two trees that differ only in E will necessarily have different branch proportions: either stems must become thicker, increasing their I , or decrease in length. Without these changes in organ proportionality, δ will increase, meaning floppier branches that may not maintain their position in the canopy. In this paper we explore the relationship between tissue mechanics and organ size and proportionalities by testing the prediction of a positive relationship of the moduli of elasticity of stem tissues with stem length for a given diameter.

We place the mechanics-proportionality relationship in an adaptive context by tracking how mechanical properties change across environments. Botanists postulate an adaptive tradeoff among the conductive, support, and storage functions of tree stems (Chave et al. 2010; Zanne & Falster 2010). In the tropical wet to dry forest continuum we study here, trees are conspicuously tall in wet forest while short, water storing plants are abundant in dry forest (Medina 1995; Borchert & Pockman 2005; see also Moles et al. 2009). Because water storage requires more cell lumen and less of the cell wall material that stiffens stems (Chapotin et al. 2006), selection favoring greater mechanical support at the expense of storage in moist areas and greater storage at the expense of support in drier areas would lead to a positive relationship between tissue and stem elastic moduli and water availability. It is this presumably adaptive mechanical variation across environments that should in turn be reflected in differing proportions between stem length and diameter.

To examine the relationship between mechanics, environment, and stem proportionalities, we focus on the members of the *simaruba* clade in the genus *Bursera* (Burseraceae; Rosell et al. in press), a group of remarkable diversity in size, habit and habitats (Fig. 1). The namesake species *B. simaruba* is an unmistakable element in virtually all lowland forests from Mexico to northern South America and the Caribbean, including southern Florida, and varies from 30 m rainforest emergents to medium sized trees of subdeciduous woods (Fig. 1A). The other 13 species in the clade range from *B. simaruba*-like subdeciduous forest trees (*B. attenuata* and *B. roseana*; Fig. 1B) to small statured trees averaging a scant 5 m tall in tropical deciduous forests (*B. arborea*, *B. grandifolia*, *B. longipes*; Fig. 1C). While the preceding species are more or less orthodox trees, two species in the clade are conspicuously eccentric. Mexican dry forest endemic *Bursera instabilis* is unusual in that its stems are self-supporting when the tree is young but as individuals attain the canopy, the branches lose the capacity to support themselves and come to rest on adjacent trees or even other branches of its own crown (Fig. 1D). In contrast, Costa Rican endemic *B. standleyana* is a hemiepiphyte that grows high in rainforest trees (Fig. 1E). Its roots, often over 20 m long, are lianescent and snake down to the forest floor, drawing water to a crown of splayed arching branches. Testing for environment-mechanics-allometry associations in the descendants of a single common ancestor is a useful approach because the species in a clade derive from the same starting

point (Day & Jayne 2007). This means that differences between species cannot be ascribed to lineage-specific differences, as might be the case if we studied distantly related plants, and it becomes much more likely that the associations observed represent adaptive responses to environmental differences. To our knowledge this is the first study to survey stem biomechanical evolution in the members of a clade across habitats (see Sterck et al. 2006; Jacobsen 2007; Chave et al. 2009).

The extraordinary morphological range of the *simaruba* clade also allows us to examine the functional integration of wood and bark and the role of ontogenetic differences in the evolution of habit diversity. Because morphological and functional diversity in woody plant stems emerges from the ways that wood and bark interact in their mechanical properties and in their proportions, it is essential to understand how wood and bark covary across species and throughout the continual ontogeny of individual stems within species (Niklas 1999a; Olson & Rosell 2006; Onoda et al. 2010). The high I of the bark places it in an ideal position to contribute to stem mechanical support (Niklas 1992, 1999b), but as in many plants, bark in *Bursera* appears to be mostly water storing tissue with low E that would not contribute substantially to support of the stem (Gómez-Vázquez & Engleman 1984). As a result, the exact role of bark in stem mechanical support is not obvious, but it clearly cannot be ignored if we hope to understand the functional diversification of the woody plants. We therefore examine the ways that whole branch behavior varies across habitats as the outcome of variation in the interaction between wood and bark. We then turn to the ways in which tissue level mechanical parameters interact to produce the behavior of intact stems from the branch tips to the older, more basal portions and relate these ontogenetic patterns with those observed across species to show that changes in the relationship between size, proportions, and mechanics can lead to the evolution of dramatic differences in habit between species (see Marroig & Cheverud 2005).

In sum, we examine the descendants of a common ancestor across an array of habitats for a demanding test of predictions regarding the adaptive associations of stem biomechanics with environment and between mechanics and stem proportionalities. We address our results in the context of the inference of adaptation through the study of convergent evolution and the web of evolutionary tradeoffs in which stem biomechanics is

likely embedded, and discuss how modulation in the size-shape-mechanics relationship is involved in the generation of morphological diversity across species.

MATERIALS AND METHODS

Sampling

We collected samples from one locality each of nine species of the *B. simaruba* clade in Mexico and Costa Rica (Appendix 1). In addition to a Mexican *B. simaruba* population, we also included one from a Costa Rican semideciduous forest to shed light on the extent to which between species mechanics-environment associations coincide with within-species plasticity. We treat these samples as separate species throughout the analyses. Due to the destructive nature of the measurements, instead of main trunks we sampled 6-13 branches from 2-4 trees per species.

Phylogeny reconstruction

We reconstructed phylogenetic relationships based on nucleotide sequences of one individual of each of the ten sampled populations. These sequences came from a phylogenetic reconstruction of the *simaruba* clade as a whole (Rosell et al. in press; Appendix 1) and include one chloroplast intergenic spacer (*psbA-trnH*, Sang et al. 1997), two low copy nuclear markers (*PEPC*, Olson 2002 and *NIAi3*, Howarth & Baum 2002), and two multiple copy nuclear loci (*ITS*, Fine et al. 2005 and *ETS*, Baldwin & Markos 1998; Weeks & Simpson 2004). Outgroup sampling included species of the two subgenera of *Bursera* and species of *Commiphora*, its sister genus (Becerra 2003). The matrix was aligned by eye using Se-AL v.2.0a11 Carbon (Rambaut 2002).

We performed a Bayesian analysis of the combined dataset with gaps treated as missing information. We partitioned the dataset by marker and determined the model of evolution that best fit each using jModelTest v. 0.1.1 (Guindon & Gascuel 2003; Posada 2008). We ran four Markov chains simultaneously for 10 million generations using MrBayes v.3.1.2 (Huelsenbeck & Ronquist 2001) on the CIPRES portal v.2.2 (Miller et al. 2009), starting with a random tree, setting the heating parameter to 0.1 to improve the probability of exchange between chains, and sampling every 200 generations. Average split deviations <0.0004, the plot of likelihood score vs. MCMC generation, and AWTY

diagnostics (Nylander et al. 2008) suggested that stationarity and convergence were reached. The initial 25% of the trees was excluded before calculating Bayesian posterior probabilities (PP). We also ran non-parametric bootstrap tests with 1000 replicates in PAUP* v.4.0 beta v.10 (Swofford 2002), holding 50 trees.

Branch allometry and maximum tree height

We measured the basal diameter (D) and total length (L) of branches tested mechanically. To estimate the scaling exponent (α) of the Huxley allometric equation $L=\gamma D^\alpha$ for each species (Niklas 1994), we \log_{10} -transformed the data and applied reduced major axis regression (RMA, Warton et al. 2006). The scaling exponent α , the intercept β ($=\log_{10} \gamma$), and their confidence intervals were calculated with the package *smatr* v.2.1 (Warton & Ormerod 2007). For *B. instabilis* we measured additional branches to document the wide variation in L:D of its lianescent branches. We measured the height of individuals sampled for branches using rappelling gear, a clipper pole, and a tape measure.

Environmental variables and indices

We extracted 19 environmental variables from WorldClim v.1.4 (Hijmans et al. 2005; Appendix 2) for all sampled populations. Many environmental variables were markedly associated with one another. To summarize the information contained in these variables, we selected those that were strongly correlated ($|R|\geq 0.7$) with E_{struct} , E_{wood} , E_{bark} , α , and tree height, and constructed indices for precipitation and temperature evenness using principal component analyses with prior standardization of the dataset. Mean temperature variables were not correlated with biological ones, so we did not construct a mean temperature index. We take not only the precipitation index as reflecting water availability but also the evenness index because higher daily or annual temperature swings are likely associated with greater evapotranspirational demands and therefore lower water availability, whereas continuous moderate temperatures are more likely to be associated with less fluctuation in water availability.

Biomechanical tests

We collected straight branches with few side branches and divided them into 2-8 segments. We measured the distance from the midpoint of each segment to the tip of the branch (hereafter "distance from the tip") and performed three-point bending tests using a digital micrometer to measure the deflection of the segment caused by adding weights to a bucket suspended at its midpoint. Segments had 1:20 diameter:length ratios to minimize the influence of shear (Vincent 1992). The flexural stiffness of the whole structure (EI_{struct}), and of the wood (EI_{wood}) were measured from intact and debarked segments respectively. Bark flexural stiffness (EI_{bark}) was inferred from the difference between EI_{struct} and EI_{wood} (Niklas 1999b; Rosell & Olson 2007). We computed second moments of area for the whole structure (I_{struct}), the wood (I_{wood}), and the bark (I_{bark}) with formulas for solid and hollow circles and ellipses (Pisarenko et al. 1979), averaging apical and basal segment diameters. Computation of elastic moduli (E_{struct} , E_{wood} , E_{bark}) was straightforward after measuring EI and I . Being minimal in *Bursera*, we ignored the pith in computations. Whereas E_{wood} and E_{bark} reflect the distinct mechanical properties of these anatomical zones, E_{struct} reflects an imaginary material, as though the entire stem made up of wood and bark were a uniform tissue.

Ontogenetic change in biomechanical variables

To establish a basis for comparison between species, it was first necessary to determine how mechanics varied with stem size (see Rosell & Olson 2007). Preliminary statistical analyses showed that E_{struct} , E_{wood} , and to a lesser degree E_{bark} , correlated with distance from the tip reaching values of $R=0.55$ ($p<0.05$) for E_{wood} in *B. attenuata* and $R=0.62$ ($p<0.05$) for E_{struct} in *B. simaruba* MX. To take this covariation into account and to rectify the imbalance in sample size between old and young portions of branches, and also between species, we classified branch segments into eight groups according to distance from the tip: 0-30, 30-60, 60-90, 90-120, 120-150, 150-180, 180-210, >210 in cm. For each category, we calculated species means for each mechanical trait, which resulted in 73 data. The oldest 3 or 4 categories were not collected for *B. grandifolia* or *B. longipes* because the stems of these species were so wide for their length that they exceeded the capacity of our mechanical testing arrangement.

To model ontogenetic change in mechanical parameters, we fit three linear models predicting average values of E_{struct} , E_{wood} , and E_{bark} based on branch segment category, which reflected the distance from the tip, species (represented by nine dummy variables), and the interaction between these two variables, allowing us to test for differences in mechanical parameters between species. Preliminary models indicated that dependent variables and distance from the tip had to be \log_{10} transformed to achieve homoscedasticity and/or to linearize the relationship between variables. All models had significant interaction terms ($p < 0.05$). The preliminary models showed that species could be grouped into two or three categories of statistically indistinguishable species. To make subsequent models more parsimonious, we used these groups rather than species. Species grouping for $\log_{10}E_{struct}$ was as follows dry: *B. cinerea*, *B. grandifolia*, *B. instabilis*, and *B. longipes*; intermediate: *B. arborea*, *B. attenuata*, and *B. roseana*; moist: *B. simaruba* MX, *B. simaruba* CR, and *B. standleyana*. For $\log_{10}E_{wood}$ dry: *B. grandifolia*, *B. instabilis*, and *B. longipes*; intermediate: *B. arborea*, *B. attenuata*, *B. cinerea*, *B. roseana*, *B. simaruba* CR; moist: *B. simaruba* MX and *B. standleyana*. For $\log_{10}E_{bark}$ dry: *B. cinerea* and *B. grandifolia*; other: remaining species. “Intermediate” or “other” acted as the reference category. After grouping species, only the model for $\log_{10}E_{wood}$ still had a significant interaction term ($p < 0.001$). Thus, we compared $\log_{10}E_{wood}$ between species groups only along the range of \log_{10} distance from the tip where regression lines did not intersect. Comparison between species groups in models lacking the interaction term was straightforward through intercept values. Unless specified, all statistical analyses were performed in R v.2.9.2 (R Development Core Team 2009).

Correlations between size, allometry, biomechanics, and environment

We estimated correlations between mechanical variables, α , maximum tree height, and the precipitation and evenness indices. Given that mechanical properties varied along branches, we used the mean value of E_{struct} , E_{wood} , and E_{bark} of the fifth category of distance from the tip (120-150cm), which was the oldest category available for all species, except *B. longipes*. For this species, we extrapolated E_{struct} , E_{wood} , and E_{bark} means based on the preliminary linear models that included species as an independent variable (instead of species groups) and no interaction term (models not shown). Correlations involving height did not include *B. standleyana*, because its hemiepiphytic habit made the height variable

not comparable with terrestrial species. Also, correlations including α were based on “conventional trees,” i.e. they excluded *B. standleyana* and *B. instabilis*.

To assess the presence of phylogenetic signal in the measured traits, which would require correcting for phylogenetic non-independence in our data, we performed a randomization procedure based on phylogenetically independent contrasts (Felsenstein 1985). We tested whether similarity between closely related species was higher than expected by chance, given the assumption that morphological trait evolution is proportional to phylogenetic branch lengths (Blomberg et al. 2003). In addition, to compare the degree of phylogenetic signal between traits, we calculated the descriptive statistic K , which when <1 indicates that a trait is less similar than expected between related species given a Brownian motion model of evolution (Blomberg et al. 2003). We performed these analyses in the R package *picante* v. 0.7-2 (Kembel et al. 2009) with the branch lengths obtained from Bayesian analysis (Fig. 2) and also with branches of unit length; the rationale for using two sets of branch lengths is described below.

When variables exhibited phylogenetic signal, we reestimated correlations using phylogenetically independent contrasts (PICs, Felsenstein 1985) as implemented in the PDAP module (Midford et al. 2005) of Mesquite v.2.71 (Maddison & Maddison 2009). We treated the polytomy of the *B. simaruba* clade phylogeny as soft and reduced degrees of freedom accordingly (Purvis & Garland 1993; Garland & Díaz-Uriarte 1999). No variables required transformation to standardize contrasts (Garland et al. 1992).

The calculation of PICs can be adjusted to reflect differing assumptions regarding the relationship between micro- and macro-evolution. Its basic implementation uses the raw branch lengths resulting from phylogenetic analysis, or a transformation that maintains proportionality between branch lengths, to standardize contrasts (Felsenstein 1985; Garland et al. 1992). This assumes that evolution proceeds via the anagenetic mode, in which evolutionary change accrues within lineages between speciation events (Jablonski 2007). The alternative is the cladogenetic mode, in which change accumulates only at speciation events. This mode is reflected in PIC calculation by setting all phylogenetic branch lengths equal, a procedure that additionally assumes that there has been no extinction in the clade (Martins & Garland 1991). Although different evolutionary modes can be reflected by different sets of branch lengths, we see no way of knowing which should be included

because it is impossible to determine which evolutionary mode was operative in the evolution of any group or how many extinct species it includes. To span these extremes of evolutionary mode, we calculated PICs using both raw and unity branch lengths.

RESULTS

Phylogeny reconstruction

The aligned matrix of the five markers had a length of 2788 bp and is available from TreeBASE (<http://purl.org/phylo/treebase/phylows/study/TB2:S10870?x-access-code=64ef9b2e143ded0e4f38927eab86e31&format=html>). The evolutionary models that best fit each marker according to the Akaike Information Criterion were TVM+G for *psbA-trnH*, HKY+I for *PEPC*, TPM2uf+G for *ETS*, GTR+G for *ITS*, and TPM3uf+G for *NIAi3*. The 50% majority-rule consensus tree from the Bayesian analysis, with posterior probabilities, bootstrap values, and branch lengths, is shown in Fig. 2. The topology was completely congruent with that recovered by Rosell et al. (in press). Support was maximal or very high for most nodes, except for that of the sisterhood of *B. standleyana* and *B. simaruba* (Fig. 2).

Branch allometry and maximum tree height

Fits for allometric models ranged from $R^2=0.63$ to $R^2=0.98$ (Table 1, Fig. 3A), except for *B. instabilis*, for which the fit was very poor ($R^2=0.23$, Fig. 3B), revealing the high variation in branch length-diameter allometry in this species. Maximum tree height per species is shown in Table 1.

Environmental variables and indices

Environmental variables reflected the habitat diversity of the *simaruba* clade species, with annual precipitation levels ranging from 680 mm at the locality of *B. cinerea*, to more than 3600 mm at that of *B. simaruba* MX. Differences in temperature evenness were also marked, e.g. with annual temperature ranges of 25 °C at the site of *B. grandifolia*, and only 14°C at that of *B. standleyana*.

Of the 19 environmental variables (Appendix 2), Table 2 includes the four precipitation variables and the three of temperature evenness that were strongly correlated

with E_{wood} , E_{struct} , and to a lesser degree with E_{bark} , α , and maximum tree height. We constructed the precipitation and evenness indices based on these variables (Table 2). We \log_{10} transformed precipitation variables to linearize their relationship with mechanical variables before performing the principal component analysis. The first principal components of precipitation and evenness explained 95% and 90% of the variability, respectively. Variables had similar loading magnitudes within each index (Table 2).

Ontogenetic change in mechanical variables and biomechanical differences between species

We tested a total of 538 segments mechanically. Segments per species ranged from 22 for *B. grandifolia* to 65 for *B. instabilis*. Standard errors within categories ranged from 0.034 to 0.469 for E_{struct} , 0.104 to 0.869 for E_{wood} , and 0.009 to 0.491 for E_{bark} .

Linear models for $\log_{10}E_{struct}$ and $\log_{10}E_{wood}$ fit the data well, explaining more than 74% of the variability in these traits (Table 3). For both models, \log_{10} distance from the tip was a highly significant variable, indicating that structural and wood stiffness increases as a given segment grows. According to the $\log_{10}E_{struct}$ model, species of drier habitats have significantly lower mean values for this trait than species of intermediate or moist sites (Table 3). For a distance from the tip of 195 cm, E_{struct} for species of dry habitats would be 1.06 GN/m², whereas that of species of intermediate and moist environments would be 1.53 and 2.38 GN/m², respectively (Table 3 and Fig. 4A).

The model predicting $\log_{10}E_{wood}$ had a significant interaction term between species group and \log_{10} distance from the tip (Table 3), but regression lines intersected only at the youngest portion of the branch, so inferences between groups of species were valid along almost the entire examined range of distance from the tip (Fig. 4B). Just as for $\log_{10}E_{struct}$, the model for $\log_{10}E_{wood}$ indicated differences between species groups, with species of dry environments having lower values of E_{wood} than those of intermediate and moist ones (Fig. 4B). Again, at a distance from the tip of 195 cm, species of moist environments would have a mean E_{wood} of 4.67 GN/m², whereas those of intermediate and dry environments would have 3.41 and 1.63 GN/m², respectively (Table 3). Dry site species did not show the marked increase in E_{wood} toward the base that was seen in the other species (Fig. 4B).

Finally, although significant, the model for $\log_{10}E_{bark}$ had a poor fit ($R^2_{adj}=0.38$), revealing that this parameter was poorly predicted by distance from the tip and species group (Table 3, Fig. 4C). The fitting process highlighted the dryland *B. cinerea* and *B. grandifolia* as having lower values than the rest of the species (Table 3).

Correlations between mechanics, environment, size, and allometry

Phylogenetic signal was strong in E_{struct} and E_{wood} , and even stronger in the precipitation index as judging by the K index, both with raw and unity branch lengths (Table 4), indicating that most correlations needed to be corrected for phylogenetic non-independence.

All biomechanical variables were strongly correlated with environmental indices, using the raw data and PICs (Table 5, Fig. 5). Correlation was always positive, meaning that resistance to bending of whole branches, wood, and bark increased with water availability. Maximum tree height was predicted well by the precipitation index with raw data but not by contrasts (Fig. 5E). Excluding *B. instabilis* and *B. standleyana*, α was positively correlated with E_{struct} , E_{wood} , and the evenness index with both raw data and contrasts, implying that longer branches for a given diameter are found in more mechanically resistant species in more even climates (Fig. 5F).

DISCUSSION

Adaptation and the size-shape-mechanics relationship

Our results bear out the expectation that an adaptive tradeoff between support and storage should result in water-storing trees with flexible stems in drier areas and stiffer ones in moist areas across the members of the *simaruba* clade. Higher precipitation and more even temperatures were positively related to the elastic moduli E_{struct} , E_{wood} , and E_{bark} , and these relationships were robust to conversion of the data to independent contrasts (Table 5, Fig. 5A-D). We take this predictable environment-mechanics relationship to reflect convergent evolution, similar adaptive responses in similar selective contexts. Interspecific associations between variables are a form of documenting convergence because they imply that given an environmental variable of value X, an organism will present Y phenotypic value regardless of its phylogenetic affinity (Bell 1989; Larson & Losos 1996). Such associations involve

several and not just one species, placing them among the most robust signatures of adaptation available because as more and more species show the convergent pattern it becomes very difficult to postulate plausible alternative causal explanations.

Following similar convergence-based reasoning, the interplay between mechanics and allometry was also congruent with adaptive predictions, with the stem length-diameter scaling constant α strongly predicting E_{struct} and E_{wood} based on both raw data and contrasts across most species (Table 5, Fig. 5F). These "conventional" trees, with stems that support their own weight borne on self-supporting trunks, describe a line in Fig. 5F, showing that species with higher E_{wood} had branches that were longer for their diameters than species with more flexible wood. This line presumably results from a reciprocal adaptive relationship between stem mechanical properties and allometry. For a given E_{struct} , selection will likely eliminate variants that cannot support their branches or that overinvest in support to the detriment of reproduction (see Niklas & Spatz 1999). Similarly, selection favoring larger or more slender trees is also likely to result in an increase in E_{struct} .

Displacement in the α - E_{wood} relationship away from the "conventional" line in Fig. 5F must produce a continuum of habits, as illustrated by *B. instabilis* with its lianescent branches and the hemiepiphyte *B. standleyana*. The "conventional" axis likely reflects constructions in which surface areas are maximized and transport distances minimized (West et al. 1997; Enquist 2003), almost certainly the reason that, despite so many morphologies being imaginable, the overwhelming majority of trees have compact crowns and do not, for example, have lianescent branches (Price et al. 2007). In most trees, the transport distances and costs associated with very long branches likely outweigh any advantage obtained in the lowered construction costs that "parasitizing" other trees for support might provide (Stevens 1987). Only in trees with large amounts of storage and consequent low costs of tissue construction, with low amounts of cell wall per unit volume, does it seem likely that selection minimizing transport distances could be overcome, permitting the evolution of lianescent branches could lianescent branches evolve. We therefore expect that trees with lianescent branches should, like *B. instabilis*, have low density wood and only be found in the frost free areas that are associated with trees with substantial xylem water storage. Bearing out this expectation may be an arborescent

tropical Chinese *Bauhinia* with lianescent branches (Rowe & Speck 2005) and the liana-tree of Zimbabwe *Adenia karibaensis* (Hearn 2006, 2009).

In contrast to *B. instabilis*, diameter predicted length well in the rigid stems of *B. standleyana* (Table 1). However, these branches were "too stubby" for their wood stiffness as compared to the conventional trees (Fig. 5F). A conventional tree with equivalent wood stiffness would be close to the height of *B. simaruba* MX. Although we did find a relationship between stature and E_{struct} (cf. van Gelder et al. 2006) based on raw data, and greater water availability in general does seem associated with taller trees (Fig. 5E; Moles et al. 2009), selection for greater stature is not the only factor that could lead to an increase in E of stem tissues. For example, it appears likely that, at least in some plants, the negative pressures in vessel interiors generate stresses that are transmitted to the non-conductive cells surrounding the vessels. In this way, selection favoring greater capacity of vessels to resist deformation or cavitation would involve cells that do not conduct water themselves (Hacke & Sperry 2001; Jacobsen et al. 2007; Alm eras 2008). This phenomenon could explain the E_{wood} of *B. standleyana*, which was higher than expected given its stem length-diameter relationship (Fig. 5F). This species draws water through extremely long roots to the rainforest canopy (Fig. 1E), making its transpiration stream from soil to leaf much longer than any other *simaruba* clade member of comparable trunk diameter. To move water such large distances, vessels in the stems of *B. standleyana* are likely subject to more highly negative xylem pressure. Selection favoring high cavitation resistance in this species would lead to thicker cell walls, higher density wood, and the relatively high E_{wood} observed.

Selection resulting in different degrees of cavitation resistance may also explain contrasting patterns between the *simaruba* clade and a recent study of Australian woody plants. In one of the few studies to examine variation in stem biomechanics with environment in multiple species, Onoda et al. (2010) recovered an association between E_{wood} and water availability opposite to the one we observed. In the sclerophyllous evergreen species they examined, higher wood density and thus higher E_{wood} is probably favored in cavitation resistance, important in plants bearing leaves even through extended drought (Maherali et al. 2004; Pratt et al. 2007). In contrast, deciduous tropical trees often lead a "dual lifestyle," in which wide vessels sustain efficient conduction and high

photosynthetic rates during the rainy season, and stem water storage permits persistence leafless through the dry season (Carlquist & Hanson 1991; Olson & Carlquist 2001). As a result, in clades of deciduous tropical trees such as *Bursera*, selection favoring stem water storage in drier areas would lead to stem tissues of lower density of cell wall per unit volume. Wood with lower density has lower E than higher density woods (Niklas 1992; Swenson & Enquist 2008), and a positive relationship between stem E and water availability will result.

The patterns of trait covariation that manifest themselves in between-species comparisons also may operate within species (Rosner et al. 2008). Although our population sampling is represented only by two different localities for *B. simaruba*, one in a Mexican rainforest and the other in a Costa Rican subdeciduous forest, our results are congruent with this notion. E_{struct} and E_{wood} values of both samples of *B. simaruba* were predicted by precipitation (Fig. 5A, C), and stem length-diameter proportions were also strikingly predicted in both samples based on E_{wood} (Fig. 5F). Clearly more sampling is required but it may be that many axes of interspecific diversification in the woody plants are the result of within-species functional associations and tradeoffs (see Schluter 1996; Marroig & Cheverud 2005; Choat et al. 2007).

Ontogenetic vs. interspecific variation in functional coordination between wood and bark

It is increasingly clear that organismal structures cannot be studied in isolation and that "atomizing" organisms into often arbitrarily defined "parts" for adaptive study overlooks the resource allocation tradeoffs and functional integration that are certainly a central part of the selective process (Lewontin 2000). Wood is often studied in isolation as though it interacted directly with the environment rather than forming part of structures of specific size and shape and which are encased in and functionally interact with the bark (Niklas 1999b; Olson & Rosell 2006). This functional integration is reflected in the *simaruba* clade, where E_{wood} and E_{bark} covaried positively across species (Table 5). Some groups, such as Malvales or Caricaceae, are notorious for long fibers in the bark that certainly assist in resisting bending. On the other hand, many plants, the *simaruba* clade included, have mostly parenchymatous bark that presumably deforms easily (Gómez-Vázquez & Engleman 1984) and thus would seem a poor candidate for contributing much to the

capacity of stems to resist bending. However, the bark is placed at the stem periphery where compression and tension loads are maximal and is thus optimally located, whatever its mechanical characteristics, to withstand bending. In other words, bark does have relatively high I , and in the *simaruba* clade natural selection appears not to have been indifferent to this fact.

The result is that, although E_{bark} is always markedly lower than E_{wood} (Appendix 3), species with stiffer wood have stiffer bark (Table 5), implying that the bark may contribute to mechanical support and that selection could favor bark of higher E in trees with greater mechanical needs. Part of this pattern may be due to selection favoring optimally-placed, low-cost bark as a significant contributor to the mechanical support of young twigs (Niklas 1999b). Whereas the contribution of bark to overall branch mechanical behavior EI is small at the basal portion of branches, its contribution to EI in twigs can be as much as 40% (Fig. 4D). The larger species that live in areas with longer rainy seasons have greater amounts of absolute extension growth each year, and as a consequence produce a greater mass of leaves and fruits that place significant loads on the branches (unpublished observations). Because E_{bark} showed no ontogenetic changes within species, with older stem segments having bark with similar tissue mechanical properties as young segments (Table 3), any variation in the contribution of bark to stem mechanics must be via I (see also Niklas 199b; Rosell & Olson 2007). These patterns exemplify that the evolution of morphological diversity necessarily involves ontogenetic differences in the size-shape-mechanics triad, and highlight that mechanical properties are related to organ size and proportions in complex ways that cannot be predicted based on morphology alone.

Ontogenetic potential, constraint, and morphological diversity

The relationship between ontogenetic potential and interspecific diversity can be generalized to a three dimensional space defined by stem diameter, length, and E_{struct} (Fig. 6). The bulk of plants will be found on a main axis along which stem diameter and length scale predictably with each other and with E_{struct} . If stems lengthen markedly for their diameter, with no change in E , a liana will result as stem deflections become increasingly large (Fig. 6; Niklas 1992; Niklas et al. 2003; Lahaye et al. 2005; Ménard et al. 2009). At another extreme, succulents are plants with short, squat stems with tissues of low E . In turn,

plants with small, self-supporting stems with very high E are found in desert shrubs, which have very dense xylem likely the result of selection favoring cavitation resistance (Hacke & Sperry 2001).

Just as important as the areas of the length-diameter-mechanics morphospace that are filled are the areas that are not. If these areas are inaccessible ontogenetically then they may be considered as resulting from some sort of developmental constraint. However, there would seem to be no reason that many of these morphologies could not be produced by plant meristems; they simply seem to be clearly maladaptive. For example, a very tall tree with very low E_{struct} could certainly be produced, but in the earth's gravity it would buckle. This is not a "constraint" in the sense of an area of morphospace that is inaccessible as the result of internal factors that are arbitrary with regard to function (Alberch 1989). Instead, it seems a clear example of natural selection eliminating morphologies that do not meet their mechanical needs (see Shanahan 2008). By the same token, plants with very wide, short stems and very high E_{struct} seem ontogenetically possible, with stumpy *Welwitschia* of the Namib Desert a possible step in this direction (Carlquist & Gowans 1995), but they are far from common.

More detailed studies of the ontogenetic potentials of the *simaruba* clade could test the notion that the empty spaces in Fig. 5F are truly inaccessible (in the manner of Beldade et al. 2002), and studies of relative fitness of the observed morphologies in different environments would also shed light on their potential adaptiveness (Larson & Losos 1996). For the moment, however, there is every indication that the pattern observed is an adaptive one, with greater mechanical support favored in moister environments and greater storage in drier ones. From this point of view, stem proportions are, in turn, the result of selection favoring stems of appropriate length and girth given the elastic moduli of stem tissues.

CONCLUSION

Size, shape, and tissue mechanical properties such as E necessarily interact to produce the mechanical behavior of all organismal structures, and the ways that the size and proportions of biological structures interact with the mechanical properties of their materials lead to the vast diversity in morphology and function observed across living things (e.g. Swartz & Middleton 2008). In the *simaruba* clade, stem mechanical properties and allometry interact

intimately in associations that seem likely adaptive. The "conventional" trees of the clade show that the evolution of similar habits of different sizes involves significant mechanical differences. From baking dry to very wet tropical forest, these species vary in predictable ways, with low-statured trees with fat, flexible stems in dry forests to tall trees with stiff, slender stems in moister ones. Deviation in this relationship has led to striking habit differentiation, such as the very long, lianescent stems and low E_{wood} of *B. instabilis*, illustrating how dramatic differences in organismal form emerge from subtle modulation of the size-proportions-mechanics relationship.

ACKNOWLEDGMENTS

This project was supported by grants from CONACYT (46475) and PAPIIT/DGAPA (IN228207). JAR acknowledges the support of CONACYT through a graduate scholarship, and the Programa de Posgrado en Ciencias Biológicas, UNAM. We thank Guillermo Ángeles, César Domínguez, Luis Eguiarte, Karl Niklas, and Horacio Paz for their comments on the manuscript and for thoughtful discussions; Rosalinda Medina for help in identifying species; Jorge López González for advice on mechanics of materials; Francisco Morales, Brad Boyle and OTS for their help during fieldwork in Costa Rica; Rosamond Coates, Martin Ricker, Jorge Vega, Ricardo Ayala, Katherine Renton, and Enrique Ramírez for their kind support; Martha García and Calixto León Gómez for their help with measurements.

LITERATURE CITED

- Alberch, P. 1989. The logic of monsters: evidence for internal constraint in development and evolution. *Geobios (mémoire spécial)* 12: 21-57.
- Alméras, T. 2008. Mechanical analysis of the strains generated by water tension in plant stems. Part II: strains in wood and bark and apparent compliance. *Tree Physiol.* 28: 1513-1523.
- Baldwin, B. G., and S. Markos. 1998. Phylogenetic utility of the external transcribed spacer (*ETS*) of 18S–26S rDNA: congruence of *ETS* and its trees of *Calycadenia* (Compositae). *Mol. Phylogenet. Evol.* 10: 449-463.
- Becerra, J. X. 2003. Evolution of Mexican *Bursera* (Burseraceae) inferred from *ITS*, *ETS*, and 5S nuclear ribosomal DNA sequences. *Mol. Phylogenet. Evol.* 26: 300–309.
- Beldade P., K. Koops, and P. M. Brakefield. 2002. Developmental constraints versus flexibility in morphological evolution. *Nature* 416: 844-847.
- Bell, G. 1989. A comparative method. *Am. Nat.* 133: 553-571.
- Blomberg, S. P., T. Garland, Jr., and A. R. Ives. 2003. Testing for phylogenetic signal in comparative data: behavioral traits are more labile. *Evolution* 57: 717-745.
- Borchert, R., and W. T. Pockman. 2005. Water storage capacitance and xylem tension in isolated branches of temperate and tropical trees. *Tree Physiol.* 25: 457-466.
- Carlquist, S., and M. A. Hanson. 1991. Wood and stem anatomy of Convolvulaceae: a survey. *Aliso* 13: 51-94.
- Carlquist, S., and D. A. Gowans. 1995. Secondary growth and wood histology of *Welwitschia*. *Bot. J. Linn. Soc.* 118: 107-121.
- Chapotin, S. M., J. H. Razanameharizaka, and N. M. Holbrook. 2006. A biomechanical perspective on the role of large stem volume and high water content in baobab trees (*Adansonia* spp.; Bombacaceae). *Am. J. Bot.* 93: 1251-1264.
- Chave, J., D. Coomes, S. Jansen, S. L. Lewis, N. G. Swenson, and A. E. Zanne. 2009. Towards a worldwide wood economics spectrum. *Ecol. Lett.* 12: 351-366.
- Choat, B., L. Sack, and N. M. Holbrook. 2007. Diversity of hydraulic traits in nine *Cordia* species growing in tropical forests with contrasting precipitation. *New Phytol.* 175: 686-698.
- Day, L. M., and B. C. Jayne. 2007. Interspecific scaling of the morphology and posture of the limbs during the locomotion of cats (Felidae). *J. Exp. Biol.* 210: 642-654.
- Enquist, B. J. 2003. Cope's Rule and the evolution of long-distance transport in vascular plants: allometric scaling, biomass partitioning and optimization. *Plant Cell Environ.* 26: 151-161.
- Felsenstein, J. 1985. Phylogenies and the comparative method. *Am. Nat.* 125: 1-15.
- Fine, P. V. A., D. C. Daly, G. Villa, I. Mesones, and K. M. Cameron. 2005. The contribution of edaphic heterogeneity to the evolution and diversity of Burseraceae trees in the Western Amazon. *Evolution* 59: 1464-1478.
- Garland, T., Jr., P. H. Harvey, and A. R. Ives. 1992. Procedures for the analysis of comparative data using phylogenetically independent contrasts. *Syst. Biol.* 41: 18-32.
- Garland, T., Jr., and R. Díaz-Uriarte. 1999. Polytomies and phylogenetically independent contrasts: an examination of the bounded degrees of freedom approach. *Syst. Biol.* 48: 547-558.

- van Gelder, H. A., L. Poorter, and F. J. Sterck. 2006. Wood mechanics, allometry, and life-history variation in a tropical rain forest tree community. *New Phytol.* 171: 367-378.
- Gere, J. M. 2002. *Mecánica de materiales*. Thomson, México, DF, Mexico.
- Gómez-Vázquez, B. G., and E. M. Engleman. 1984. Bark anatomy of *Bursera longipes* (Rose) Standley and *Bursera copallifera* (Sessé and Moc.) Bullock. *IAWA Bull.* 5: 335-340.
- Guindon, S., and O. Gascuel. 2003. A simple, fast and accurate method to estimate large phylogenies by maximum-likelihood. *Syst. Biol.* 52: 696-704.
- Habib, M. 2010. The structural mechanics and evolution of aquaflying birds. *Biol. J. Linn. Soc.* 99: 687-698.
- Hacke, U. G., and J. S. Sperry. 2001. Functional and ecological xylem anatomy. *Perspect. Plant Ecol. Evol. Syst.* 4: 97-115.
- Hearn, D. J. 2006. *Adenia* (Passifloraceae) and its adaptive radiation: phylogeny and growth form diversification. *Syst. Bot.* 31: 805-821.
- Hearn, D. J. 2009. Developmental patterns in anatomy are shared among separate evolutionary origins of stem succulent and storage root-bearing growth habits in *Adenia*. *Am. J. Bot.* 96: 1941-1956.
- Hijmans, R. J., S. E. Cameron, J. L. Parra, P. G. Jones, and A. Jarvis. 2005. Very high resolution interpolated climate surfaces for global land areas. *Int. J. Climatol.* 25: 1965-1978.
- Howarth, D. G., and D. A. Baum. 2002. Phylogenetic utility of a nuclear intron from nitrate reductase for the study of closely related plant species. *Mol. Phylogenet. Evol.* 23: 525-528.
- Huelsenbeck, J. P., and F. Ronquist. 2001. MrBayes: Bayesian inference of phylogenetic trees. *Bioinformatics* 17: 754-755.
- Jacobsen, A. L., B. Pratt, F. W. Ewers, and S. D. Davis. 2007. Cavitation resistance among 26 chaparral species of southern California. *Ecol. Monogr.* 77: 99-115.
- Jablonski, D. 2007. Scale and hierarchy in macroevolution. *Palaeontology* 50: 87-109.
- Kembel, S.W., D. D. Ackerly, S. P. Blomberg, P. D. Cowan, M. R. Helmus, H. Morlon, and C. O. Webb. 2009. picante: R tools for integrating phylogenies and ecology. R package version 0.7-2. Available at <http://picante.r-forge-r.project.org>.
- Lahaye, R., L. Civeyrel, T. Speck, and N. P. Rowe. 2005. Evolution of shrub-like growth forms in the lianoid subfamily Secamonoideae (Apocynaceae s.l.) of Madagascar: phylogeny, biomechanics, and development. *Am. J. Bot.* 92: 1381-1396.
- Larson, A., and J. B. Losos. 1996. Phylogenetic systematics of adaptation. Pp. 187-220 in M. R. Rose, and G. V. Lauder, eds. *Adaptation*. Academic Press, San Diego, CA.
- Lewontin, R. 2000. The triple helix. *Gene, organism, and environment*. Harvard Univ. Press, Cambridge, MA.
- Maddison, W. P., and D.R. Maddison. 2009. Mesquite: A modular system for evolutionary analysis. Version 2.71. Available at <http://mesquiteproject.org>.
- Maherali H., W. T. Pockman, and R. B. Jackson. 2004. Adaptive variation in the vulnerability of woody plants to xylem cavitation. *Ecology* 85: 2184-2199.
- Marroig, G., and J. M. Cheverud. 2005. Size as a line of evolutionary least resistance: diet and adaptive morphological radiation in New World monkeys. *Evolution* 59: 1128-1142.

- Martins, E. P., and T. Garland, Jr. 1991. Phylogenetic analyses of the correlated evolution of continuous characters: a simulation. *Evolution* 45: 534-557.
- Medina, E. 1995. Diversity of life forms in neotropical dry forests. Pp. 221-242 in S. H. Bullock, H. A. Mooney, and E. Medina, eds. *Seasonally dry tropical forests*. Cambridge Univ. Press, Cambridge.
- Ménard, L., D. McKey, and N. Rowe. 2009. Developmental plasticity and biomechanics of treelets and lianas in *Manihot* aff. *quinquepartita* (Euphorbiaceae): a branch-angle climber of French Guiana. *Ann. Bot.* 103: 1249-1259.
- Midford, P. E., T. Garland Jr., and W. P. Maddison. 2008. PDAP Package of Mesquite. Version 1.14. Available at http://mesquiteproject.org/pdap_mesquite/.
- Miller, M. A., M. T. Holder, R. Vos, P. E. Midford, T. Liebowitz, L. Chan, P. Hoover, and T. Warnow. 2009. The CIPRES Portals. CIPRES. Available at http://www.phylo.org/sub_sections/portal.
- Moles, A. T., D. I. Warton, L. Warman, N. G. Swenson, S. W. Laffan, A. E. Zanne, A. Pitman, F. A. Hemmings, and M. R. Leishman. 2009. Global patterns in plant height. *J. Ecol.* 97: 923-932.
- Niklas, K. J. 1992. *Plant biomechanics*. Univ. Chicago Press, Chicago, IL.
- Niklas, K. J. 1993. Influence of tissue density-specific mechanical properties on the scaling of plant height. *Ann. Bot.* 72: 173-179.
- Niklas, K. J. 1994. *Plant allometry. The scaling of form and process*. Univ. Chicago Press, Chicago, IL.
- Niklas, K. J. 1999a. Changes in the factor of safety within the superstructure of a dicot tree. *Am. J. Bot.* 86: 688-696.
- Niklas, K. J. 1999b. The mechanical role of bark. *Am. J. Bot.* 86: 465-469.
- Niklas, K. J., F. Molina-Freaner, C. Tinoco-Ojanguren, C. J. Hogan, and D. J. Paolillo. 2003. On the mechanical properties of the rare endemic cactus *Stenocereus eruca* and the related species *S. gummosus*. *Am. J. Bot.* 90: 663-674.
- Niklas, K. J., and H.-C. Spatz. 1999. Methods for calculating factors of safety of plant stems. *J. Exp. Biol.* 202: 3273-3280.
- Nylander, J. A. A., J. C. Wilgenbusch, D. L. Warren, and D. L. Swofford. 2008. AWTY (are we there yet?): a system for graphical exploration of MCMC convergence in Bayesian phylogenetics. *Bioinformatics* 24: 581-583.
- Olson, M. E., and S. Carlquist. 2001. Stem and root anatomical correlations of life-form diversity, ecology and systematics in *Moringa* (Moringaceae). *Bot. J. Linn. Soc.* 135: 315-348.
- Olson, M. E. 2002. Combining data from DNA sequences and morphology for a phylogeny of Moringaceae (Brassicales). *Syst. Bot.* 27: 55-73.
- Olson, M. E., and J. A. Rosell. 2006. Using heterochrony to detect modularity in the evolution of stem diversity in the plant family Moringaceae. *Evolution* 60: 724-734.
- Onoda, Y., A. E. Richards, and M. Westoby. 2010. The relationship between stem biomechanics and wood density is modified by rainfall in 32 Australian woody species. *New Phytol.* 185: 493-501.
- Pisarenko, G. S., A. P. Yákovlev, and V. V. Matvéev. 1979. *Manual de resistencia de materiales*. Mir, Moscow, URSS.
- Posada, D. 2008. jModelTest: phylogenetic model averaging. *Mol. Biol. Evol.* 25: 1253-1256.
- Pratt, R. B., A. L. Jacobsen, F. W. Ewers, and S. D. Davis. 2007. Relationships among

- xylem transport, biomechanics and storage in stems and roots of nine Rhamnaceae species of the California chaparral. *New Phytol.* 174: 787-798.
- Price, C. A., B. J. Enquist, and V. M. Savage. 2007. A general model for allometric covariation in botanical form and function. *P. Natl. Acad. Sci. USA* 104: 13204–13209.
- Purvis, A., and T. Garland, Jr. 1993. Polytomies in comparative analyses of continuous characters. *Syst. Biol.* 42: 569-575.
- R Development Core Team. 2009. R: A language and environment for statistical computing. Version 2.9.2. R Foundation for Statistical Computing, Vienna, Austria. Available at <http://www.R-project.org>.
- Rambaut, A. 2002. SE-AL v.2.0a11: sequence alignment editor. Available at <http://tree.bio.ed.ac.uk/software/seal>.
- Rosell, J., and M. E. Olson. 2007. Testing implicit assumptions regarding the age vs. size dependence of stem biomechanics using *Pittocaulon* (~*Senecio*) *praecox* (Asteraceae). *Am. J. Bot.* 94: 161-172.
- Rosell, J. A., M. E. Olson, A. Weeks, A. de-Nova, R. Medina, J. Pérez-Camacho, T. P. Ferial, R. Gómez-Bermejo, J. C. Montero, and L. E. Eguiarte. in press. Diversification in species complexes: tests of species origin and delimitation in the *Bursera simaruba* clade of tropical trees (Burseraceae). *Mol. Phylogenet. Evol.* <http://dx.doi.org/10.1016/j.ympev.2010.08.004>.
- Rosner, S., A. Klein, U. Müller, and B. Karlsson. 2008. Tradeoffs between hydraulic and mechanical stress responses of mature Norway spruce trunk wood. *Tree Physiol.* 28: 1179-1188.
- Rowe, N., and T. Speck. 2005. Plant growth forms: an ecological and evolutionary perspective. *New Phytol.* 166: 61-72.
- Sang, T., D. J. Crawford, and T. F. Stuessy. 1997. Chloroplast DNA phylogeny, reticulate evolution, and biogeography of *Paeonia* (Paeoniaceae). *Am. J. Bot.* 84: 1120–1136.
- Schluter, D. 1996. Adaptive radiation along genetic lines of least resistance. *Evolution* 50: 1766-1774.
- Shanahan, T. 2008. Why don't zebras have machine guns? Adaptation, selection, and constraints in evolutionary theory. *Stud. Hist. Phil. Biol. and Biomed. Sci.* 39: 135-146.
- Sterck, F. J., H. A. van Gelder, and L. Poorter. 2006. Mechanical branch constraints contribute to life-history variation across tree species in a Bolivian forest. *J. Ecol.* 94: 1192-1200.
- Stevens, G. C. 1987. Lianas as structural parasites: the *Bursera simaruba* example. *Ecology* 68: 77-81.
- Swartz, S. M., and K. M. Middleton. 2008. Biomechanics of the bat limb skeleton: scaling, material properties and mechanics. *Cells Tissues Organs* 187: 59-84.
- Swenson, N. G., and B. J. Enquist. 2008. The relationship between stem and branch wood specific gravity and the ability of each measure to predict leaf area. *Am. J. Bot.*, 95: 516-519.
- Swofford, D. L. 2002. PAUP*. Phylogenetic analysis using parsimony (*and Other Methods). Version 4. Sinauer, Sunderland, MA.
- Vincent, J. F. 1992. Biomechanics- Materials. A practical approach. Oxford Univ. Press, Oxford, UK.

- Vogel, S. 2003. Comparative biomechanics: life's physical world. Princeton Univ. Press, Princeton, NJ.
- Warton, D. I., I. J. Wright, D. S. Falster, and M. Westoby. 2006. Bivariate line-fitting methods for allometry. *Biol. Rev.* 81: 259-291.
- Warton, D. I., and J. Ormerod, 2007. smatr: (Standardised) Major Axis Estimation and Testing Routines. R package version 2.1. Available at <http://cran.r-project.org/web/packages/smatr/index.html>
- Weeks, A., and B. B. Simpson. 2004. Molecular genetic evidence for interspecific hybridization among endemic Hispaniolan *Bursera* (Burseraceae). *Am. J. Bot.* 91: 976-984.
- West, G., J. H. Brown, and B. J. Enquist. 1997. A general model for the origin of allometric scaling laws in biology. *Science* 276: 122-126.
- Worcester, S. E. 1996. The scaling of the size and stiffness of primary flight feathers. *J. Zool.* 239: 609-624.
- Zanne, A. E., and D. S. Falster. 2010. Plant functional traits-linkages among stem anatomy, plant performance and life history. *New Phytol.* 185: 348-351.

TABLES

Table 1. Branch length-diameter allometric models and maximum tree height for the species of the *simaruba* clade. Using RMA regression of \log_{10} transformed data, we estimated the scaling exponent α of the Huxley allometric equation $L=\gamma D^\alpha$. The \log_{10} of the scaling constant γ equals the RMA regression intercept β . 95% confidence intervals are given in parentheses.

Species/Population	n	R ²	α (95% C. I.)	β (95% C. I.)	Max height (m)
<i>B. arborea</i>	10	0.629	1.308 (0.811-2.111)	1.664 (1.276-2.051)	10.44
<i>B. attenuata</i>	8	0.875	0.891 (0.630-1.260)	1.880 (1.620-2.140)	10.5
<i>B. cinerea</i>	11	0.692	0.790 (0.526-1.187)	1.907 (1.627-2.187)	14.58
<i>B. grandifolia</i>	12	0.675	0.794 (0.536-1.174)	1.972 (1.783-2.162)	9.28
<i>B. instabilis</i>	18	0.229	1.640 (1.045-2.572)	1.673 (1.175-2.172)	9.75
<i>B. longipes</i>	11	0.872	0.752 (0.576-0.982)	1.903 (1.820-1.986)	8.69
<i>B. roseana</i>	13	0.856	1.047 (0.816-1.344)	1.815 (1.618-2.012)	16.85
<i>B. simaruba CR</i>	12	0.847	1.052 (0.801-1.381)	1.836 (1.698-1.974)	14
<i>B. simaruba MX</i>	10	0.758	1.416 (0.957-2.093)	1.479 (0.996-1.963)	25.15
<i>B. standleyana</i>	6	0.985	0.964 (0.812-1.145)	2.121 (2.051-2.191)	5.36

Table 2. Precipitation (ppt) and temperature evenness (T) indices based on principal component analyses of environmental data. Variables reflecting precipitation were \log_{10} transformed before PCA.

Index	Variables	Loadings
Precipitation	Annual ppt	0.509
	Ppt wettest qtr	0.504
	Ppt coldest qtr	0.482
	Ppt wettest month	0.504
Range	T annual range	-0.597
	Mean diurnal range	-0.581
	Min T coldest month	0.554

Table 3. Linear models describing ontogenetic variation in mechanical behavior. E_{struct} , E_{wood} , and the relative contribution of bark to overall stem flexural stiffness EI_{struct} are predicted well by distance from the tip of the stem ("Distance") and species group. However, E_{bark} apparently does not vary strongly ontogenetically. Species falling in the dry, moist, and intermediate (the reference category) groups can be found in the Materials and Methods section. Standard errors of estimates are given in parentheses. All cases had $p < 0.001$, except for * $p < 0.01$ or n.s. (non-significant). R^2 adj=adjusted R^2 .

	$\log_{10}E_{struct}$	$\log_{10}E_{wood}$	$\log_{10}E_{bark}$	Contribution EI_{bark}
R^2_{adj}	0.743	0.77	0.375	0.55
Model Anova	$F_{(3,69)}=70.51$	$F_{(5,67)}=49.25$	$F_{(2,69)}=22.28$	$F_{(3,68)}=29.86$
Intercept	-0.671 (0.081)	-0.1035 (0.071) ^{n.s.}	-0.737 (0.108)	26.814 (1.672)
\log_{10}Distance	0.374 (0.039)	0.278 (0.036)	0.168 (0.054)	-
Distance	-	-	-	-0.056 (0.011)
Dry species	-0.1620 (0.035)	0.3696 (0.125) [*]	-0.287 (0.051)	7.643 (1.872)
Moist species	0.192 (0.036)	0.1824 (0.134) ^{n.s.}	-	-6.489 (1.637)
\log_{10}Distance*Dry species	-	-0.302 (0.065)	-	-
\log_{10}Distance*Moist species	-	-0.020 (0.067) ^{n.s.}	-	-

Table 4. Tests for phylogenetic signal and the K index of Blomberg et al. (2003) using the original branch lengths of Fig. 2 to reflect anagenetic change as well as all branches set to one to reflect the cladogenetic mode. Variables with significant phylogenetic signal are in bold.

Variable	Anagenetic		Cladogenetic	
	K	p	K	p
E_{struct}	1.493	0.008	1.446	0.038
E_{wood}	1.377	0.014	1.356	0.028
E_{bark}	0.672	0.707	0.553	0.279
a _{RMA}	0.522	0.730	0.373	0.933
Max. Height	0.889	0.196	0.850	0.389
Ppt index	1.733	0.011	1.761	0.014
Evenness index	1.343	0.064	1.050	0.058

Table 5. Correlations between elastic moduli, environmental indices, stem length-diameter scaling exponents, and maximum tree height based on raw data and phylogenetically independent contrasts. Correlations involving the scaling exponent excluded *B. standleyana* and *B. instabilis*, whereas those involving height excluded *B. standleyana*. PIC_{anag}=correlations involving contrasts calculated with original branch lengths and assuming anagenetic change, PIC_{clad}=correlations involving contrasts calculated with branch lengths set to one, assuming cladogenetic change and no extinction. * p<0.05, ** p<0.01, *** p<0.001, ns. ps.=non-significant phylogenetic signal for neither variables involved in the correlation.

	<i>E_{struct}</i>			<i>E_{wood}</i>			<i>E_{bark}</i>			α (-stan, -inst)			Max. height (-stan)		
	Raw	PIC _{anag}	PIC _{clad}	Raw	PIC _{anag}	PIC _{clad}	Raw	PIC _{anag}	PIC _{clad}	Raw	PIC _{anag}	PIC _{clad}	Raw	PIC _{anag}	PIC _{clad}
<i>E_{struct}</i>	-	-	-	-	-	-	-	-	-	0.879**	0.889**	0.862**	0.728*	0.368	0.437
<i>E_{wood}</i>	0.947***	0.933***	0.933***	-	-	-	-	-	-	0.845**	0.828*	0.810*	0.653	0.272	0.330
<i>E_{bark}</i>	0.812**	0.809**	0.743*	0.750*	0.695*	0.630	-	-	-	0.687	ns ps	ns ps	0.319	ns ps	ns ps
PPt index	0.896***	0.846**	0.857**	0.819**	0.803**	0.831**	0.730*	0.641*	0.586	0.669	0.645	0.636	0.732*	0.449	0.545
Evenness index	0.830**	0.793**	0.767*	0.697*	0.657*	0.642*	0.753*	ns ps	ns ps	0.782*	ns ps	ns ps	0.494	ns ps	ns ps

FIGURES

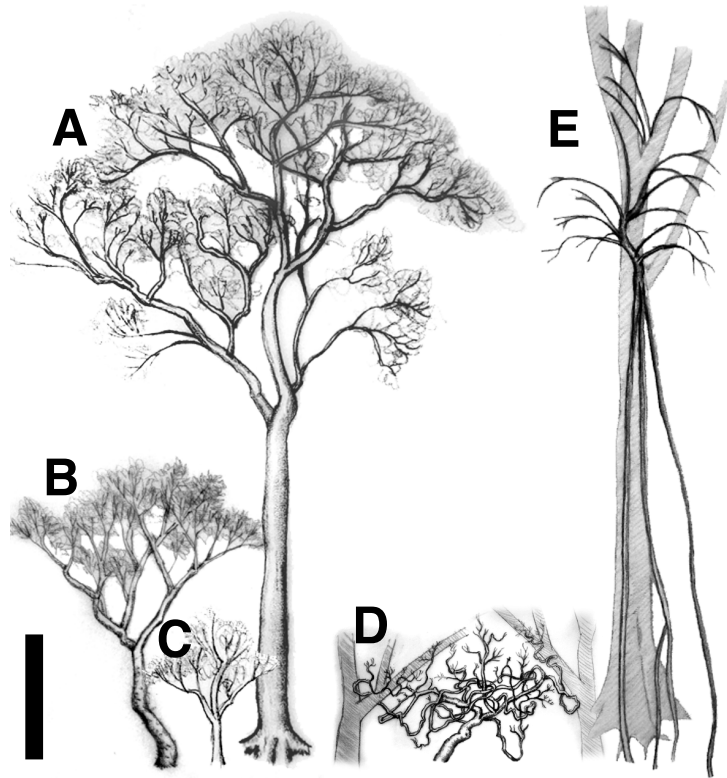


Figure 1. Diversity in shape, size, and habit in the *Bursera simaruba* clade. A-C. "Conventional" trees. A. The largest member of the clade, *B. simaruba*, ranges from rainforest to subdeciduous forest. B. Intermediate sized trees of subdeciduous and moister deciduous forests include *B. ovalifolia* and *B. attenuata*. C. Small trees of tropical dry forest include *B. longipes* and *B. arborea*. D. *Bursera instabilis* has stems that support their own weight when young and become lianescent with age. Neighboring trees supporting *B. instabilis* branches are indicated in gray. E. *Bursera standleyana* grows high in rainforest trees, with arching branches and long roots that draw water from the forest floor. The host tree is indicated in gray. Scale bar = 5 m.

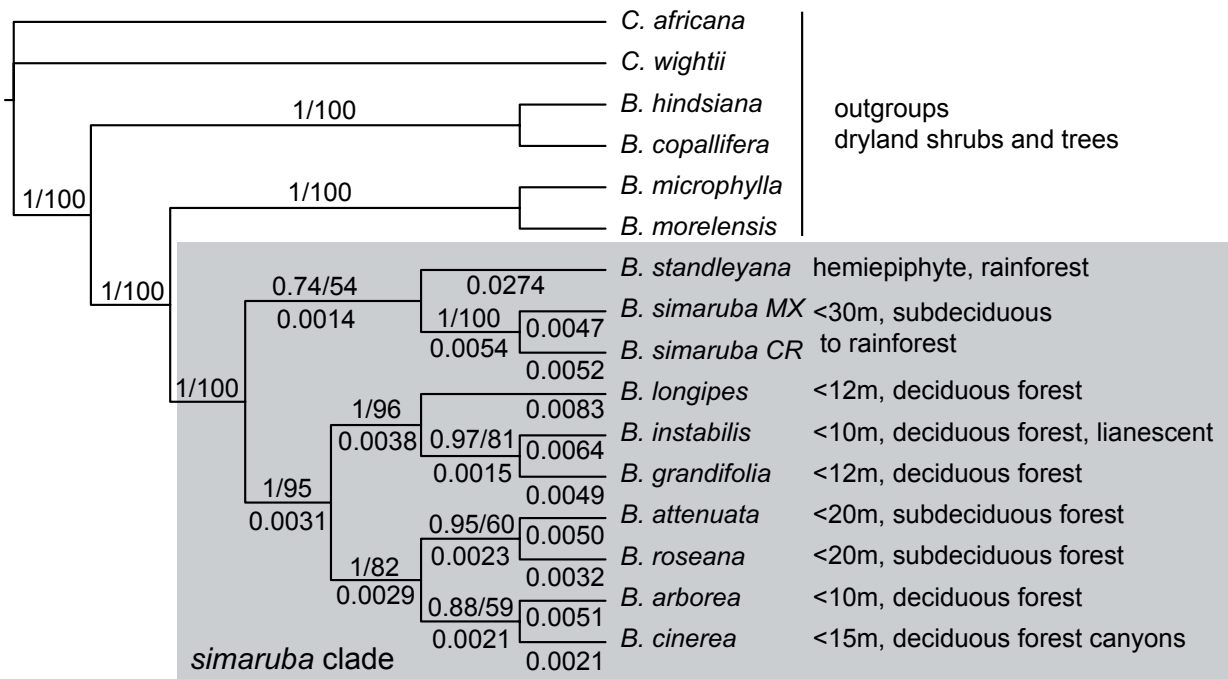


Figure 2. Habitat and size characteristics of the sampled species and their phylogenetic relationships based on five nucleotide markers. The tree is a Bayesian 50% majority-rule consensus with posterior probabilities/bootstraps above branches and branch lengths below. The outgroup included members of the Old World genus *Commiphora* as well as members from throughout the rest of genus *Bursera*.

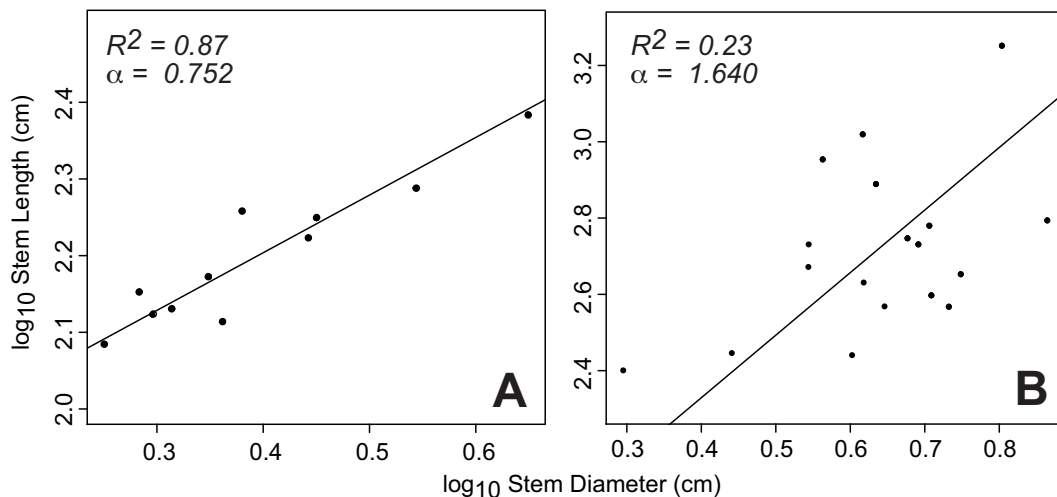


Figure 3. Branch length-diameter allometric models for two species in the *simaruba* clade. A. *Bursera longipes*, a "conventional" tree, showing that stem length is predicted well based on diameter. B. In contrast, in *Bursera instabilis*, the tree with lianescent branches, stems may vary markedly in length for a given diameter.

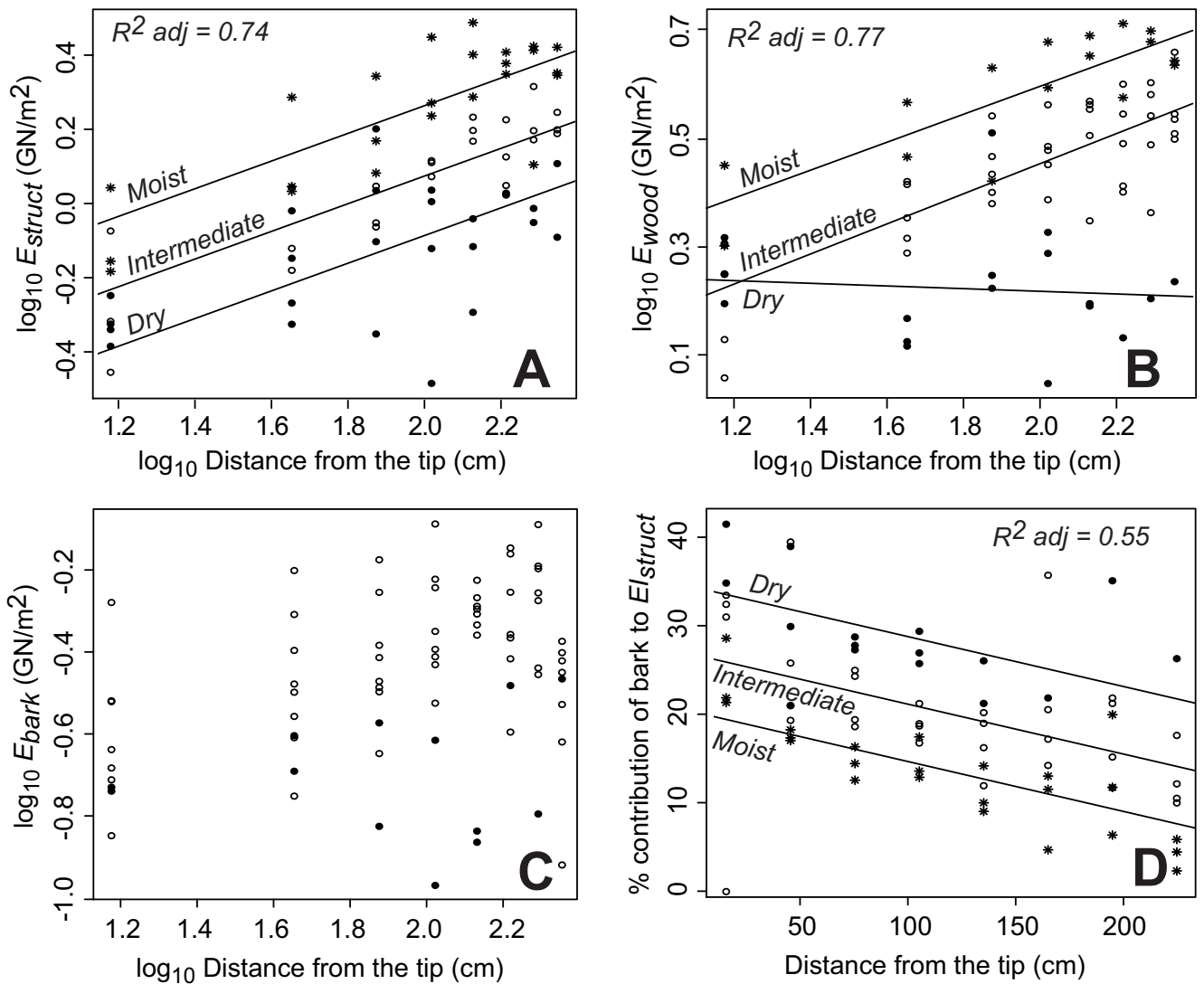


Figure 4. Ontogenetic changes in mechanical properties and differences between species. A. E_{struct} increased with distance from the tip and was higher in species of moist locales and lower in those of dry environments (moist: *B. simaruba* MX, *B. simaruba* CR, and *B. standleyana*; intermediate: *B. arborea*, *B. attenuata*, and *B. roseana*; dry: *B. cinerea*, *B. grandifolia*, *B. instabilis*, and *B. longipes*). B. E_{wood} varied with distance from the tip of the stem in all species but the dryland ones. Species grouping as for E_{struct} , except for *B. cinerea* and *B. simaruba* CR which fell in the intermediate group. C. E_{bark} was less strongly predicted by distance, and species from dry environments (*B. cinerea* and *B. grandifolia*) tended to have lower values. D. Although E_{bark} did not show a marked increase along the stem, the mechanical contribution of bark to resisting bending varied drastically through ontogeny; bark is especially important in supporting the terminal sections of stems. Species grouping as for E_{wood} , except for *B. simaruba* CR which fell in the moist group. Symbols are as follows: black circle = species of dry environments; hollow circle = species of intermediate environments (and also moist environments for C); asterisk = species of moist environments.

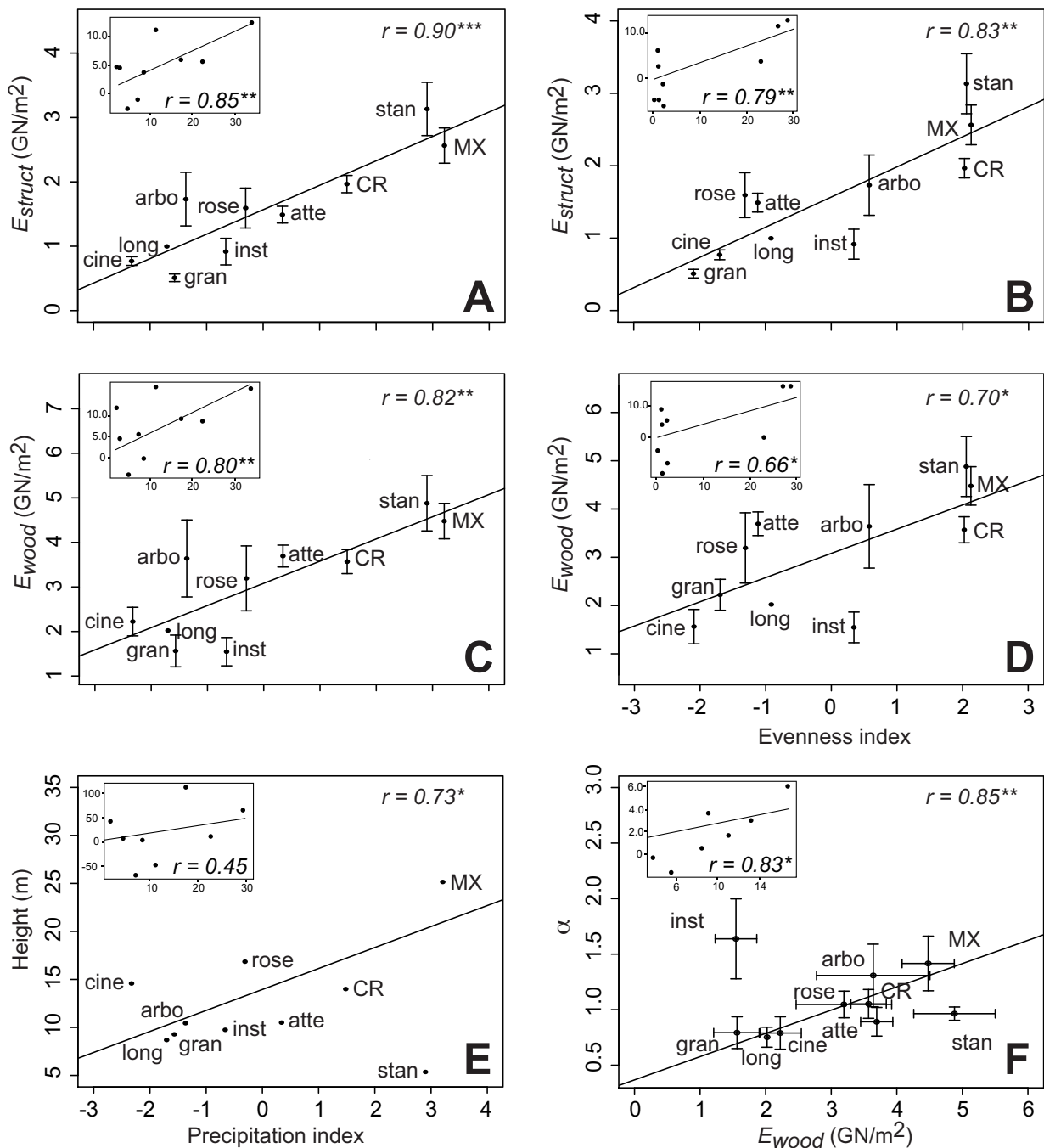


Figure 5. Correlations between elastic moduli, plant height, and environmental indices, and between the stem allometry and the wood elastic modulus. Insets are with phylogenetically independent contrasts (PIC) with original branch lengths from Fig. 2. Bars represent standard errors. A, B. E_{struct} vs. precipitation and temperature evenness, showing that stem tissue stiffness increases with water availability and more even temperatures. C, D. A similar pattern was shown by E_{wood} vs. precipitation and climate evenness. E. Maximum tree height vs. precipitation showing that *simaruba* clade trees are taller in moister habitats based on raw data but not contrasts (the hemiepiphyte *B. standleyana* was excluded from

correlations and PICs). F. Stem length-diameter scaling exponent α vs. wood mechanical properties, showing that in the conventional trees E_{wood} predicts stem length-diameter proportions. The lianescent *B. instabilis* and the hemiepiphyte *B. standleyana* are displaced from the conventional tree axis. The non-self supporting branches of *B. instabilis* had much lower E_{wood} as compared to the self-supporting species. On the other hand, *B. standleyana* had stiffer wood than expected for its stem proportions, possibly reflecting selection favoring resistance of more negative xylem pressure potentials than the other species. Fit and correlation were calculated based only on conventional trees. Abbreviations are as follows: arbo = *B. arborera*, atte = attenuata, cine = *B. cinerea*, CR = *B. simaruba* CR, gran = *B. grandifolia*, inst = *B. instabilis*, long = *B. longipes*, MX = *B. simaruba* MX, rose = *B. roseana*, stan = *B. standleyana*.

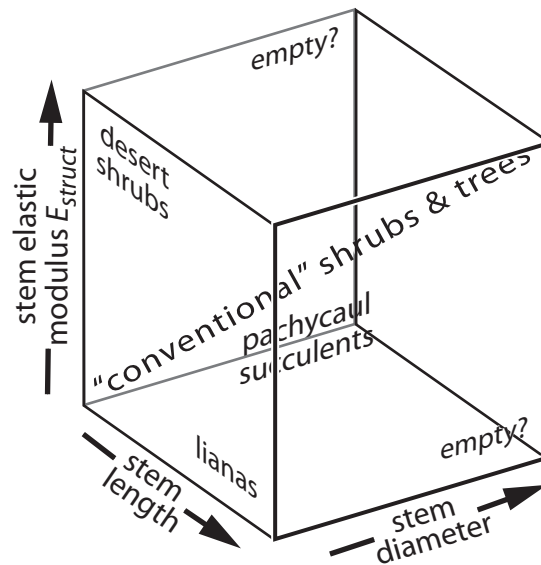


Figure 6. Heuristic morphospace defined by E_{struct} , stem length, and stem diameter. Most woody plants likely describe a "conventional" axis with length, diameter, and tissue stiffness increasing more or less predictably, with surface area maximized and transport distances minimized. Displacement from this relationship should result in lianas, succulents, and cavitation-resistant shrubs with dense wood. Empty areas seem ontogenetically accessible but maladaptive.

Appendix 1. Locality, voucher, and GenBank accession numbers (*psbA-trnH*, *PEPC*, *ETS*, *ITS*, *NIAi3*) of species and populations of *B. simaruba* included in the phylogenetic reconstruction. All vouchers are deposited in MEXU, unless otherwise stated. Mx: Mexico. GenBank accession numbers of previously published sequences are designated by a superscript corresponding to the following publications: ^a Becerra (2003), ^b Weeks & Simpson (2004), ^c Weeks et al. (2005), ^d Weeks & Simpson (2007).

B. ARBOREA: Chamela, Jalisco, Mx (Rosell 16), GQ377870, GQ377934, GQ378006, GQ378070, GQ378140. **B. ATTENUATA:** Tepic, Nayarit, Mx (R. Medina 3412), GQ377871, GQ377935, GQ378007, GQ378071, GQ378141. **B. CINEREA:** Jayacatlán, Oaxaca, Mx (Rosell 40), GQ377874, GQ377938, GQ378010, GQ378074, GQ378144. **B. GRANDIFOLIA:** Atlacholoaya, Morelos, Mx (Rosell 5), GQ377877, GQ377941, GQ378013, GQ378078, GQ378148. **B. INSTABILIS:** Chamela, Jalisco, Mx (Rosell 11), GQ377882, GQ377946, GQ378018, GQ378084, GQ378156. **B. LONGIPES:** Xalitla, Guerrero, Mx (Cervantes 5), GQ377891, GQ377955, GQ378027, GQ378093, GQ378165. **B. ROSEANA:** Río Cupatitzio, Michoacán, Mx (Rosell 25), GQ377899, GQ377963, GQ378035, GQ378101, GQ378175. **B. SIMARUBA:** Los Tuxtlas, Veracruz, Mx (Rosell 44), GQ377909, GQ377973, GQ378045, GQ378111, GQ378186; **CR=** Palo Verde, Guanacaste, Costa Rica (A. Fernández & C. Hood 1128, MO), GQ377913, GQ377977, GQ378049, GQ378115, GQ378192. **B. STANDLEYANA:** **CR=** La Cangreja, San José, Costa Rica (J.F. Morales 1944, MO), GQ377931, GQ377996, GQ378067, GQ378133, GQ378212. **OUTGROUP SPECIES: B. COPALLIFERA:** Taxco, Guerrero, Mx (R. Medina 3975), AY831897^d, GQ377999, AY315042-AY315044^c, AF445833^a, GQ378216. **B. HINDSIANA:** Sonora, Mx (J. Núñez-Farfán sn), AY831899^d, GQ378001, AY315048-AY315050^c, GQ378136, GQ378220. **B. MICROPHYLLA:** Sonora, Mx (J. Núñez-Farfán sn), AY309396^b, AY309370^b, AY309326-AY309328^b, AF445855^a, GQ378222. **B. MORELENSIS:** Cuicatlán, Oaxaca, Mx (R. Medina 3971), AY309397^b, AY309371^b, AY309329-AY309331^b, AF445852^a, GQ378223. **COMMIPHORA AFRICANA:** South Africa (Weeks 02-XII-09-03, TEX), AY831901^d, GQ378003, AY831869^d, GQ378137, GQ378227. **C. WIGHTII:** India (Weeks-00-VIII-18-3, TEX), AY831936^d, GQ378005, AY315081-AY315083^c, GQ378139, GQ378229.

Becerra, J. X. 2003. Evolution of Mexican *Bursera* (Burseraceae) inferred from *ITS*, *ETS*, and 5S nuclear ribosomal DNA sequences. *Mol. Phylogenet. Evol.* 26: 300-309.

Weeks, A., and B. B. Simpson. 2004. Molecular genetic evidence for interspecific hybridization among endemic Hispaniolan *Bursera* (Burseraceae). *Am. J. Bot.* 91: 976-984.

Weeks, A., D. C. Daly, and B. B. Simpson. 2005. The phylogenetic history and biogeography of the frankincense and myrrh family (Burseraceae) based on nuclear and chloroplast sequence data. *Mol. Phylogenet. Evol.* 35: 85-101.

Weeks, A., and B. B. Simpson. 2007. Molecular phylogenetic analysis of *Commiphora* (Burseraceae) yields insight on the evolution and historical biogeography of an “impossible” genus. *Mol. Phylogenet. Evol.* 42: 62-79.

Appendix 2. Environmental variables extracted from WorldClim v.1.4 (Hijmans et al. 2005).

Annual mean temperature
 Mean diurnal range
 Isothermality
 Temperature seasonality
 Maximum temperature warmest month
 Minimum temperature coldest month
 Temperature annual range
 Mean temperature wettest quarter
 Mean temperature driest quarter
 Mean temperature warmest quarter
 Mean temperature coldest quarter
 Annual precipitation
 Precipitation wettest month
 Precipitation driest month
 Precipitation seasonality
 Precipitation wettest quarter
 Precipitation driest quarter
 Precipitation warmest quarter
 Precipitation coldest quarter

Appendix 3. α =the stem length-diameter scaling exponent; PPT=the precipitation index; evenness=the evenness index, which indicates the degree of temperature oscillation

Species/ Population	E_{struct} (GN/m ²)	E_{wood} (GN/m ²)	E_{bark} (GN/m ²)	α	Max. height (m)	PPT	Evenness
<i>B. arborea</i>	1.73	3.64	0.49	1.31	10.44	-1.37	0.58
<i>B. attenuata</i>	1.49	3.69	0.46	0.89	10.50	0.34	-1.12
<i>B. cinerea</i>	0.77	2.22	0.14	0.79	14.58	-2.33	-1.70
<i>B. grandifolia</i>	0.51	1.56	0.15	0.79	9.28	-1.57	-2.09
<i>B. instabilis</i>	0.92	1.55	0.44	1.64	9.75	-0.66	0.34
<i>B. longipes</i>	1.00	2.02	0.35	0.75	8.69	-1.70	-0.91
<i>B. roseana</i>	1.59	3.19	0.51	1.05	16.85	-0.31	-1.31
<i>B. simaruba</i> CR	1.97	3.57	0.54	1.05	14.00	1.48	2.03
<i>B. simaruba</i> MX	2.56	4.48	0.50	1.42	25.15	3.21	2.13
<i>B. standleyana</i>	3.13	4.88	0.59	0.96	5.36	2.90	2.06

CAPÍTULO 3.

INTEGRACIÓN FUNCIONAL Y DIVERSIFICACIÓN ADAPTATIVA EN LOS TALLOS DEL CLADO *SIMARUBA* (*BURSEREA*, BURSERACEAE).

RESUMEN

Las estructuras biológicas suelen realizar dos o más funciones simultáneamente, lo que resulta en una fuerte integración funcional. Cuando estas funciones compiten por recursos y/o son antagónicas, los patrones de covariación entre funciones son negativos y pueden reflejar trade-offs. Los trade-offs y la integración funcional pueden tener un impacto en la diversificación morfológica al restringir los fenotipos posibles. Este efecto en la diversificación es evaluado en este trabajo utilizando tallos leñosos como sistema de estudio. Este sistema es ideal por ser estructuralmente sencillo y desempeñar tres funciones principales, sostén mecánico, almacenamiento de agua y productos fotosintéticos, y conducción hidráulica. La naturaleza antagónica y la competencia por recursos resultan en trade-offs entre estas tres funciones del tallo. Se estudiaron los patrones de integración positiva y los trade-offs en los niveles interpoblacional, intraespecífico e interespecífico en los tallos leñosos del clado *Bursera simaruba* (Burseraceae), un grupo de árboles tropicales de gran diversidad estructural y ambiental. Midiendo ocho poblaciones y nueve especies dentro del grupo y variables que reflejaron las tres funciones del tallo, se encontró que los patrones de integración funcional en los tallos estuvieron conservados entre niveles evolutivos, excepto en un par de casos a nivel poblacional, donde las diferencias resultaron del relajamiento de algunas correlaciones. Los trade-offs se ubicaron principalmente entre variables relacionadas con el sostén mecánico y aquellas que reflejaron el almacenamiento de agua. Se encontraron correlaciones positivas entre las variables reflejando una misma función. La conductividad no presentó covariación con otras funciones, pero al interior se detectó un trade-off entre la eficiencia y la seguridad. Si bien los patrones de covariación se conservaron entre especies, hay cambios importantes en los valores medios de desempeño de las diferentes funciones que se asocian con condiciones ambientales, sugiriendo que la selección natural es responsable de los cambios de desempeño en la función que se optimiza, además de ser el agente causal que mantiene los patrones de covariación observados. La integración funcional que afecta los patrones de diversificación en el clado *simaruba* podría estar impactando la diversificación de los tallos leñosos en general, dado el reporte reiterado de ciertos trade-offs en la madera de diversos sistemas.

ABSTRACT

Biological structures are multitasking units with strong functional integration between parts. When there is strong competition for resources or functions are antagonistic, negative covariation patterns reflecting trade-offs may emerge between parts. Trade-offs, and functional integration in general, can strongly impact morphological diversification, restricting possible phenotypes. We evaluate this effect in diversification using woody stems as a model system. Wood is an ideal system due to its relative structural simplicity and because it performs three main functions, mechanical support, water and starch storage, and water conduction. The antagonistic nature of these functions and the competition for resources result in functional trade-offs. We studied the patterns of functional integration at the interpopulation, intraspecific, and interspecific levels using the woody stems of the *Bursera simaruba* clade (Burseraceae), a group of tropical trees of exceptional environmental and morphological diversity. We measured eight populations, nine species, and several variables reflecting the three functions, and found that the functional integration patterns were similar between levels, except for two populations in which some correlations were relaxed. Main trade-offs were found between variables regarding mechanical support and storage. Positive covariation was observed between variables reflecting the same function. Conductivity did not covary with other functions, but showed a strong trade-off between efficiency and security. Although covariation patterns were conserved between species, mean performance values changed for different functions in association with environmental conditions, suggesting the adaptive nature for these changes. Natural selection is also suggested as the causal agent maintaining functional covariation patterns. Functional integration affecting the patterns of diversification in the *simaruba* clade could affect that of woody stems in general, given the pervasive nature of trade-offs that have been reported for this tissue.

1. INTRODUCCIÓN

Todas las estructuras biológicas suelen realizar varias funciones de manera simultánea, lo que resulta en fuertes patrones de integración entre sus partes (Olson y Miller, 1958; Van Valen, 1965; Schwenk, 2001; Pigliucci y Preston, 2004). Es frecuente que una misma estructura desempeñe funciones antagónicas y que como resultado se detecten patrones de covariación negativa entre sus partes (Reznick y Travis, 1996). Además, las funciones pueden estar compitiendo por recursos, lo que refuerza su antagonismo. Cuando existe una asociación funcional tan fuerte que cambios en una parte acarrear alteraciones en otra parte, y estos cambios tienen efectos opuestos en la adecuación del organismo, emergerá un trade-off (Roff y Fairbairn, 2007). Los trade-offs son un caso particular dentro de las posibles manifestaciones de la integración fenotípica y pueden tener un efecto muy fuerte en las posibilidades de diversificación de las morfologías. Es precisamente este efecto el que motiva el presente estudio de tradeoffs y de integración funcional en los tallos leñosos. Aunque se conocen disyuntivas evolutivas en los tallos, no se ha explorado el impacto de estas negociaciones en la diversificación adaptativa de estas estructuras multifuncionales.

1.1. LOS TRADE-OFFS Y EL ESTUDIO DE LA ADAPTACIÓN

Los estudios que buscan caracteres adaptativos suelen ignorar que las estructuras biológicas tienen fuertes relaciones entre sus partes (p.e. Elstrott e Irschick, 2004). Atomizar arbitrariamente una estructura tiene el supuesto implícito y fuerte de que las estructuras se optimizan independientemente durante el proceso de adaptación (Gould y Lewontin, 1979). Sin embargo, la fuerte integración fenotípica en una estructura, que se traduce en patrones de covariación entre sus partes, puede imponer “frenos” o restringir el proceso adaptativo (Pigliucci, 2004). Además, en una estructura con interacciones entre partes se vuelve un reto reconocer la característica que es blanco de la selección natural y que “arrastra” a otras características al cambio (Lewontin, 1977; Lande y Arnold, 1983). Como puede apreciarse, los trade-offs y la adaptación están íntimamente ligados: el estudio de trade-offs involucra directamente el de la adaptación, y en cualquier estudio adaptativo

estaremos frente al fenómeno omnipresente de correlación entre caracteres, en muchos casos correspondiente a un trade-off.

Se ha comentado ya que los patrones de covariación han sido interpretados como restricciones al proceso evolutivo. La genética cuantitativa ha producido modelos teóricos que muestran cómo la matriz de varianzas y covarianzas genéticas podría generar estas restricciones (Schluter 1996, 2000; Marroig y Cheverud, 2005). Cuando hay fuertes correlaciones genéticas, el cambio morfológico tenderá a darse a lo largo de la llamada “línea de resistencia mínima” (LRM), que corresponde a la dirección de varianza máxima (Schluter, 1996). La trayectoria evolutiva hacia un pico adaptativo estará entonces influida por la dirección de la LRM. Si la dirección del gradiente de selección y de la LRM no coinciden, entonces la trayectoria evolutiva será desviada y podría, en casos extremos, ser dirigida hacia otro pico adaptativo diferente (Schluter, 2000). Este escenario ejemplifica el porqué la correlación entre caracteres puede ser interpretada como una restricción.

Sin embargo, también existe la posición que sostiene que los patrones de covariación podrían facilitar la adaptación (Wagner, 1988; Merilä y Björklund, 2004) o ser el resultado de la selección natural (Cheverud, 1988; Marroig y Cheverud, 2010). La “facilitación” resultaría de un aumento en la eficiencia de la selección al actuar sobre un número de combinaciones restringido por los patrones de covariación (Schlichting y Pigliucci, 1998; Merilä y Björklund, 2004). La respuesta evolutiva de una población también sería más rápida cuando la dirección de la LRM y el gradiente de selección coincidieran (Björklund, 1996). Tomar cualquiera de estas dos posturas extremas en cuanto al papel de los patrones de covariación podría ser erróneo (Schlichting y Pigliucci, 1998; Pigliucci, 2004; Schwenk y Wagner, 2004), pues el efecto restrictivo o adaptativo de estos patrones depende totalmente del contexto selectivo. Por ejemplo, la integración favorecerá la adaptación cuando la LRM coincida con el gradiente de selección, pero actuará como una restricción en caso contrario (Merilä y Björklund, 2004).

1.2. APROXIMACIONES AL ESTUDIO DE LOS TRADE-OFFS Y DE LA INTEGRACIÓN FENOTÍPICA

Los trade-offs pueden ser estudiados a partir de diferentes aproximaciones. Una muy popular es la de la genética cuantitativa, en donde se elaboran modelos teóricos de

trade-offs entre características o funciones y se pone a prueba su existencia a través de modelos, p.e. el modelo de adquisición y alocaión de recursos (de Jong and van Noordwijk, 1992; Roff y Fairbairn, 2007). Esta aproximación ha mostrado ser sumamente exitosa para el estudio de las historias de vida (Roff, 2002), pero requiere condiciones de laboratorio y cálculos de parámetros de la genética cuantitativa, condiciones que no siempre pueden alcanzarse en un estudio. Por otro lado, existen estudios que infieren la existencia de trade-offs a partir de la correlación negativa entre variables. Esta aproximación requiere estudios posteriores que aclaren si la correlación detectada ocurre verdaderamente entre las variables, y no es consecuencia de una correlación indirecta, y que también permitan determinar las causas próximas del trade-off, es decir, si existe competencia por recursos y/o antagonismo funcional. No obstante, el uso de la covariación negativa es un primer paso fundamental en la búsqueda de trade-offs, sobre todo en estudios que efectúan las búsquedas entre especies.

Los estudios sobre trade-offs se enfocan en el nivel poblacional, sobre todo aquellos con la perspectiva de la genética cuantitativa (p.e. Roff y Gélina, 2003), o en el nivel interespecífico (p.e. Badyaev y Ghalambor, 2001; Shiota y Kimura, 2007). Aunque los trabajos a nivel poblacional tienen como motivación principal generalizar lo observado hacia niveles más altos (p.e. Stepan et al., 2002; Roff y Gélina, 2003; Begin y Roff, 2004; Ghalambor et al., 2004; Nespolo et al., 2009), son muy escasos los trabajos dirigidos explícitamente a validar esta extrapolación. Por su parte, los estudios con enfoque interespecífico suelen obviar el que los trade-offs a ese nivel se observarán también a niveles más bajos (p.e. Pratt et al., 2007), y son muy pocos los estudios que abordan explícitamente este aspecto (p.e. Choat et al., 2007). Es por ello que en este proyecto planteamos someter a prueba explícitamente este supuesto de generalización entre niveles tan importante estudiando trade-offs en el nivel poblacional y comparativo en el mismo linaje.

A diferencia de los estudios enfocados directamente en trade-offs, las comparaciones entre niveles evolutivos han sido un objetivo explícito en algunos estudios de integración fenotípica. Estas comparaciones se han realizado para determinar si la diversificación de los linajes ha seguido la dirección de los patrones de covariación dentro de poblaciones, es decir, si ha ocurrido por deriva, o si la selección ha intervenido en el

proceso desviando la diversificación de la dirección impuesta por la covariación (Merilä y Björklund, 1999; Eroukhmanoff y Svensson, 2008; Marroig y Cheverud, 2010). Si la divergencia entre poblaciones ocurre en la misma dirección que los patrones de covariación dentro de poblaciones, en particular a lo largo de las LRMs, no se descarta que el cambio haya ocurrido por deriva genética (Merilä y Björklund, 1999; Marroig y Cheverud, 2004). En contraste, cuando los patrones de covariación no coinciden entre niveles, se concluye que en el proceso de diversificación ha intervenido la selección natural (Arnold et al., 2001; Marroig y Cheverud, 2004). No obstante, el no rechazar la acción de la deriva no constituye una prueba definitiva de la ausencia de selección (Marroig y Cheverud, 2004; Merilä y Björklund, 2004), como parece ser el caso de la integración funcional de los tallos que será abordado en este trabajo.

Los resultados de la comparación entre niveles evolutivos de los estudios de integración ofrecen evidencia en los dos sentidos: algunos han encontrado conservación de los patrones entre niveles (Arnold y Phillips, 1999; Begin y Roff, 2004; Blows y Hoffmann, 2005; Eroukhmanoff y Svensson, 2008), y otros han detectado diferencias (Merilä y Björklund, 1999; Waldmann y Andersson, 2000; Game y Caley, 2006; Renaud et al., 2006; Monteiro y Noguera, 2009). Estos últimos resultados ponen en duda las generalizaciones entre niveles que se hacen a partir de estudiar un solo nivel y refuerzan la necesidad de seguir documentando la conservación o alteración de los patrones de integración a diferentes escalas evolutivas.

1.3. MATRICES DE VARIANZAS Y COVARIANZAS GENOTÍPICAS VS. FENOTÍPICAS EN EL ESTUDIO DE LOS TRADE-OFFS Y LA INTEGRACIÓN FENOTÍPICA

Con origen en la genética cuantitativa, la gran mayoría de los trabajos sobre trade-offs están basados en la matriz G o matriz de varianzas y covarianzas genéticas (Roff, 2002; Sinervo y Svensson, 2002; Roff y Fairbairn, 2007). Esta matriz, que refleja la “arquitectura genética”, ha permitido modelar detalladamente algunos trade-offs entre caracteres (Roff, 2002), e incluso predecir la evolución de estos (Stearns, 1989; Roff y Fairbairn, 2007). Sin embargo, la matriz G ha recibido varias críticas, principalmente en cuanto a su existencia ontológica, la dependencia de su construcción en los caracteres

elegidos, el contexto ambiental y el estadio de desarrollo del organismo (Pigliucci, 2006). Otro problema de esta matriz es que no captura aspectos de covariación epigenética, ecofenotípica o filogenética (Eble, 2004). Por estas razones, algunos consideran que la matriz G no es un buen indicador de trade-offs o restricciones evolutivas (Pigliucci, 2006).

Este trabajo aborda trade-offs desde un punto de vista morfológico y se fundamenta en la matriz de varianzas y covarianzas fenotípicas (matriz P). Se ha argumentado que la matriz P es una fuente de información por sí misma (Eble, 2003), y se ha encontrado que tiene cierto grado de correspondencia con la matriz G (Cheverud, 1988; Roff, 2000). La matriz P se fundamenta en caracteres observados directamente y captura aspectos de plasticidad y variación ambiental que son parte esencial del proceso adaptativo. Al igual que la matriz G , la matriz P depende fuertemente de los caracteres incluidos en su construcción. En este trabajo se abordan todas las funciones principales de un tallo, por lo que las matrices P reflejarán los patrones de integración generales de estas estructuras.

1.4. LOS TALLOS Y EL CLADO *SIMARUBA* COMO MODELOS DE ESTUDIO

Los tallos de las plantas son modelos ideales para el estudio de trade-offs y de la integración funcional en general. Estas estructuras tienen un número reducido de tipos celulares y desempeñan tres funciones principales: almacenamiento de productos fotosintéticos y agua, sostén mecánico y conducción de agua. Estas funciones son generalmente llevadas a cabo por diferentes tipos celulares (Fig. 1.1). Puesto que todas las células en la madera derivan de las mismas células meristemáticas cambiales (Carlquist, 2001), hay una competencia fuerte por recursos entre las funciones del tallo, una de las condiciones más importantes para el surgimiento de trade-offs (de Jong and van Noordwijk, 1992; Sinervo et al., 1992; Emlen, 2001). Además de esta competencia, las funciones del tallo son también antagónicas por la naturaleza misma de las células especializadas en llevarlas a cabo. El parénquima, un tejido que almacena una gran cantidad de agua y productos fotosintéticos, es pobre desde el punto de vista mecánico. En consecuencia, además de la competencia por recursos entre el almacenamiento y el sostén mecánico, las células destinadas a almacenar agua y fotosintatos disminuyen el desempeño mecánico de un tallo. Es por esto que las relaciones entre las funciones del tallo pueden ilustrarse a

través de un triángulo (Fig. 1.1, Chave et al., 2009). Una especie ocupará un punto en el triángulo de acuerdo a su combinación particular de requerimientos, en cuanto a las tres tareas mencionadas.

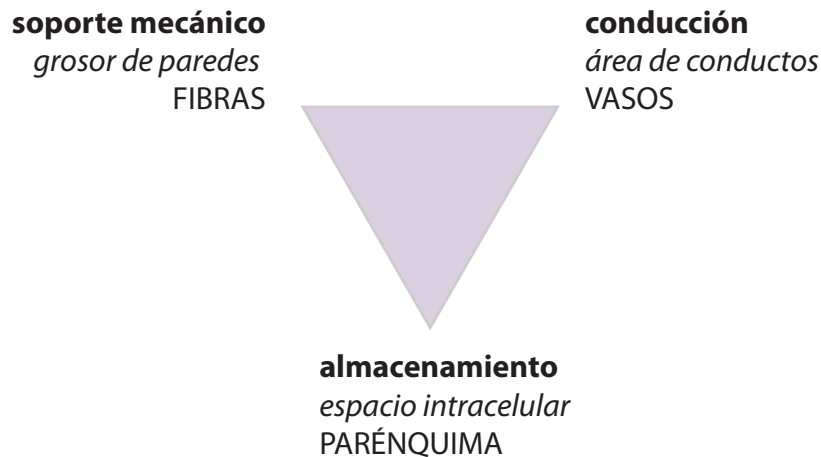


Figura 1.1. El "modelo del triángulo" en la evolución de los tallos leñosos. En los vértices se muestran las tres funciones principales de los tallos (negritas), los tipos celulares especializados para cada función (mayúsculas), y características que tienden a maximizarse (cursivas) con el aumento en el desempeño de cada función.

Trabajos recientes han destinado grandes esfuerzos a la búsqueda de patrones de covariación en los tallos y han detectado trade-offs en la madera a partir de la correlación negativa de variables estructurales y funcionales. Los trade-offs más citados involucran al sostén mecánico y la conductividad (Meinzer et al., 2003; Preston et al., 2006; Sperry et al., 2008), y la eficiencia hidráulica y la seguridad conductiva (Wheeler et al., 2005, Hacke et al., 2006; Sperry et al., 2008). Hasta hace poco, el almacenamiento de agua en los tallos había recibido poca atención (Holbrook, 1995; Bucci et al., 2004; Borchert and Pockman, 2005; Gartner and Meinzer, 2005; Chapotin et al., 2006), por lo que los trade-offs involucrando esta función están comenzándose a revelar, siendo aquel entre la capacitancia (una medida de la capacidad de almacenamiento de los tejidos) o el contenido de agua y la mecánica, a través de la densidad de la madera, uno de los más comúnmente encontrados (Meinzer et al., 2003; Bucci et al., 2004; Pratt et al., 2007a; Scholz et al., 2007; Sperry et al., 2008; Poorter et al., 2010).

Usualmente, estos trabajos realizan búsquedas de covariación entre variables relacionadas con una o dos funciones, y son pocos los que abordan las tres (p.e. Pratt et al., 2007a; Méndez-Alonzo, en revisión). Al mismo tiempo, la mayoría de los estudios abordan esta búsqueda en comunidades vegetales (Choat et al., 2005; Scholz et al., 2007; Meinzer et al., 2008; Onoda et al., 2010), en lugar de clados (p.e. Pratt et al., 2007a,b; Choat, et al., 2007). Sin embargo, utilizar como sistema un clado tiene la ventaja de que las especies parten de un mismo punto al tener un mismo ancestro común (Day y Jayne, 2007). Por ello, las diferencias entre las especies no pueden ser adjudicadas a diferencias entre los linajes, y es más probable que las diferencias reflejen respuestas adaptativas al ambiente. Es precisamente este aspecto el que se explota en este trabajo, pues usando un clado de muy alta diversidad se explora la integración funcional entre las tres funciones del tallo, relacionando el desempeño funcional diferencial con las condiciones ambientales.

Para un estudio de trade-offs e integración funcional en el tallo como el que aquí se propone, es necesario un clado con alta diversidad morfológica y ambiental a nivel interespecífico, y también a nivel interpoblacional, para permitir las comparaciones de los patrones de integración entre niveles evolutivos. El clado *simaruba* de *Bursera* reúne justamente estas características. Contiene un número razonable de especies de muy alta diversidad para el enfoque interespecífico, además de especies de muy amplia distribución como *Bursera simaruba* y *B. grandifolia*, ocupando ambientes muy contrastantes que resultan en diversidad también entre poblaciones (Rosell et al., 2010; Capítulo 1). La gran diversidad morfológica y estructural dentro del clado se asocia a la variación en hábitat (del bosque tropical muy seco a selva alta perennifolia; Capítulo 1 y 2). Las especies son muy diferentes en cuanto a su tamaño (árboles de 3 a 25 m), arquitectura (ramas erectas, curvadas, lianescentes e incluso una epífita), proporción de tejidos (áreas porcentuales de médula, corteza y madera variables), propiedades mecánicas y anatomía.

La variación estructural y ambiental dentro del clado sugiere que las especies ocupan distintos puntos dentro del triángulo de las funciones. Con base en las inferencias del capítulo dos, parece que los ambientes más secos han empujado a las poblaciones hacia el vértice del almacenamiento, a costa de una disminución en la función del sostén mecánico. En las zonas más húmedas, la selección ha impulsado el desplazamiento hacia el vértice del sostén mecánico, a costa del espacio disponible para el almacenamiento. La

exploración de estas negociaciones está incompleta si no se incluye la conductividad hidráulica. La necesidad de mantener un sistema de conducción que maximice la cantidad de agua transportada, sin incrementar excesivamente el riesgo a la cavitación, ejercerá fuerte influencia sobre los límites de la selección sobre el almacenamiento y el sostén mecánico. Por ello, en este capítulo se añade esta función y se completa la tríada funcional de los tallos leñosos.

1.5. HIPÓTESIS Y OBJETIVOS

En este trabajo ponemos a prueba la hipótesis de que los trade-offs entre las tres funciones del tallo son el resultado de fuerte competencia por recursos y antagonismo funcional a nivel individual, y que estas disyuntivas ontogenéticas estarán presentes de igual forma durante el desplazamiento de las diferentes poblaciones y especies hacia otras zonas del triángulo funcional (Fig. 1.1). Como resultado de esto, los patrones de covariación observados entre las poblaciones y entre las especies serán similares a los que emergen a nivel de los individuos. La alta diversidad morfológica y en hábitat del clado *simaruba* permite abarcar un amplio rango de manifestación de los trade-offs en los tallos. Midiendo variables que reflejan el desempeño mecánico, de almacenamiento y conductivo de los tallos, se exploran los patrones de covariación negativa que pudieran indicar trade-offs, y aquellos positivos, que sugerirían la participación de las variables dentro de una misma función.

Los escenarios posibles resultantes de la comparación entre niveles evolutivos tienen diferentes implicaciones para el estudio de trade-offs funcionales y la diversificación morfológica de los tallos. Aunque las comparaciones en este trabajo consideran todas las funciones del tallo simultáneamente, para la ilustración de estos escenarios se maneja el trade-off entre el sostén mecánico y el almacenamiento. Este trade-off puede describirse con una recta de pendiente negativa (Fig. 1.2A; Capítulo 2), indicando un patrón común para todas las especies, y cambio solamente en las combinaciones de desempeño funcional asociado al ambiente que las especies ocupan. La comparación entre niveles podría resultar en patrones equivalentes entre especies, entre poblaciones, e incluso dentro de una misma población, escenario congruente con la hipótesis de este trabajo (Fig. 1.2B). Similitud en

los patrones entre niveles sería el resultado de que la fuerte competencia por recursos y el antagonismo funcional que se presenta a nivel individual, también están presentes en niveles superiores. Aunque la concordancia entre niveles puede ser tomada como evidencia de evolución por deriva (Merilä y Björklund, 1999; Marroig y Cheverud, 2004), en los tallos de las plantas hay argumentos fuertes para postular que esta concordancia sería el resultado de la acción de la selección natural.

En contraste, podría observarse una ausencia de concordancia en los patrones de covariación entre niveles evolutivos. Por ejemplo, si los individuos dentro de las poblaciones analizadas tienen valores muy similares para las dos funciones analizadas por encontrarse sometidos a las mismas condiciones ambientales, no se observará covariación dentro de las poblaciones. Esto no rechazaría la existencia de un trade-off, pero éste será “fijo” (Roff y Fairbairn, 2007) y no será detectable a nivel intrapoblacional (Fig. 1.2C). Otro escenario posible de discordancia entre niveles implicaría que el trade-off no se observa a nivel intrapoblacional, pero tampoco interpoblacional, implicando que la combinación de valores para las dos funciones está fija para toda la especie, y no hay expresión diferencial de las poblaciones, incluso cuando éstas se encuentran ocupando ambientes distintos (Fig. 1.2D). Un escenario de esta naturaleza podría ocurrir cuando una única combinación de valores para los caracteres o las funciones es indispensable, y existen muchos mecanismos homeostáticos para generar dicha combinación, aun en presencia de diferencias ambientales (p.e. Olson et al., 2009). Un último escenario de discordancia sería aquel en donde el signo del patrón de covariación fuera distinto entre cualquiera de los tres niveles. En la Figura 1.2E se ilustra el caso en donde el patrón intrapoblacional tiene un signo positivo en lugar del negativo observado al nivel interpoblacional e interespecífico. Por su naturaleza, este escenario es muy poco probable para el trade-off sostén-almacenamiento. Sin embargo, esta discordancia con cambio en signo podría presentarse entre otras variables funcionales dentro de los tallos leñosos. Por ejemplo, si a nivel intrapoblacional mantener una alometría particular fuera indispensable, pero a nivel interespecífico hubiera fuerte selección independiente de esta relación alométrica.

Todos estos escenarios alternativos tienen implicaciones importantes desde varios puntos de vista. Por ejemplo, si los patrones de covariación se presentan de igual manera entre las especies, entre las poblaciones y también dentro de las poblaciones (Fig. 1.2B), se

sugiere una fuerte restricción en todos los niveles: a pesar de su diversidad, las especies, poblaciones e individuos del clado *simaruba* pueden transitar solamente a lo largo de ciertos trayectos. Un escenario de esta naturaleza también sugeriría que los tallos leñosos en general estarían dirigidos en su diversificación por estos patrones de covariación. Si los trade-offs están fijados o tienen varianza en cualquier dirección dentro de poblaciones (Fig. 1.2C), y también entre poblaciones (Fig. 1.2D), la integración funcional en el tallo sería interpretada como de menor fuerza. Además, si se observara cualquiera de los escenarios, con excepción del primero, existirían diferencias entre niveles jerárquicos en cuanto a la presencia y manifestación de la integración funcional y sugerirían que las generalizaciones entre niveles no deben hacerse de manera automática sin verificar su validez.

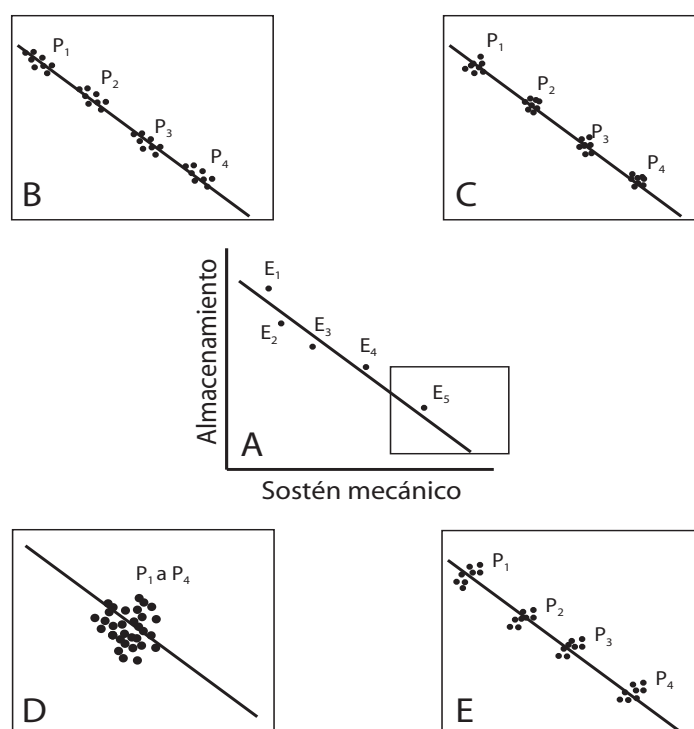


Figura 1.2. Escenarios alternativos al comparar los patrones de covariación entre niveles evolutivos. Se considera el trade-off almacenamiento-mecánica (A). El muestreo de cuatro poblaciones (P_1 a P_4) para la especie 5 (E_5) puede resultar en un patrón de covariación intra e interpoblacional que coincida con el observado entre especies (B). Si el trade-off está “fijo” entre individuos, no se recuperará a nivel intrapoblacional (C) y si está fijo entre poblaciones, tampoco será recuperado a nivel interpoblacional (D). Finalmente, los patrones de covariación pueden ser opuestos entre niveles (E).

2. MATERIALES Y MÉTODOS

2.1. MUESTREO DE ESPECIES Y DE POBLACIONES

Para contar con datos a nivel específico y poblacional, se colectaron ramas de nueve especies dentro del clado *simaruba*, de cuatro poblaciones de *B. grandifolia* y de cuatro más de *B. simaruba* (Tabla 2.1). La colecta poblacional abarcó ambientes contrastantes, reflejados en los rangos de precipitación anual entre sitios. Para *B. grandifolia* este rango abarcó de 817 hasta 1100mm de lluvia, mientras que para *B. simaruba* el rango fue de 785 a 3670mm. Para cada especie o población se colectaron 18 ramas de individuos distintos que fueran rectas, sin ramificación o poco ramificadas, de 150 a 200 cm de largo, y de edades diversas.

Tabla 2.1. Localidades, coordenadas y hábitat de las especies y poblaciones colectadas.

BTC = bosque tropical caducifolio, BTSC= bosque tropical subcaducifolio, BTP = bosque tropical perennifolio.

Población/ Especie	Localidad	Latitud	Longitud	Hábitat
<i>B. arborea</i>	Chamela-Cuixmala, Jalisco	19° 28' 20.52"	104° 58' 22.3"	BTC
<i>B. attenuata</i>	Tepic, Nayarit	21° 31' 10.3"	104° 58' 17.6"	BTSC
<i>B. grandifolia</i>	Chamela-Cuixmala, Jalisco	18° 44' 14.3"	99° 11' 15.5"	BTC
<i>B. grandifolia</i>	Tlaltizapán, Morelos	21° 27' 9.9"	104° 31' 54.7"	BTC
<i>B. grandifolia</i>	Aguamilpas, Nayarit	19° 04' 45.8"	103° 46' 23.2"	BTC
<i>B. grandifolia</i>	Tecomán, Colima	19° 21' 42.12"	104° 55' 41.5"	BTC
<i>B. instabilis</i>	Chamela-Cuixmala, Jalisco	19° 30' 35.73"	105° 02' 12.01"	BTC
<i>B. krusei</i>	Río Papagayo, Guerrero	17° 07' 44.38"	99° 33' 14.74"	BTC
<i>B. laurihuertae</i>	Tehuantepec, Oaxaca	16° 19' 35.8"	95° 18' 5.2"	BTC
<i>B. longipes</i>	Xalitla, Guerrero	18° 0' 12"	99° 32' 37.5"	BTC
<i>B. ovalifolia</i>	Tierra Colorada, Guerrero	17° 07' 47.9"	99° 33' 36.1"	BTC
<i>B. simaruba</i>	La Palma, Guerrero	17° 03' 33.6"	99° 29' 57.8"	BTSC
<i>B. simaruba</i>	Cozumel, Quintana Roo	20° 33' 8.51"	86° 54' 48.5"	BTSC, manglar
<i>B. simaruba</i>	Los Tuxtlas, Veracruz	18° 35' 6.9"	95° 4' 27"	BTP
<i>B. simaruba</i>	Agua Caliente, Jalisco	19° 21' 4.32"	104° 53' 35.52"	BTSC

La colecta se realizó de agosto de 2008 a finales de marzo de 2009, abarcando la temporada de lluvias y la primera parte de la temporada de secas. La colecta terminó mucho antes del brote de las inflorescencias (mayo-junio) y de las hojas (junio-julio), y de que las reservas de carbohidratos y de agua en el tallo y la corteza fueran mermadas por estos eventos (Chapotin et al., 2006; Rojas-Jiménez et al., 2007). No obstante, para explorar posibles diferencias entre los tallos colectados en la época de lluvias y los colectados al comienzo de la época de secas, se compararon los contenidos relativos de agua de la madera y la corteza (ver sección 2.3.2).

2.2. EDAD DE LAS RAMAS Y CÁLCULO DE LAS TASAS DE CRECIMIENTO

La edad de los segmentos procesados para las pruebas funcionales (mecánicas, hidráulicas y de almacenamiento) fue determinada contando las cicatrices del crecimiento anual desde la punta del tallo hasta el punto medio del segmento medido (Rosell y Olson, 2007). Aunque se ha mostrado que la edad no es una variable muy relevante desde el punto de vista mecánico (Rosell y Olson, 2007; Anexo B), sí permitió la estimación de las tasas de crecimiento.

La tasa de crecimiento en longitud se estimó para cada rama midiendo los incrementos de crecimiento anual. La tasa fue calculada como la pendiente del modelo de regresión de la longitud anual acumulada (distancia de la punta del tallo a las cicatrices anuales) con base en la edad. Para tomar en cuenta el que las longitudes anuales acumuladas dentro de una misma rama no son datos independientes, se modelaron los residuos con un modelo autorregresivo de orden uno (Zuur et al., 2009). Las tasas de crecimiento en longitud fueron comparadas entre especies y correlacionadas con las variables ambientales mencionadas en la sección 2.4. Todos los análisis estadísticos en este capítulo fueron realizados en R v.2.9.2 (R Development Core Team, 2009).

2.3. MEDICIÓN DE VARIABLES FUNCIONALES EN LOS TALLOS

Para detectar de mejor manera los trade-offs entre funciones, todas las mediciones funcionales se realizaron sobre los mismos segmentos de rama o sobre las secciones adyacentes. Las variables medidas, sus unidades y su abreviatura se muestran en la Tabla

2.2. Las mediciones funcionales se realizaron inmediatamente después de la colecta, excepto las mecánicas, que se hicieron dentro de los tres días posteriores a la colecta. Para estas mediciones, las ramas fueron mantenidas en refrigeración.

2.3.1. Mediciones de propiedades mecánicas: Módulos elásticos y de ruptura

Las propiedades mecánicas fueron reflejadas a través de los módulos elásticos del segmento completo (E_{estr} , incluyendo la madera y la corteza), de la madera (E_{mad}) y de la corteza (E_{cor}), del módulo de ruptura de la madera (MOR), y de la rigidez a la flexión estructural (EI_{estr}), de la madera (EI_{mad}), y de la corteza (EI_{cor}). Para medir los módulos elásticos se realizaron pruebas de flexión en tres puntos en los segmentos utilizados para la medición de la conductividad hidráulica. Las pruebas fueron realizadas en una máquina universal INSTRON 3345, utilizando una celda de carga de 5kN (Instron Corporation, Canton, MA, USA). Los segmentos tuvieron una relación 20:1 entre la longitud y el diámetro para minimizar la fuerza cortante (Vincent, 1992). El módulo elástico estructural fue estimado a partir de pruebas de flexión de los tallos completos con el programa SYSTEM IX/S INSTRON, que lo calculó como la pendiente de la porción lineal de la gráfica de desplazamiento vs. fuerza aplicada, la longitud de prueba (L) y el momento de inercia (I). Para calcular I , se aproximó la sección transversal del tallo a un círculo (Pisarenko et al., 1979) de radio (R) igual al promedio de los diámetros mayor y menor, tanto apicales como basales de cada segmento. Para el cálculo del módulo elástico de la madera (E_{mad}) se descortezó el segmentos y se repitió la prueba de flexión. A partir de la estimación de E_{estr} y E_{mad} , se calculó la rigidez a la flexión estructural (EI_{estr}) y de la madera (EI_{mad}). El módulo elástico de la corteza (E_{cor}) fue estimado a partir de EI_{cor} que resulta de la diferencia en la rigidez a la flexión del tallo completo y de la madera ($EI_{\text{estr}}-EI_{\text{mad}}$, Niklas, 1999). Finalmente, el módulo de ruptura de la madera (MOR) fue estimado como $(F_{\text{max}} \times L \times R)/4I$, donde F_{max} es la carga máxima aplicada al momento en que la madera falla (Gere y Timoshenko, 1999).

2.3.2. Mediciones de almacenamiento: Contenido de agua, densidad, contenido relativo de agua, volúmenes de agua, material celular y almidón, y capacitancia

Las mediciones relativas al almacenamiento en la madera y la corteza fueron realizadas en un disco de tallo de 1cm de alto tomado de la porción adyacente a la parte basal del segmento utilizado para las mediciones hidráulicas y mecánicas. Los volúmenes de madera y corteza fueron cuantificados usando el principio de Arquímedes (volumen fresco, V_{fresco}) y el peso fresco (W_{fresco}) con una balanza analítica. Posteriormente, ambos tejidos fueron saturados en agua por 24 horas, pesados nuevamente (peso saturado, W_{satur}) y secados en la estufa a 80°C hasta alcanzar un peso constante (W_{seco}). El volumen en base seca (V_{seco}) solamente fue determinado para la madera, resultando imposible medirlo con precisión para la corteza que se enrolla con el secado.

El contenido de agua en la madera y la corteza (CA_{mad} , CA_{cor}), expresado como el porcentaje de agua por unidad de peso de tejido seco, fue estimado como:

$$CA (\%) = 100 \times (W_{\text{fresco}} - W_{\text{seco}}) / W_{\text{seco}}$$

La densidad de la madera (D_{mad}) fue calculada en base seca, mientras que la de la corteza (D_{cor}) fue medida en base fresca:

$$D_{\text{mad}} (\text{g/cm}^3) = W_{\text{seco}} / V_{\text{seco}}$$

$$D_{\text{cor}} (\text{g/cm}^3) = W_{\text{fresco}} / V_{\text{fresco}}$$

El contenido relativo de agua de la madera y la corteza (CRA_{mad} , CRA_{cor}), que refleja la cantidad de agua en estos tejidos al momento de la colecta, respecto de la cantidad de agua que podrían contener en base saturada, fue calculado como sigue:

$$CRA (\%) = 100 \times (W_{\text{fresco}} - W_{\text{seco}}) / ((W_{\text{satur}} - W_{\text{seco}}) \times D_{\text{agua}})$$

Los volúmenes porcentuales de agua (V_a) y de material celular (paredes celulares y almidón, V_p) fueron calculados para la madera y la corteza como:

$$V_a (\%) = 100 \times (W_{\text{fresco}} - W_{\text{seco}}) / (V_{\text{fresco}} \times D_{\text{agua}})$$

$$V_p (\%) = 100 \times (W_{\text{seco}}) / (V_{\text{fresco}} \times D_{\text{par/alm}})$$

La densidad de pared y almidón ($D_{\text{par/alm}}$) fue obtenida promediando la densidad de la pared celular hecha de lignina (1.53 g/cm³, Siau, 1984) y la densidad del almidón (1.55 g/cm³, Isleib, 1957; International Starch Institute). La densidad del agua (D_{agua}) fue considerada como 1 g/cm³. Aunque V_p fue calculado también para la corteza, es probable

que el cálculo esté subestimado, pues la densidad de las paredes primarias de celulosa presentes en la corteza es menor a la densidad de paredes lignificadas.

Las áreas porcentuales de madera ($\%_{\text{mad}}$) y de corteza ($\%_{\text{cor}}$) fueron calculadas con respecto al total del tallo a partir de la medición promedio de los diámetros de cada tejido en los extremos basal y apical de cada segmento.

Finalmente, la capacitancia de la madera (C_{mad}) fue medida sobre los tallos recién colectados para determinar la facilidad con la que este tejido pierde el agua almacenada. Para cuantificar esta variable, se tomaron discos de 8x5mm, dimensiones máximas impuestas por las cámaras Wescor C-52 (Wescor Inc., Logan, UT, USA) utilizadas para medir el potencial hídrico. Cada muestra se saturó en agua por dos horas, fue pesada (W_{capsatur}) y colocada en la cámara, misma que fue conectada a un psicrómetro Wescor. De acuerdo con pruebas preliminares, la temperatura y la humedad dentro de la cámara se estabilizaron una o dos horas después de su cierre, por lo que transcurrido ese tiempo se realizó la medición del potencial hídrico utilizando el método de punto de rocío. Posteriormente se pesó la muestra ($W_{\text{capfresco}}$) y se dejó secar a temperatura ambiente por dos horas. Transcurrido ese tiempo se introdujo de nuevo en la cámara para repetir la medición de potencial hídrico. Este ciclo se repitió cuatro o cinco veces por muestra, hasta alcanzar potenciales hídricos entre -5 y -7 MPa, según la especie. Cada muestra fue pesada después de haber sido secada en la estufa a 80°C por dos días (W_{capseco}). El psicrómetro fue calibrado antes de iniciar cada serie de mediciones usando una solución salina de potencial conocido. Para cada punto de medición de potencial se calculó el CRA de los discos de madera como $(W_{\text{capfresco}} - W_{\text{capseco}})/(W_{\text{capsatur}} - W_{\text{capseco}})$. C_{mad} fue calculada como la pendiente de la recta de cambio en $\log_{10}\text{CRA}$ y cambio en potencial hídrico. Se procesaron de 10 a 18 fragmentos procesados por especie o población.

2.3.3. Mediciones de conductividad hidráulica: eficiencia conductiva y vulnerabilidad a la cavitación

Los segmentos para estas mediciones fueron cortados sumergiendo las ramas recién colectadas en agua y tuvieron un largo de 25cm y un diámetro de 13mm, dimensiones que corresponden al largo mínimo y ancho máximo posible para el uso de las mangas de

presión que permiten inducir la cavitación y estimar la vulnerabilidad de los tallos a experimentar este evento de manera natural. Los segmentos fueron sometidos a una inyección de una solución desgasificada, filtrada ($0.2 \mu\text{m}$) y acidificada con HCl ($\text{pH}=3.0$) por 10 minutos usando una presión de 1.5 bares (0.15MPa). Con esta inyección se revirtió la cavitación nativa en los tallos rellenando los conductos con agua. Después de esta inyección, la conductividad hidráulica fue medida utilizando un aparato de Sperry (Sperry et al. 1988), aplicando una presión de 5-10 kPa. El flujo de agua fue cuantificado con ayuda de una balanza analítica y un cronómetro. El ciclo de inyección a 1.5 bares fue repetido hasta que no hubo incrementos significativos en la conductividad, lo que ocurrió usualmente después de dos o tres ciclos. Esta conductividad máxima fue dividida entre el área de xilema para obtener la conductividad específica máxima (k_{max}), una medida de la eficiencia conductiva.

Para determinar la vulnerabilidad a la cavitación de los tallos, estimamos la presión necesaria para alcanzar un 50% de pérdida en la conductividad hidráulica (P50). Para ello se construyeron curvas de vulnerabilidad utilizando el método de inyección de aire en los tallos (Sperry y Saliendra, 1994). Los mismos tallos utilizados para la medición de k_{max} fueron sometidos a una inyección de aire (nitrógeno), a una presión de 2 bares (0.2MPa) por 10 minutos utilizando mangas de presión y tapones de goma. Posteriormente, la conductividad fue medida en el tallo y el porcentaje de pérdida en conductividad fue calculado con respecto a k_{max} . El ciclo de inyección fue repetido cuatro veces más a intervalos variables para los diferentes tallos hasta alcanzar los 20 bares (2MPa). Para calcular P50, se calculó el valor medio de porcentaje de pérdida en conductividad por nivel de presión por población o especie y se graficó contra la presión de aire aplicada. Aquellos tallos con valores de pérdida $>90\%$ después de la primera inyección, o que no mostraron una disminución en la conductividad, fueron eliminados del ajuste (13% del total de tallos medidos). El cálculo de P50 se realizó a partir de los datos de al menos 10 ramas por especie. Una curva tipo Michaelis-Menten fue ajustada a los datos de cada población utilizando la función para cuadrados mínimos no lineales nls en R y añadiendo la coordenada (0,0) al conjunto de datos (sin pérdida de conductividad cuando no se ha inyectado aire). El valor de presión al cual se alcanza una pérdida de 50% en la

conductividad (P50) fue determinado a partir del modelo ajustado para cada especie o población.

Tabla 2.2. Variables funcionales medidas en los tallos del clado *simaruba*. Se incluye la función o funciones con las que la variable está más asociada. M = mecánica, A = almacenamiento, C = conductividad.

Variable	Etiqueta	Función
Rigidez a la flexión estructural (MNm ²)	EI _{estr}	M
Rigidez a la flexión de la madera (MNm ²)	EI _{mad}	M
Rigidez a la flexión de la corteza (MNm ²)	EI _{cor}	M
Módulo elástico estructural (MPa)	E _{estr}	M
Módulo elástico de la madera (MPa)	E _{mad}	M
Módulo elástico de la corteza (MPa)	E _{cor}	M
Módulo de ruptura de la madera (MPa)	MOR	M
Densidad de la madera (gcm ⁻³)	D _{mad}	M, A
Densidad de la corteza (gcm ⁻³)	D _{cor}	M, A
Contenido de agua de la madera (%)	CA _{mad}	A
Contenido de agua de la corteza (%)	CA _{cor}	A
Volumen porcentual de pared y almidón en la madera (%)	V _{pmad}	M, A
Volumen porcentual de agua en la madera (%)	V _{amad}	A
Volumen porcentual de pared en la corteza (%)	V _{pcor}	M
Volumen porcentual de agua en la corteza (%)	V _{acor}	A
Capacitancia de la madera ($\Delta \log_{10} CA / \Delta \Psi$)	C _{mad}	A
Conductividad específica máxima (gs ⁻¹ MPa ⁻¹)	K _{max}	C
Vulnerabilidad al embolismo (MPa)	P50	C
Área porcentual de la madera (%)	% _{mad}	M, A
Área porcentual de la corteza (%)	% _{cor}	M, A

2.4. EXTRACCIÓN DE VARIABLES AMBIENTALES

Se extrajeron 19 variables ambientales de la base WorldClim v.1.4 (Hijmans et al., 2005) a partir de las coordenadas de colecta de las poblaciones o especies (Tabla 2.3).

Tabla 2.3. Variables climáticas extraídas para cada población y especie.

Variables de temperatura	Variables de precipitación
Temperatura media anual	Precipitación anual
Rango diario de temperatura	Precipitación del mes más húmedo
Isotermalidad	Precipitación del mes más seco
Estacionalidad en la temperatura	Estacionalidad en la precipitación
Temperatura máxima del mes más cálido	Precipitación del cuarto más húmedo
Temperatura mínima del mes más frío	Precipitación del cuarto más seco
Rango anual de temperatura	Precipitación del cuarto más cálido
Temperatura media del cuarto más húmedo	Precipitación del cuarto más frío
Temperatura media del cuarto más seco	
Temperatura media del cuarto más cálido	
Temperatura media del cuarto más frío	

2.5. COMPARACIÓN DE PATRONES DE COVARIACIÓN ENTRE NIVELES EVOLUTIVOS

Las comparaciones entre niveles evolutivos se realizaron para las 20 variables funcionales medidas y para un subconjunto de siete variables que reflejan las tres funciones principales de la madera. Las comparaciones incluyeron (1) los niveles *intrapoblacional* vs. *interpoblacional*, al contrastar los patrones de covariación entre las cuatro poblaciones de *B. grandifolia* (matrices intrapoblacionales) y repetir el procedimiento para las cuatro poblaciones de *B. simaruba*, y (2) los niveles *intraespecífico* vs. *interespecífico*, al comparar los patrones al interior de cada especie (matrices intraespecíficas) y aquellos descritos por las matriz de medias entre especies (matriz interespecífica, Figura 2.1). Para todo lo relativo al nivel de especie se usó la población de Colima como representante de *B. grandifolia* y la de Veracruz como representante de *B. simaruba*.

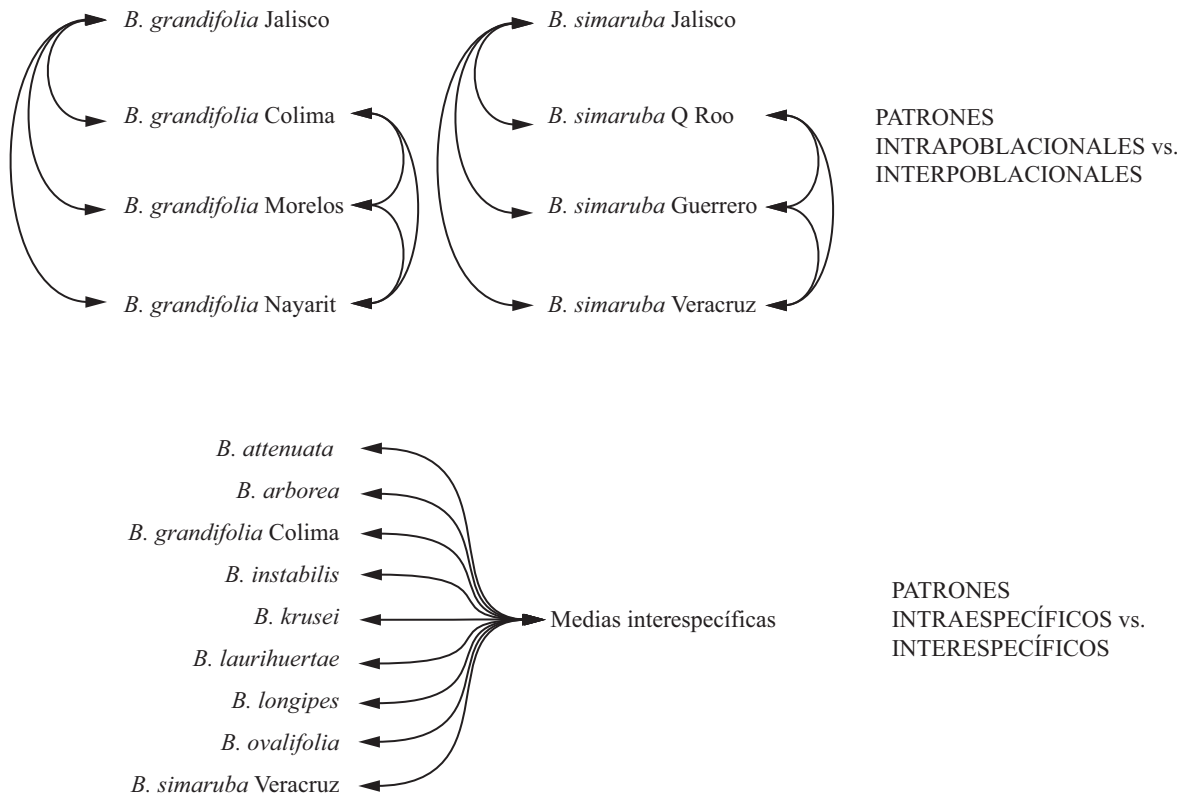


Figura 2.1. Comparación de los patrones de integración entre niveles evolutivos. Las comparaciones interpoblacionales se realizaron entre las cuatro poblaciones de *B. grandifolia* y *B. simaruba* (n=18). Las comparaciones interespecíficas se efectuaron entre los datos intraespecíficos (n=18) y las medias por especie (n=9). Estas comparaciones se aplicaron al conjunto de todas las variables funcionales y al conjunto de siete variables funcionales de la madera.

2.5.1. Comparación de los patrones de covariación entre todas las variables funcionales medidas

Para todas las variables funcionales se contó con valores para cada segmento y para cada población o especie, excepto en el caso de P50, para la que únicamente existe el dato poblacional o específico. Es por ello que P50 fue excluida de estas comparaciones y únicamente es tomada en cuenta en el análisis de los trade-offs a partir de las medias por especie. Los patrones de covariación incluyendo todas las variables funcionales medidas se compararon a través de los coeficientes de correlación observados entre parejas de

matrices. Para ello se calculó la correlación entre los coeficientes de correlación de una matriz y los coeficientes equivalentes en la segunda matriz (Merilä y Björklund, 1999; Eroukhmanoff y Svensson, 2008). Estas comparaciones pareadas se llevaron a cabo entre las poblaciones de *B. grandifolia*, entre las poblaciones de *B. simaruba*, y entre cada especie o población y la matriz interespecífica basada en las medias por especie (Fig. 2.1). Para cada correlación entre coeficientes de Pearson se estimó un intervalo de confianza. Puesto que la matriz interespecífica y las matrices intraespecíficas no son independientes, el intervalo de confianza de las correlaciones involucrando la matriz interespecífica fue estimado con un procedimiento bootstrap (Manly, 2007) utilizando el paquete boot v.1.2-41 en R (Canty y Ripley, 2009).

2.5.2. Comparación de los patrones de covariación entre siete variables funcionales de la madera

Una comparación más detallada de los patrones de covariación se realizó sobre un subconjunto de siete variables funcionales de la madera que reflejaron las tres funciones principales del tallo: E_{mad} y MOR representaron el sostén mecánico; D_{mad} y V_{pamad} reflejaron la capacidad de sostén, pero también el almacenamiento; CA_{mad} y C_{mad} informaron sobre la capacidad de almacenamiento de agua; la conductividad fue incluida a través de K_{max} . Nuevamente, las comparaciones se realizaron entre las poblaciones de *B. grandifolia* y *B. simaruba*, y contrastando las matrices intraespecíficas con la interespecífica (Fig. 2.1).

Las matrices fueron comparadas a través del modelo CPC (Phillips y Arnold, 1999) y del método de jackknife-MANOVA (Roff, 2002; Apéndice A). Estos métodos dieron información complementaria y contribuyeron a fortalecer la inferencia de similitud o disimilitud entre las matrices (Apéndice A). Aunque se han implementado sobre matrices de correlación (p.e. Eroukhmanoff y Svensson, 2008), estos métodos parecen funcionar mejor sobre matrices de varianzas y covarianzas (Phillips y Arnold, 1999). Para disminuir la heteroscedasticidad de algunas variables (Roff, 2002), y el efecto de las diferentes escalas de medición, se calcularon las matrices de varianzas y covarianzas sobre datos transformados logarítmicamente. Previamente se verificó que las matrices de correlación

con los datos crudos y transformados logarítmicamente fueran muy similares. El modelo CPC fue implementado con el programa CPC de Phillips (Phillips y Arnold, 1999).

Para el método jackknife-MANOVA se generaron matrices de pseudovalores para las varianzas y covarianzas y posteriormente se compararon los grupos utilizando un MANOVA y la estadística de Wilks. Cuando se detectaron diferencias significativas, se procedió a ubicar la(s) variable(s) y el (los) grupo(s) responsable(s) de dicha diferencia utilizando análisis de varianza y pruebas de Tukey. Cuando se detectaron niveles fuertes de heteroscedasticidad entre las variables a través de la prueba de Levene, las comparaciones se realizaron con un MANOVA no paramétrico (Anderson, 2001), pruebas de Kruskal-Wallis y pruebas posthoc no paramétricas de Behrens-Fisher (Munzel y Hothorn, 2001). Las comparaciones intra e interpoblacionales se realizaron incluyendo las cuatro poblaciones de *B. grandifolia* y *B. simaruba* simultáneamente. Las comparaciones entre las matrices intraespecífica y la interespecífica se realizaron pareadamente y únicamente para las covarianzas (no para las varianzas), dado que la matriz interespecífica solamente contó con datos. Dado que el interés es comparar las covarianzas, eliminar las varianzas de la comparación no tuvo ningún efecto en la interpretación. Para las pruebas no paramétricas se utilizaron los paquetes *vegan* v.1.15-4 (Oksanen et al., 2009) y *npmc* v.1.0-7 (Helms y Munzel, 2008) en R.

2.6. DETECCIÓN DE CONJUNTOS DE COVARIACIÓN FUNCIONAL DE LA MADERA Y ASOCIACIÓN DE ESTOS CONJUNTOS CON VARIABLES AMBIENTALES

Con el objetivo de detectar conjuntos de covariación funcional en la madera, se realizaron análisis de componentes principales (PCA) sobre cada matriz de correlación intraespecífica e intrapoblacional. La tendencia a la agrupación de caracteres se exploró a través de las variables incluidas en cada componente principal. Estos conjuntos se compararon con los detectados por un PCA sobre la matriz de correlación interespecífica. La recuperación de conjuntos de covariación similares implicaría patrones similares entre niveles evolutivos.

Aunque los patrones de covariación funcional sean similares entre especies, los valores mismos de desempeño de las diferentes funciones pueden variar entre especies de

acuerdo al ambiente que éstas ocupan. Si existe esta asociación con variables ambientales, se puede inferir que las combinaciones en los valores de desempeño podrían representar adaptaciones. Para poner a prueba esta idea, los dos primeros PCs de la matriz de correlación interespecífica fueron correlacionados con variables ambientales.

3. RESULTADOS

3.1. TASAS DE CRECIMIENTO Y SU RELACIÓN CON VARIABLES AMBIENTALES

Algunas ramas de *B. ovalifolia* y *B. simaruba* correspondieron al brote del último año, por lo que fue imposible calcular su tasa de crecimiento en longitud. Las medias de la tasa de crecimiento por especie o población se muestran en la Tabla 3.1. Una prueba de Kruskal-Wallis detectó diferencias en las tasas de al menos una especie ($\chi^2_{13g.l.}=74.41$, $p<0.0001$). Las especies con tasas más extremas fueron las que tendieron a presentar las diferencias, en particular *B. instabilis* y *B. simaruba*-Quintana Roo, especies de rápido crecimiento, y *B. laurihuertae*, *B. grandifolia*-Jalisco y *B. simaruba*-Guerrero, especies de crecimiento más lento. Las tasas se correlacionaron con la precipitación del mes más húmedo ($r=0.659$, $p<0.05$) y del cuarto más húmedo ($r=0.668$, $p<0.05$).

Tabla 3.1. Tasas de crecimiento en longitud (cm/año) por especie o población.

Pob/Especie	Tasa	Pob/Especie	Tasa
<i>B. arborea</i>	0.416	<i>B. laurihuertae</i>	0.270
<i>B. attenuata</i>	0.464	<i>B. longipes</i>	0.476
<i>B. grandifolia</i> -Jalisco	0.386	<i>B. ovalifolia</i>	0.595
<i>B. grandifolia</i> -Colima	0.429	<i>B. simaruba</i> -Jalisco	0.548
<i>B. grandifolia</i> -Morelos	0.412	<i>B. simaruba</i> -Quintana Roo	0.746
<i>B. grandifolia</i> -Nayarit	0.404	<i>B. simaruba</i> -Guerrero	0.343
<i>B. instabilis</i>	0.707	<i>B. simaruba</i> -Veracruz	0.711
<i>B. krusei</i>	0.557		

3.2. MEDICIÓN DE LAS VARIABLES FUNCIONALES

Se midieron variables funcionales en 270 segmentos con diámetros de 1-1.3cm, pero con alta variación en edad y posición relativa respecto de la punta de la rama, dadas las diferencias en tasas de crecimiento y alometría en las ramas del clado (Capítulo 2). Las edades promedio de los segmentos fluctuaron entre 1.3 años en *B. ovalifolia* y 12.6 en *B. longipes*, y la distancia promedio a la punta de la rama fue de 0.40 cm para *B. grandifolia* de Morelos y 0.98 cm para *B. grandifolia* de Nayarit.

Los valores promedio para cada variable funcional se muestran en la Tabla 3.2. La estimación de las variables funcionales fue directa, excepto en el caso de la capacitancia (C_{mad}) y la vulnerabilidad al embolismo (P50), que provienen de ajustes estadísticos. Los modelos lineales para el cálculo de C_{mad} tuvieron un coeficiente de determinación entre 0.75 y 0.99. Los ajustes de una curva no lineal para el cálculo de P50 alcanzaron convergencia rápidamente (pocos pasos) y se muestran en el Apéndice B.

Tabla 3.2. Valores promedio de las variables funcionales medidas en los tallos para cada especie y población medida (n=18).

Especie/Población	E_{estr}	E_{mad}	E_{cor}	MOR	EI_{estr}	EI_{mad}	EI_{cor}	$\%_{mad}$	$\%_{cor}$
<i>B. arborea</i>	3485.2	5995.2	1252.3	27.2	3.11E-06	2.54E-06	5.76E-07	65.5	31.8
<i>B. attenuata</i>	1831.5	4669.2	587.5	35.8	2.33E-06	1.92E-06	4.98E-07	51.1	43.8
<i>B. grandifolia</i> -Jal	2835.6	5167.2	924.1	38.1	2.92E-06	2.43E-06	4.95E-07	63.5	32.2
<i>B. grandifolia</i> -Col	2439.7	5218.8	589.8	34.2	3.12E-06	2.71E-06	4.37E-07	54.9	36.6
<i>B. grandifolia</i> -Mor	1109.4	3185.8	548.9	18.3	1.01E-06	6.50E-07	3.96E-07	37.5	52.2
<i>B. grandifolia</i> -Nay	2391.7	5346.5	431.4	45.7	4.22E-06	3.86E-06	4.16E-07	60.7	36.0
<i>B. instabilis</i>	2259.1	4256.9	801.0	21.2	2.12E-06	1.69E-06	4.34E-07	62.2	35.2
<i>B. krusei</i>	2674.8	5171.3	1216.2	27.3	1.64E-06	1.21E-06	4.28E-07	56.3	37.8
<i>B. laurihuertae</i>	1952.2	4881.4	553.4	27.1	1.34E-06	1.11E-06	2.47E-07	56.3	42.4
<i>B. longipes</i>	1231.3	3143.2	616.4	26.8	8.96E-07	6.05E-07	3.07E-07	46.5	49.9
<i>B. ovalifolia</i>	1875.1	3225.1	896.0	18.0	1.86E-06	1.39E-06	4.72E-07	57.1	33.7
<i>B. simaruba</i> -Jal	1896.1	3641.2	677.0	33.5	2.70E-06	2.20E-06	4.94E-07	54.5	35.6
<i>B. simaruba</i> -QRoo	2266.5	4705.3	884.8	21.1	1.96E-06	1.54E-06	4.60E-07	54.7	38.8
<i>B. simaruba</i> -Gro	2505.5	5305.8	752.9	23.5	2.18E-06	1.92E-06	3.63E-07	52.8	35.6
<i>B. simaruba</i> -Ver	1817.5	4230.5	504.4	37.8	2.41E-06	2.03E-06	4.13E-07	48.9	40.9

Especie/Población	D_{mad}	D_{cor}	CA_{mad}	CA_{cor}	V_{pmad}	V_{amad}	V_{pcor}	V_{acor}	K_{max}	C_{mad}	P50
<i>B. arborea</i>	0.46	1.05	111.6	365.3	26.7	46.4	15.1	81.7	0.023	0.146	0.708
<i>B. attenuata</i>	0.42	1.04	129.2	368.1	25.0	48.1	14.7	81.3	0.037	0.175	0.231
<i>B. grandifolia</i> -Jal	0.49	1.08	93.0	288.4	29.3	41.5	18.4	79.5	0.029	0.149	0.726
<i>B. grandifolia</i> -Col	0.44	1.08	108.5	268.0	25.9	42.8	19.6	77.6	0.047	0.147	0.310
<i>B. grandifolia</i> -Mor	0.44	0.95	118.0	293.9	25.9	46.4	15.9	70.3	0.014	0.169	0.597
<i>B. grandifolia</i> -Nay	0.53	1.06	107.7	314.0	29.4	47.3	17.2	80.0	0.039	0.142	0.317
<i>B. instabilis</i>	0.45	1.07	109.8	388.6	26.9	44.8	14.8	84.6	0.031	0.170	0.284
<i>B. krusei</i>	0.42	1.08	123.2	339.9	24.6	48.3	17.1	78.9	0.026	0.211	0.678
<i>B. laurihuertae</i>	0.47	0.98	129.9	333.0	27.4	53.8	15.3	74.2	0.019	0.143	0.581
<i>B. longipes</i>	0.48	1.08	95.9	132.2	29.6	43.1	30.7	61.2	0.017	0.145	0.699
<i>B. ovalifolia</i>	0.34	1.01	159.4	405.3	20.1	47.5	13.5	80.4	0.032	0.217	0.672
<i>B. simaruba</i> -Jal	0.45	1.09	104.5	214.1	27.6	42.3	23.6	72.7	0.034	0.168	0.387
<i>B. simaruba</i> -QRoo	0.38	1.03	170.9	396.9	22.1	56.7	13.7	82.4	0.027	0.149	0.790
<i>B. simaruba</i> -Gro	0.38	0.98	124.9	255.9	22.7	43.2	19.6	70.8	0.039	0.175	0.170
<i>B. simaruba</i> -Ver	0.51	1.10	96.5	272.0	31.2	44.0	19.7	79.9	0.026	0.169	0.519

En cuanto al uso del contenido relativo de agua como indicador de diferencias entre épocas de colecta, no se detectó ninguna tendencia a que los tallos colectados durante las lluvias tuvieran niveles más altos de contenido de agua que aquellos colectados ya iniciada la época de secas.

3.3. CORRELACIONES Y TRADE-OFFS ENTRE LAS VARIABLES FUNCIONALES

3.3.1. *Correlaciones y trade-offs entre todas las variables funcionales (madera, corteza y tallo)*

Con base en las medias para las 15 poblaciones o especies colectadas, se detectaron numerosas asociaciones entre las variables funcionales de la madera, la corteza y del tallo (Tabla 3.3). Existe fuerte covariación positiva entre las variables relacionadas con una misma función, p.e. entre variables relacionadas con el sostén mecánico, como los diferentes módulos elásticos, la rigidez a la flexión, MOR, D_{mad} y V_{pamad} . De igual manera, existe asociación positiva entre variables relacionadas con el almacenamiento como CA_{mad} , V_{amad} y C_{mad} , aunque para esta última variable las correlaciones no son altas ni significativas. En contraste, las variables relacionadas con la conductividad, K_{max} y P50, tienen una fuerte covariación negativa, implicando un trade-off entre la seguridad y la eficiencia en la conducción del agua.

Las correlaciones entre variables que reflejan diferentes funciones suelen ser negativas, sugiriendo la presencia de trade-offs. Así, variables mecánicas como D_{mad} , D_{cor} , V_{pamad} , V_{pcor} covarían de manera inversa con el contenido de agua y C_{mad} , aunque no siempre con valores significativos de correlación. K_{max} casi no presentó correlaciones significativas con las otras funciones, salvo para el caso de la rigidez a la flexión. Lo mismo sucedió con P50. Hubo correspondencia entre las propiedades mecánicas y de almacenamiento entre la madera y la corteza, pero no siempre fueron significativas las correlaciones.

Tabla 3.3. Correlaciones entre todas las variables funcionales basadas en los valores medios por especie o población (n=15). Los coeficientes de correlación de Pearson se muestran debajo de la diagonal y los valores de significancia se muestran por encima. Se resaltan las correlaciones significativas a un nivel $\alpha=0.05$.

	E_{estr}	E_{mad}	E_{cor}	MOR	EI_{estr}	EI_{mad}	EI_{cor}	%_{mad}	%_{cor}	D_{mad}	D_{cor}	CA_{mad}	CA_{cor}	V_{pmad}	V_{amad}	V_{pcor}	V_{acor}	K_{max}	C_{mad}	P50
E_{estr}	-	0.00	0.01	0.44	0.02	0.02	0.05	0.00	0.00	0.97	0.37	0.89	0.18	0.79	0.94	0.22	0.03	0.22	0.69	0.88
E_{mad}	0.87	-	0.20	0.14	0.02	0.01	0.37	0.01	0.03	0.60	0.69	0.81	0.30	0.87	0.67	0.23	0.08	0.18	0.25	0.58
E_{cor}	0.67	0.35	-	0.19	0.92	0.74	0.05	0.05	0.05	0.14	0.66	0.41	0.15	0.15	0.74	0.33	0.22	0.61	0.20	0.06
MOR	0.22	0.40	-0.36	-	0.00	0.00	0.60	0.36	0.48	0.00	0.03	0.03	0.31	0.01	0.26	0.40	0.59	0.11	0.15	0.28
EI_{estr}	0.61	0.61	-0.03	0.72	-	0.00	0.04	0.02	0.01	0.19	0.11	0.33	0.66	0.37	0.37	0.60	0.05	0.01	0.27	0.18
EI_{mad}	0.58	0.62	-0.09	0.74	1.00	-	0.09	0.02	0.01	0.16	0.15	0.31	0.75	0.33	0.39	0.65	0.08	0.00	0.21	0.13
EI_{cor}	0.52	0.25	0.52	0.15	0.54	0.46	-	0.11	0.03	0.56	0.21	0.88	0.15	0.54	0.53	0.23	0.02	0.24	0.55	0.82
%_{mad}	0.84	0.64	0.52	0.25	0.61	0.59	0.43	-	0.00	0.77	0.18	0.95	0.11	0.99	0.94	0.24	0.01	0.20	0.67	0.93
%_{cor}	-0.82	-0.57	-0.52	-0.20	-0.67	-0.64	-0.56	-0.88	-	0.62	0.23	0.84	0.17	0.52	0.61	0.25	0.01	0.03	0.71	0.75
D_{mad}	-0.01	0.15	-0.40	0.71	0.36	0.39	-0.16	0.08	0.14	-	0.11	0.00	0.11	0.00	0.27	0.17	0.67	0.55	0.01	0.86
D_{cor}	0.25	0.11	0.12	0.57	0.43	0.39	0.34	0.36	-0.33	0.43	-	0.06	0.37	0.05	0.14	0.12	0.42	0.30	0.75	0.96
CA_{mad}	-0.04	-0.07	0.23	-0.57	-0.27	-0.28	0.04	-0.02	-0.06	-0.80	-0.50	-	0.01	0.00	0.00	0.02	0.29	0.97	0.17	0.43
CA_{cor}	0.36	0.29	0.39	-0.28	0.12	0.09	0.39	0.43	-0.38	-0.43	-0.25	0.65	-	0.04	0.02	0.00	0.00	0.78	0.24	0.73
V_{pmad}	-0.07	0.04	-0.39	0.66	0.25	0.27	-0.17	0.00	0.18	0.97	0.51	-0.86	-0.54	-	0.12	0.06	0.48	0.46	0.03	0.92
V_{amad}	-0.02	0.12	0.09	-0.31	-0.25	-0.24	-0.18	0.02	0.14	-0.31	-0.40	0.78	0.61	-0.42	-	0.02	0.28	0.29	0.94	0.21
V_{pcor}	-0.33	-0.33	-0.27	0.24	-0.15	-0.13	-0.33	-0.32	0.32	0.37	0.42	-0.60	-0.95	0.50	-0.58	-	0.00	0.78	0.36	0.94
V_{acor}	0.56	0.46	0.34	0.15	0.51	0.47	0.61	0.62	-0.62	-0.12	0.22	0.29	0.84	-0.20	0.30	-0.78	-	0.19	0.55	0.86
K_{max}	0.33	0.36	-0.14	0.42	0.68	0.69	0.32	0.35	-0.56	-0.17	0.29	0.01	0.08	-0.21	-0.29	-0.08	0.36	-	0.78	0.00
C_{mad}	-0.11	-0.31	0.35	-0.39	-0.31	-0.34	0.17	-0.12	-0.11	-0.62	-0.09	0.37	0.32	-0.57	-0.02	-0.26	0.17	0.08	-	1.00
P50	0.04	-0.16	0.49	-0.30	-0.36	-0.41	0.06	0.02	0.09	-0.05	0.01	0.22	0.10	-0.03	0.34	-0.02	-0.05	-0.69	0.00	-

3.3.2. Correlaciones y trade-offs entre siete variables funcionales de la madera

La matriz de correlación basada en las medias por especie para las siete variables de la madera se presenta en la Tabla 3.4. Las matrices correspondientes a cada población y especie por separado se incluyen en el Apéndice C. La matriz interespecífica, y también las intrapoblacionales e intraespecíficas (Apéndice C), muestran trade-offs entre las propiedades mecánicas y el contenido de agua, que se traducen en covariaciones negativas de las variables D_{mad} , V_{pmad} y MOR con índices de almacenamiento de agua como CA_{mad} y C_{mad} , aunque aquellas relaciones con MOR no son significativas. La variable mecánica E_{mad} presentó asociaciones en este mismo sentido con variables de almacenamiento, pero de baja magnitud y no significativas en la matriz interespecífica (Tabla 3.4), pero cobran más fuerza en algunas poblaciones y especies (Apéndice C). No se detectaron trade-offs entre la conductividad, a través de K_{max} , y las otras variables, salvo en el caso de *B. simaruba*-Guerrero (Apéndice C). Usualmente K_{max} no covaría fuertemente con ninguna otra variable, exceptuando P50, con quien parece tener un fuerte trade-off.

Tabla 3.4. Correlaciones entre las siete variables que reflejan las tres funciones principales de la madera. Esta matriz está basada en las medias por especie (n=9). Se muestran en la diagonal inferior los coeficientes de correlación de Pearson y en la diagonal superior los valores de significancia. Se resaltan las correlaciones significativas a un nivel $\alpha=0.10$.

	E_{mad}	MOR	D_{mad}	CA_{mad}	V_{pmad}	K_{max}	C_{mad}	P50
E_{mad}	-	0.358	0.664	0.708	0.880	0.690	0.459	0.766
MOR	0.348	-	0.142	0.168	0.134	0.502	0.345	0.295
D_{mad}	0.169	0.530	-	0.002	0.000	0.234	0.020	0.933
CA_{mad}	-0.146	-0.503	-0.869	-	0.001	0.649	0.065	0.776
V_{pmad}	0.059	0.539	0.988	-0.897	-	0.265	0.041	0.933
K_{max}	0.155	0.259	-0.442	0.177	-0.416	-	0.624	0.030
C_{mad}	-0.284	-0.358	-0.750	0.637	-0.686	0.190	-	0.711
P50	-0.116	-0.393	-0.033	0.111	-0.033	-0.715	0.144	-

3.4. CORRELACIÓN ENTRE LAS SIETE VARIABLE FUNCIONALES DE LA MADERA Y LAS VARIABLES AMBIENTALES

Las correlaciones entre las variables funcionales y las ambientales considerando nueve especies se muestran en la Tabla 3.5. Existieron asociaciones importantes entre las variables funcionales y las variables de precipitación y temperatura, y en menor medida con las variables que reflejan rangos ambientales.

Tabla 3.5. Correlaciones entre las variables funcionales de la madera y variables ambientales. Se resaltan las correlaciones significativas a un nivel $\alpha=0.10$. T = temperatura, máx = máximo, mín = mínimo, ppt = precipitación.

Variable ambiental	E_{mad}	MOR	D_{mad}	CA_{mad}	V_{pamad}	K_{max}	C_{mad}	P50
T media anual	-0.126	-0.673	-0.252	0.269	-0.257	-0.407	0.283	0.742
Rango medio diurno de T	-0.241	-0.418	-0.511	0.251	-0.503	0.196	0.126	0.010
Isotermalidad	0.171	-0.744	-0.744	0.617	-0.796	0.159	0.424	0.225
Estacionalidad en T	0.022	0.661	0.589	-0.533	0.603	0.002	-0.475	-0.472
T máx mes más cálido	-0.433	-0.638	-0.303	0.242	-0.271	-0.413	0.305	0.758
T mín mes más frío	-0.048	-0.434	-0.122	0.242	-0.124	-0.405	0.322	0.672
Rango anual de T	-0.379	-0.067	-0.150	-0.073	-0.114	0.125	-0.118	-0.131
T cuarto más húmedo	0.065	-0.647	-0.177	0.253	-0.207	-0.429	0.233	0.683
T cuarto más seco	-0.187	-0.562	-0.199	0.183	-0.171	-0.402	0.400	0.750
T cuarto más caliente	-0.193	-0.654	-0.156	0.169	-0.151	-0.523	0.232	0.820
T cuarto más frío	-0.128	-0.689	-0.337	0.334	-0.340	-0.352	0.358	0.724
Ppt anual	-0.191	0.476	0.293	-0.224	0.379	-0.040	0.248	-0.009
Ppt mes más húmedo	-0.179	0.390	0.092	-0.025	0.173	0.038	0.445	-0.061
Ppt mes más seco	-0.103	0.573	0.516	-0.419	0.586	-0.095	-0.024	-0.033
Estacionalidad en ppt	0.172	-0.527	-0.559	0.555	-0.646	0.128	0.088	-0.051
Ppt cuarto más húmedo	-0.173	0.450	0.134	-0.096	0.221	0.075	0.406	-0.101
Ppt cuarto más seco	-0.122	0.552	0.527	-0.447	0.601	-0.111	-0.033	-0.013
Ppt cuarto más cálido	-0.003	0.602	0.268	-0.216	0.318	0.204	0.095	-0.474
Ppt cuarto más frío	-0.095	0.592	0.494	-0.428	0.569	-0.046	0.002	-0.067

3.5. COMPARACIÓN DE LOS PATRONES DE COVARIACIÓN ENTRE NIVELES

3.5.1. Patrones de covariación entre niveles considerando todas las variables del tallo.

Para comparar los patrones de covariación de todas las variables del tallo se utilizó la correlación de los valores de correlación entre diferentes niveles. Las correlaciones entre

las cuatro poblaciones de *B. grandifolia* (comparación intra vs. interpoblacional) fueron mayores a 0.4 y tuvieron intervalos de confianza lejanos a cero, indicando que hay correspondencia entre las matrices de correlación de las diversas poblaciones (Tabla 3.6). Los valores de correlación entre las poblaciones de *B. simaruba* fueron considerablemente mayores (Tabla 3.6), sugiriendo mayor correspondencia entre los patrones de correlación.

Tabla 3.6. Correlación de Pearson entre los valores de correlación de las matrices poblacionales de *B. grandifolia* y *B. simaruba*. LI = límite inferior, LS = límite superior.

<i>B. grandifolia</i>					<i>B. simaruba</i>				
Pob. 1	Pob. 2	r	I.C. 95%		Pob. 1	Pob. 2	r	I.C. 95%	
			LI	LS				LI	LS
Jalisco	Colima	0.557	0.444	0.652	Jalisco	QRoo	0.497	0.375	0.602
Jalisco	Morelos	0.551	0.437	0.647	Jalisco	Guerrero	0.699	0.613	0.768
Jalisco	Nayarit	0.488	0.364	0.594	Jalisco	Veracruz	0.601	0.496	0.689
Colima	Morelos	0.446	0.317	0.559	QRoo	Guerrero	0.577	0.467	0.669
Colima	Nayarit	0.421	0.289	0.537	QRoo	Veracruz	0.626	0.525	0.709
Morelos	Nayarit	0.443	0.314	0.556	Guerrero	Veracruz	0.63	0.529	0.712

En lo que respecta a las correlaciones en la comparación de los patrones intraespecíficos vs. los interespecíficos, los valores fueron variables (0.30 a 0.79, Tabla 3.7). Los intervalos de confianza al 95% no incluyen al cero, indicando relaciones entre los patrones de covariación. Las gráficas correspondientes a los extremos encontrados en estas comparaciones (*B. krusei* y *B. simaruba*-Ver) se muestran en la Figura 3.2.

Tabla 3.7. Correlación de Pearson entre los valores de correlación de las matrices intraespecíficas vs. la matriz interespecífica. LI = límite inferior, LS = límite superior.

Especie/Pob.	r	I.C. 95%	
		LI	LS
<i>B. arborea</i>	0.536	0.424	0.663
<i>B. attenuata</i>	0.612	0.517	0.715
<i>B. grandifolia</i> -Col	0.452	0.323	0.596
<i>B. instabilis</i>	0.405	0.272	0.569
<i>B. krusei</i>	0.296	0.176	0.458
<i>B. laurihuertae</i>	0.417	0.284	0.569
<i>B. longipes</i>	0.417	0.297	0.574
<i>B. ovalifolia</i>	0.610	0.516	0.719
<i>B. simaruba</i> -Ver	0.735	0.666	0.823

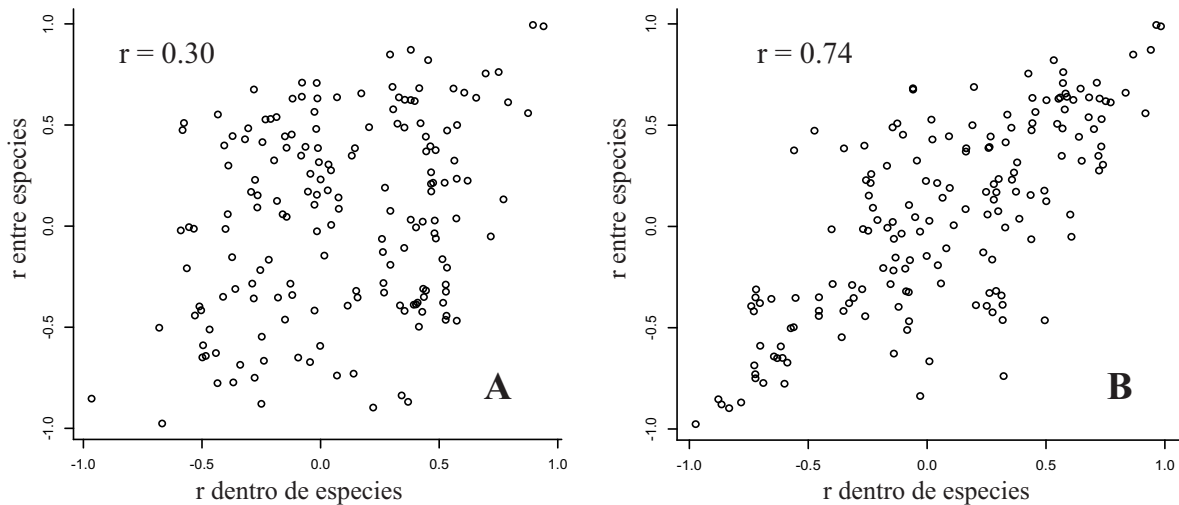


Figura 3.2. Correlaciones entre los valores de correlación de la matriz de covariación interespecífica y las matrices intraespecíficas de *B. krusei* (A) y *B. simaruba-Veracruz* (B)

3.5.2. Patrones de covariación entre niveles considerando siete variables funcionales de la madera

3.5.2.1. Comparación de los patrones intrapoblacionales vs. interpoblacionales en *B. grandifolia*

Excepto en un caso, todas las comparaciones pareadas de las matrices de varianzas y covarianzas poblacionales de *B. grandifolia* a través del modelo CPC resultaron en algún grado de similitud entre las matrices (Tabla 3.8). La similitud abarcó desde el caso de compartir el primer componente principal (CPC(1)) hasta compartirlos todos (CPC). Aunque las estrategias Step-up y Jump-up para la evaluación de los diferentes modelos no coincidió de manera exacta, en la mayoría de los casos eligieron modelos vecinos en la jerarquía de Flury. Las matrices de Colima y Morelos fueron las únicas sin similitud (Tabla 3.8). El método de jacknife-MANOVA no detectó diferencias entre las cuatro matrices poblacionales de *B. grandifolia*. (Tabla 3.8).

3.5.2.2. Comparación de los patrones intrapoblacionales vs. interpoblacionales en *B. simaruba*

Al igual que para *B. grandifolia*, las comparaciones a través del modelo de CPC recuperaron mucha estructura común entre las poblaciones de *B. simaruba*, excepto para las poblaciones de Jalisco y Guerrero que resultaron sin relación (Tabla 3.8). Para las demás comparaciones, la similitud entre las matrices abarcó desde compartir el primer componente principal, hasta la igualdad.

La matriz de pseudovalores de varianzas y covarianzas con las cuatro poblaciones de *B. simaruba* presentaba un nivel muy alto de heteroscedasticidad con 11 de 28 variables violando este supuesto. Fue por ello que la comparación se aplicó a través de un MANOVA no paramétrico. Esta prueba detectó diferencias en al menos una de las varianzas o covarianzas de las cuatro poblaciones de *B. simaruba* ($p < 0.01$, Tabla 3.8). Estas diferencias fueron ubicadas a través de las pruebas Kruskal-Wallis en una varianza y varias covarianzas indicadas en la Tabla 3.9. Las diferencias se debieron principalmente a que ciertas covarianzas en las poblaciones de Quintana Roo y Guerrero eran débiles y positivas a diferencia de las presentadas por todas las demás poblaciones (Tabla 3.9).

Tabla 3.8. Comparación de las matrices de varianzas y covarianzas entre las cuatro poblaciones de *B. grandifolia* (Jalisco, Colima, Morelos y Nayarit) y de *B. simaruba* (Jalisco, Quintana Roo, Guerrero y Veracruz). Las comparaciones con el modelo CPC (Flury) se hicieron por pares de poblaciones. Se incluye el modelo elegido por la estrategia Step-up y Jump-Up y las estadísticas asociadas al rechazo del modelo superior al modelo elegido. La comparación por el método de jacknife-MANOVA se realizó con todas las poblaciones simultáneamente. En el caso de *B. simaruba* se realizó un MANOVA no paramétrico. gl = grados de libertad, n = numerador, d = denominador, P = p-value asociado a la prueba, iguald. = igualdad, sin rel. = sin relación, no par. = MANOVA no paramétrico

	Pob. 1	Pob. 2	Modelo CPC (Flury)								Método jacknife-MANOVA			
			Step-up				Jump-Up				Wilks	F	gl (n,d)	P
			Modelo	χ^2	gl	P	Modelo	χ^2	gl	P				
<i>B. grandifolia</i>	Jalisco	Colima	CPC (4)	6.491	2	0.0389	CPC	62.44	27	0.0001	0.1575	1.257	84, 123.5	0.123
	Jalisco	Morelos	CPC (1)	12.316	5	0.0307	CPC	51.829	27	0.0028				
	Jalisco	Nayarit	CPC (1)	17.578	5	0.0035	CPC (1)	24.222	11	0.0118				
	Colima	Morelos	Sin rel.	15.536	6	0.0165	Sin rel.	15.536	6	0.0165				
	Colima	Nayarit	CPC (3)	10.053	3	0.0181	CPC	49.135	27	0.0057				
	Morelos	Nayarit	CPC (1)	14.169	5	0.0146	CPC (2)	30.775	15	0.0094				
<i>B. simaruba</i>	Jalisco	Q. Roo	CPC	18.643	6	0.0048	Iguald.	34.902	28	0.1728	no par.	2.2573	3, 68	0.009
	Jalisco	Guerrero	Sin rel.	16.266	6	0.124	Sin rel.	16.266	6	0.0124				
	Jalisco	Veracruz	CPC (4)	8.069	2	0.0177	CPC	42.896	27	0.0268				
	Q. Roo	Guerrero	CPC	52.103	6	<0.001	CPC	68.841	27	<0.001				
	Q. Roo	Veracruz	CPC	21.201	6	0.0017	CPC	45.723	27	0.0136				
	Guerrero	Veracruz	CPC (1)	22.496	5	0.0004	CPC (1)	24.693	11	0.0101				

Tabla 3.9. Variables con diferencias significativas en la comparación interpoblacional para *B. simaruba* causantes de la diferencias en el MANOVA no paramétrico. Se muestran los resultados de las pruebas de Kruskal-Wallis y las parejas de poblaciones con diferencias significativas de acuerdo a las pruebas de Behrens-Fisher. La columna de diferencias menciona la pareja con diferencias significativas en la varianza y las poblaciones que difieren de las demás por cambio en signo y magnitud de sus covarianzas. Var = varianza, cov=covarianza, +=covarianza positiva.

Variable	$\chi^2_{(3)}$	P	Diferencias
var C_{mad}	8.450	0.0376	Ver-Gro
cov $D_{mad}-K_{max}$	8.811	0.0319	QRoo + y débil
cov $D_{mad}-C_{mad}$	8.007	0.046	Gro + y débil
cov $V_{pamad}-K_{max}$	8.465	0.0373	QRoo + y débil
cov $V_{pamad}-C_{mad}$	8.896	0.0307	Gro + y débil

3.5.2.3. Comparación de los patrones intraespecíficos vs. interespecíficos

El modelo CPC detectó similitud entre la matriz interespecífica y las matrices intraespecíficas en todos los casos (Tabla 3.10). La similitud abarcó desde compartir el primer componente principal hasta la proporcionalidad entre matrices. Las estrategias step-up y jump-Up coincidieron en el modelo seleccionado o eligieron modelos vecinos en la jerarquía de Flury. Las pruebas de jacknife-MANOVA también sugieren similitud entre las las covarianzas para todos los casos.

3.6. CONJUNTOS DE COVARIACIÓN FUNCIONAL DENTRO DE LA MADERA

3.6.1. Conjuntos de covariación detectados en las matrices intraespecíficas e intrapoblacionales

Los resultados de los PCAs sobre los siete caracteres de la madera se muestran en la Tabla 3.11. Los dos primeros componentes principales explican un porcentaje considerable de la variación observada (55.7-83.8%). El conteo del número de veces en que cada variable aparece en el PC1 o en el PC2 muestra tendencias de asociación entre las variables,

es decir, sugieren conjuntos de covariación funcional en la madera. Las variables funcionales relacionadas con el sostén mecánico, tales como MOR, D_{mad} , V_{pamad} , tienden a ser relevantes en el PC1, en donde sus cargas presentan los mismos signos, sugiriendo una asociación positiva entre ellas. Covariando de manera opuesta aparece también en el PC1 CA_{mad} . En aquellos casos en que alguna de las variables mecánicas aparece como importante en el PC2, ésta suele acompañarse de las otras variables y/o de CA_{mad} .

Por su parte, el PC2 suele tener como variables relevantes E_{mad} , K_{max} y C_{mad} . Aunque en varios casos E_{mad} aparece acompañada de otras variables mecánicas como MOR o D_{mad} en el PC2, la mayoría de las veces solamente se presenta con K_{max} y C_{mad} (Tabla 3.11). E_{mad} tiende a presentar el mismo signo que K_{max} , a diferencia de C_{mad} , que tiende a covariar de manera inversa con las otras dos variables.

Tabla 3.10. Comparación de la matriz de varianzas y covarianzas interespecífica y aquellas intraespecíficas. Para el modelo CPC se incluyen el modelo elegido por la estrategia Step-up y Jump-Up y las estadísticas asociadas al rechazo del modelo superior al modelo elegido. La comparación con jackknife-MANOVA se realizó sobre las covarianzas entre variables, excluyéndose las varianzas por limitaciones del tamaño muestral dadas por la matriz interespecífica. gl= grados de libertad, num=numerador, den=denominador, P=p-value asociado a la prueba.

Especie	Modelo CPC (Flury)								Método jackknife-MANOVA				
	Step-up				Jump-Up				Wilks	F	gl num	gl den	P
	Modelo	χ^2	gl	P	Modelo	χ^2	gl	P					
<i>B. arborea</i>	CPC (1)	13.569	5	0.0186	CPC (2)	26.093	15	0.0371	0.418	0.332	21	5	0.967
<i>B. attenuata</i>	CPC (5)	6.348	1	0.0117	CPC	85.002	27	<0.0001	0.145	1.403	21	5	0.379
<i>B. grandifolia</i> -Col	CPC (5)	8.947	1	0.0028	CPC	81.391	27	<0.0001	0.206	0.919	21	5	0.604
<i>B. instabilis</i>	CPC (3)	20.979	3	0.0001	CPC (3)	31.328	18	0.0264	0.231	0.795	21	5	0.682
<i>B. krusei</i>	CPC (2)	11.229	4	0.0241	CPC (3)	32.611	18	0.0186	0.338	0.467	21	5	0.900
<i>B. laurihuertae</i>	CPC (3)	43.622	3	<0.0001	CPC (3)	62.131	18	<0.0001	0.138	1.491	21	5	0.350
<i>B. longipes</i>	CPC (1)	11.237	5	0.0469	CPC (2)	28.108	15	0.0209	0.392	0.369	21	5	0.952
<i>B. ovalifolia</i>	CPC	30.947	6	<0.0001	CPC	52.088	27	0.0026	0.289	0.585	21	5	0.824
<i>B. simaruba</i> -Ver	CPC (4)	10.956	2	0.0042	CPC	69.699	27	<0.0001	0.145	1.401	21	5	0.379

Tabla 3.11. Análisis de componentes principales sobre siete caracteres de la madera. Para cada variable funcional se resalta el componente principal para el que la carga tiene un valor absoluto mayor.

	<i>arborea</i>		<i>attenuata</i>		<i>grandifolia-Jal</i>		<i>grandifolia-Col</i>		<i>grandifolia-Mor</i>		<i>grandifolia-Nay</i>		<i>instabilis</i>		<i>krusei</i>	
	PC1	PC2	PC1	PC2	PC1	PC2	PC1	PC2	PC1	PC2	PC1	PC2	PC1	PC2	PC1	PC2
E_{mad}	0.118	-0.025	-0.409	0.440	0.308	-0.543	0.055	-0.456	-0.373	-0.399	0.423	-0.154	0.366	0.215	0.223	-0.167
MOR	0.220	-0.036	-0.340	0.315	0.227	-0.545	0.155	-0.620	-0.454	-0.391	0.436	-0.089	0.350	0.436	0.225	-0.540
D_{mad}	0.540	0.343	-0.440	-0.209	-0.426	-0.437	-0.445	-0.255	-0.443	0.448	0.302	0.251	0.492	-0.236	-0.586	-0.065
CA_{mad}	-0.201	0.627	0.462	0.200	0.521	-0.004	0.462	-0.047	0.259	-0.396	-0.455	0.273	-0.294	0.495	-0.258	0.530
V_{pamad}	0.562	0.249	-0.478	-0.325	-0.484	-0.409	-0.544	-0.324	-0.549	0.227	0.507	-0.186	0.458	-0.335	-0.577	-0.118
K_{max}	-0.263	0.652	-0.016	0.705	0.135	-0.076	0.510	-0.229	0.286	0.192	-0.202	-0.669	0.209	0.570	0.368	0.298
C_{mad}	-0.469	0.035	0.288	-0.145	-0.385	0.211	-0.070	0.428	-0.091	-0.492	-0.188	-0.591	0.401	0.162	0.146	0.542
%	35.0	23.8	48.1	21.5	38.2	28.5	34.1	21.5	35.7	24.9	41.0	21.8	45.3	27.3	38.3	27.8
% acum	35.0	58.8	48.1	69.6	38.2	66.7	34.1	55.7	35.7	60.7	41.0	62.7	45.3	72.6	38.3	66.2

	<i>laurihuertae</i>		<i>longipes</i>		<i>ovalifolia</i>		<i>simaruba-Jal</i>		<i>simaruba-QRoo</i>		<i>simaruba-Gro</i>		<i>simaruba-Ver</i>		conteo	
	PC1	PC2	PC1	PC2	PC1	PC2	PC1	PC2	PC1	PC2	PC1	PC2	PC1	PC2	PC1	PC2
E_{mad}	-0.180	0.684	-0.392	0.423	0.336	-0.445	0.266	-0.642	0.251	-0.519	0.116	0.430	0.171	-0.680	4	11
MOR	-0.358	0.526	-0.438	0.333	0.402	-0.266	0.430	-0.020	0.390	-0.366	0.471	0.236	0.405	-0.228	10	5
D_{mad}	-0.549	-0.216	-0.442	-0.311	0.488	0.289	0.433	-0.058	0.501	0.091	0.521	-0.010	0.469	0.048	13	2
CA_{mad}	0.457	0.378	0.469	0.258	-0.456	0.268	-0.393	-0.327	-0.407	-0.031	-0.464	0.273	-0.409	-0.242	11	4
V_{pamad}	-0.493	-0.118	-0.480	-0.180	0.497	0.235	0.442	0.028	0.524	0.029	0.522	0.005	0.468	0.078	15	0
K_{max}	-0.050	0.207	-0.080	0.616	0.080	0.071	-0.351	-0.539	-0.151	-0.671	0.020	0.597	-0.214	-0.613	5	10
C_{mad}	0.289	-0.096	-0.045	-0.368	-0.160	-0.718	-0.290	0.432	-0.267	-0.370	0.076	-0.573	-0.393	0.206	6	9
%	41.8	24.1	52.4	20.0	47.9	19.2	65.9	14.5	45.6	17.3	50.7	28.1	60.2	23.6		
% acum	41.8	65.8	52.4	72.4	47.9	67.1	65.9	80.5	45.6	63.0	50.7	78.8	60.2	83.8		

3.6.2. Conjuntos de covariación detectados en la matriz interespecífica

Los resultados del análisis de componentes principales para la matriz interespecífica se muestran en la Tabla 3.12. Las variables de mayor relevancia para el PC1 son las relacionadas con el almacenamiento y el sostén mecánico, mientras que para el PC2 resultan importantes las dos variables de conductividad. Los signos opuestos de las cargas asociadas a las variables de almacenamiento y de sostén mecánico indican un trade-off entre estas funciones también en la matriz interespecífica. El PC2 también muestra un fuerte trade-off entre la eficiencia (K_{max}) y la seguridad (P50) en la conductividad, y en menor grado entre la seguridad y el sostén mecánico.

Estos dos componentes principales se correlacionan con algunas variables ambientales, principalmente aquellas relacionadas con la temperatura, y en menor grado y de manera no significativa con variables de precipitación (Tabla 3.13)

Tabla 3.12. Análisis de componentes principales para los siete caracteres de la madera con base en la matriz interespecífica (n=9).

Variable	PC1	PC2
E_{mad}	-0.133	0.269
MOR	-0.319	0.372
D_{mad}	-0.494	-0.106
CA_{mad}	0.458	-0.002
V_{pamad}	-0.487	-0.112
K_{max}	0.148	0.633
C_{mad}	0.406	-0.021
P50	0.061	-0.603
%	49.0	25.5
% acum	49.0	74.5

Tabla 3.13. Correlaciones entre los componentes principales para los siete caracteres de la madera y las variables ambientales. T = temperatura, Máx = máximo, mín = mínimo. Se resaltan las correlaciones significativas a un nivel $\alpha=0.10$.

Variable ambiental	PC1	PC2	Variable ambiental	PC1	PC2
T media anual	0.355	-0.659	T cuarto más frío	0.433	-0.620
Rango diurno de T	0.434	0.003	Ppt anual	-0.234	0.020
Isotermalidad	0.738	-0.076	Ppt mes más húmedo	-0.030	0.084
Estacionalidad en T	-0.638	0.294	Ppt mes más seco	-0.468	0.018
Máx T mes más cálido	0.385	-0.712	Estacionalidad en ppt	0.526	0.063
Mín T del mes más frío	0.246	-0.572	Ppt cuarto más seco	-0.479	-0.008
Rango anual de T	0.066	0.044	Ppt cuarto más cálido	-0.271	0.401
T cuarto más húmedo	0.290	-0.610	Ppt cuarto más frío	-0.456	0.064
T cuarto más seco	0.312	-0.655	Ppt cuarto más		
T cuarto más cálido	0.267	-0.765	húmedo	-0.085	0.127

4. DISCUSIÓN

Si bien la pregunta central de este trabajo es la comparación de los patrones de covariación entre niveles evolutivos, para discutir el efecto de estos patrones en la morfología de los tallos y en la diversificación de las especies es necesario abordar primero qué trade-offs y patrones de covariación positiva fueron encontrados en los tallos del clado *simaruba*. Es por ello que los primeros apartados de esta sección abordan estos patrones y trade-offs con más detalle, comparando los resultados con lo encontrado en otros sistemas leñosos. Posteriormente se discute la posibilidad de que existan conjuntos de covariación en los tallos del clado, después de lo cual se discute la comparación entre niveles evolutivos y las causas de esta covariación, para concluir con la potencial naturaleza adaptativa de los cambios en los valores de desempeño que se observan en los tallos del clado en los diferentes ambientes que ocupan las especies.

4.1. COVARIACIÓN POSITIVA Y TRADE-OFFS ENTRE LAS FUNCIONES DE LOS TALLOS DEL CLADO *SIMARUBA*

Aunque la mayoría de los patrones de covariación positiva y trade-offs detectados en este análisis coinciden con lo reportado en otros grupos leñosos, existen algunas asociaciones de reporte reiterado que no fueron recuperadas aquí. Entre las asociaciones positivas más fuertes están las relacionadas con la densidad de la madera, una de las variables más importantes y más conocidas por la facilidad con la que se mide (Williamson y Wiemann, 2010), y por su frecuente asociación con funciones (Chave et al., 2009; Martínez-Cabrera et al., 2009) e historias de vida (Falster, 2006; Poorter et al., 2010). La densidad de la madera covaría positivamente con la mecánica a través de MOR y E_{mad} (Jacobsen, 2005, Sterck et al., 2006; Méndez-Alonzo et al., en revisión), y también con la vulnerabilidad al embolismo (Hacke et al., 2001; Jacobsen et al., 2005). En el clado *simaruba* la densidad no estuvo asociada con E_{mad} a nivel interespecífico (Tabla 3.4) y a nivel intraespecífico solamente en *B. simaruba*-Jalisco (Apéndice C). En contraste, MOR estuvo asociado con la densidad (Tablas 3.3 y 3.4), aunque a nivel intraespecífico solamente fue significativa la asociación en pocos casos. La magnitud intermedia de la

covariación entre D_{mad} y las variables mecánicas, en comparación con algunos otros estudios que recuperaron fuerte correlación, puede deberse a la gran cantidad de almidón que almacenan los tallos del clado *simaruba* (observación personal), misma que tendrá un efecto incrementando la densidad, pero no la resistencia mecánica.

El efecto que produce el almidón en las mediciones también fue tangible en el volumen porcentual de material celular (pared y almidón, es decir, carbohidratos estructurales y no estructurales). Esta variable, que se esperaba se relacionara de manera muy fuerte con la mecánica, no presentó relación con E_{mad} , y con MOR tiene una magnitud media ($r=0.539$, Tabla 3.4), pero no significativa. Este mismo patrón se observó en las matrices intraespecíficas. Para aclarar si estas relaciones fueron bajas por la inclusión del almidón en las variables V_{pamad} y D_{mad} , será necesario cuantificar esta sustancia de reserva y restarla de V_{pamad} y D_{mad} para únicamente dejar la contribución de la pared celular.

El trade-off entre las capacidades mecánicas y de almacenamiento del tallo es una de las disyuntivas más citadas en la literatura (Meinzer et al., 2003; Pratt et al., 2007; Méndez-Alonzo, et al., en revisión). La competencia por recursos entre estas dos funciones se observó a través de la correlación entre CA_{mad} y V_{pamad} y en menor grado con D_{mad} , probablemente a causa de lo comentado sobre el abundante almidón en el clado. La covariación negativa entre CA_{mad} y la función mecánica expresada como MOR, resultó más fuerte dentro de especies que entre ellas (Tabla 3.4 y Apéndice C). Este relajamiento de la magnitud de la covariación sugiere que el trade-off es fuerte, como se aprecia a nivel interindividual, pero que el cálculo de las medias oscurece un poco su presencia, pues los datos ya no provienen de un mismo individuo exhibiendo los resultados directos de las disyuntivas en la misma estructura. Algo muy similar sucedió con la covariación entre MOR y E_{mad} , que usualmente es fuerte (Jacobsen et al., 2005; Pratt et al., 2007a; Méndez-Alonzo et al., en revisión), pero aquí solamente se detectó en el nivel intraespecífico y fue muy débil en el interespecífico.

El trade-off mecánica-almacenamiento también fue inferido a partir de las correlaciones entre la facilidad de la madera para liberar agua (C_{mad}) y sus capacidades mecánicas. Al igual que en otros estudios (Meinzer et al., 2003; Pratt et al., 2007a; Zanne et al., 2010), las maderas con mayor capacitancia fueron aquellas con menor densidad, menor volumen de pared y almidón y mayor contenido de agua (Tabla 3.4). Estos patrones se

mantuvieron dentro de las poblaciones y especies, pero generalmente sin significancia estadística (Apéndice C).

Las variables de conductividad hidráulica no se asociaron prácticamente con ninguna otra. Aunque la competencia por recursos predeciría trade-offs involucrando esta función, existen reportes recientes de que K_{max} no está asociada a la densidad de la madera (Martínez-Cabrera, 2009, Zanne et al., 2010), y por lo tanto tampoco con los aspectos mecánicos del tallo. Sin embargo, el aspecto de seguridad en la conducción de agua, P50, sí ha estado asociado con la densidad (Jacobsen et al., 2005, Méndez-Alonzo et al., en revisión), relación que no fue recuperada en este estudio. El trade-off que sí se observó fue aquel entre la eficiencia y la seguridad en la conductividad (Tabla 3.4). Este trade-off, que ha sido extensamente reportado en la literatura y ha sido objeto de estudios detallados (Wheeler et al., 2005; Hacke et al., 2006), no refleja compromisos entre las tres funciones principales, pero sí evidencia que al interior de las mismas también ocurren disyuntivas importantes.

La corteza es un tejido que ha sido ignorado por la mayoría de los trabajos de caracteres funcionales de las plantas, pero comienza a cobrar importancia (Niklas, 1999; Onoda et al., 2010; Paine et al., 2010). En los tallos del clado *simaruba* la corteza puede llegar a ser muy abundante (>50% del área porcentual de los tallos jóvenes, datos no publicados) y parece tener una contribución mecánica al sostén mecánico de los tallos jóvenes (Capítulo 2), por lo que su análisis en el contexto de la integración funcional del tallo es muy importante. En este análisis, la corteza se comportó de manera parecida a la madera mostrando un mayor nivel de almacenamiento en aquellas especies con madera de mayor contenido de agua ($r=0.65$, $p<0.05$, Tabla 3.3). Sin embargo, a diferencia de lo que pasa en la madera, en la corteza no se detectó un trade-off entre la mecánica y el almacenamiento de agua. Aunque los módulos elásticos de la madera y de la corteza están asociados positivamente en tallos más viejos (Capítulo 2), en los tallos más jóvenes usados para este estudio, esta asociación no fue significativa ($r=0.35$, $p>0.05$, Tabla 3.3). Esto podría deberse a que las diferencias entre especies en cuanto a la corteza se vuelven más pronunciada con la edad de los tallos, detectándose mejor en los tallos de mayor edad. La densidad y el volumen porcentual de pared y almidón de la corteza y la madera parece también ser proporcional ($r=0.43$, $p>0.05$ y $r=0.50$, $p<0.05$, respectivamente, Tabla 3.3).

4.2. CONJUNTOS DE COVARIACIÓN EN LOS TALLOS DEL CLADO *SIMARUBA*

Los resultados de los análisis de componentes principales de los valores medios por especie sugieren la existencia de dos conjuntos de covariación funcional en los tallos, uno relacionado con el aspecto mecánico y de almacenamiento, y un segundo conjunto reflejando aspectos de conductividad. Dentro de especies y poblaciones estos conjuntos emergieron con una tendencia similar (Tabla 3.11). Entre niveles se observaron solamente dos discrepancias. Tanto E_{mad} como C_{mad} tendieron a ser relevantes en el PC2 de algunas especies y poblaciones, asociándose con K_{max} (Tabla 3.11), pero claramente formaron parte del PC1 en el PCA interespecífico (Tabla 3.12). Esta inconsistencia puede deberse a la inclusión de P50 solamente en el PCA interespecífico. Si se pudiera contar con el valor de P50 para cada tallo, es probable que la asociación con K_{max} fuera muy fuerte en las matrices intrapoblacionales e intraespecíficas y desplazara a E_{mad} y C_{mad} del PC2 al PC1, y que como resultado los conjuntos de covariación entre niveles fueran equivalentes.

La relativa independencia que parecen tener las variables de conductividad respecto de las demás variables funcionales del tallo se ha reportado en otros estudios para la conductividad específica (Zanne et al., 2010). Sin embargo, la resistencia al embolismo suele asociarse positivamente con variables que reflejan las propiedades mecánicas, asociación que fue recuperada aquí con el signo contrario, aunque sin significancia estadística ($r=-0.39$, $p>0.05$; Tabla 3.4). Se ha explicado la asociación de P50 y las variables del sostén mecánico a través de las fibras, que son las células especializadas en el sostén mecánico y que en algunos casos parecen ayudar a evitar el colapso de las células conductivas (Hacke et al., 2001; Jacobsen et al., 2005). Muchos de estos estudios se han basado en sistemas leñosos con una matriz de fibras formada por células muertas, como la flora del chaparral californiano (Carlquist y Hoekman, 1985; Jacobsen et al., 2005) o el matorral xerófilo (Hacke et al., 2001). En contraste, las fibras en el clado *simaruba*, y en muchos árboles del trópico seco, son células vivas muy importantes para el almacenamiento de almidón. Esta doble función de las fibras en este grupo podría restarle importancia a las fibras en la labor del sostén mecánico y también como refuerzo de los vasos en condiciones de bajo potencial hídrico. Para aclarar la contribución de las fibras a

una y otra función será necesario correlacionar las características a nivel anatómico con el desempeño funcional.

La existencia de un segundo componente principal explicando un porcentaje considerable de la variación en este estudio impidió comparar si la dirección de la varianza máxima coincide entre niveles. Muchos estudios utilizan el PC1 para esta comparación que tiene por objetivo determinar si la dirección de la “línea de resistencia mínima” se mantiene entre niveles (Schluter 1996, 2000). Usualmente el PC1 en estos estudios tiene un fuerte efecto del tamaño y explica un alto porcentaje de la variación (Merilä y Björklund, 1999; Marroig y Cheverud, 2005). Si bien el PC1 explicó un porcentaje considerablemente mayor de la variación que el PC2 en las matrices intrapoblacionales e intraespecíficas, este último siguió teniendo una aportación significativa a la explicación (15-30%, Tabla 3.11). Además, el PC2 recogió información relativa a la conductividad, y en menor grado información mecánica, por lo que comparar únicamente el PC1 dejaría fuera la información relativa a la tercera función (Tablas 3.11 y 3.12).

Los conjuntos de covariación detectados en los tallos del clado *simaruba* podrían ser considerados módulos funcionales, pues reúnen caracteres con fuertes relaciones al interior y tienen relaciones más difusas con otros conjuntos (Klingenberg, 2008). Esta interpretación de los conjuntos funcionales lleva a preguntar cómo ocurre esta coordinación funcional a niveles más bajos, p.e. genéticos, y si esta coordinación se lleva a cabo de igual manera en otras plantas leñosas. El estudio de los trade-offs y la integración funcional en el tallo cuenta ya con datos suficientes para comenzar a hacer estas preguntas y para abordar preguntas de modularidad en el tallo (Olson y Rosell, 2006), aplicando técnicas analíticas que vayan más allá del cálculo de coeficientes de correlación (Magwene, 2001; Mitteroecker y Bookstein, 2007)

4.3. COMPARACIÓN DE LOS PATRONES DE COVARIACIÓN ENTRE NIVELES EVOLUTIVOS

Los patrones de covariación en los tallos del clado *simaruba* fueron muy similares entre niveles evolutivos, tanto para las 20 variables funcionales, como para las siete variables de la madera. Los patrones de integración coincidieron dentro y entre poblaciones y también dentro y entre especies, sugiriendo que los trade-offs y las asociaciones positivas

entre funciones afectan de la misma manera a los individuos, las poblaciones y las especies. Los únicos contraejemplos de esta tendencia ocurrieron entre poblaciones y se debieron a la relajación de las correlaciones en las matrices intrapoblacionales. Un nivel de integración alto en los tallos predecía justamente este escenario (Fig. 1.2B).

Al comparar los patrones de covariación incluyendo las 20 variables se concluye que hay similitud entre niveles. Las correlaciones entre los coeficientes así lo sugirieron al ser mayores a 0.4 (excepto *B. krusei* vs. matriz interespecífica) y significativamente distintas de cero en todos los casos. Además, las magnitudes de las correlaciones fueron similares, independientemente del nivel de comparación (intra-interpoblacional o intra-interespecífico), aunque destacó una mayor correspondencia entre las matrices poblacionales de *B. simaruba* con valores más altos de correlación en la comparación (Tabla 3.6). En contraste con *B. grandifolia*, las matrices para esta especie mostraron valores más fuertes de covariación entre caracteres (Apéndice C), y como resultado se corresponden mejor con los patrones de covariación fuertes observados en la matriz interespecífica (Tabla 3.4). En general, la tendencia a presentar valores más fuertes de asociación parece estar presente en plantas con mayor resistencia mecánica. Al correlacionar MOR con el grado de correspondencia intra-interespecífico (r de esas comparaciones, Tabla 3.7), se observó que aquellas especies con MOR más alto tendieron a ser también las que presentaron grados de correspondencia más elevados ($r=0.44$). Esta observación sugiere que en aquellas plantas con mayores necesidades mecánicas, la integración tiende a ser más fuerte, sugiriendo que existe cierto grado de plasticidad en los patrones de integración funcional de estos tallos leñosos. Otra explicación alternativa sería que la confusión introducida por los altos contenidos de almidón en los tallos del grupo está afectando más a las plantas con mayores niveles de almacenamiento de este carbohidrato, reduciendo la magnitud de sus correlaciones y disminuyendo el nivel de integración de sus tallos. La cuantificación del almidón permitirá resolver este aspecto.

La comparación de matrices de varianzas y covarianzas de las siete variables de la madera también sugirió la conservación de los patrones de covariación entre niveles evolutivos. Los resultados de las comparaciones a través del modelo CPC y del jackknife-MANOVA coincidieron en sugerir que existe fuerte correspondencia en la integración funcional a todos los niveles. El modelo CPC sugirió en casi todos los casos que las

matrices comparten más que el primer componente principal, y en muchos casos todos los componentes principales. Las únicas dos comparaciones que resultaron en matrices sin relación se dieron a nivel interpoblacional (Tabla 3.8). Una exploración de las matrices intrapoblacionales sugiere que en ambos casos las diferencias se deben a diferencias en magnitud, pero no en signo, de las correlaciones (Apéndice C). Por su parte, el método jackknife-MANOVA no detectó diferencias entre las poblaciones de *B. grandifolia*, pero sí entre las de *B. simaruba*. De nuevo, las diferencias se debieron a que algunas covariaciones en las poblaciones de Guerrero y Quintana Roo fueron de signo opuesto, pero de magnitud muy pequeña. En general, las pocas discrepancias observadas entre las matrices de varianzas y covarianzas entre niveles ocurrieron por falta de asociación entre caracteres y no por una asociación de diferente signo entre los mismos. No se detectó ninguna diferencia significativa entre matrices en las comparaciones intra-interespecíficas, y el modelo CPC sugirió fuerte similitud con dos o más componentes principales comunes entre ellas.

La fuerza de integración funcional en los tallos leñosos, que se manifiesta a todos los niveles analizados, debe tener implicaciones importantes en la diversificación del clado *simaruba*. Estos patrones de integración sugieren que especies de gran talla con un alto nivel de almacenamiento no se observarán (Capítulo 2). Sin embargo, aunque las especies dentro del clado no pueden desviarse fuertemente de estos patrones de covariación, sí pueden alcanzar cambios morfológicos importantes al modificar drásticamente alguna de las tres funciones del tallo, pero dentro de los límites impuestos por estos patrones. En el Capítulo 2 se abordó el caso de *B. instabilis*, la especie del clado con ramas lianescentes que combinan un bajo valor de E_{mad} con ramas más largas de lo esperado para su diámetro. Aunque difiere un poco de otras matrices, la matriz intraespecífica de *B. instabilis* no resultó significativamente diferente del resto, sugiriendo que aún con estos cambios en el aspecto mecánico, la integración funcional en el tallo es similar al de otras especies. De igual forma, la única especie hemiepífita del género, *B. standleyana*, posee madera muy rígida a pesar de no tener una talla muy grande, que más bien podría relacionarse con un aumento en la resistencia a la cavitación (Jacobsen et al., 2005), al transportar agua a lo largo de los más de 20m que suelen medir sus raíces. Aunque no se realizaron mediciones de las tres funciones del tallo para *B. standleyana*, es probable que, al igual que en *B.*

instabilis, los patrones de covariación se mantengan. La fuerte integración funcional de la madera sugeriría que un hábito como el de *B. standleyana* no podría surgir en el trópico seco, pues el incremento en densidad que seguramente ocurre incrementando los valores de E_{mad} estaría frenado por la necesidad de almacenamiento de agua en la madera que ocurre en las especies de este grupo que ocupan los ambientes secos.

4.4. CAUSAS DE LA COVARIACIÓN FUNCIONAL EN LOS TALLOS DEL CLADO *SIMARUBA*

La covariación entre caracteres pueden tener como causas las restricciones de desarrollo (Arnold, 1992; Schwenk, 2004) o la selección natural (Brodie, 1992; Schwenk, 2001). En el caso de los tallos leñosos, la integración funcional parece ser un ejemplo de covariación producida y mantenida por la selección natural por las razones que se argumentan a continuación. Bajo ciertas ópticas, la covariación entre mecánica y almacenamiento que se ha venido discutiendo, y que impide que un árbol con una gran cantidad de agua almacenada en la madera alcance más de 20m, puede ser interpretada como una “restricción arquitectónica” (p.e. Gould y Lewontin, 1979). Sin embargo, es muy importante distinguir entre las restricciones impuestas por el sistema ontogenético, que impiden el acceso a ciertas zonas del morfoespacio (Alberch, 1989), de aquellas combinaciones de caracteres que al resultar en una menor adecuación y ser eliminadas por la selección natural, no son observadas y se interpretan erróneamente como una restricción (Shanahan, 2007). Por la forma en que se producen las células del tallo, es sencillo imaginar un meristemo produciendo una gran cantidad de fibras y de tejido de almacenamiento al mismo tiempo. Sin embargo, este gasto excesivo en recursos tendrá efectos en la adecuación del organismo. De igual forma, la disminución de una de las funciones al mínimo también parece ontogenéticamente posible, pero de baja adecuación. Todo esto sugiere que en el clado *simaruba* habría posibilidad de acceder a otras zonas del morfoespacio, pero que esto no ocurre a causa de un proceso de optimización funcional. Esto contrasta con otras estructuras orgánicas donde restricciones de desarrollo impiden el acceso a ciertas zonas del morfoespacio (p.e. Wagner y Chiu, 2001).

Si como se ha argumentado, la selección es la causa de los patrones que observamos en el tallo, surge la pregunta de cuál es entonces el blanco de la selección natural (Lande y

Arnold, 1983; Ghalambor et al., 2003). Es muy probable que, al menos en el caso del trade-off entre la mecánica y el almacenamiento, el aumento de una función tendrá un efecto positivo en la adecuación del organismo, pero la disminución en la otra función involucrada en el trade-off tendrá el efecto opuesto en la adecuación. Estos efectos opuestos sugieren que la covariación asociada a un trade-off funcional en el tallo no corresponde a un escenario de selección correlacionada. Sin embargo, otros patrones de covariación dentro de la madera podrían ocurrir por esta causa. Determinar qué carácter es blanco de la selección natural en las relaciones tipo trade-offs es muy importante para los estudios futuros de integración en los tallos y para entender la diversificación adaptativa de estas estructuras (Skinner y Lee, 2009).

4.5. COVARIACIÓN FUNCIONAL Y ADAPTACIÓN EN LOS TALLOS DEL CLADO *SIMARUBA*

Las variables funcionales se asocian con condiciones ambientales, sugiriendo que un aumento en el desempeño funcional podría ser resultado de un proceso adaptativo. Al considerarlas aisladamente (Tabla 3.5), las variables mecánicas, principalmente MOR, reflejan asociación reiterada con los valores medios y la estacionalidad de la temperatura, y la precipitación. Así, las especies con mayores capacidades mecánicas son aquellas que ocupan ambientes de temperatura media más baja, más estable y con mayor precipitación. En estos ambientes, el incremento en las capacidades mecánicas podría representar una ventaja selectiva, por ejemplo cuando hay fuerte competencia por luz y las plantas requieren alcanzar mayores tallas (Iwasa et al., 1985; Mäkelä, 1985; Niklas, 1992; Sterck y Bongers, 1998; Clark y Clark, 2001; Grime, 2001; Westoby et al. 2002; Enquist, 2003; Kessler et al. 2007). En contraste, las variables relacionadas con el almacenamiento aumentan en sitios con temperaturas más altas, más variables y de menor precipitación, condiciones en donde un mayor almacenamiento representaría una ventaja selectiva. Aunque las correlaciones entre el almacenamiento y la precipitación no son estadísticamente significativas, sí sugieren un patrón general (Tabla 3.5). En cuanto a la conductividad, la vulnerabilidad al embolismo mostró fuertes correlaciones con la temperatura; aquellas especies con mayor resistencia al embolismo son aquellas que habitan ambientes con temperaturas medias más altas y menor precipitación. Esta

asociación de P50 y el almacenamiento con los ambientes más secos y cálidos se da de manera independiente, pues P50 no presentó ninguna asociación fuerte con las variables funcionales que reflejan almacenamiento. En general, la magnitud de las correlaciones función-ambiente en los tallos delgados usados en este capítulo fueron menores que las calculadas para los tallos de más edad del Capítulo 2. Esto pudo deberse a que la madera de ramas jóvenes tiene un mayor parecido entre especies, a diferencia del xilema de ramas más viejas y diferenciadas, que ha estado sujeto a condiciones ambientales particulares por más tiempo y, como resultado, exhibe diferencias interespecíficas mucho más fuertes. Se espera que esto sea especialmente cierto en los brotes nuevos, donde el ambiente selectivo –la época de lluvias- es el mismo. Esto contrastará fuertemente con los tallos más viejos, que han experimentado ya las diferencias selectivas de los distintos sitios.

Los conjuntos de covariación en el tallo reflejan igualmente asociación con variables ambientales. El PC1, relacionado con la mecánica y el almacenamiento, se asocia principalmente con la variación ambiental de la temperatura y en menor grado con la precipitación y su estacionalidad (Tabla 3.13). Aquellas especies con mayores capacidades de almacenamiento y menores en sostén mecánico ocupan ambientes más extremos (mayor isothermalidad, que a pesar del nombre es un índice de variación, pues resulta del cociente de los rangos diurno y anual en temperatura; menor estacionalidad, índice que se incrementa en condiciones de temperaturas medias menores y más precipitación). Por su parte, el PC2, relacionado con la capacidad conductiva, se asocia negativamente con ambientes de mayor temperatura, en los que habrá mayor resistencia al embolismo y menor conductividad específica.

Estas asociaciones ambientales con la mayoría de las variables que reflejan las tres funciones del tallo lleva nuevamente a la pregunta de cuál es la función que es objeto de la selección natural, y por lo tanto la que está reflejando adaptación. Los árboles del grupo tienen un crecimiento lento, que dificulta el enfoque experimental para determinar qué función o funciones están cambiando como respuesta a la selección natural. Sin embargo, una aproximación con el enfoque comparativo podría contribuir a contestar esta pregunta (Butler y King, 2004). Mediante la reconstrucción de estados ancestrales, basada en las relaciones filogenéticas del grupo, sería posible determinar en qué dirección dentro del triángulo funcional del tallo ha ocurrido el cambio en cada uno de los taxones actuales. Una

alternativa más compleja sería reconstruir las matrices ancestrales de covariación (Steppan, 1997a y b) y determinar en qué dirección han ocurrido los cambios en el desempeño funcional.

La búsqueda de la función que es blanco de selección y que podría constituir una adaptación está fundamentada en la visión adaptacionista tradicional que busca el reconocimiento de un carácter como adaptación (Larson y Losos, 1996). Aún cuando se reconoce la existencia de trade-offs, se adjudica al cambio en una de las funciones el impacto en la adecuación. Sin embargo, bajo otras ópticas, las combinaciones de valores funcionales podrían ser adaptaciones, por ejemplo, para la escuela de la optimalidad. Para esta aproximación, los trade-offs son centrales al modelar los costos y beneficios del fenotipo o el comportamiento que se espera será optimizado por la selección natural (Maynard Smith, 1978; Parker and Maynard Smith, 1990). Los trade-offs derivados de la competencia por recursos son particularmente importantes para estos modelos de optimización (Seeger y Stubblefield, 1996). Los tallos podrían ser un ejemplo de esto, con combinaciones particulares de desempeño funcional resultando en la máxima adecuación. Con el creciente interés de la posición adaptacionista en la integración funcional (Toro et al., 2004), los trade-offs podrían servir como una liga conceptual entre la escuela optimalista y la adaptacionista.

Otra pregunta más, derivada de la constancia en los patrones de covariación entre niveles, es si los valores medios de desempeño para las diferentes funciones se encuentran restringidos en las especies o si hay una gama plástica amplia. Los resultados de este estudio sugieren que, a pesar de las grandes diferencias en talla y arquitectura que se observan entre las especies, los valores de desempeño tienen una gama plástica amplia dentro de las especies. Al graficar los dos PCs del análisis de ocho variables funcionales de la madera basado en todas las especies y poblaciones medidas, se observa que las poblaciones de *B. simaruba* y *B. grandifolia* se distribuyen a lo largo de los dos ejes, exhibiendo amplios rangos en sus valores de desempeño (Fig. 4.1). Este análisis de componentes principales no se incluyó en los resultados, pero produce componentes con cargas equivalentes y con porcentajes de explicación similares a los obtenidos en el PCA que solamente incluye a las especies. Para confirmar que las especies tienen amplias gamas plásticas, habría que asegurar que las diferencias entre sus poblaciones no resultan de un

rango de expresión acotado y sin traslape, sino que representan partes de la gama plástica de la especie. Esta hipótesis podría ponerse a prueba a través de trasplantes recíprocos, que permitieran conocer si las diferentes poblaciones de *B. grandifolia* se comportarán de manera similar a la *B. simaruba* de Los Tuxtlas al ser sembradas en el bosque tropical perenifolio. La confirmación de rangos plásticos amplios en las especies sería de mucho interés para el estudio de la plasticidad y de la integración. Aunque algunos estudios han encontrado que los rangos plásticos de los caracteres son inversamente proporcionales al número de sus asociaciones con otras características (Gianoli y Palacio-López, 2009), un sistema altamente integrado, como los tallos leñosos, tiene todavía la opción de cambios plásticos importantes a través de cambios fuertes en las combinaciones de caracteres permitidos por la integración funcional.

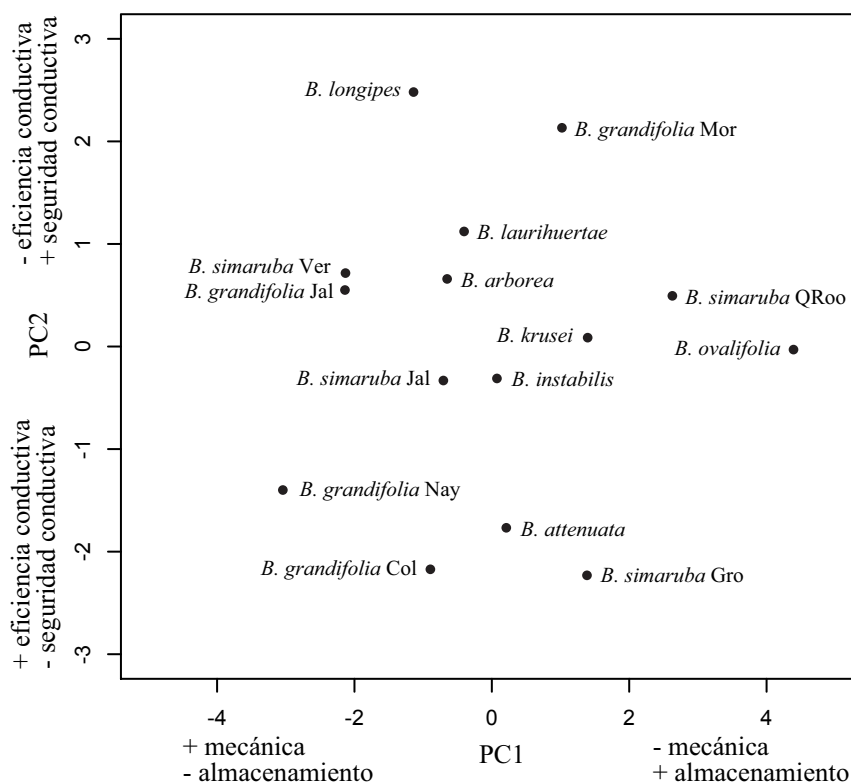


Figura 4.1. Proyección de los dos primeros componentes principales del análisis sobre ocho variables funcionales de la madera (las siete usadas en las comparaciones entre matrices y P50) considerando todas las poblaciones y especies medidas.

5. CONCLUSIONES

1. En general, los trade-offs y los patrones de covariación positiva entre las funciones de los tallos del clado *simaruba* se conservan entre niveles. Aunque se detectaron algunas diferencias entre algunas poblaciones, resultado de la relajación de correlaciones, y también hay indicación de posible plasticidad en la magnitud de la integración (p.e. más fuerte en *B. simaruba*), no parecen ocurrir cambios drásticos en los patrones de covariación. La integración funcional en el tallo del clado *simaruba* podría estar afectando la diversificación a niveles macroevolutivos en este grupo, y parece probable que se observen patrones parecidos en otros sistemas leñosos.

2. Estos trade-offs y patrones de covariación positiva son probablemente mantenidos por selección natural, pues no parecen existir restricciones ontogenéticas que les impidan a los tallos acceder a todas las posibles combinaciones del morfoespacio. En este estudio, la conservación de los patrones de covariación entre niveles argumenta a favor de la selección natural, a diferencia de otros estudios donde son las diferencias al comparar entre niveles las se interpretan como resultado de selección.

3. Las siete variables analizadas en la madera a nivel interespecífico parecen formar dos conjuntos de covariación. El primero y más importante incluye a las variables relacionadas con la mecánica y el almacenamiento, ligadas a través de un trade-off. El segundo conjunto incluye las dos variables relacionadas con la conductividad hidráulica, que también reflejan un trade-off dentro de la misma función. A diferencia de otros estudios, la conductividad no se asoció de manera fuerte con el sostén mecánico.

4. Si bien los patrones de covariación están conservados entre los individuos, las poblaciones y las especies, los valores medios de desempeño funcionales cambian entre funciones. Estos cambios están asociados con condiciones ambientales por lo que sugieren adaptación. El rango de desempeño dentro de una especie no parece estar restringido a una zona del morfoespacio. Por el contrario, las poblaciones muestran altos niveles de plasticidad para optimizar una u otra función, disminuyendo la otra función incluida en el

trade-off. Para entender más sobre el impacto de las disyuntivas en la diversificación macroevolutiva es necesario rastrear las funciones que son blanco de la selección natural. Ante las dificultades de una aproximación experimental, este blanco de selección podría ubicarse utilizando una estrategia comparativa que incluya la reconstrucción de estados ancestrales.

5. Para un entendimiento más detallado de los trade-offs y la integración funcional en los tallos leñosos sería necesario realizar mediciones a nivel anatómico. La información derivada permitiría asociar los cambios funcionales con cambios a nivel estructural, aspecto que es fundamental cuando es a este último nivel que se manifiestan directamente las disyuntivas de asignación de recursos, a través de diferencias en las características a nivel celular y en la abundancia relativa de tejidos. Además, los datos anatómicos contribuirían a entender más sobre el doble papel de las fibras en el clado *simaruba*.

LITERATURA CITADA

- Alberch, P. 1989. The logic of monsters: evidence for internal constraint in development and evolution. *Geobios*, mémoire spéciale 12: 21-57
- Arnold, S. J. 1992. Constraints on phenotypic evolution. *American Naturalist* 140, supp: S85-S107.
- Arnold, S. J, Pfrender, M. E. y A. G. Jones. 2001. The adaptive landscape as a conceptual bridge between micro- and macroevolution. *Genetica* 112-113: 9-32.
- Arnold, S. J. y P. C. Phillips. 1999. Hierarchical comparison of genetic variance-covariance matrices: II. Coastal-inland divergence in the garter snake, *Thamnophis elegans*. *Evolution* 53: 1516-1527.
- Badyaev, A. V. y C. K. Ghalambor. 2001. Evolution of life histories along elevational gradients: trade-off between parental care and fecundity. *Ecology* 82: 2948-2960.
- Begin, M. y D. A. Roff. 2004. From micro- to macroevolution through quantitative genetic variation: positive evidence from field crickets. *Evolution* 58: 2287-2304.
- Björklund, M. 1996. The importance of evolutionary constraints in ecological time scales. *Evolutionary Ecology* 10: 423-431.
- Blows, M. W. y A. A. Hoffmann. 2005. A reassessment of genetic limits to evolutionary change. *Ecology* 86: 1371-1384.
- Borchert, R. y W. T. Pockman. Water storage capacitance and xylem tension in isolated branches of temperate and tropical trees. *Tree Physiology* 25: 457-466.
- Brodie, E. D. 1992. Correlational selection for color pattern and antipredator behavior in the garter snake *Thamnophis ordinoides*. *Evolution* 46: 1284-1298.
- Bucci, S. J., Goldstein, G., Meinzer, F. C., Scholz, F. G., Franco, A. C. y M. Bustamante. 2004. Functional convergence in hydraulic architecture and water relations of tropical savanna trees: from leaf to whole plant. *Tree Physiology* 24: 891-899.
- Butler M. A. y A. A. King. 2004. Phylogenetic comparative analysis: A modeling approach for adaptive evolution. *American Naturalist* 164: 683-695.
- Canty, A. y B. Ripley (2009). boot: Bootstrap R (S-Plus) Functions. R package
- Carlquist, S. 2001. *Comparative Wood Anatomy*. Springer, Heidelberg.
- Carlquist, S. y D. A. Hoekman. 1985. Ecological wood anatomy of the woody southern Californian flora. *International Association of Wood Anatomists Bulletin* 6: 319-347.
- Chapotin, S.M., J.H. Razanameharizaka, y N.M. Holbrook. 2006. Water relations of baobab trees (*Adansonia spp.* L.) during the rainy season: does stem water buffer daily water deficits? *Plant, Cell and Environment* 29: 1021-1032.
- Chave, J., D. Coomes, S. Jansen, S. L. Lewis, N. G. Swenson y A. E. Zanne. 2009. Towards a worldwide wood economics spectrum. *Ecology Letters* 12: 351-366.
- Cheverud, J. M. 1988. A comparison of genetic and phenotypic correlations. *Evolution* 42: 958-968.
- Choat, B., Ball, M. C., Luy, J. G. y J. A. M. Holtum. 2005. Hydraulic architecture of deciduous and evergreen dry rainforest tree species from north-eastern Australia. *Trees* 19: 305-311.
- Choat, B., Sack, L., y N. M. Holbrook. 2007. Diversity of hydraulic traits in nine *Cordia* species growing in tropical forests with contrasting precipitation. *New Phytologist* 175: 686-698.
- Clark, D. A. y D. B. Clark. 2001. Getting to the canopy: tree height growth in a neotropical rain forest. *Ecology* 82: 1460-1472.
- Day, L. M., y B. C. Jayne. 2007. Interspecific scaling of the morphology and posture of the limbs during the locomotion of cats (Felidae). *Journal of Experimental Biology* 210: 642-654.
- De Jong, G. y A. J. Van Noordwijk. 1992. Acquisition and allocation of resources: genetic (co)variances, selection, and life histories. *American Naturalist* 139: 749-770.
- Eble, G. J. 2003. Morphological modularity and macroevolution: conceptual and empirical aspects. En Callebaut, W. y D. Rasskin Gutman (eds.). *Modularity: understanding the development and evolution of complex natural systems*. MIT Press, Cambridge: 221-238.

- Eble, G. J. 2004. The macroevolution of phenotypic integration. En Pigliucci, M. y K. Preston (eds.). *Phenotypic integration. Studying the ecology and evolution of complex phenotypes*. Oxford University Press, Oxford: 253-273.
- Elstrott, J. y D. J. Irschick. 2004. Evolutionary correlations among morphology, habitat use and clinging performance in Caribbean *Anolis* lizards. *Biological Journal of the Linnean Society* 83: 389-398.
- Emlen, D. J. 2001. Costs and the diversification of exaggerated animal structures. *Science* 291: 1534-1536.
- Enquist, B. J. 2003. Cope's Rule and the evolution of long-distance transport in vascular plants: allometric scaling, biomass partitioning and optimization. *Plant Cell and Environment* 26: 151-161.
- Eroukhmanoff, F. y E. I. Svensson. 2008. Phenotypic integration and conserved covariance structure in calopterygid damselflies. *Journal of Evolutionary Biology* 21:514-526.
- Falster, D. S. 2006. Sapling strength and safety: the importance of wood density in tropical forests. *New Phytologist* 171: 237-239.
- Game, E. T. y M. J. Caley. 2006. The stability of P in coral reef fishes. *Evolution* 60: 814-823.
- Gartner, B. L. And F. C. Meinzer. 2005. Structure-function relationships in sapwood water transport and storage. In Holbrook, N. M. and M. A. Zwieniecki (eds). *Vascular Transport in Plants*. Elsevier Academic Press, Boston: 307-331.
- Gere, J. M. y S. P. Timoshenko. 1999. *Mechanics of Materials*. Tanly Thornes Publisher Ltd. Cheltenham, UK.
- Ghalambor, C. K., Walker, J. A. y D. N. Reznick. 2003. Multi-trait selection, adaptation, and constraints on the evolution of burst swimming performance. *Integrative Comparative Biology* 43: 431-438.
- Ghalambor, C. K., Reznick, D. N. y J. A. Walker. 2004. Constraints on adaptive evolution: the functional trade-off between reproduction and fast-start swimming performance in the Trinidadian guppy (*Poecilia reticulata*). *American Naturalist* 164: 38-50.
- Gianoli, E. y K. Palacio-López. 2009. Phenotypic integration may constrain phenotypic plasticity in plants. *Oikos* 118: 1924-1928.
- Gould, S. J. y R. C. Lewontin. 1979. The spandrels of San Marco and the Panglossian paradigm; a critique of the adaptationism programme. *Proceedings of the Royal Society of London B* 205: 147-164.
- Grime, J. P. 2001. *Plant strategies, vegetation processes, and ecosystem properties*. John Wiley and Sons, Nueva York.
- Hacke, U. G., Sperry, S. S., Pockman, W. T., Davis, S. D. y K. A. McCulloh. 2001. Trends in wood density and structure are linked to prevention of xylem implosion by negative pressure. *Oecologia* 126: 457-461.
- Hacke, U. G., J. S. Sperry, J. K. Wheeler y L. Castro. 2006. Scaling of angiosperm xylem structure with safety and efficiency. *Tree Physiology* 26: 689-701.
- Helms, J. y U. Munzel. 2008. nptc: nonparametric multiple comparisons. R package version 1.0-7.
- Hijmans, R. J., Cameron, S. E., Parra, J. L., Jones, P. G. y A. Jarvis. 2005. Very high resolution interpolated climate surfaces for global land areas. *International Journal of Climatology* 25: 1965-1978.
- Holbrook, N. M. 1995. Stem water storage. En Gartner, B. L. (ed). *Plant Stems: Physiology and Functional Morphology*. Academic Press, San Diego, pp. 151-174.
- International Starch Institute. www.starch.dk/isi/starch/tmstarch.htm.
- Isleib, D. R. 1957. Density of potato starch. *American Potato Journal* 35: 428.
- Iwasa, Y., Cohen, D. y J. A. Leon. 1985. Tree height and crown shape, as results of competitive games. *Journal of Theoretical Biology* 112:279-297.
- Jacobsen, A. L., Ewers, F. W., Pratt, R. B., Paddock III, W. A., y S. Davis. 2005. Do xylem fibers affect vessel cavitation resistance? *Plant Physiology* 139: 546-556.

- Kessler, M., Bohner, J. y J. Kluge. 2007. Modelling tree height to assess climatic conditions at tree lines in the Bolivian Andes. *Ecological Modelling* 207: 223-233.
- Klingenberg, C. P. 2008. Morphological integration and developmental modularity. *Annual Review of Ecology, Evolution, and Systematics* 39: 115-132.
- Lande, R. y S. Arnold. 1983. The measurement of selection on correlated characters. *Evolution* 37: 1210-1226.
- Larson, A. y J. B. Losos. 1996. Phylogenetic Systematics of Adaptation. En Rose, M. R., y G. V. Lauder (eds.). *Adaptation*. Academic Press, San Diego: 1-10.
- Lewontin, R. 1977. Adattamento. En Einaudi, G. (ed.). *Enciclopedia Einaudi*, vol. 1, Turin, Italia. Reimpreso en inglés en Levins, R. y R. Lewontin. 1985 *The Dialectical Biologist*. Harvard University Press, Cambridge, Massachusetts.
- Magwene, P. M. 2001. New tools for studying integration and modularity. *Evolution* 55: 1734-1745.
- Mäkelä, A. 1985. Differential games in evolutionary theory: height growth strategies of trees. *Theoretical Population Biology* 27: 239-267.
- Manly, B. F. J. 2007. *Randomization, bootstrap and Monte Carlo methods in biology*. Chapman & Hall, Florida.
- Marroig, G. y J. M. Cheverud. 2004. Did natural selection or genetic drift produce the cranial diversification of Neotropical monkeys? *American Naturalist* 163: 417-428.
- Martínez-Cabrera, H. I., Jones, C. S., Espino, S. E. y H. J. Schenk. 2009. Wood anatomy and wood density in shrubs: responses to varying aridity along transcontinental transects. *American Journal of Botany* 96: 1388-1398.
- Marroig, G. y J. M. Cheverud. 2005. Size as a line of least resistance: diet and adaptive morphological radiation in New World monkeys. *Evolution* 59: 1128-1142.
- Marroig, G. y J. M. Cheverud. 2010. Size as a line of least resistance II: direct selection on size or correlated response due to constraints. *Evolution* 65: 1470-1488.
- Maynard Smith, J. 1978. Optimization theory in evolution. *Annual Review of Ecology and Systematics* 9: 31-56.
- Meinzer, F. C., James, S. A., Goldstein, G. y D. Woodruff. 2003. Whole-tree water transport scales with sapwood capacitance in tropical forest canopy trees. *Plant, Cell and Environment* 26: 1147-1155.
- Meinzer, F. C., Woodruff, D. R., Domec, J.-C., Goldstein, G., Campanello, P. I., Gatti, M. G., Villalobos-Vega, R. 2008. Coordination of leaf and stem water transport properties in tropical forest trees. *Oecologia* 156: 31-41.
- Méndez-Alonzo, R., Paz, H., Rosell, J. A., y M. E. Olson. En revisión. Coordination between leaf phenology and xylem traits: the fugacious pachycaul-tardy leptocaul spectrum. *Ecology*.
- Merilä, J. y M. Björklund. 1999. Population divergence and morphometric integration in the greenfinch (*Carduelis chloris*)-evolution against the trajectory of least resistance. *Journal of Evolutionary Biology* 12: 103-112.
- Merilä, J. y M. Björklund. 2004. Phenotypic integration as a constraint and adaptation. En Pigliucci, M. y K. Preston (eds.). *Phenotypic integration. Studying the ecology and evolution of complex phenotypes*. Oxford University Press, Oxford: 107-129.
- Mitteroecker, P. y F. Bookstein. 2007. The conceptual and statistical relationship between modularity and morphological integration. *Systematic Biology* 56: 818-836.
- Monteiro, L. R. y M. R. Nogueira. 2009. Adaptive radiations, ecological specialization, and the evolutionary integration of complex morphological structures. *Evolution* 64: 724-744.
- Munzel, U. y L. A. Hothorn. 2001. A unified approach to simultaneous rank test procedures in the unbalanced one-way layout. *Biometrical Journal* 43: 553-569.
- Nespolo, R. F., Halkett, F., Figueroa, C. C., Plantegenest, M. y J.-C. Simon. 2009. The role of reproductive plasticity in the genetic architecture of aphid life histories. *Evolution* 63: 2402-2412.

- Niklas, K. J. 1992. *Plant biomechanics*. Univ. Chicago Press, Chicago.
- Niklas, K. J. 1999. The mechanical role of bark. *American Journal of Botany* 86: 465-469.
- Oksanen, J., Kindt, R., Legendre, P., O'Hara, B., Simpson, G. L., Solymos, P., Jari Oksanen, Roeland Kindt, Pierre Legendre, Bob O'Hara, Gavin L. Simpson, Peter Solymos, M., Stevens, M. H. H. y H. Wagner. 2009. vegan: Community Ecology Package. R package version 1.15-4. <http://CRAN.R-project.org/package=vegan>.
- Olson, E. y R. Miller. 1958. *Morphological Integration*. The University of Chicago Press, Chicago, Illinois.
- Olson, M. E. y J. A. Rosell. 2006. Using heterochrony to detect modularity in the evolution of stem diversity in the plant family Moringaceae. *Evolution* 60: 724-734.
- Olson, M. E., Aguirre-Hernández, R. y J. A. Rosell. 2009. Universal foliage-stem scaling across environments and species in dicot trees: plasticity, biomechanics and Corner's Rules. *Ecology Letters* 12: 210-219.
- Onoda, Y., Richards, A. E. y M. Westoby. 2010. The relationship between stem biomechanics and wood density is modified by rainfall in 32 Australian woody plant species. *New Phytologist* 185: 493-501.
- Paine, C. E. T., Stahl, C., Courtois, E., Patiño, S., Sarmiento, C. y C. Baraloto. 2010. Functional explanations for variation in bark thickness in tropical rain forest trees. *Functional Ecology*. DOI: 10.1111/j.1365-2435.2010.01736.x
- Parker, G. A. y J. Maynard Smith. 1990. Optimality theory in evolutionary biology. *Nature* 348: 27-33.
- Phillips, P. C. y S. J. Arnold. 1999. Hierarchical comparison of genetic variance-covariance matrices. I. Using the Flury hierarchy. *Evolution* 53: 1506-1515.
- Pigliucci, M. 2004. Studying mutational effects of G-matrices. En Pigliucci, M. y K. Preston (eds.). *Phenotypic integration. Studying the ecology and evolution of complex phenotypes*. Oxford University Press, Oxford: 231-248.
- Pigliucci, M. 2006. Genetic variance-covariance matrices: a critique of the evolutionary quantitative genetics research program. *Biology and Philosophy* 21: 1-23.
- Pigliucci, M. y K. Preston. 2004. *Phenotypic integration. Studying the ecology and evolution of complex phenotypes*. Oxford University Press, Oxford.
- Pisarenko, G. S., Yákovlev, A. P., y V. V. Matvéev. 1979. *Manual de resistencia de materiales*. Mir, Moscú.
- Poorter, L., McDonald, I., Alarcón, A., Fichtler, E., Licona, J., Peña-Calors, M., Sterck, F., Villegas, Z. y U. Sass-Klaassen. 2010. The importance of wood traits and hydraulic conductance for the performance and life history strategies of 42 rainforest tree species. *New Phytologist* 185: 481-492.
- Pratt, R. B., Jacobsen, A. L., Ewers, F. W. and S. D. Davis. 2007a. Relationships among xylem transport, biomechanics and storage in stems and roots of nine Rhamnaceae species of the California chaparral. *New Phytologist* 174: 787-798.
- Pratt, R. B., Jacobsen, A. L., Golgotiu, K. A., Sperry, J. S., Ewers, F. W. y S. D. Davis. 2007b. Life history type and water stress tolerance in nine California chaparral species (Rhamnaceae). *Ecological Monographs* 77: 239-253.
- Preston, K. A., Cornwell, W. K., y J. L. DeNoyer. 2006. Wood density and vessel traits as distinct correlates of ecological strategy in 51 California coast range angiosperms. *New Phytologist* 170: 807-818.
- R Development Core Team, 2009. R: A language and environment for statistical computing, v.2.9.2. <http://www.R-project.org>. Accessed 2009.
- Renaud, S., Auffray, J. C y J. Michaux. 2006. Conserved phenotypic variation patterns, evolution along lines of least resistance, and departure due to selection in fossil rodents. *Evolution* 60: 1701-1717.

- Reznick, D. N. y J. Travis. 1996. The empirical study of adaptation in natural populations. En Rose, M. R. y G. V. Lauder (eds.). *Adaptation*. Academic Press, San Diego: 243-289.
- Roff, D. 2000. The evolution of the G matrix: selection or drift? *Heredity* 84: 135-142.
- Roff, D. 2002. Comparing G matrices: a manova approach. *Evolution* 56: 1286-1291.
- Roff, D. A. y D. J. Fairbairn. 2007. The evolution of trade-offs: where are we? *Journal of Evolutionary Biology* 20: 433-447.
- Roff, D. A. y M. B. Gélinas. 2003. Phenotypic plasticity and the evolution of trade-offs: the quantitative genetics of resource allocation in the wing dimorphic cricket, *Gryllus firmus*. *Journal of Evolutionary Biology* 16: 55-63.
- Rojas-Jimenez, K., N.M. Holbrook y M.V. Gutierrez-Soto. 2007. Dry- season leaf flushing of *Enterolobium cyclocarpum* (ear-pod tree): above and belowground phenology and water relations. *Tree Physiology* 27: 1561-1568.
- Rosell, J. A. y M. E. Olson. 2007. Testing implicit assumptions regarding the age vs. size dependence of stem biomechanics using *Pittocaulon* (~*Senecio*) *praecox* (Asteraceae). *American Journal of Botany* 94:161-172.
- Rosell, J. A., Olson, M. E., Weeks, A., De-Nova, J. A., Medina, R., Pérez-Camacho, R., Gómez-Bermejo, R., Ferial, T. P., Montero, J. C. y L. Eguiarte. 2010. Diversification in species complexes: tests of species origin and delimitation in the *Bursera simaruba* clade of tropical trees (Burseraceae). *Molecular Phylogenetics and Evolution*.
- Schlichting, C.D. y M. Pigliucci. 1998. *Phenotypic evolution. A reaction norm perspective*. Sinauer Associates, Massachussets.
- Schluter, D. 1996. Adaptive radiation along genetic lines of least resistance. *Evolution* 50: 1766-1764.
- Schluter, D. 2000. *The ecology of adaptive radiation*. Oxford University Press, Oxford.
- Scholz, F. G., Bucci, S. J., Goldstein, G., Meinzer, F. C., Franco, A. C. y F. Miralles-Wilhelm. 2007. Biophysical properties and functional significance of stem water storage tissues in Neotropical savanna trees. *Plant, Cell and Environment* 30: 236-248.
- Schwenk, K. 2001. Functional units and their evolution. En Wagner, G. P. (ed.). *The Character Concept in Evolutionary Biology*. Academic Press, San Diego: 165-198.
- Schwenk, K. y G. P. Wagner. 2004. The relativism of constraints on phenotypic evolution. En Pigliucci, M. y K. Preston, eds. *Phenotypic integration. Studying the ecology and evolution of complex phenotypes*. Oxford University Press, Oxford: 390-408.
- Seeger, J. y J. W. Stubblefield. 1996. Optimization and adaptation. En Rose, M. R. y G. V. Lauder (eds.). *Adaptation*. Academic Press, San Diego: 93-123.
- Shanahan, T., 2008. Why don't zebras have machine guns? Adaptation, selection, and constraints in evolutionary theory. *Studies in History and Philosophy of Biological and Biomedical Sciences* 39: 135-146.
- Shiota, H. y M. T. Kimura. 2007. Evolutionary trade-offs between thermal tolerance and locomotor and developmental performance in drosophilid flies. *Biological Journal of the Linnean Society* 90:375-380.
- Siau, J.F. 1984. *Transport processes in wood*. Springer, Berlin.
- Sinervo, B., Doughty, P., Huey, R. B. y K. Zamudio. 1992. Allometric engineering: a causal analysis of natural selection on offspring size. *Science* 258: 1927-1930.
- Sinervo, B. y E. Svensson. 2002. Correlational selection and the evolution of genomic architecture. *Heredity* 89: 329-338.
- Skinner, A. y M. S. y Lee. 2009. Body-form evolution in the scincid lizard clade *Lerista* and the mode of macroevolutionary transitions. *Evolutionary Biology* 36: 292-300
- Sperry, J.S. y M.T. Tyree. 1988. Mechanism of water-stress induced xylem embolism. *Plant Physiology* 88: 581-587.
- Sperry J. S. y N. Z. Saliendra. 1994. Intra- and inter- plant variation in xylem cavitation in *Betula occidentalis*. *Plant, Cell and Environment* 17: 1233-1241

- Sperry, J. S., Meinzer, F. C. y K. A. McCulloh. 2008. Safety and efficiency conflicts in hydraulic architecture: scaling from tissues to trees. *Plant, Cell and Environment* 31: 632-645.
- Stearns, S. C. 1989. Trade-offs in life-history evolution. *Functional Ecology* 3: 259-268.
- Sterck, J., y F. Bongers. 1998. Ontogenetic changes in size, allometry, and mechanical design of tropical rain forest trees. *American Journal of Botany* 85: 266-272.
- Sterck, F. J., van Gelder, H. A. y L. Poorter. 2006. Mechanical branch constraints contribute to life-history variation across tree species in a Bolivian forest. *Journal of Ecology* 94: 1192-1200.
- Steppan, S. J. 1997a. Phylogenetic analysis of phenotypic covariance structure. I. Contrasting results from matrix correlation and common principal component analyses. *Evolution* 51: 571-586.
- Steppan, S. J. 1997b. Phylogenetic analysis of phenotypic covariance structure. II. Reconstructing matrix evolution. *Evolution* 51: 587-594.
- Steppan, S. J., Phillips, P. C. y D. Houle. 2002. Comparative quantitative genetics: evolution of the G matrix. *Trends in Ecology and Evolution* 17: 321-327.
- Van Valen, L. 1965. The study of morphological integration. *Evolution* 19: 347-349.
- Vincent, J. F. 1992. *Biomechanics- Materials. A Practical Approach*. IRL Press.
- Wagner, G. P. 1988. The significance of developmental constraints for phenotypic evolution by natural selection. En De Jong, G.(ed.). *Population genetics and evolution*. Springer Verlag, Berlin: 222-229.
- Wagner, G. P. y C. Chiu. 2001. The tetrapod limb: a hypothesis on its origin. *Journal of Experimental Zoology* 291: 226-240.
- Waldmann, P. y S. Andersson. 2000. Comparison of genetic (co)variance matrices within and between *Scabiosa canescens* and *S. columbaria*. *Journal of Evolutionary Biology* 13: 826-835.
- Westoby, M., Falster, D. S., Moles, A. T., Vesk, P. A. e I. J. Wright. 2002. Plant ecological strategies: Some leading dimensions of variation between species. *Annual Review of Ecology and Systematics* 33: 125-159.
- Wheeler, J. K., Sperry, J. S., Hacke, U. G. y N. Hoang. 2005. Inter-vessel pitting and cavitation in woody Rosaceae and other vesselled plants: a basis for safe-y versus efficiency trade-off in xylem transport. *Plant, Cell and Environment* 28: 800-812.
- Williamson G. B. y M. C. Wiemann. 2010. Measuring wood specific gravity... correctly. *American Journal of Botany* 97: 519-524.
- Zanne, A. E., Westoby, M., Falster, D. S., Ackerly, D. D., Loarie, S. R., Arnold, S. E. J., y D. A. Coomes. 2010. Angiosperm wood structure: global patterns in vessel anatomy and their relation to wood density and potential conductivity. *American Journal of Botany* 97: 207-215.
- Zuur, A. F., Ieno, E. N., Walker, N. J., Saveliev, A. A. y G. M. Smith. 2009. *Mixed effects models and extensions in ecology with R*. Springer, Berlin.

APÉNDICE A. Métodos para la comparación de matrices de covariación

Existen numerosos métodos para la comparación de matrices que pueden ser utilizados para el análisis de matrices de covariación (ver Steppan et al., 2002 para una revisión; Cheverud y Marroig, 2007). Dos de ellos son el método de componentes principales comunes (CPC, Flury, 1988; Phillips y Arnold, 1999) y el método jackknife-MANOVA de Roff (2002). A pesar de que se desconocen los detalles del comportamiento de estos métodos bajo diferentes circunstancias (Phillips y Arnold, 1999; Roff, 2002), y de que existe una fuerte discusión sobre problemas asociados al método de CPC (Houle et al., 2002), estos dos métodos siguen siendo los más populares para la comparación de matrices en el contexto de la integración fenotípica. Estudios recientes han aplicado ambos con el objetivo de comparar sus resultados y robustecer las inferencias derivadas. A continuación se explica de manera muy breve en qué consiste cada método.

A.1. COMPONENTES PRINCIPALES COMUNES (CPC, FLURY, 1988)

Este procedimiento permite ir más allá de la inferencia de igualdad o desigualdad entre matrices de covariación explorando similitud entre los componentes principales de las matrices a comparar (Flury, 1988). Así, el método distingue relaciones de igualdad o proporcionalidad entre matrices (eigenvectores iguales, eigenvalores multiplicados por un escalar), matrices que comparten todos sus componentes principales (eigenvectores iguales, eigenvalores distintos), o que comparten uno, dos o hasta $p-2$ componentes principales ($p \times p$ siendo la dimensión de la matriz).

Comenzando con la hipótesis de que no existe relación entre las matrices comparadas, el procedimiento evalúa de manera jerárquica y ascendente la probabilidad de que las matrices compartan el primer componente principal (CPC(1)), los dos primeros componentes principales (CPC(2)), los $p-2$ primeros componentes principales (CPC($p-2$)), todos los componentes principales (CPC), el que sean proporcionales o iguales. Esta sucesión puede realizarse entre los modelos vecinos en la jerarquía, p.e. comparando la no relación vs CPC(1), CPC(1) vs. CPC(2), etc., estrategia conocida como step-up, o puede realizarse dando saltos entre niveles (jump-up). En particular, las comparaciones se realizan entre el modelo de no relación y todos los modelos superiores (Phillips y Arnold, 1999, Fig.

CPC). Las comparaciones entre modelos se realizan a través de la estadística de cociente de verosimilitudes que tiene una distribución ji-cuadrada (Phillips y Arnold, 1999). Las comparaciones se realizan sobre parejas de modelos vecinos en la jerarquía (estrategia step-up) o entre el modelo de no relación y cualquier otro. La comparación se puede interpretar como la verosimilitud de que el modelo superior será cierto, dado que el modelo inferior también es cierto. Si la comparación es estadísticamente significativa, se rechaza el modelo superior. Si por el contrario, no hay significancia en la comparación, se procede a la siguiente comparación superior en la jerarquía (Documentación asociada al programa CPC, Phillips y Arnold, 1999).

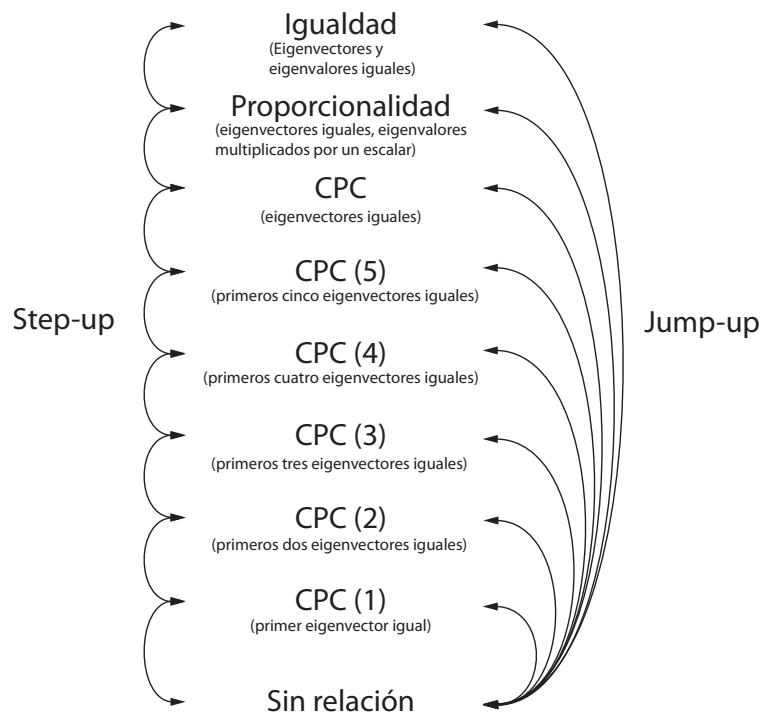


Figura A.1. Modelos comparados en el método de Componentes Principales Comunes. Se ilustra el caso de una matriz de covariación de 7 caracteres (dimensión 7x7). La comparación de matrices comienza con el modelo de no relación entre las matrices y continúa de manera ascendente con el caso donde las matrices comparten uno, dos, tres, cuatro, cinco o todos los componentes principales, son proporcionales o equivalentes. La estrategia de comparación Step-up involucra modelos vecinos, mientras que la estrategia Jump-Up compara el modelo de la ausencia de relación con todos los modelos superiores.

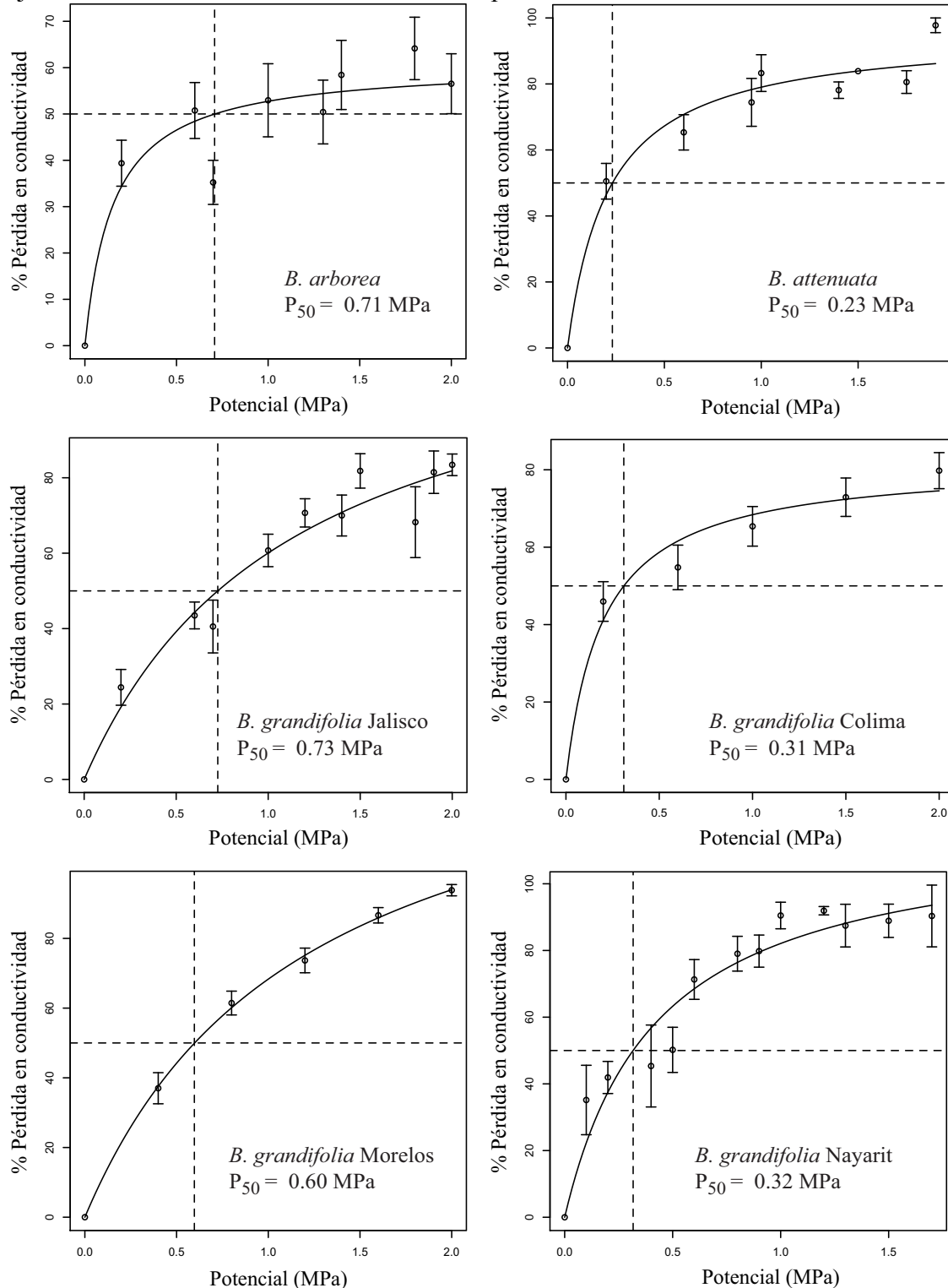
A.2. COMPARACIÓN DE MATRICES A TRAVÉS DEL MÉTODO JACKNIFE-MANOVA DE ROFF (2002).

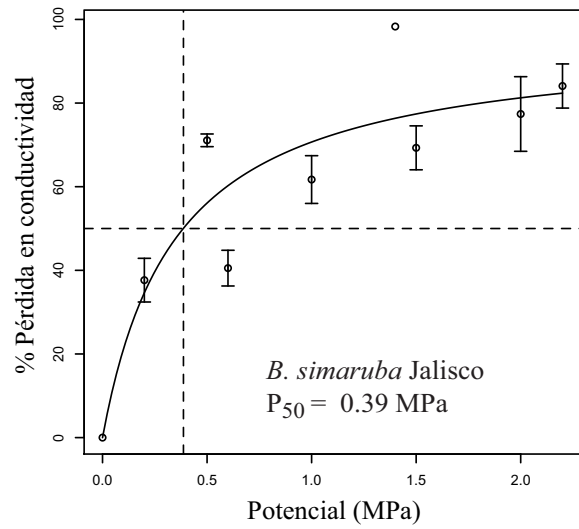
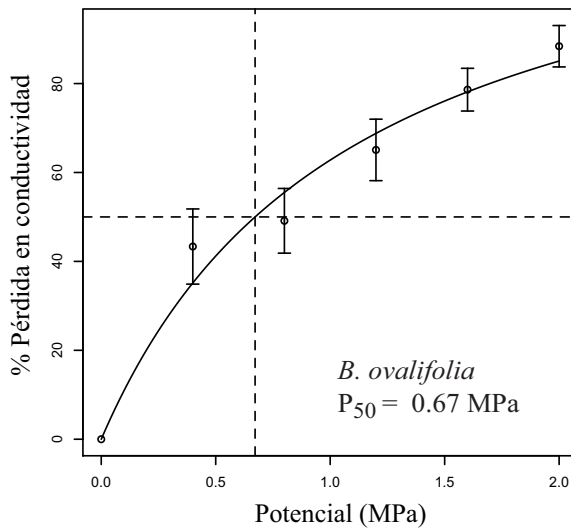
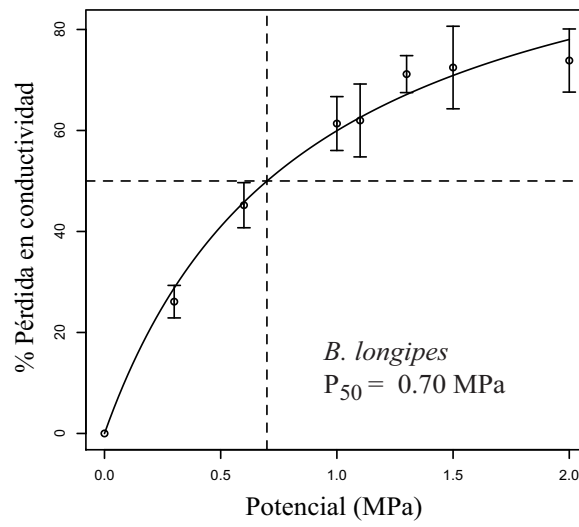
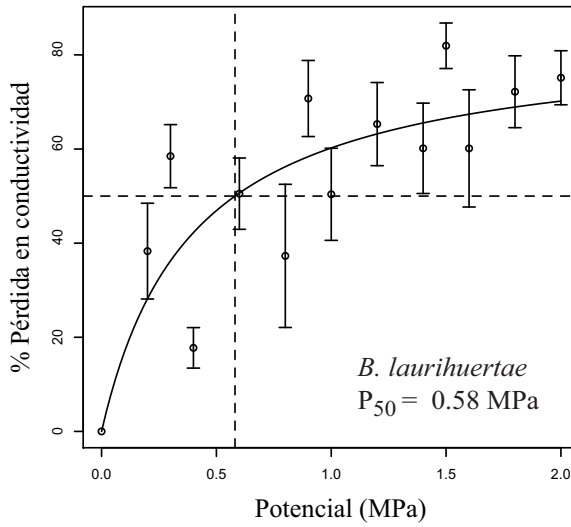
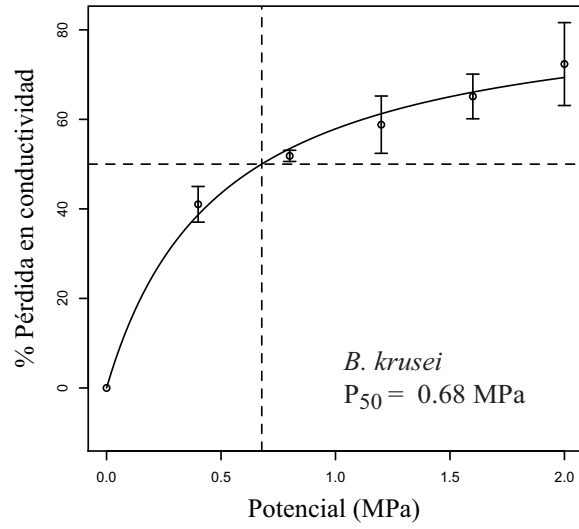
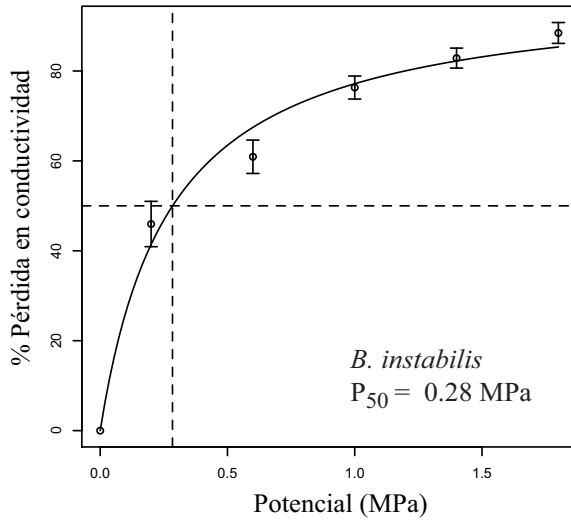
Este método se fundamenta en el MANOVA para realizar las comparaciones entre matrices, considerando a cada elemento de una matriz una variable dependiente. Puesto que dentro de una matriz solamente hay un valor de varianza para cada variable o de covarianza entre variables, es necesario replicar estos datos para poder realizar una comparación a través de un MANOVA. Esto se logra con el procedimiento jacknife, con el que se generan pseudovalores para cada uno de estos datos (Manly, 2007). La aplicación de un MANOVA sobre estos datos permite comparar múltiples matrices simultáneamente y ubicar puntualmente las diferencias en las covarianzas entre especies, algo que el método de Flury no permite rastrear.

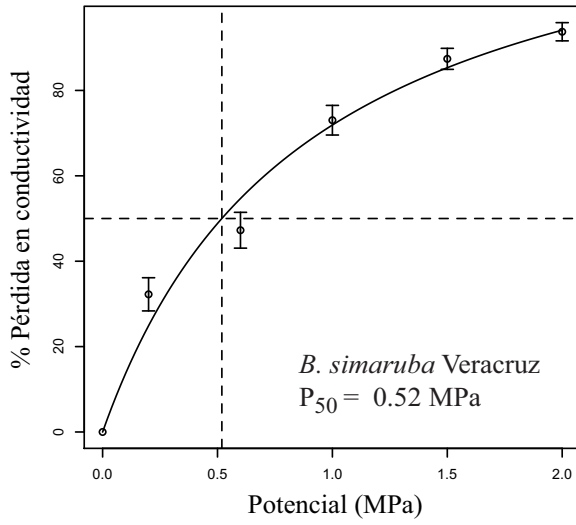
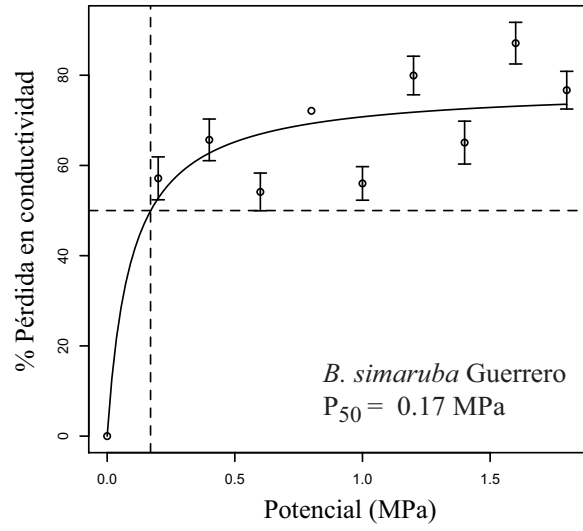
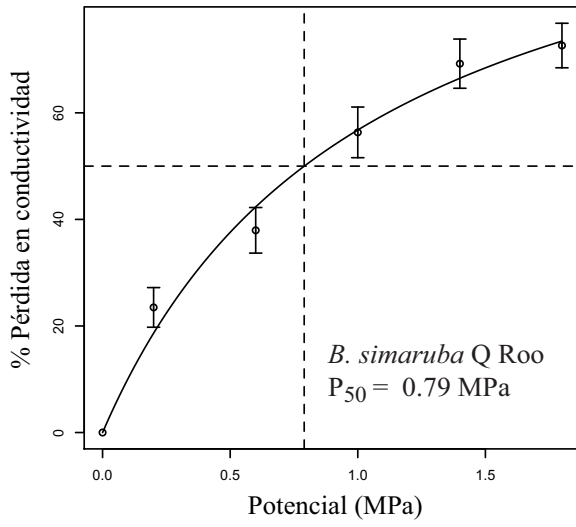
LITERATURA CITADA

- Cheverud, J.M. y G. Marroig. 2007. Comparing covariances matrices: random skewers method compared to the common principal components model. *Genetics and Molecular Biology* 30: 461-469.
- Flury, B. 1988. *Common principal components and related multivariate models*. Wiley, New York.
- Houle, D., Mezey, J., y P. Galpern. 2002. Interpretation of the results of the common principal components analyses. *Evolution* 56: 433-440.
- Manly, B. F. J. 2007. *Randomization, bootstrap and Monte Carlo methods in biology*. Chapman & Hall, Florida.
- Phillips, P. C. y S. J. Arnold. 1999. Hierarchical comparison of genetic variance-covariance matrices. I. Using the Flury hierarchy. *Evolution* 53: 1506-1515.
- Roff, D. 2002. Comparing G matrices: a manova approach. *Evolution* 56: 1286-1291.
- Steppan, S. J., Phillips, P. C. y D. Houle. 2002. Comparative quantitative genetics: evolution of the G matrix. *Trends in Ecology and Evolution* 17: 321-327.

Apéndice B. Curvas de vulnerabilidad para las 15 especies y poblaciones incluidas en este trabajo. Los puntos representan el promedio y los bigotes el error estándar del porcentaje en la pérdida de conductividad a un potencial determinado. Las rectas indican el potencial hídrico al que ocurre un 50% de pérdida en la conductividad del tallo (P_{50}). El modelo ajustado a los datos es un modelo no lineal tipo Michaelis-Menten.







Apéndice C. Matrices de correlación para siete variables funcionales de la madera por especie y población. Cada matriz está basada en los resultados para 18 tallos.

Tabla C.1. Matriz de correlación para *B. arborea* incluyendo siete caracteres de la madera. Se resaltan las correlaciones significativas a un nivel $\alpha=0.05$.

	E_{mad}	MOR	D_{mad}	CA_{mad}	V_{pmad}	K_{max}
MOR	0.519					
D_{mad}	-0.011	0.117				
CA_{mad}	0.045	-0.055	-0.014			
V_{pmad}	0.109	0.142	0.947	-0.111		
K_{max}	-0.076	-0.070	0.036	0.686	-0.101	
C_{mad}	0.019	-0.181	-0.501	0.076	-0.454	0.390

Tabla C.2. Matriz de correlación para *B. attenuata* incluyendo siete caracteres de la madera. Se resaltan las correlaciones significativas a un nivel $\alpha=0.05$.

	E_{mad}	MOR	D_{mad}	CA_{mad}	V_{pmad}	K_{max}
MOR	0.684					
D_{mad}	0.422	0.299				
CA_{mad}	-0.509	-0.428	-0.552			
V_{pmad}	0.427	0.304	0.823	-0.867		
K_{max}	0.405	0.115	-0.096	0.150	-0.213	
C_{mad}	-0.359	-0.169	-0.415	0.294	-0.328	-0.162

Tabla C.3. Matriz de correlación para *B. grandifolia*-Jalisco incluyendo siete caracteres de la madera. Se resaltan las correlaciones significativas a un nivel $\alpha=0.05$.

	E_{mad}	MOR	D_{mad}	CA_{mad}	V_{pmad}	K_{max}
MOR	0.770					
D_{mad}	0.058	0.073				
CA_{mad}	0.421	0.213	-0.466			
V_{pmad}	0.021	0.085	0.953	-0.606		
K_{max}	0.156	0.020	-0.045	-0.011	-0.130	
C_{mad}	-0.352	-0.266	0.100	-0.531	0.255	-0.253

Tabla C.4. Matriz de correlación para *B. grandifolia*-Colima incluyendo siete caracteres de la madera. Se resaltan las correlaciones significativas a un nivel $\alpha=0.05$.

	E_{mad}	MOR	D_{mad}	CA_{mad}	V_{pmad}	K_{max}
MOR	0.201					
D_{mad}	-0.094	0.038				
CA_{mad}	-0.039	0.168	-0.174			
V_{pmad}	0.028	0.161	0.712	-0.488		
K_{max}	0.035	0.436	-0.292	0.533	-0.471	
C_{mad}	-0.270	-0.127	0.015	-0.040	-0.002	-0.075

Tabla C.5. Matriz de correlación para *B. grandifolia*-Morelos incluyendo siete caracteres de la madera. Se resaltan las correlaciones significativas a un nivel $\alpha=0.05$.

	E_{mad}	MOR	D_{mad}	CA_{mad}	V_{pmad}	K_{max}
MOR	0.534					
D_{mad}	0.137	0.153				
CA_{mad}	0.089	0.074	-0.452			
V_{pmad}	0.405	0.465	0.776	-0.361		
K_{max}	-0.073	-0.551	-0.077	0.190	-0.112	
C_{mad}	0.392	0.238	-0.219	-0.035	-0.089	-0.068

Tabla C.6. Matriz de correlación para *B. grandifolia*-Nayarit incluyendo siete caracteres de la madera. Se resaltan las correlaciones significativas a un nivel $\alpha=0.05$.

	E_{mad}	MOR	D_{mad}	CA_{mad}	V_{pmad}	K_{max}
MOR	0.689					
D_{mad}	0.281	0.253				
CA_{mad}	-0.372	-0.389	-0.083			
V_{pmad}	0.409	0.420	0.410	-0.921		
K_{max}	0.015	-0.116	-0.361	0.071	-0.179	
C_{mad}	-0.166	-0.174	-0.092	0.088	-0.055	0.540

Tabla C.7. Matriz de correlación para *B. instabilis* incluyendo siete caracteres de la madera. Se resaltan las correlaciones significativas a un nivel $\alpha=0.05$.

	E_{mad}	MOR	D_{mad}	CA_{mad}	V_{pmad}	K_{max}
MOR	0.342					
D_{mad}	0.390	0.329				
CA_{mad}	-0.221	0.052	-0.541			
V_{pmad}	0.267	0.266	0.960	-0.642		
K_{max}	0.448	0.652	0.128	0.288	0.017	
C_{mad}	0.507	0.574	0.466	-0.189	0.351	0.191

Tabla C.8. Matriz de correlación para *B. krusei* incluyendo siete caracteres de la madera. Se resaltan las correlaciones significativas a un nivel $\alpha=0.05$.

	E_{mad}	MOR	D_{mad}	CA_{mad}	V_{pmad}	K_{max}
MOR	0.132					
D_{mad}	-0.293	-0.211				
CA_{mad}	0.016	-0.680	0.369			
V_{pmad}	-0.391	-0.186	0.940	0.222		
K_{max}	-0.016	-0.043	-0.530	0.030	-0.504	
C_{mad}	-0.288	-0.282	-0.278	0.330	-0.339	0.271

Tabla C.9. Matriz de correlación para *B. laurihuertae* incluyendo siete caracteres de la madera. Se resaltan las correlaciones significativas a un nivel $\alpha=0.05$.

	E_{mad}	MOR	D_{mad}	CA_{mad}	V_{pmad}	K_{max}
MOR	0.754					
D_{mad}	0.056	0.354				
CA_{mad}	0.126	-0.143	-0.885			
V_{pmad}	0.120	0.436	0.788	-0.619		
K_{max}	0.184	0.005	0.068	0.020	-0.034	
C_{mad}	-0.120	-0.271	-0.428	0.210	-0.196	-0.173

Tabla C.10. Matriz de correlación para *B. longipes* incluyendo siete caracteres de la madera. Se resaltan las correlaciones significativas a un nivel $\alpha=0.05$.

	E_{mad}	MOR	D_{mad}	CA_{mad}	V_{pmad}	K_{max}
MOR	0.899					
D_{mad}	0.359	0.477				
CA_{mad}	-0.458	-0.625	-0.855			
V_{pmad}	0.532	0.616	0.908	-0.844		
K_{max}	0.297	0.251	-0.086	-0.024	0.036	
C_{mad}	-0.032	-0.047	-0.006	-0.275	0.065	-0.059

Tabla C.11. Matriz de correlación para *B. ovalifolia* incluyendo siete caracteres de la madera. Se resaltan las correlaciones significativas a un nivel $\alpha=0.05$.

	E_{mad}	MOR	D_{mad}	CA_{mad}	V_{pmad}	K_{max}
MOR	0.540					
D_{mad}	0.313	0.478				
CA_{mad}	-0.558	-0.576	-0.644			
V_{pmad}	0.324	0.498	0.981	-0.707		
K_{max}	0.171	0.183	0.048	0.019	0.032	
C_{mad}	0.053	-0.049	-0.422	-0.058	-0.364	-0.171

Tabla C.12. Matriz de correlación para *B. simaruba*-Jalisco incluyendo siete caracteres de la madera. Se resaltan las correlaciones significativas a un nivel $\alpha=0.05$.

	E_{mad}	MOR	D_{mad}	CA_{mad}	V_{pmad}	K_{max}
MOR	0.541					
D_{mad}	0.486	0.834				
CA_{mad}	-0.439	-0.743	-0.701			
V_{pmad}	0.442	0.849	0.988	-0.750		
K_{max}	-0.091	-0.658	-0.575	0.793	-0.657	
C_{mad}	-0.411	-0.523	-0.556	0.243	-0.558	0.378

Tabla C.13. Matriz de correlación para *B. simaruba*-Quintana Roo incluyendo siete caracteres de la madera. Se resaltan las correlaciones significativas a un nivel $\alpha=0.05$.

	E_{mad}	MOR	D_{mad}	CA_{mad}	V_{pmad}	K_{max}
MOR	0.384					
D_{mad}	0.178	0.520				
CA_{mad}	-0.277	-0.433	-0.549			
V_{pmad}	0.340	0.549	0.929	-0.603		
K_{max}	0.073	0.008	-0.136	0.327	-0.185	
C_{mad}	-0.120	-0.136	-0.452	0.059	-0.422	0.203

Tabla C.14. Matriz de correlación para *B. simaruba*-Guerrero incluyendo siete caracteres de la madera. Se resaltan las correlaciones significativas a un nivel $\alpha=0.05$.

	E_{mad}	MOR	D_{mad}	CA_{mad}	V_{pmad}	K_{max}
MOR	0.296					
D_{mad}	0.137	0.849				
CA_{mad}	-0.030	-0.616	-0.821			
V_{pmad}	0.151	0.857	0.997	-0.821		
K_{max}	0.394	0.261	0.030	0.251	0.039	
C_{mad}	-0.208	-0.204	0.118	-0.466	0.089	-0.484

Tabla C.15. Matriz de correlación para *B. simaruba*-Veracruz incluyendo siete caracteres de la madera. Se resaltan las correlaciones significativas a un nivel $\alpha=0.05$.

	E_{mad}	MOR	D_{mad}	CA_{mad}	V_{pmad}	K_{max}
MOR	0.566					
D_{mad}	0.291	0.734				
CA_{mad}	-0.002	-0.573	-0.782			
V_{pmad}	0.254	0.679	0.983	-0.833		
K_{max}	0.435	-0.235	-0.455	0.493	-0.455	
C_{mad}	-0.397	-0.655	-0.722	0.559	-0.727	0.095

CONCLUSIONES GENERALES

La integración funcional ha sido un tema central en la biología evolutiva desde hace mucho tiempo (p.e., el principio de correlación funcional de Cuvier, 1817), pero no es sino hasta recientemente que su impacto en los estudios adaptativos está siendo reconocido de manera explícita (Schwenk, 2001; Ghalambor et al., 2004; Toro et al., 2004). Esta tesis aborda la integración funcional y su impacto en la adaptación de los organismos, y la vincula con algunos de los temas más importantes de la biología evolutiva actual, como el origen de la covariación en unidades funcionales (Schwenk, 2001), las restricciones evolutivas (Schwenk y Wagner, 2004) y la modularidad (Olson y Rosell, 2006). Aunque esta tesis está enfocada en la integración funcional de los tallos leñosos, los resultados y las preguntas que emergieron del estudio de estas estructuras resultan de interés para cualquier sistema altamente integrado.

Es mucho lo que falta por entender sobre la integración funcional en los tallos. Sin embargo, la comparación entre niveles evolutivos realizada en este trabajo informa sobre el impacto de los patrones de covariación en la diversificación morfológica de los árboles. Aunque existieron diferencias en los patrones de integración de algunas poblaciones, en general las correlaciones encontradas aquí sugieren que los árboles tienen un eje de variación dado por el trade-off mecánica-almacenamiento y otro eje relacionado con la conductividad. De acuerdo con lo discutido en este trabajo, combinaciones fuera de estos ejes son posibles ontogenéticamente, pero probablemente no son favorecidas por la selección natural. Las combinaciones que sí son favorecidas parecen limitadas, pero permiten cambios drásticos de hábito en las plantas, como se discutió para *B. instabilis* y *B. standleyana* (Capítulos 2 y 3).

Uno de los aspectos que hace falta abordar en los estudios de la integración de los tallos es la vinculación entre los patrones a nivel funcional y aquellos que ocurren a niveles de organización más bajos. Aunque se ha vinculado la covariación funcional con las características anatómicas, se desconocen los procesos de desarrollo del xilema, que controlan esta covariación, i.e., los procesos detrás de la “decisión” de un meristemo de producir un elemento de vaso o una célula de parénquima. El estudio de la evolución de los tallos se beneficiará, sin duda, de continuar la documentación de los patrones de

covariación en nuevos sistemas y en otros ambientes, pero sería un paso muy importante combinar el estudio de la integración funcional con la integración del desarrollo (Breuker et al., 2006), sobre todo cuando se ha encontrado que la función puede inducir la integración a niveles más bajos, como el epigenético (Zelditch et al., 2009).

Una pregunta de mucho interés desde el punto de vista de la integración y evolución fenotípica es determinar qué carácter o caracteres son el blanco de la selección natural en una relación tipo trade-off y qué constituye una adaptación en este contexto. Se discutió en el Capítulo 3 una forma de determinar el carácter que es blanco de selección usando una aproximación comparativa, las relaciones filogenéticas e información ambiental. Sin embargo, una aproximación experimental a esta pregunta complementaría la comparativa y podría contribuir a determinar si es el carácter aislado o las combinaciones de dos o más caracteres lo que constituye una adaptación.

De este trabajo también se concluye que, por su combinación de caracteres de alta y baja disparidad, el clado *simaruba* provee un sistema ideal para estudios que aborden los factores evolutivos internos y externos que modelan el fenotipo de los organismos (Frankino et al., 2007). El número limitado de fenotipos para las hojas, las flores y los frutos, que ha complicado tanto la taxonomía del complejo (Capítulo 1), invita a realizar estudios de restricciones de desarrollo en este sistema (Brakefield, 2006). En contraste, la alta diversidad estructural que se asocia con condiciones ambientales, lo convierte en un grupo ideal para estudiar adaptación. La filogenia generada en este trabajo es un marco indispensable para cualquier estudio de este tipo.

LITERATURA CITADA

- Brakefield, P. M. 2006. Evo-devo and constraints on selection. *Trends in Ecology and Evolution* 21: 362-368.
- Breuker, C. J., Debat, V. y P. Klingenberg. 2006. Functional evo-devo. *Trends in Ecology and Evolution* 21: 488-492.
- Cuvier, G. 1817. *Le Règne animal distribué d'après son organisation*. Imprenta de A. Berlin, París. Traducción en inglés Animal Kingdom arranged according to its organization.
- Frankino, W. A., Zwaan, B. J., Stern, D. L. y P. M. Brakefield. 2007. Internal and external constraints in the evolution of morphological allometries in a butterfly. *Evolution* 61: 2958-2970.
- Ghalambor, C. K., Reznick, D. N. y J. A. Walker. 2004. Constraints on adaptive evolution: the functional trade-off between reproduction and fast-start swimming performance in the Trinidadian guppy (*Poecilia reticulata*). *American Naturalist* 164: 38-50.
- Olson, M. E. y J. A. Rosell. 2006. Using heterochrony to detect modularity in the evolution of stem diversity in the plant family Moringaceae. *Evolution* 60: 724-734.

- Schwenk, K. 2001. Functional units and their evolution. In Wagner, G. P. (ed.). *The Character Concept in Evolutionary Biology*. Academic Press, San Diego: 165-198.
- Schwenk, K. y G. P. Wagner. 2004. The relativism of constraints on phenotypic evolution. En Pigliucci, M. y K. Preston, eds. *Phenotypic integration. Studying the ecology and evolution of complex phenotypes*. Oxford University Press, Oxford: 390-408.
- Toro, E., Herrel, A., y D. Irschick. 2004. The evolution of jumping performance in Caribbean *Anolis* lizards: solutions to biomechanical trade-offs. *American Naturalist* 163: 844-856.
- Zelditch, M. L., Wood, A. R. y D. L. Swiderski. 2009. Building developmental integration into functional systems: function-induced integration of mandibular shape. *Evolutionary Biology* 36: 71-87.

ANEXO A.

**PROBANDO SUPUESTOS IMPLÍCITOS SOBRE LA DEPENDENCIA EN LA
EDAD O EN EL TAMAÑO POR PARTE DE LA BIOMECÁNICA DE LOS TALLOS
USANDO *PITTOCAULON PRAECOX* (ASTERACEAE)**

TESTING IMPLICIT ASSUMPTIONS REGARDING THE AGE VS. SIZE DEPENDENCE OF STEM BIOMECHANICS USING *PITTOCAULON* (~*SENECIO*) *PRAEcox* (ASTERACEAE)¹

JULIETA A. ROSELL AND MARK E. OLSON²

Instituto de Biología, Universidad Nacional Autónoma de México, Departamento de Botánica, Tercer Circuito s/n,
Ciudad Universitaria, Copilco, Coyoacán A.P. 70–367, México, Distrito Federal, C.P. 04510, Mexico

Strong covariation between organismal traits is often taken as an indication of a potentially adaptively significant relationship. Because one of the main functions of woody stems is mechanical support, identifying the factors that covary with biomechanics is essential for inference of adaptation. To date in such studies, stem biomechanics is plotted against stem age or size, thus with implicit assumptions regarding the importance of each in determining mechanics. Likewise, comparing ontogenies between individuals is central to the study of ontogenetic evolution (e.g., heterochrony). Both absolute age and size have been used, but the rationale for choosing one over the other has not been examined. Sampling a plant of simple architecture across microsites with differing sizes for the same absolute age, we compared regressions of stem length, mechanics, and tissue areas against age and size. Stem length was predicted by diameter but not by age, and stem biomechanics and tissue areas were better explained by stem length rather than age. We show that the allometric and mechanical properties observed across microsites are uniform despite great plasticity in other features (e.g., size and wood anatomy) and suggest that this uniformity is an example of developmental homeostasis. Finally, we discuss reasons for preferring size over absolute age as a basis for comparing ontogenies between individuals.

Key words: adaptation; allometry; Asteraceae; developmental homeostasis; heterochrony; ontogenetic autocorrelation; plasticity; Young's modulus.

Covariation between morphological characters has often been interpreted as an indication of functional relationships that may be of adaptive significance. From this point of view, close correlations suggest selectively important relationships, whereas a lack of covariation between characters suggests that their synergy is not essential for survival (cf. Berg, 1960; Frankino et al., 2005). For example, the observation that many tree species have constant trunk–crown allometric relationships throughout ontogeny (Sterck and Bongers, 1998) thus could be interpreted as indicating that the maintenance of specific allometric relationships may be of strong functional significance. The same reasoning leads to the idea that dissociation between characters such as the lack of phenotypic integration between vegetative and reproductive characters (e.g., Pigliucci et al., 1991) implies that strong covariation between these features is not essential for organismal function and thus not favored by natural selection. Covariation between features in ontogeny or across the adults of a clade has also been interpreted as an indication of developmental constraint (e.g., Zelditch et al., 1990; Marroig and Cheverud, 2005). To begin to unravel the causes of trait covariation and to identify

relationships of adaptive significance, we first need to identify the characters involved and the strength and direction of their covariation.

The stems of woody plants are studied from many points of view such as anatomical, hydraulic, biomechanical, allometric, yet many assumptions remain untested regarding the covariation of these traits with stem size and age. For example, on what basis can it be said that the wood of species A is stiffer than the wood of species B, that the xylem of one is more vulnerable to cavitation than another, or that the libriform fibers have thicker walls in one than the other? Such ranking of traits is based on some standard, but what standard best predicts the traits of interest has not been widely addressed. Some workers prefer to compare features between stems of similar size (e.g., Tyree and Yang, 1992; Kavanaugh et al., 1999; Carlquist and Grant, 2005), whereas others have reason to favor comparisons between stem segments of similar absolute age (e.g., Bailey and Tupper, 1918; Panshin and de Zeeuw, 1980; Moltenberg and Hoibo, 2006). A notable exception is the work of Spicer and Gartner (2001), who found that tree ring age was not sufficient to explain the specific conductivity (k_s) of a given sample of xylem but that position within the stem was strongly associated with k_s . The use of stem age vs. stem size as a basis for the comparison of stem properties between individuals (whether anatomical, hydraulic, mechanical, or otherwise) implies differing scenarios regarding the adaptive significance of these variables. Plotting stem characteristics against age invokes the implicit hypothesis that certain features are dependably associated with the same age between individuals. In contrast, comparing stem features in the context of stem size between individuals involves the notion that, regardless of its age, the structure and function of a stem must keep pace with its proportions.

In this article, we focus on the biomechanical behavior of stems and ask whether mechanics are best predicted by the

¹ Manuscript received 24 June 2006; revision accepted 1 November 2006.

The authors thank F. Sánchez-Sesma, K. Niklas, F. Ewers, and G. Ángeles for helpful discussions, C. Díaz for assistance with the calculation of growth rates, R. Aguirre for statistical advice, and C. León for laboratory assistance. Field and lab work were supported by the Instituto de Biología, UNAM, the Dirección General de Asuntos del Personal Académico/Programa de Apoyo a Proyectos de Investigación e Innovación Tecnológica, UNAM, Project #IN229202, and Consejo Nacional de Ciencia y Tecnología Project #46475, both awarded to M.E.O.; scholarship #172233 from the Consejo Nacional de Ciencia y Tecnología, and a Karling Award from the Botanical Society of America, were both awarded to J.A.R.

² Author for correspondence (e-mail: explore@explorelifeonearth.org)

absolute age or by the size of a stem segment. Because one of the major functions of woody plant stems is mechanical support, stem biomechanical data provide crucial information for inferences of adaptation in these organisms. Despite the importance of understanding the interrelationship between mechanics, size, and age, in most biomechanical studies of woody plant stems, variation in mechanical behavior has been considered either in the context of absolute age or growth rates (e.g., Bhat and Priya, 2004) or of stem allometry (e.g., Niklas and Buchman, 1994) but not both simultaneously. Similarly, in various studies the relationship between allometry in relation to size or age has been considered, but the mechanical parameters were not examined or were inferred indirectly (e.g., Sterck and Bongers, 1998; Briand et al., 1999; Poorter et al., 2003). Taken together, these studies imply that the mechanical behavior of a stem is related to its size, age, and allometry, but to what extent each plays a part cannot be determined when these factors are considered separately. Identifying whether or not woody stem features are more strongly predicted by stem size or age would permit a biologically justified selection of one or the other for a given study. To provide information to guide the inference of woody plant stem evolution and to distinguish between these very different implicit visions of ontogeny, it is vital to understand the ways that structure, size, age, and allometry interact to produce mechanical behavior.

It might be argued that age and size are clearly and necessarily related in woody stems, an assertion that highlights the differences between within-stem and between-individual comparisons. Within individual stems, age and size vary predictably in that the direction of the correlation between size and age can always be predicted; because woody stems grow via the accretion of xylem layers, an older stem segment will inevitably have accumulated more layers than a more distal and therefore younger segment. Greater stem segment diameter implies greater second moment of area I , the mechanical parameter that describes the geometric arrangement and size of a given beam in cross section and mathematically reflects how well this arrangement of material can resist bending. As a result, larger, more basal segments can confidently be predicted to be less flexible than more distal segments, although the magnitude of this difference cannot be predicted (see Niklas, 1995, 1997a–c, 1999a). However, the relationship of mechanics with size and age in comparisons between individuals is less clear, because stems of the same age growing in different environments or microsites can have differing sizes (e.g., Rozas, 2003; Parish and Antos, 2004; Brienen and Zuidema, 2006). For example, a stem growing slowly in a dry environment will be much smaller than a rapidly growing stem in a moist one, even though they may be clones of the same age (cf. Weiner, 2004). Thus, in contrast to comparisons of segments within the same stem, larger stem size does not necessarily indicate greater age between individuals. It is precisely this plasticity that gives rise to the problem of whether size or age better reflects stem properties, mechanical and otherwise. To test the relative importance of each requires a model system in which age can be readily determined.

We compare the relationship of mechanical behavior to both size and age using the Asteraceous “broomstick tree” *Pittocaulon* (~*Senecio*) *praecox* (Cav.) H. Rob. and Brettell, endemic to seasonally dry tropical areas of southern central Mexico. This species is ideal for such tests for several reasons. First, the pattern of leaf scars on the stem permits the inference of the age of any segment (Pérez and Franco, 2000). Early in

the yearly rainy season, the internodes are long, and the leaf scars on the stem are well separated, but as the rains dwindle, the internodes become so short that the scars of the final leaves produced nearly touch one another, leaving a conspicuous ring of scars around the stem (Fig. 1B, C). Each scar ring thus indicates the growth of one season. We are not aware of other woody dicots in which these annual scars can be so readily detected, even in stems decades old. Second, detailed anatomical information is available for *P. praecox* and its relatives (Olson, 2005), which allows us to pinpoint the anatomical features responsible for some of the ontogenetic changes in biomechanical behavior observed. Finally, *P. praecox* has relatively simple architecture, consisting of thick stems that branch only occasionally, thus providing long, straight beams ideal for mechanical bending tests (Fig. 1A). There is relatively little xylem in the stems of *Pittocaulon*, with the bulk taken up by thick, water-storing pith and bark that fuel flowering and fruiting at the end of the 6-month dry season (Fig. 1A inset, D; Olson, 2005).

By sampling a variety of situations, from old, slow-growing individuals atop exposed lava boulders to younger trees of rapid growth in shady hollows, we tested stems spanning an array of size–age relations (Fig. 2; cf. Niklas, 1995). Our general strategy to address whether the mechanical properties of a stem are better explained by its absolute age or by its size was to compare the fit of a linear regression that included age as a covariable with one using stem length. First, we asked whether or not stem length–diameter proportions should resemble each other more strongly between stems of similar size or between those of similar absolute ages. Likewise, are similar materials properties, i.e., tissue and structural Young’s moduli (E), observed between stems of similar sizes or between stems of similar absolute ages? We also examined the changes in areas occupied by bark, wood, and pith along the length of the stems studied. These tissue areas are important because, in addition to E , the mechanical behavior of a structure is also determined by the amount and arrangement of its materials, as reflected by the second moment of area I . Therefore, we determined whether the percentage of the cross-sectional area of the stem occupied by bark, wood, and pith were best predicted by segment age or by stem diameter. Furthermore, because it is the performance of the entire branch that is of greatest adaptive relevance, we examined flexural stiffness EI . Because I is related directly to stem diameter, then stem size would be expected to predict EI well. However, it is not clear to what extent age should be associated with stem EI . We therefore also examined how well the age of a given stem segment predicts its flexural stiffness. Finally, many studies have suggested that differences between environments or growth rates result in differences in mechanical properties (Kliger et al., 1998; Bhat and Priya, 2004). We examined which features change with the great differences in environments and growth rates sampled and how these are involved in the interplay between size, allometry, and mechanics. Finally, we highlight which stem features appear to be of chief adaptive importance in woody stems and discuss the merits of size vs. age in studies of ontogenetic evolution.

MATERIALS AND METHODS

Plants were collected from a highland, dry tropical scrub community on the Pedregal de San Ángel lava field in the southwestern part of the Valley of

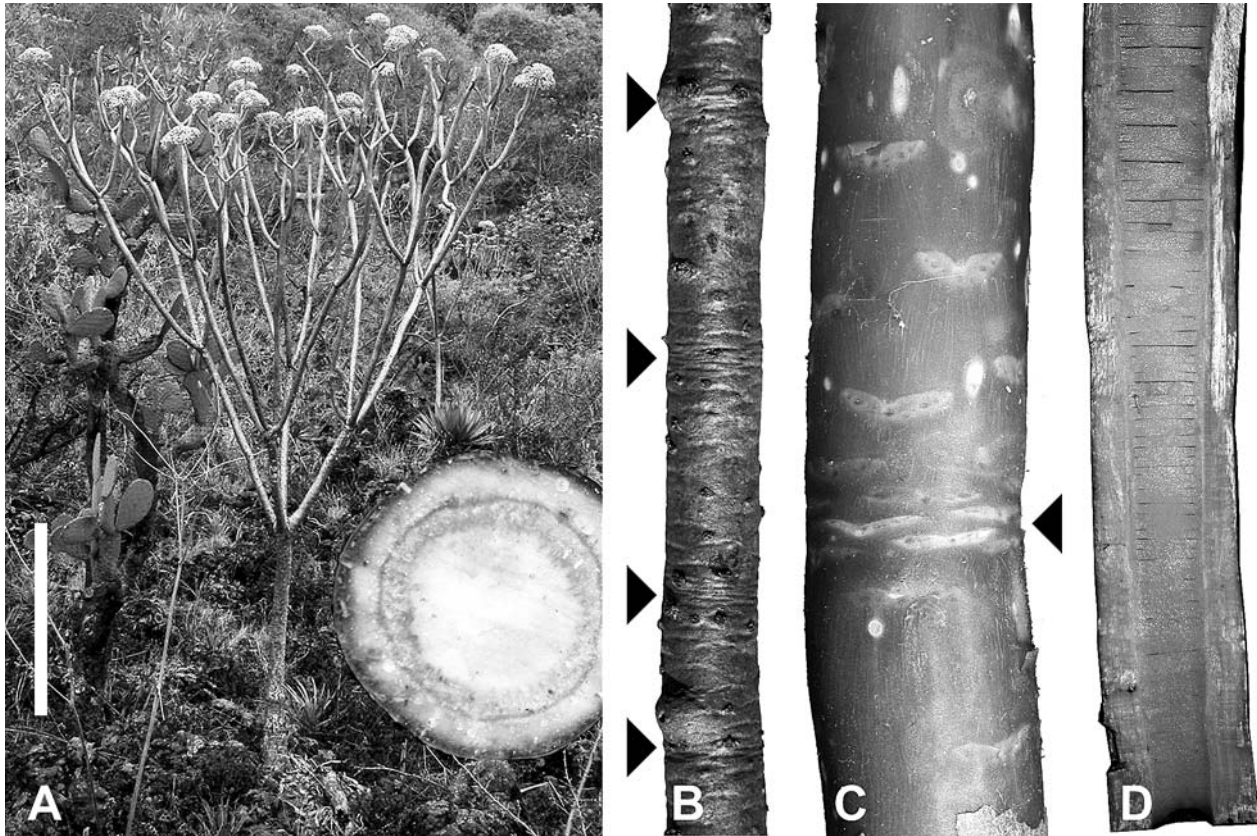


Fig. 1. *Pittocaulon* habit and stem construction. (A) Habit, with thick stems and sparse branching. Scale bar = 1 m. Inset, 6.5 cm diameter stem in transection to show the very wide pith, thin xylem cylinder, and bark with thick, water-storing cortex. (B) Stem with annular scars left at the end of each growing season. Four such rings are shown here (arrows). Stem = 1.5 cm in diameter. (C) In older stems, the annular scars can become obscured by the phellem, but they are preserved and readily detected by exposing the phellogen. A large amount of phellem was removed from this stem to show separated mid-season leaf scars and the aggregated end-of-season scars (arrow); only a very small amount was removed from stems subjected to mechanical testing. Stem = 5.5 cm in diameter. (D) Stem split lengthwise to show very wide pith replete with water at the end of the wet season. Stem = 6 cm in diameter.

Mexico (19°19'14" N 99°11'40" W) at an elevation of 2315 m a.s.l. Vouchers are deposited as *Olson 1020* in the MEXU herbarium. We selected a single branch from each of 16 individuals from microsites describing a range of water availability within a single 0.5 km² locality. The driest habitats were exposed lava outcrops, and the moistest were areas of deeper soil where the natural vegetation was shaded by native and invasive trees. To provide optimal beams for mechanical testing, we selected stems that branched well above the base, had fewer than three orders of branching, and had long, straight segments. Like many water-storing dryland plants, *Pittocaulon* stem water content changes drastically throughout the year (Olson, 2005); mechanical tests could produce differing results between dry and wet seasons (see Jacobsen et al., 2005). To eliminate any such possibility, all allometric measurements and mechanical tests were conducted at the same time of the year, at the end of the 2005 rainy season. The collected stems were immediately taken to the laboratory for processing.

Data were analyzed using simple and multiple linear regressions, checking all assumptions. All variables were log₁₀ transformed to meet assumptions and/or to increase model fit. Statistical analyses employed Statistica v.6.0. (StatSoft, Inc., Tulsa, Oklahoma, USA) and S-Plus 2000 (MathSoft, Inc., Cambridge, Massachusetts, USA).

Stem age—The age of stems was determined by counting the annual growth increment scars (Fig. 1B). These scars were no longer apparent on the older phellem of some lower stems. In these cases, we removed small amounts of phellem to expose the phellogen, where these scars are clearly preserved (a stem with a large amount of phellem removed is shown in Fig. 1C).

Allometric relationships: variation of stem length with diameter and age—We sampled plants of very different heights that were of similar ages and plants of differing ages but similar heights (cf. Niklas, 1995). To test our hypothesis that length is better predicted by its relationship with basal diameter than absolute age, we used linear regressions to estimate the relationships between these variables.

Bending tests and variation of mechanical properties with size and age—For mechanical testing, the branches were divided into segments with a 1 : 20 diameter to length ratio to minimize shear (Vincent, 1992). Each segment was submitted to three-point bending tests using a digital micrometer to measure the deflection of the stem caused by adding weights to a bucket suspended at the midpoint of the tested segment (Vincent, 1990). The taper of each segment was less than 10% of its mean diameter, except for a few terminal segments, which tapered ~20%. The flexural stiffness for each segment (structural flexural stiffness, EI_{struct}) was computed from the formula (Gere, 2002):

$$EI_{\text{struct}} = \frac{L^3}{48m},$$

where m is the slope of the linear relationship resulting from observed deflections of stem segments upon adding a sequence of weights and L is the length between the supports on which the segment ends rested. After testing, each segment was debarked to repeat the bending test and to compute the flexural stiffness of the wood (EI_{wood}). The flexural stiffness of the bark (EI_{bark}) was inferred by taking the difference of EI_{struct} and EI_{wood} (Niklas, 1999b). For most of the terminal segments of the stems, EI_{wood} and thus EI_{bark} could not be

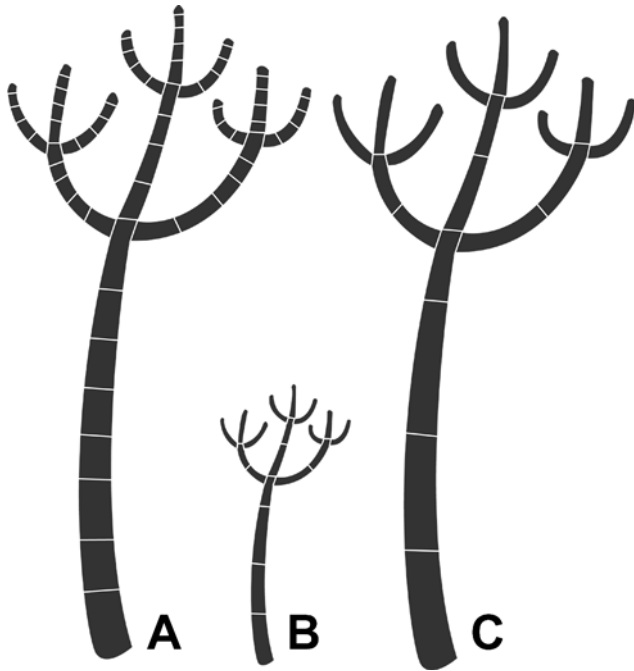


Fig. 2. Age and size in *Pittocaulon*. The black silhouettes represent three individuals of *Pittocaulon*; ages can be determined by annual scars (white lines). All three have flowered twice and thus have undergone two branching events. Despite having similar architecture, the three plants have very different age–size relationships. (A) Tall individual; annual scars show it is 17 years old. (B) Small individual, 7 years old. (C) Tall individual, 7 years old.

computed, because the xylem fascicular areas were not yet united into a continuous cylinder (see Olson, 2005; cf. Esau, 1977, p. 297), making removal of the bark impossible without damaging the xylem. Because the cross sections of the tested segments were nearly circular, the second moments of area (I) were calculated with the formulas of Pisarenko et al. (1979) for circles and hollow circles. To obtain the measurements necessary for calculating I , apical and basal diameters of the bark, wood cylinder, and pith were measured before bending tests for each segment and averaged for computing I_{struct} , I_{wood} , and I_{bark} . After calculating both flexural stiffness (EI) and second moment of area (I), the computation of the different Young's moduli (E_{struct} , E_{wood} , and E_{bark}) was straightforward. The structural Young's modulus (E_{struct}) refers to the heterogeneous composite material formed by the bark and wood when the whole stem is mechanically tested. In tests both with the pith and with the pith removed with a rod, the pith contributes minimally to the flexural stiffness of older stems (data not shown). As a result, we ignored this tissue, although in the terminal segments it likely makes a significant mechanical contribution. The measurements of each segment used for computing I were used to calculate areas occupied by bark, wood, and pith in stem transection.

We regressed the mechanical characteristics EI_{struct} , EI_{wood} , EI_{bark} , E_{struct} , E_{wood} , and E_{bark} on the stem segment midpoint–stem tip distance. We selected this distance as a measure of size based on the expectation that it should reflect the amount of load that a given segment has to bear. We compared these results with regressions of the same mechanical characteristics against stem age. The number of stems tested (16) exceeded the average number of segments per stem (3.6), which made it seem unlikely that similarity between segments due to membership in the same stem would influence our results (i.e., that mechanical data would be ontogenetically autocorrelated, because samples were taken from along the same stem). To check this supposition, in all regressions, “individual” was entered as a random effect to check for its potential influence in the fitting of the model (Longford, 1993). All regressions with distance from the tip and “individual” as independent variables resulted in estimated coefficients and associated standard errors that were practically identical to those estimated in the models without individual as a variable. In contrast, some of the regressions with age as an independent variable had a significant effect of

individual, with the fit slightly increasing. This increase can be attributed to the markedly poor fit of the regressions with age as an explanatory variable. Therefore, we report the fitting of simple models with only distance from the tip or age as independent variables, thus allowing direct comparisons between all models.

Growth rate as a proxy environmental variable—The marked differences in age and size observed (Fig. 2) in plants from a range of environments imply differing growth rates, an observation that is of interest because growth rate has been implicated in many plants as being associated with mechanical differences. We assumed that the average growth rate of a stem should reflect the long-term water availability of a microsite, and we thus considered growth rate a stand-in for water availability, referred to here as “environment.” The plants sampled were collected from the same general area, climate, and soils. However, fine-grained microsite differences led to extreme situations, such as short, old plants on exposed sites on bare rock growing adjacent to tall, young ones in sheltered spots.

To calculate growth rates, stem age was determined, the length of each annual growth increment was measured with a tape measure, and the diameter of the base of each growth increment was measured with digital calipers. Growth rate in length was calculated for each individual as the slope of the simple linear regression line defined by the relationship between annual cumulative length (distance from tip to annual scars) and age. Because we were dealing with cumulative lengths along the same stem, one value could not be considered entirely independent of another. This autocorrelation was taken into account in a variance–covariance matrix (\mathbf{W}), which was incorporated into the estimation process of the regression coefficients as follows (Kutner et al., 2005):

$$\beta = (\mathbf{X}'\mathbf{W}\mathbf{X})^{-1}\mathbf{X}'\mathbf{W}\mathbf{Y},$$

where β is the vector of the least-squares regression coefficients (β_0 and β_1), \mathbf{X} is the matrix that contains the explanatory variable (age in yr), and \mathbf{Y} is the vector of the response variable (annual cumulative length). To construct \mathbf{W} , we performed a preliminary regression of annual cumulative length vs. age to estimate the residuals. Using these residuals, we then estimated the average autocovariance between age difference categories, that is, between all pairs of residuals that differed by 1 year, then between all that differed by 2 years, and so on, until the maximum distance of the total branch age minus one was reached. These values were placed in the off-diagonal cells of the matrix. For example, for a 5-year-old branch, the autocovariance for the 1-year age difference category would be the average autocovariance between the residuals for years 1 and 2, 2 and 3, 3 and 4, and 4 and 5. This value would be placed in all cells that represent a difference of 1 year between segments. The autocovariance for the 2-year category would correspond to the average autocovariance between residuals for years 1 and 3, 2 and 4, and 3 and 5; that for the 3-year category would correspond to the average between years 1 and 4 and 2 and 5, whereas the 4-year category would consist only of the value between years 1 and 5. For the diagonal elements of the matrix, we calculated the average variance for the annual cumulative length of each stem age. That is, the length from the stem tip to the first annual scar was measured and the average variance across all stems calculated. Similarly, the average variance in length from the second annual scar to the stem tip was calculated using data from all stems. This procedure was followed for all ages. The same approach was followed with respect to growth rates in diameter.

To examine whether or not different environmental situations were associated with differences in allometry and mechanics, we used multiple regression models introducing growth rate as an explanatory variable to 13 of the 26 simple regressions in Table 1. These 13 models were selected because they did not include age, which is closely related to growth rate ($r = -0.87$; $P < 0.05$) and could therefore be a source of collinearity. As for simple regressions of mechanical parameters vs. distance from the tip or age, in these multiple models the effect of the “individual” was tested and was also not significant. We inferred a significant environmental effect when $\beta_{\text{growth rate}}$ differed from zero and when the adjusted coefficient of multiple determination r_a^2 increased with respect to the simple model without growth rate. The strength of the contribution of environment to explaining allometric or mechanical response variables was evaluated using semipartial correlations. We preferred semipartial over partial correlations because they readily identified which variable explained more of the variation in the response variable in each multiple model and were thus useful indicators of the relevance of growth rate (Etxeberria, 1999).

TABLE 1. Simple ordinary least-squares regressions of *Pittocaulon* stem length, tissue areas, and mechanical parameters vs. size and age, showing that dimensional variables in all cases predict far more effectively than age. Regressions for stem allometry (a), tissue area (b–d), flexural stiffness (e–g), Young’s modulus (h–j), and moment of inertia (k–m). All variables are log₁₀ transformed. Diameter = basal diameter of the stem (m); Distance = distance from tip of stem to midpoint of segment (m); Age = average age of segment (yr). *F* test for lack of fit of model; β₀ = intercept; β₁ = slope. * = significant at *P* < 0.05; ** = significant at *P* < 0.01; ns = not significant, *P* > 0.05.

	Response	Explanatory	<i>r</i> ²	<i>N</i>	<i>F</i> test	β ₀ ± SE	β ₁ ± SE
(a)	Stem length (m)	Diameter	0.69	16	<i>F</i> _{1,14} = 31.16**	2.20 ± 0.36**	1.33 ± 0.24**
		Age	<0.1	16	<i>F</i> _{1,14} < 0.01, ns	ns	ns
(b)	Bark area (m ²)	Distance	0.69	54	<i>F</i> _{1,52} = 114.01**	-3.61 ± 0.02**	0.60 ± 0.05**
		Age	0.13	58	<i>F</i> _{1,56} = 7.99**	-3.90 ± 0.08**	0.28 ± 0.10**
(c)	Wood area (m ²)	Distance	0.75	53	<i>F</i> _{1,51} = 154.03**	-3.92 ± 0.04**	1.15 ± 0.09**
		Age	0.26	57	<i>F</i> _{1,55} = 19.77**	-4.61 ± 0.13**	0.76 ± 0.17**
(d)	Pith area (m ²)	Distance	0.55	54	<i>F</i> _{1,52} = 62.28**	-3.70 ± 0.05**	0.87 ± 0.11**
		Age	<0.1	58	<i>F</i> _{1,56} = 0.76, ns	-3.93 ± 0.14**	ns
(e)	<i>E</i> _{struct} (GN·m ²)	Distance	0.86	54	<i>F</i> _{1,52} = 322.60**	1.11 ± 0.06**	2.5 ± 0.14**
		Age	0.19	58	<i>F</i> _{1,56} = 12.714**	ns	1.34 ± 0.38**
(f)	<i>E</i> _{wood} (GN·m ²)	Distance	0.91	45	<i>F</i> _{1,43} = 450.30**	1.05 ± 0.05**	2.95 ± 0.14**
		Age	<0.1	46	<i>F</i> _{1,44} = 4.37*	ns	1.03 ± 0.49*
(g)	<i>E</i> _{bark} (GN·m ²)	Distance	0.63	39	<i>F</i> _{1,37} = 63.19**	ns	1.63 ± 0.21**
		Age	<0.1	41	<i>F</i> _{1,39} = 1.02, ns	ns	ns
(h)	<i>E</i> _{struct} (GN/m ²)	Distance	0.8	54	<i>F</i> _{1,52} = 213.82**	-0.36 ± 0.03**	1.02 ± 0.07**
		Age	0.34	58	<i>F</i> _{1,56} = 28.08**	-1.06 ± 0.11**	0.76 ± 0.14**
(i)	<i>E</i> _{wood} (GN/m ²)	Distance	0.74	44	<i>F</i> _{1,42} = 117.04**	0.30 ± 0.03**	0.85 ± 0.08**
		Age	0.12	46	<i>F</i> _{1,44} = 5.95*	ns	0.38 ± 0.15*
(j)	<i>E</i> _{bark} (GN/m ²)	Distance	<0.1	39	<i>F</i> _{1,37} = 0.30, ns	-1.18 ± 0.06**	0.09 ± 0.1706
		Age	<0.1	41	<i>F</i> _{1,39} = 0.08, ns	-1.14 ± 0.15**	-0.05 ± 0.1763
(k)	<i>I</i> _{struct} (m ⁴)	Distance	0.75	54	<i>F</i> _{1,52} = 156.64**	-7.53 ± 0.05**	1.49 ± 0.12**
		Age	<0.1	58	<i>F</i> _{1,56} = 5.16*	-8.15 ± 0.20**	0.57 ± 0.25**
(l)	<i>I</i> _{wood} (m ⁴)	Distance	0.8	53	<i>F</i> _{1,51} = 199.20**	-8.26 ± 0.06**	2.00 ± 0.14**
		Age	0.15	57	<i>F</i> _{1,55} = 9.80**	-9.21 ± 0.24**	0.97 ± 0.31**
(m)	<i>I</i> _{bark} (m ⁴)	Distance	0.76	54	<i>F</i> _{1,52} = 159.90**	-7.72 ± 0.05**	1.36 ± 0.11**
		Age	<0.1	58	<i>F</i> _{1,56} = 5.96*	-8.32 ± 0.18**	0.55 ± 0.23*

RESULTS

The 16 measured stems ranged in age from 5 to 26 yr old, in total length from 1.2 to 3.4 m and from 2.2 to 4.5 cm in diameter. Branches were divided into an average of 3.6 segments for a total of 58 segments tested mechanically.

Allometry: stem dimensions and areas of bark, wood, and pith—To compare how stem length is related to diameter and age, we performed two regressions, which showed that the length of a stem cannot be predicted from its age, but is well explained by its diameter (Table 1a, Fig. 3A, B). The model with diameter as an explanatory variable takes the form of a Huxley-type allometric equation (log₁₀ length = β + αlog₁₀ diameter; Niklas, 1994), that explains variation in length reasonably well (Table 1a, Fig. 3A). Because the confidence interval of its scaling exponent α includes unity (0.82–1.84), the allometric relationship of branch length and diameter does not deviate significantly from isometry, with large plants showing the same proportions as small ones. Areas of bark, wood, and pith were also better predicted by distance from the tip of the stem than age (Table 1b–d, Fig. 3C, D).

Stem mechanical properties—The mechanical parameters *E*, *I*, and *EI* decreased from the stem bases to the tips in all situations but in Young’s modulus of the bark. As was

observed for allometry, a size variable was a better predictor of the mechanical parameters than was age (Table 1e–m). *E*_{struct} ranged from a minimum of 0.27 GN/m² near the branch tips to 1.82 GN/m² at the stem base (*N* = 58). Likewise, *E*_{wood} varied from 0.2 GN/m² in terminal segments to 5.31 GN/m² in segments 2 m or more from the stem tips (*N* = 46). In contrast, the Young’s modulus of the bark (*E*_{bark}) was more or less constant, showing no trend with age or with distance to the tip (Table 1j) and an average of 0.083 GN/m² (*N* = 40, SE = 0.009) at any given point. With respect to the flexural stiffness of the stem (*EI*_{struct}), the data ranged from 0.02 to 320.52 GN·m² (*N* = 58), whereas *EI*_{wood} varied from 0.03 to 312.11 GN·m² (*N* = 46) and *EI*_{bark} between 0.03 and 8.93 GN·m² (*N* = 41). Table 1 gives the regressions modelling *EI* (Table 1e–g, Fig. 4), *E* (Table 1h–j, Fig. 5), as well as the second moments of area (*I*) (Table 1k–m) based on the distance from the tip of the stem or age. Except for *E*_{bark}, which remained constant along the stem, mechanical variables were better explained by the size variables than by age, which in all cases yielded very poor regression models (cf. Fig. 4A, C vs. 4B, D and Fig. 5A, C vs. 5B, D).

Effect of environment on allometry and mechanical properties—The wide variety of environments occupied by *Pittocaulon* was reflected in the range of growth rates in length observed, which varied from 0.060 m/yr in the most highly

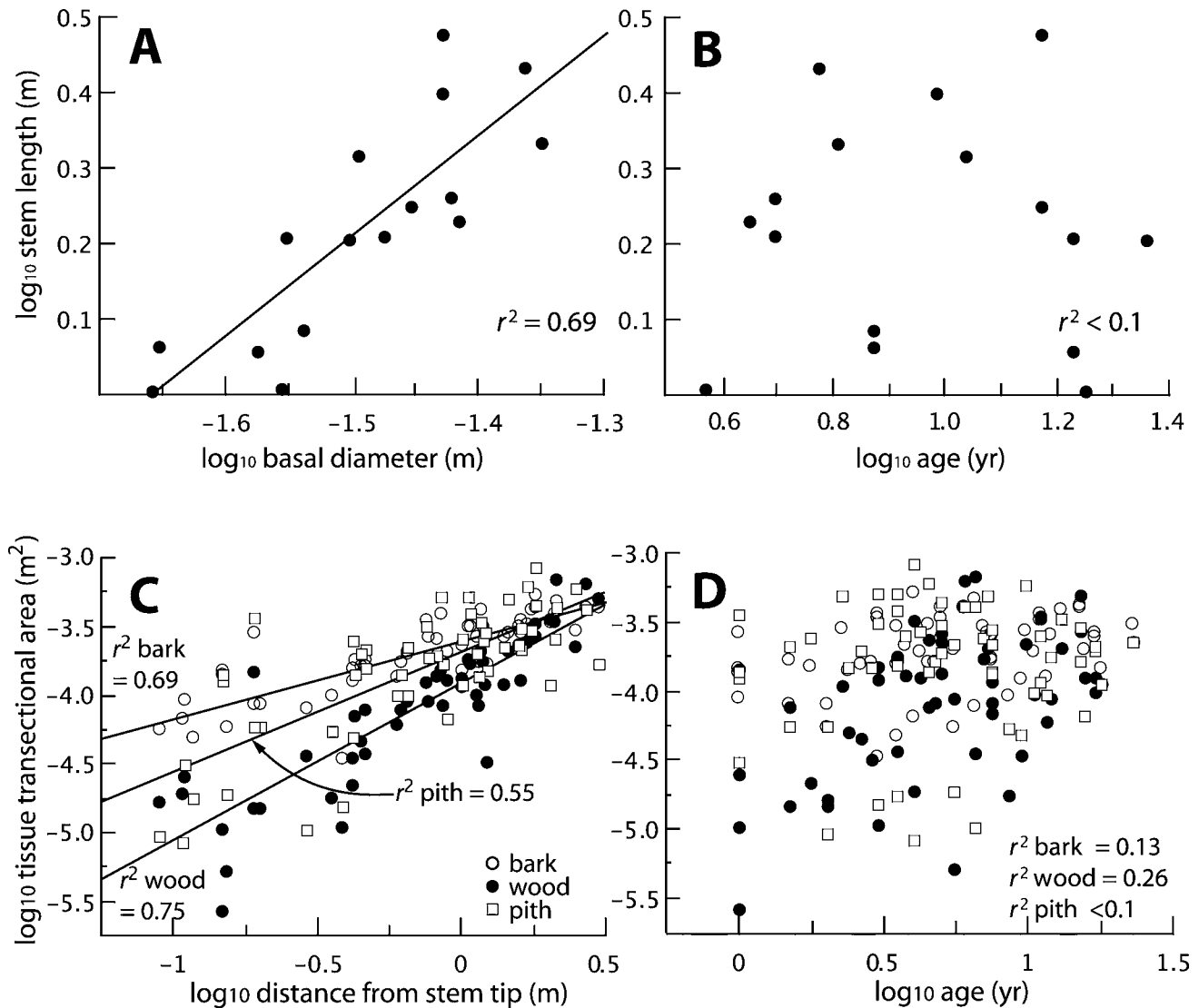


Fig. 3. Size vs. age in *Pittocaulon* allometry and proportions of bark, wood, and pith. (A, B) Stem length is better explained by diameter than by age. (A) Total stem length is predicted well by basal diameter. (B) Stem length has no statistical relationship to total stem age. (C–D) Similarly, areas of bark, wood, and pith per unit of stem transectional area are predicted better by stem size than by stem age. (C) Wood and bark, the tissues with greatest mechanical contributions, are predicted better than the pith. (D) Bark, wood, and pith plotted against segment age, showing that age is a poor predictor.

exposed location to 0.496 m/yr in the most sheltered, with a mean of 0.237 (SE = 0.018). The high uniformity in diameter along the length of *P. praecox* stems prevented in most cases the calculation of a growth rate in diameter.

Multiple regressions that included growth rate showed that stem length to diameter relations apparently do not vary across environments but that environment does play a role, albeit very slight, in explaining bark and pith areas. When stem length was explained by diameter and growth rate, the coefficient associated with growth rate was not significant ($N = 16$, $\beta_{\log_{10} \text{ growth rate}} \pm \text{SE} = -0.10 \pm 0.10$, $P = 0.38$), showing that the same allometric relationship is maintained regardless of habitat. In contrast, the environment was significant in the multiple regressions explaining both bark and pith areas based on distance from the tip and growth rate (Table 2a, b). Despite these significant coefficients, the contribution of growth rate is slight, with semipartial correlations showing that the distance

from the tip explains much more of the total variation in bark or pith areas than growth rate (Table 2a, b). The effect of environment was also detected in the regressions involving flexural stiffness and moment of inertia, but it was again slight. EI_{struct} , EI_{wood} , and EI_{bark} increased with distance from the tip of the stem and also with environment, tending very slightly to be greater in faster-growing plants in moister locations (Table 2c–e). The same pattern applied to I_{struct} , I_{wood} , and I_{bark} (Table 2f–h). In contrast, no influence of environment on the elastic moduli was detected ($E_{\text{struct}} N = 54$, $\beta_{\log_{10} \text{ growth rate}} \pm \text{SE} = 0.01 \pm 0.11$, $P = 0.94$; $E_{\text{wood}} N = 44$, $\beta_{\log_{10} \text{ growth rate}} \pm \text{SE} = 0.14 \pm 0.10$, $P = 0.18$; $E_{\text{bark}} N = 39$, $\beta_{\log_{10} \text{ growth rate}} \pm \text{SE} = 0.12 \pm 0.21$, $P = 0.59$). As a result, the pattern of increase in EI with increased growth rate must be attributed only to the increase observed in I . When the environment had any effect on the models, the effect was very slight, as shown by the low semipartial correlations associated with growth rate in Table 2.

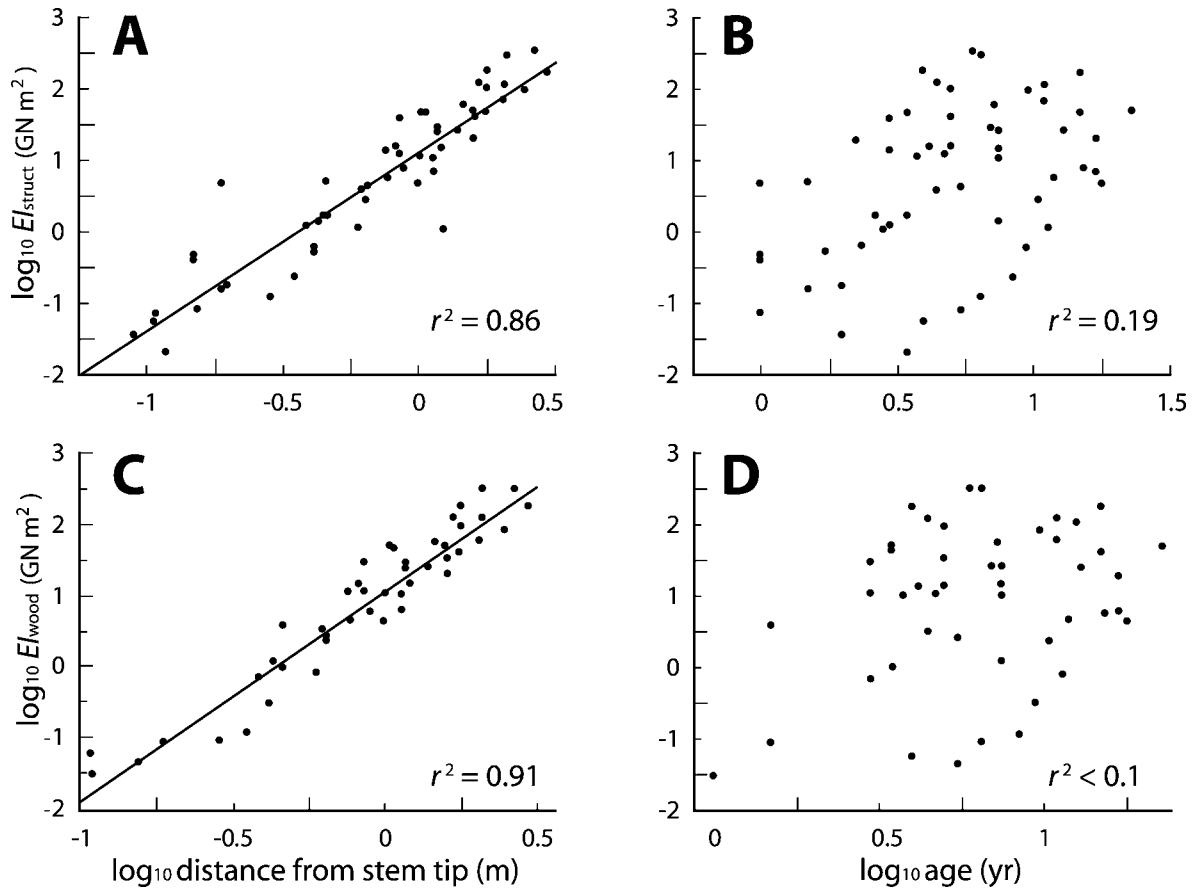


Fig. 4. Structural (E_{struct}) and wood flexural stiffness (E_{wood}) are poorly explained by stem age. (A) As could be expected given the allometric relationship between stem length and diameter, the E_{struct} of a stem segment is predicted very well based only on the distance of the midpoint of the segment to the tip of the stem. (B) In striking contrast, the average age of the segment is a poor predictor of E_{struct} . (C) Likewise, E_{wood} of a stem segment is largely explained by the distance from the tip of the stem, whereas (D) it is not explained at all by age.

For example, for E_{struct} (Table 2c), the semipartial correlation for distance was 0.85, more than four times that for the growth rate at 0.19. Also, the increase in the coefficient of determination when growth rate was added to the simple model that included only distance from the tip was minimal, changing from 0.86 to 0.89 (Table 1e and 2c). The very slight association between growth rate and tissue areas or mechanical parameters was readily evident in scatter plots (Fig. 6).

DISCUSSION

The allometric and biomechanical attributes of a given section of *P. praecox* stem were far better predicted by stem size than by age. Stems of the same size could have very different ages and come from very different environments, but they maintained very similar length to diameter proportions (Fig. 3). Likewise, mechanical parameters of similarly sized segments and their tissues were comparable regardless of absolute age (Figs. 4, 5). Our results thus support the notion that time can be rejected as a meaningful basis for comparison for many evolutionary studies, and with it the implicit assumption of plant ontogeny characterized by particular developmental events occurring at particular absolute times. In contrast, the correlation of mechanics with size could be

expected based on basic mechanical theory, which predicts that the stress experienced by a given sector of a beam is directly related to the amount of material that must be supported and its distribution (Niklas, 1999a; Gere, 2002; cf. Holbrook and Putz, 1989). As a result, the mechanical needs of a stem of a given length by diameter proportion would be the same regardless of age. We discuss the implications of these findings for inferring variables of adaptive importance in woody plants and argue that variables describing stem size are more appropriate for comparing ontogenies between individuals than are those that represent absolute ages.

The *Pittocaulon* allometric and biomechanical “model,” adaptation, and plasticity—Perhaps the most surprising result of our study was the observation that, although they were collected across a marked amplitude of microhabitats and displayed a greater than eightfold range in growth rate, the stems measured were for the most part mechanically and allometrically interchangeable. In other words, there was no way to distinguish an old stem covered with annual scars (Fig. 2A) from similarly sized stems produced in just one or a few seasons (Fig. 2B) based on allometry or mechanics. To predict the flexural stiffness of a stem segment (E_{struct}), it was necessary only to know the length of stem that the segment must support (i.e., its distance from the tip of the stem; cf. Fig.

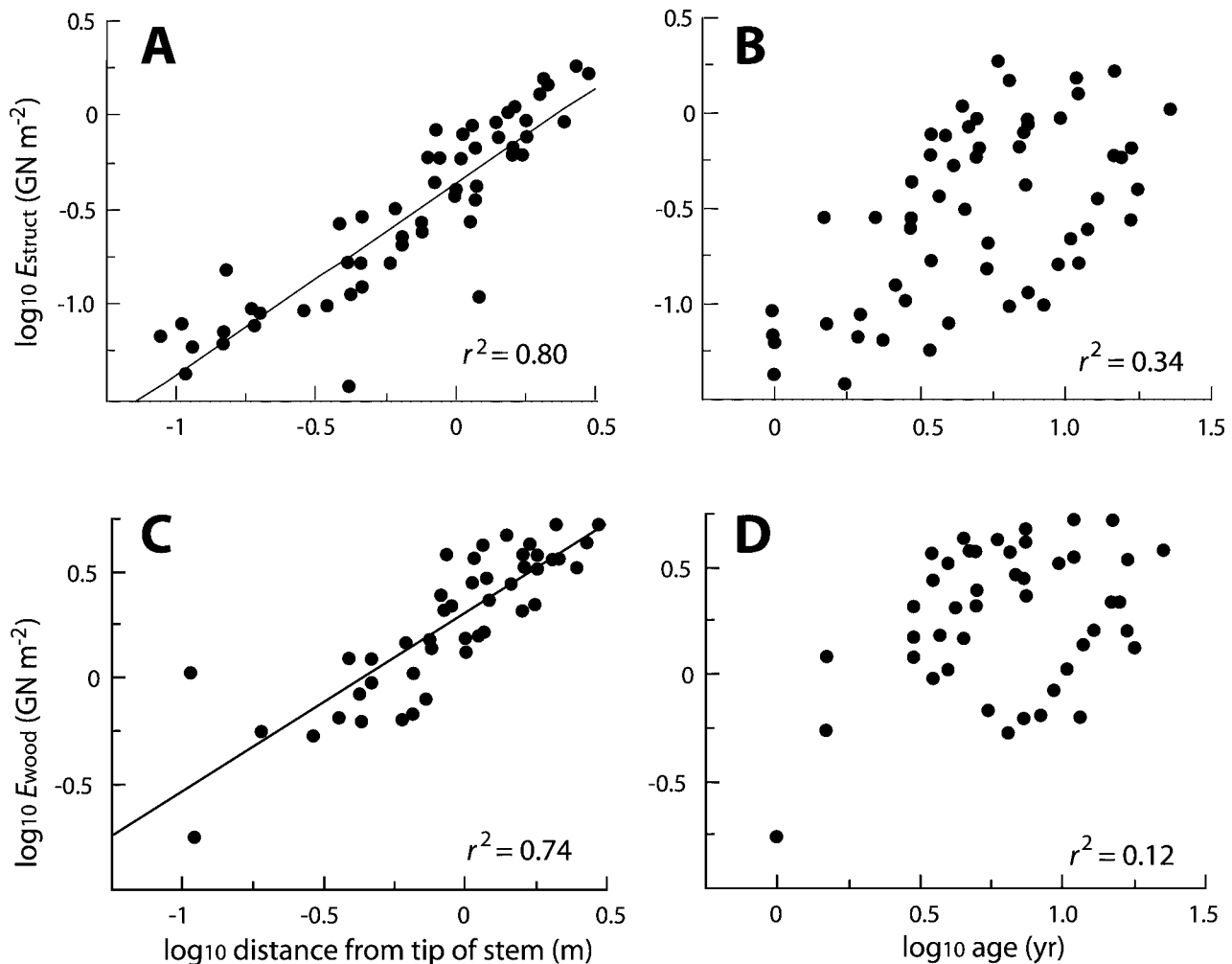


Fig. 5. Structural (E_{struct}) and wood Young's moduli (E_{wood}) are closely related to size and not to stem age. (A) The E_{struct} of a segment correlates remarkably well with the distance of the midpoint of the segment to the tip of the stem. (B) In contrast, E_{struct} is only very loosely correlated with the average age of the same stem segments. (C) Likewise, E_{wood} is explained in large part by the distance from the tip of the stem, whereas (D) E_{wood} cannot be explained by age.

4A, B). Likewise, at the tissue level, the Young's modulus of the wood was associated to a striking degree with the distance to the stem tip (Fig. 5C), regardless of age (Fig. 5D).

The production of a relatively invariant phenotype despite internal or external perturbing factors, as in *Pittocaulon* allometry and mechanics, has been referred to as developmental homeostasis. Developmental homeostasis is commonly explained as a result of natural selection favoring ontogenetic systems capable of producing a specific, perhaps even optimal, phenotype (Fenster and Galloway, 1997; Møller and Shykoff, 1999). Our study thus directs attention to allometry and mechanics as factors that are likely under strong selection. But what features are of primary selective importance? In most situations, allometry seems unlikely to be the direct object of selection. Instead, we suggest that the most plausible hypothesis is that allometry follows selection for storage, mechanics, conduction, or size. For example, given constant materials properties (e.g., wood and bark E), selection for increased stature will require concomitant changes in allometry to maintain a mechanically viable structure (Niklas, 1992;

Vogel, 2003). In the case of *Pittocaulon*, selection for storage has clearly played a role in shaping its allometric and biomechanical syndrome. In Asteraceae and in many other plants, selection for increased stem water storage has led to massive zones of parenchyma in pith and bark (e.g., *Kleinia*, *Pachythamnus*); parenchymatized xylem does not seem to be a typical mode of water storage in asters (cf. Carlquist, 1966). Many ways could be imagined to arrange a given cross-sectional area of xylem within a stem. Nevertheless, in all plants with extensive stem water storage outside of the xylem, the xylem is not in a central rod-like cylinder with a conventional tiny pith. Instead, the pith is always greatly enlarged, and the xylem cylinder is close to the stem periphery, where it is better located to resist tension and compression (that is, with higher I) as compared to a central rod (cf. Fig. 1A and structures such as the vertebrate femur). Selection for storage thus almost certainly results not only in a thick stem, but also in an arrangement of tissues that accommodates water storage while at the same time providing mechanical adequacy. More detailed testing of these hypotheses will require examination of

TABLE 2. Multiple regressions of *Pittocaulon* tissue areas and mechanical parameters predicted by the inclusion of environment (growth rate) with distance from the stem tip, showing that the effect of environment is slight in all cases. Multiple regressions for tissue areas (a–b), flexural stiffness (c–e), and moments of inertia (f–h). All variables are \log_{10} transformed. r_a^2 = adjusted coefficient of multiple determination; β_D = coefficient associated with distance from the tip of the stem; β_{GR} = coefficient associated with growth rate (proxy environmental variable). The semipartial correlations indicate the relative contribution of stem diameter (PD) and growth rate (PGR) in predicting the response variable of interest. Distance from the tip never has partial correlations less than 0.60, whereas those for environment never are above 0.4. Other abbreviations and units are as in Table 1.

Response	r_a^2	N	F test	$\beta_D \pm SE$	$\beta_{GR} \pm SE$	$\beta_{GR} \pm SE$	PD	PGR
(a) Bark area	0.72	54	$F_{2,51} = 68.49^{**}$	$-3.46 \pm 0.57^{**}$	$0.53 \pm 0.05^{**}$	$0.21 \pm 0.08^{**}$	0.75	0.21
(b) Pith area	0.69	54	$F_{2,51} = 59.06^{**}$	$-3.21 \pm 0.10^{**}$	$0.75 \pm 0.10^{**}$	$0.70 \pm 0.14^{**}$	0.62	0.39
(c) $E_{I_{struct}}$	0.89	54	$F_{2,51} = 224.64^{**}$	$1.66 \pm 0.14^{**}$	$2.37 \pm 0.13^{**}$	$0.79 \pm 0.18^{**}$	0.85	0.19
(d) $E_{I_{wood}}$	0.95	45	$F_{2,42} = 398.74^{**}$	$1.65 \pm 0.11^{**}$	$2.69 \pm 0.12^{**}$	$0.81 \pm 0.15^{**}$	0.80	0.19
(e) $E_{I_{bark}}$	0.68	39	$F_{2,36} = 40.38^{**}$	$0.54 \pm 0.19^{**}$	$1.46 \pm 0.20^{**}$	$0.63 \pm 0.24^*$	0.68	0.25
(f) I_{struct}	0.83	54	$F_{2,51} = 133.85^{**}$	$-6.99 \pm 0.11^{**}$	$1.35 \pm 0.10^{**}$	$0.78 \pm 0.15^{**}$	0.76	0.30
(g) I_{wood}	0.83	53	$F_{2,50} = 128.29^{**}$	$-7.80 \pm 0.14^{**}$	$1.89 \pm 0.13^{**}$	$0.67 \pm 0.19^{**}$	0.82	0.20
(h) I_{bark}	0.83	54	$F_{2,51} = 126.78^{**}$	$-7.26 \pm 0.10^{**}$	$1.24 \pm 0.09^{**}$	$0.66 \pm 0.14^{**}$	0.77	0.28

more than one species, preferably in a clade of broad anatomical, biomechanical, and ecological diversity.

The mechanical properties of *Pittocaulon* wood (as reflected by E) could also be expected to differ with respect to non

water-storing plants. Selection pressure for bark and pith storage could lead to pressure for a xylem cylinder of great diameter but minimal wall thickness, thereby maximizing pith diameter. Given the mass of such thick, water-filled stems, the

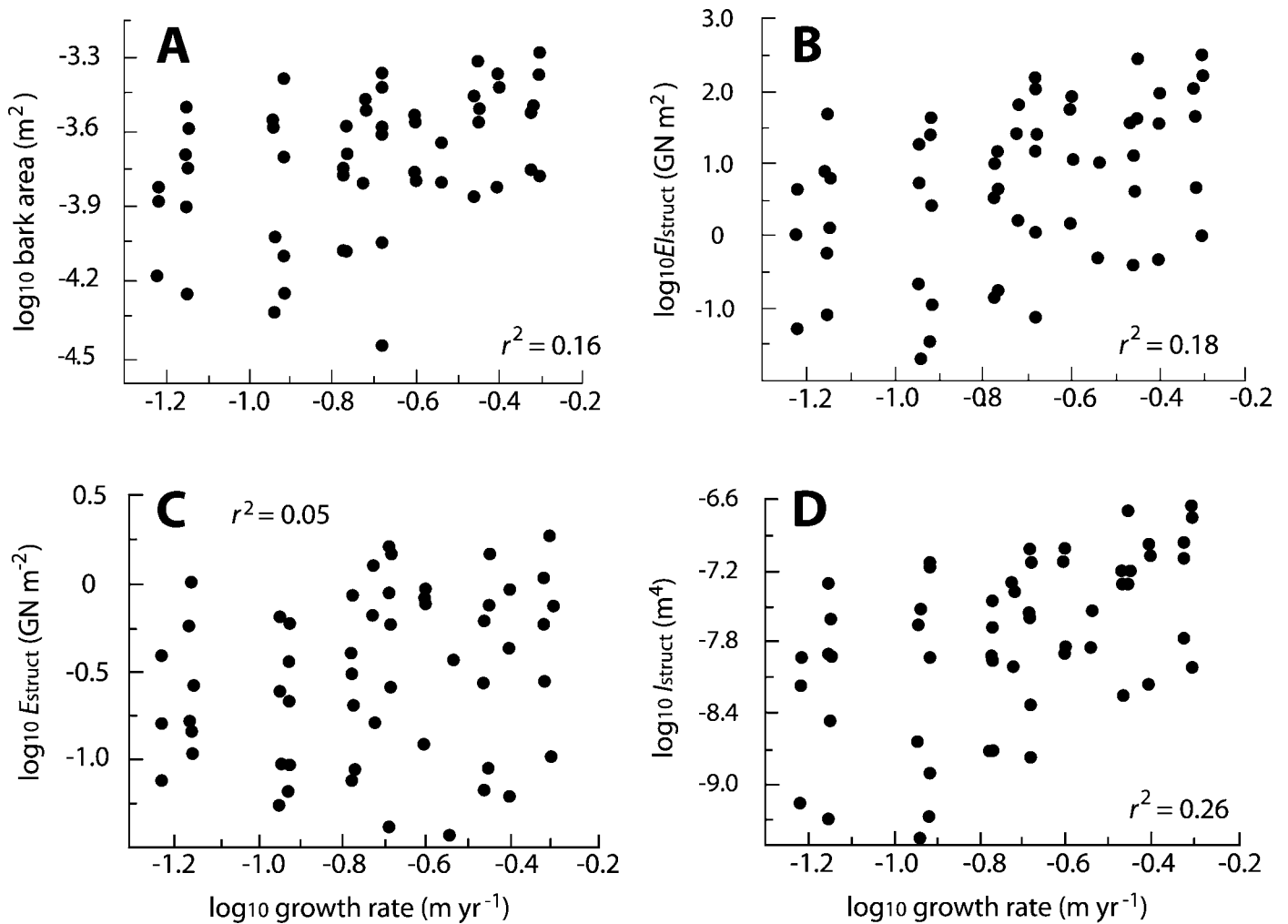


Fig. 6. Growth rate is only very slightly correlated with tissue areas and mechanical parameters; its contribution to their prediction is very poor. (A) Growth rate is poorly correlated with bark area, (B) structural flexural stiffness ($E_{I_{struct}}$), (C) structural Young's modulus (E_{struct}), and (D) structural second moment of area (I_{struct}). No relationship between environment and Young's modulus (E) was detected.

little xylem that is present would be expected to be relatively stiff. Congruent with this expectation, *Pittocaulon* wood is comparable with plants of much larger stature (see Niklas, 1992).

The relatively constant allometric and mechanical phenotype observed in *Pittocaulon* is all the more striking given the host of other characters with high levels of plasticity. The most obvious plastic response is represented by the strong differences in size that were observed between individuals. Plants on exposed lava ridges were short, slender-stemmed, and branched far below the height at which more sheltered plants did. In the allometric and mechanical characteristics examined, the only exception to the pattern of uniformity across habitats was a tendency for stems in moister environments to have marginally larger pith and bark areas (Table 2a, b). Greater pith area implies higher I_{pith} and also higher I_{wood} and I_{bark} (Table 2f–h) because the xylem-bark cylinder lies farther from the neutral axis if pith area increases. This environmental effect on I seems to be responsible for the minor tendency for EI to increase with growth rate (Table 2c–e), because E had no environmental differences (cf. Klinger et al., 1998). Similarly, in a previous anatomical study (Olson, 2005), cellular features thought to be of great functional importance varied substantially. For example, both vessel wall diameter and libriform fiber length and diameter had coefficients of variation on the order of 20–25%, whereas variation in vessel wall thickness and the number of vessels per group was even broader at 40%. The cambium thus appears to modulate the mechanical properties and the arrangement of tissues it produces in such a way that the *Pittocaulon* “model” is produced despite a remarkable degree of variation in growth rate and cellular level variation. This pattern of higher-level uniformity despite lower-level variation corresponds exactly with what would be expected if developmental homeostasis were responsible for the constancy of the *Pittocaulon* “model.”

Size and stem properties—Because the mechanical properties of a stem are the result of its characteristics at lower hierarchical levels (Niklas, 1992; cf. Alfaro et al., 2004), size attributes should correlate not only with mechanical characteristics at the whole-structure level but also with lower-level features such as anatomy and hydraulics. The correlation of cell size with stem size within species, well known to wood anatomists and foresters (Carlquist, 1975; Panshin and De Zeeuw, 1980; Gartner, 1995; Carlquist and Grant, 2005; Olson and Rosell, 2006), would seem to bear out this expectation, as does the observation that *Pittocaulon* bark, wood, and xylem proportions can be predicted based on stem size (Fig. 3A). Similarly, authors such as Tyree and Yang (1992) and Tyree and Zimmermann (2002) have shown that features of hydraulic architecture are well predicted by stem size.

If comparisons between individuals are based on size rather than age, then the interpretation of phenomena such as dwarfing could differ from conventional interpretations. For example, Bailey and Tupper (1918) present tracheid lengths from “vigorous” and “stunted” individuals plotted against growth ring age. In all cases, the cells for stunted individuals are smaller for a given growth ring age. Authors such as Baas et al. (1984) and Moltenberg and Hoibo (2006) also reported smaller cell sizes for suboptimal individuals. It seems likely that comparisons between similar distances from the pith rather than age would reveal cell sizes that more closely resemble one another (cf. Mäkinen et al., 2002).

Comparing ontogenies—Explicitly identifying whether stem mechanics are better predicted by size or age can also inform studies of the evolution of ontogeny in woody plants. Morphology is produced via ontogeny, and as a result, morphological differences between species are associated with ontogenetic differences (Gould, 1977; Raff, 1996; West-Eberhard, 2003). Comparing ontogenies between species can thus serve as a means of inferring the evolutionary mechanisms responsible for the differences observed. To accomplish these comparisons, a suitable common axis is needed against which ontogenetic data from different species can be plotted in the same space. The most commonly studied evolutionary alteration to ontogeny is heterochrony, which involves interspecific differences in the timing of developmental events (Alberch et al., 1979). The very name implies differences with respect to time, and indeed those working with animals are often emphatic that ontogenetic data from different individuals must be plotted against absolute time (e.g., Godfrey and Sutherland, 1995). As we show here, woody plant stems may have different sizes and be at different ontogenetic stages at similar ages (see also Parish and Antos, 2004; Brienen and Zuidema, 2006). As a result, mechanical and other features are unlikely to correlate well with age between individuals. The identification of an axis with points corresponding to comparable events in different individuals is thus a significant challenge in studies of ontogenetic evolution in woody plants.

For many organisms, there may be measures of “biological time” that are more relevant than absolute time (Strauss, 1987). From our results in *Pittocaulon*, absolute time can be rejected as a meaningful axis for comparisons between individuals (e.g., Figs. 3B, D; 4B, D; 5B, D), whereas size is clearly correlated with crucial characteristics such as proportions of tissues and mechanical attributes (e.g., Figs. 3A, C; 4A, C; 5A, C; Olson and Rosell, 2006; Olson, in press). It could be argued that simply observing a correlation is not sufficient justification for the use of size as a basis for comparison between species. However, size is of prime biological relevance in woody stems because stems increase in girth as the result of the accumulation of new layers of wood and bark; the diameter of a stem reflects how many layers it has accumulated. Thus, across species that share similar allometry (cf. Müller et al., 2000), variables such as diameter would appear to offer a more biologically defensible measure of “biological time” than would absolute age (Strauss, 1987; Olson and Rosell, 2006).

Conclusion—We suggest that there is reason to justify the selection of stem size as a basis for comparing stem structure and function between individuals over absolute age. Conversely, the degree of fit when modelling wood properties, whether mechanical, hydraulic, or structural, based on age is likely to vary to the extent that age and size are decoupled. Results from *Pittocaulon* can be used to generate hypotheses regarding woody plants generally. For example, a prediction meriting examination is that allometry and mechanical characteristics always respond to stem size more than absolute age in plants in general. The stem of *Pittocaulon* has a somewhat unusual stem construction resembling a columnar cactus in having more water-storing cortex and pith than xylem (Gibson and Nobel, 1986; Niklas et al., 2000; Olson, 2005). It could be argued that the results we obtained might not apply to a typical arborescent dicot in which the xylem predominates. However, the need for the mechanical characteristics of a structure to meet the demands imposed by its size would seem to apply to any

structure regardless of its construction, and thus we feel that results similar to those in *Pittocaulon* could be expected in most if not all woody plant stems. In fact, finding that there is a lack of correspondence between mechanics or allometry and size would be noteworthy and perhaps point to factors such as developmental constraint. Similarly, the hypothesis that woody plants in general have ontogenetic systems that produce a narrow, perhaps optimal, range of allometry and mechanics warrants examination.

LITERATURE CITED

- ALBERCH, P., S. J. GOULD, G. F. OSTER, AND D. B. WAKE. 1979. Size and shape in ontogeny and phylogeny. *Paleobiology* 5: 296–317.
- ALFARO, M. E., D. I. BOLNICK, AND P. C. WAINWRIGHT. 2004. Evolutionary dynamics of complex biomechanical systems: an example using the four-bar mechanism. *Evolution* 58: 495–503.
- BAAS, P., C. LEE, X. ZHANG, K. CUI, AND Y. DENG. 1984. Some effects of dwarf growth on wood structure. *International Association of Wood Anatomists Bulletin, New Series* 5: 45–63.
- BAILEY, I. W., AND W. W. TUPPER. 1918. Size variation in tracheary cells. I. A comparison between the secondary xylems of vascular cryptogams, gymnosperms, and angiosperms. *Proceedings of the National Academy of Sciences, USA* 54: 149–204.
- BERG, R. L. 1960. The ecological significance of correlation pleiades. *Evolution* 14: 171–180.
- BHAT, K. M., AND P. B. PRIYA. 2004. Influence of provenance variation on wood properties of teak from the Western Ghat region in India. *International Association of Wood Anatomists Journal* 25: 273–282.
- BRIAND, C. H., S. M. CAMPION, D. A. DZAMBO, AND K. A. WILSON. 1999. Biomechanical properties of the trunk of the devil's walking stick (*Aralia spinosa*; Araliaceae) during the crown-building phase: implications for tree architecture. *American Journal of Botany* 86: 1677–1682.
- BRIENEN, J. W., AND P. A. ZUIDEMA. 2006. Lifetime growth patterns and ages of Bolivian rain forest trees obtained by tree ring analysis. *Journal of Ecology* 94: 481–493.
- CARLQUIST, S. J. 1966. Wood anatomy of Compositae: a summary, with comments on factors controlling wood evolution. *Aliso* 6: 1–23.
- CARLQUIST, S. J. 1975. Ecological strategies of xylem evolution. University of California Press, Berkeley, California, USA.
- CARLQUIST, S. J., AND J. R. GRANT. 2005. Wood anatomy of Gentianaceae, tribe Helieae, in relation to ecology, habit, systematics, and sample diameter. *Brittonia* 57: 276–291.
- ESAU, K. 1977. Anatomy of seed plants, 2nd ed. Wiley, New York, New York, USA.
- ETXEBERRIA, J. 1999. Regresión múltiple. La Muralla, Madrid, Spain.
- FENSTER, C. B., AND L. F. GALLOWAY. 1997. Developmental homeostasis and floral form: evolutionary consequences and genetic basis. *International Journal of Plant Sciences* 158(Supplement): S121–S130.
- FRANKINO, W. A., B. J. ZWAAN, D. L. STERN, AND P. M. BRAKEFIELD. 2005. Natural selection and developmental constraints in the evolution of allometries. *Science* 307: 718–720.
- GARTNER, B. 1995. Patterns of xylem variation within a tree and their hydraulic and mechanical consequences. In B. Gartner [ed.], Plant stems. Physiology and functional morphology, 125–149. Academic Press, San Diego, California, USA.
- GERE, J. M. 2002. Mecánica de materiales. Thomson Publishers, Mexico City, Mexico.
- GIBSON, A., AND P. S. NOBEL. 1986. The cactus primer. Harvard University Press, Cambridge, Massachusetts, USA.
- GODFREY, L. R., AND M. R. SUTHERLAND. 1995. Flawed inference: why size-based tests of heterochronic processes do not work. *Journal of Theoretical Biology* 172: 43–61.
- GOULD, S. J. 1977. Ontogeny and phylogeny. Harvard University Press, Cambridge, Massachusetts, USA.
- HOLBROOK, N. M., AND F. E. PUTZ. 1989. Influence of neighbors on tree form: effects of lateral shade and prevention of sway on the allometry of *Liquidambar styraciflua* (sweet gum). *American Journal of Botany* 76: 1740–1749.
- JACOBSEN, A. L., F. W. EWERS, R. B. PRATT, W. A. PADDOCK III, AND S. D. DAVIS. 2005. Do xylem fibers affect vessel cavitation resistance? *Plant Physiology* 139: 546–556.
- KAVANAGH, K. L., B. J. BOND, S. N. AITKEN, B. L. GARTNER, AND S. KNOWE. 1999. Shoot and root vulnerability to xylem cavitation in four populations of Douglas-fir seedlings. *Tree Physiology* 19: 31–37.
- KLIGER, I. R., M. PERSTORPER, AND G. JOHANSSON. 1998. Bending properties of Norway spruce timber. Comparison between fast- and slow-grown stands and influence of radial position of sawn timber. *Annales des Sciences Forestières* 55: 349–358.
- KUTNER, M. H., C. J. NACHTSHEIM, J. NETER, AND W. LI. 2005. Applied linear statistical models. McGraw-Hill, New York, New York, USA.
- LONGFORD, N. T. 1993. Random coefficient models. Oxford University Press, Oxford, UK.
- MÄKINEN, H., P. SARAPÄÄ, AND S. LINDER. 2002. Effect of growth rate on fibre characteristics in Norway spruce (*Picea abies* (L.) Karst.). *Holzforchung* 56: 449–460.
- MARROIG, G., AND J. M. CHEVERUD. 2005. Size as a line of least evolutionary resistance: diet and adaptive morphological radiation in new world monkeys. *Evolution* 59: 1128–1142.
- MÖLLER, A. P., AND J. A. SHYKOFF. 1999. Morphological developmental stability in plants: patterns and causes. *International Journal of Plant Sciences* 160(6 Supplement): S135–S146.
- MOLTENBERG, D., AND O. HOIBO. 2006. Development and variation of wood density, kraft pulp yield and fibre dimensions in young Norway spruce (*Picea abies*). *Wood Science and Technology* 40: 173–189.
- MÜLLER, I., B. SCHMID, AND J. WEINER. 2000. The effect of nutrient availability on biomass allocation patterns in 27 species of herbaceous plants. *Perspectives in Plant Ecology, Evolution and Systematics* 3: 115–127.
- NIKLAS, K. J. 1992. Plant biomechanics. University of Chicago Press, Chicago, Illinois, USA.
- NIKLAS, K. J. 1994. Plant allometry. The scaling of form and process. University of Chicago Press, Chicago, Illinois, USA.
- NIKLAS, K. J. 1995. Size-dependent allometry of tree height, diameter and trunk-taper. *Annals of Botany* 75: 217–227.
- NIKLAS, K. J. 1997a. Mechanical properties of black locust (*Robinia pseudoacacia*) wood: correlations among elastic and rupture moduli, proportional limit, and tissue density and specific gravity. *Annals of Botany* 79: 479–485.
- NIKLAS, K. J. 1997b. Mechanical properties of black locust (*Robinia pseudoacacia*) wood: size- and age-dependent variations in sap- and heartwood. *Annals of Botany* 79: 265–272.
- NIKLAS, K. J. 1997c. Size- and age-dependent variations in the properties of sap- and heartwood in black locust (*Robinia pseudoacacia* L.). *Annals of Botany* 79: 473–478.
- NIKLAS, K. J. 1999a. Changes in the factor of safety within the superstructure of a dicot tree. *American Journal of Botany* 86: 688–696.
- NIKLAS, K. J. 1999b. The mechanical role of bark. *American Journal of Botany* 86: 465–469.
- NIKLAS, K. J., AND S. L. BUCHMAN. 1994. The allometry of saguaro height. *American Journal of Botany* 81: 1161–1168.
- NIKLAS, K. J., F. MOLINA-FREANER, AND C. TINOCO-OJANGUREN. 2000. Wood biomechanics and anatomy of *Pachycereus pringlei*. *American Journal of Botany* 87: 469–481.
- OLSON, M. E. 2005. Wood, bark, and pith anatomy in *Pittocaulon* (~*Senecio*, Asteraceae): water storage and systematics. *Journal of the Torrey Botanical Society* 132: 173–186.
- OLSON, M. E. In press. Wood ontogeny as a model for studying heterochrony. *Systematics and Biodiversity*.
- OLSON, M. E., AND J. A. ROSELL. 2006. Using heterochrony to detect modularity in the evolution of stem diversity in the plant family Moringaceae. *Evolution* 60: 724–734.
- PANSHIN, A. J., AND C. DE ZEEUW. 1980. Textbook of wood technology. McGraw-Hill, New York, New York, USA.

- PARISH, R., AND J. A. ANTOS. 2004. Structure and dynamics of an ancient montane forest in coastal British Columbia. *Oecologia* 141: 562–576.
- PÉREZ, R., AND M. FRANCO. 2000. *Senecio praecox* (Cav.) DC. var. *praecox*: toda una vida impresa en su arquitectura. *Cactáceas y Suculentas Mexicanas* 45: 62–65.
- PIGLIUCCI, M., C. PAOLETTI, S. FINESCHI, AND M. E. MALVOLI. 1991. Phenotypic integration in chestnut (*Castanea sativa* Mill.): leaves versus fruits. *Botanical Gazette* 152: 514–521.
- PISARENKO, G. S., A. P. YÁKOVLEV, AND V. V. MATVÉEV. 1979. Manual de resistencia de materiales. Mir, Moscow, USSR.
- POORTER, L., F. BONGERS, F. J. STERCK, AND H. WOLL. 2003. Architecture of 53 rain forest tree species differing in adult stature and shade tolerance. *Ecology* 84: 602–608.
- RAFF, R. A. 1996. The shape of life. University of Chicago Press, Chicago, Illinois, USA.
- ROZAS, V. 2003. Tree age estimates in *Fagus sylvatica* and *Quercus robur*: testing previous and improved methods. *Plant Ecology* 167: 193–212.
- SPICER, R., AND B. L. GARTNER. 2001. The effects of cambial age and position within the stem on specific conductivity in Douglas-fir (*Pseudotsuga menziesii*) sapwood. *Trees—Structure and Function* 15: 222–229.
- STERCK, F. J., AND F. BONGERS. 1998. Ontogenetic changes in size, allometry and mechanical design of tropical rain forest trees. *American Journal of Botany* 85: 266–272.
- STRAUSS, R. E. 1987. On allometry and relative growth in evolutionary studies. *Systematic Zoology* 36: 72–75.
- TYREE, M. T., AND S. YANG. 1992. Hydraulic conductivity recovery versus water pressure in xylem of *Acer saccharum*. *Plant Physiology* 100: 669–676.
- TYREE, M. T., AND M. ZIMMERMANN. 2002. Xylem structure and the ascent of sap, 2nd ed. Springer-Verlag, Berlin, Germany.
- VINCENT, J. F. 1990. Structural biomaterials. Princeton University Press, Princeton, New Jersey, USA.
- VINCENT, J. F. 1992. Biomechanics—Materials. A practical approach. Oxford University Press, Oxford, UK.
- VOGEL, S. 2003. Comparative biomechanics: life's physical world. Princeton University Press, Princeton, New Jersey, USA.
- WEINER, J. 2004. Allocation, plasticity and allometry in plants. *Perspectives in Plant Ecology, Evolution and Systematics* 6: 207–215.
- WEST-EBERHARD, M. J. 2003. Developmental plasticity and evolution. Oxford University Press, Oxford, UK.
- ZELDITCH, M. L., D. O. STRANEY, D. L. SWIDERSKI, AND A. C. CARMICHAEL. 1990. Variation in developmental constraints in *Sigmodon*. *Evolution* 44: 1738–1747.

ANEXO B.

REGRESIÓN LOGÍSTICA EN LA ANATOMÍA COMPARADA DE LA MADERA: TIPOS DE TRAQUEIDAS, TERMINOLOGÍA ANATÓMICA, Y NUEVAS INFERENCIAS DEL CONJUNTO DE DATOS DE CARLQUIST Y HOEKMAN DEL SUR DE CALIFORNIA

Logistic regression in comparative wood anatomy: tracheid types, wood anatomical terminology, and new inferences from the Carlquist and Hoekman southern Californian data set

JULIETA A. ROSELL¹, MARK E. OLSON^{1*}, REBECA AGUIRRE-HERNÁNDEZ² and SHERWIN CARLQUIST FLS³

¹Instituto de Biología, Universidad Nacional Autónoma de México, 3er Circuito s/n CU, México DF 04510, Mexico

²Facultad de Medicina, Universidad Nacional Autónoma de México, Circuito Escolar s/n CU, México DF 04510, Mexico

³Santa Barbara Botanical Garden, 1212 Mission Canyon Road, Santa Barbara, CA 93105, USA

Received September 2006; accepted for publication March 2007

Despite collecting copious amounts of data, wood anatomists rarely perform appropriate statistical analyses, especially in the case of categorical variables. Nevertheless, anatomists have succeeded in identifying strong ecological trends. We show that, with only a slightly more sophisticated analysis, the strength and significance of ‘well-known’ associations can be quantified, and new associations pinpointed. Using logistic regression to reanalyse the classic Carlquist and Hoekman data set for the southern Californian flora, we show strong support for the notion that true tracheid presence lowers vessel grouping; in contrast, vasicentric tracheids are associated with a diversity of vessel grouping strategies. We show that statistical models can refine anatomical interpretations by identifying unusual species. For example, *Fremontodendron californicum* and *Baccharis salicifolia* (= *B. glutinosa*) were identified as unusual in lacking vasicentric tracheids; a consultation of preparations revealed that they are indeed present. For purposes of ecological wood anatomy, anatomical terminology should reflect cell function; we suggest that terminological systems that yield better predictive power in statistical models such as ours are preferable. Finally, we make recommendations ranging from the statistical, e.g. the need to check assumptions and the need for the inclusion of phylogeny, to the biological, e.g. gathering data expressly designed to test functional hypotheses rather than all of the information in standardized lists. © 2007 The Linnean Society of London, *Botanical Journal of the Linnean Society*, 2007, 154, 331–351.

ADDITIONAL KEYWORDS: adaptation – categorical data – character correlation – contingency tables – data coding – ecological wood anatomy – evolution – relative risk – vasicentric tracheids.

INTRODUCTION

Comparative wood anatomists use laborious methods to generate large quantities of data. Despite the considerable work involved, statistical procedures have only rarely been used to guide data collection, and analyses of wood anatomical data have been restricted to descriptive statistics or the application of basic techniques that do not extract the maximum amount

of information from the data (Burley & Miller, 1982). As a result, there are many opportunities for expanding the use of statistics in the analysis of anatomical information, including strategies for the collection of wood samples from wild populations and the sampling of anatomical information from preparations. However, perhaps the greatest opportunity for improving results while taking advantage of the prodigious amount of information already possessed by wood anatomists is data analysis. In one of the few works to treat statistics in comparative wood anatomy explic-

*Corresponding author. E-mail: explore@explorelifeonearth.org

itly, Burley & Miller (1982) highlighted a variety of techniques that could be used to analyse quantitative anatomical data. However, categorical data frequently arise in comparative wood anatomy. They include nominal (e.g. crystal type, presence/absence of true tracheids) and ordinal (e.g. vessel diameter coded as narrow, medium and wide) variables. Here we complement the work of Burley and Miller by providing an example of the analysis of qualitative data using logistic regression and other statistical methods for categorical data. We illustrate our novel recommendations with a reanalysis of a well-known ecological wood anatomy data set (Carlquist & Hoekman, 1985) to show that, with only a slightly more sophisticated analysis, new associations can be demonstrated, support for previously recognized trends can be quantified, and directions for further research can be identified.

Wood identification, systematics, and ecological wood anatomy comprise the three main efforts that can be identified within comparative wood anatomy (Olson, 2005). Although improved statistical treatment could substantially contribute to each of these fields, as the one that relies the most on the statistical treatment of data, ecological wood anatomy stands to benefit most from more sophisticated analytical techniques. Ecological wood anatomy attempts to relate anatomical information with plant habit or environmental variables thought to be important in determining plant structural adaptations. Wood characters can vary remarkably, even between closely related species, in relation to habit and ecology. The repeated documentation of the same correlations between anatomical characteristics and environmental variables or habit (e.g. Carlquist, 1975, 2001; Carlquist & Hoekman, 1985; Arias & Terrazas, 2001; Jansen *et al.*, 2004; Lens *et al.*, 2004), and of the co-occurrence of given suites of anatomical characteristics (e.g. Carlquist, 1984) thus forms the basis of ecological wood anatomy. Whatever the specific variables used, the overall aim is to identify the occurrence of similar anatomical characteristics in similar environmental situations.

Although comparative wood anatomists have typically collected many qualitative data, the association between categorical variables has rarely been subjected to statistical analysis, and when it has, the treatment has been mainly descriptive (e.g. Alves & Angyalossy-Alfonso, 2000, 2002). One of our main aims was thus to highlight statistical methods that can be used with categorical data, and to illustrate their extraordinary utility in comparative wood anatomy with a reanalysis of the data set from Carlquist & Hoekman's (1985) ecological wood anatomy study of the flora of southern California. Although this study has been frequently cited because of the large quanti-

ties of ecological hypotheses and concepts it embodies, the original statistical analysis was, like those of most ecological wood anatomy studies, somewhat superficial. As a result, less obvious trends have remained hidden, but can be recovered with the appropriate statistical methods, such as logistic regression.

LOGISTIC REGRESSION MODELS AND COMPARATIVE WOOD ANATOMY

Although they are rarely used in ecological wood anatomy, methods are available for studying the association between categorical variables. For example, these associations can be examined using contingency tables (Sokal & Rohlf, 1995; Quinn & Keough, 2002), but this procedure is impractical for analysing more than three variables simultaneously. Furthermore, if continuous variables are to be included in the analysis, the contingency table approach cannot be used unless the numerical variables are categorized, a practice that is undesirable for both statistical and biological reasons (Olson, 2005; Royston, Altman & Sauerbrei, 2006). To describe more complex patterns of association between categorical variables, statistical models are available. Apart from modelling association, these models can also predict the probability of the presence or absence of one variable based on the values of other variables. They share many properties with linear regression and analysis of variance, and include logistic regression models.

Logistic models are the most widely used tools for studying the relationship between a binary trait of interest (the response variable) and a set of characteristics thought to influence this trait (the explanatory variables), which can be categorical and/or continuous (Kleinbaum, 2002). It is an ideal statistical technique for modelling the association between the presence or absence of a given type of cell and a set of environmental and anatomical variables. Because several explanatory variables can be included in a given model, logistic regression is ideal for discovering complex patterns of association that cannot be easily extracted with pairwise estimation of correlations, and much less with a descriptive analysis of the data (Kutner *et al.*, 2005). Suppose we are interested in modelling the way in which vessel grouping (*vg*) and the presence or absence of scalariform perforation plates (*sc*) predict the presence of vasicentric tracheids (*i*). We can use a logistic regression model with two explanatory variables (one continuous, *vg*, one categorical, *sc*), and a binary response variable (the presence or absence of *i*). Such a model has the following form:

$$\ln\left[\frac{\pi_i}{1-\pi_i}\right] = \beta_0 + \beta_1 vg + \beta_2 sc$$

The left part of the expression is called the logit transformation of π_i , that is, the logarithm of the ratio of the probability of the presence of vascentric tracheids (referred to by statisticians as the 'probability of success', π_i) and the probability of absence (the 'probability of failure', $1 - \pi_i$). The probability of success varies from one species to another depending on the value of the two explanatory variables (*vg* and *sc*). This probability is expressed as a nonlinear function of the parameters β_0 , β_1 , and β_2 , which are also known as regression coefficients. After a process of modelling, which is detailed below, a logistic model contains the explanatory variables that influence the response. As we will show, information regarding the direction and magnitude of the associations between each explanatory variable and the response can be extracted from the estimated parameters of the model. Logistic models can thus be used to unveil complex patterns of association between several variables, a property of evident utility in ecological wood anatomy.

REANALYSIS OF THE CARLQUIST AND HOEKMAN ECOLOGICAL ANATOMY DATA SET

Carlquist & Hoekman (1985) used the ecologically and phylogenetically diverse woody flora of southern California to examine variation in anatomical features associated with the conduction of water, such as vessel diameter, grouping, and perforation plate type. They included over 200 species in all of the woody genera then recognized in the region and examined the relationship of anatomical variables with habit (shrub, tree, vine, etc.) and environmental factors represented by habitat categories (e.g. alpine, riparian, woodland, etc.). With this large data set, Carlquist and Hoekman detected trends for the whole flora and illustrated numerous ecological hypotheses that still guide ecological wood anatomy studies to the present.

The original statistical analysis of Carlquist and Hoekman focused mainly on descriptive statistics (means and percentages), but two statistical tests (Mann–Whitney and chi-squared) were mentioned. The general approach was to divide the data into subsets according to the categories of a given qualitative variable. Then, means for the different subsets were calculated for continuous variables. These statistics were then compared with their global counterparts calculated using all of the data. The signs of the differences (positive or negative) were used to determine whether the woods of a given category tend to be xeromorphic or mesomorphic. The process was repeated for all of the qualitative variables in the data set. Although the main focus of the discussion of the paper centred on how mesomorphic or xeromorphic the wood of a given category appeared to be, the authors also highlighted associations between some variables.

Additionally, they commented on categories and species that did not follow the predicted patterns. Significant findings of Carlquist and Hoekman were that low vessel density, wide vessels, low vessel grouping, a lack of vascentric tracheids, a lack of helical sculpture on vessel walls, and the absence of growth rings are common in woods in moister situations. Because the sign of these associations (positive or negative) has repeatedly been corroborated in many ecological wood anatomy studies, they are often regarded as well known. However, the magnitudes of these associations have rarely or never been quantified, making it impossible to establish comparisons between regions or taxa.

In our reanalysis, we chose to focus on the presence or absence of the different types of conductive imperforate tracheary elements included in the data set, both because they are a major focus of the original work and because the identification of these cells has been the object of a debate among wood anatomists (e.g. Bailey, 1936; Baas, 1986; Carlquist, 1986, 2001, etc.). Using Carlquist's classification (see Carlquist, 2001), the conductive imperforate tracheary elements in this study included true tracheids, vascentric tracheids, and vascular tracheids. True tracheids have dense, fully bordered pits and are generally present as ground tissue. In general, true tracheids are assumed to be symplexiomorphic with the tracheids of gymnosperms, but this assumption is still controversial (e.g. Feild, Brodribb & Holbrook, 2002). Vascentric tracheids are so called because they are found only in association with vessels, and are thought to provide a safer, if slower, alternative conductive path to the vessels with which they are associated. In contrast, vascular tracheids are never found in association with vessels and are instead typical of the latewood of soft-leaved shrubs whose leaves, and sometimes branches, desiccate in the summer dry season. Both vascentric and vascular tracheids are thought to be derived evolutionarily from vessel elements, and are morphologically similar to one another. Despite the different evolutionary origins that these cell types are thought to have, for convenience we refer to them collectively as 'tracheid types' or 'conductive imperforate tracheary elements'.

The Carlquist and Hoekman data set is ideal for examining the associations of tracheid types with other variables because it is one of the few studies to examine these cells and because its sampling covered a wide variety of environmental conditions, anatomical variables, and plant families. In addition to allowing us to show that the analyses employed in traditional wood anatomical studies overlook important information, our reanalysis illustrates important issues in cell classification and data coding. Standard practice in comparative wood anatomy (e.g. IAWA

Committee, 1989) emphasizes the classification of cell types and wood features, e.g. growth ring types, imperforate tracheary element types, ray types, etc. How 'real' or biologically defensible these classifications are could be tested using approaches such as the one we propose. We also show how incorrect coding can lead to a loss of inferential power. Finally, we illustrate how the unusual species pointed out by logistic models as deviating from the general behaviour of the data could be revealing unrecognized anatomical strategies or could be indicating the need for new observations of preparations to verify that the information was collected correctly.

MATERIAL AND METHODS

ADJUSTMENTS TO THE CARLQUIST AND HOEKMAN DATA SET AND DEFINITION OF VARIABLES

All of the 207 species in the Carlquist and Hoekman data set were included in the analysis. The variables considered in this analysis are summarized in Table 1. Two variables required modification, whereas an additional two were deemed unsuitable for inclusion in logistic models and were eliminated. The 'average number of bars in scalariform perforation plate' was converted to a binary presence/absence character because only a very small fraction (5%) of the species had scalariform plates and maintaining it as a numerical variable would have produced a strongly right-

Table 1. Variables in the Carlquist and Hoekman data set that were included in our reanalysis. Variables included continuous vessel characteristics and categorical variables with two possible states (p/a: presence/absence) or with more than two states (growth ring and habit). Tracheid types (vasicentric, true, and vascular) were used as response variables in the analyses

Variable	Type of variable
Vessels mm ⁻²	Continuous
Vessel element length (µm)	Continuous
Vessel diameter (µm)	Continuous
Vessels per group	Continuous
Vasicentric tracheids	Categorical (p/a)
True tracheids	Categorical (p/a)
Vascular tracheids	Categorical (p/a)
Scalariform perforation plates	Categorical (p/a)
Helical sculpture in earlywood	Categorical (p/a)
Helical sculpture in latewood	Categorical (p/a)
Growth ring type	Categorical (ring porous, semiring porous, and diffuse porous)
Habit	Categorical (shrubs, subshrubs, other)

skewed distribution of the data, with most of the species having zero bars. 'Helical sculpture' was separated into two variables: helical sculpture in earlywood and helical sculpture in latewood. 'Habitat' and 'mesomorphy index' were not included in the analyses. For 16 species the habitat was not assigned, and the distribution of the 181 remaining species among the 11 habitat categories was so uneven that the estimation of some parameters would probably have been inaccurate because there would have been too few data in some categories to serve as a basis for inference (Collett, 2003). The mesomorphy index was eliminated because it was computed based on continuous variables of the same data set and would therefore be a source of collinearity in the logistic models.

The original data set had a problem with the coding of vascular tracheids. When a given species had both vascular and vasicentric tracheids, it was coded by Carlquist and Hoekman as having vasicentric but not vascular tracheids. Therefore, some woods that have vascular tracheids are coded as lacking them. Although they did not mention how many species were coded in this way, Carlquist & Hoekman (1985) stated that they were few. Because apparently relatively few species were incorrectly coded and because the patterns of association of vascular tracheids and the other variables were also of interest, we did not discard vascular tracheids in the analyses.

FITTING OF LOGISTIC REGRESSION MODELS

The aim of our analyses was to obtain three models, one for each of the tracheid types. Each model attempts to predict the presence or absence of a tracheid type based on the rest of the nontracheid type variables. None of the tracheid types was used to predict the presence or absence of another one because, as coded by Carlquist and Hoekman, they are mutually exclusive, and such variables can cause numerical problems when the regression coefficients and their standard errors are estimated (Hosmer & Lemeshow, 2000). We outline the general strategy adopted for the fitting of the logistic models (see Fig. 1) before treating each step in greater detail. Broadly, the model-building process involved three main steps, which are very similar to those taken when fitting a multiple regression model: (1) univariate analyses; (2) construction of a preliminary multiple logistic model; and (3) construction of the final multivariate logistic model (Hosmer & Lemeshow, 2000; Quinn & Keough, 2002). The iterative nature of this process is designed to eliminate uninformative variables and identify and correct problems with the data or models, and is illustrated graphically in Figure 1. Each of these steps, which were carried out using the PC program STATA vs. 7 (Stata Corpora-

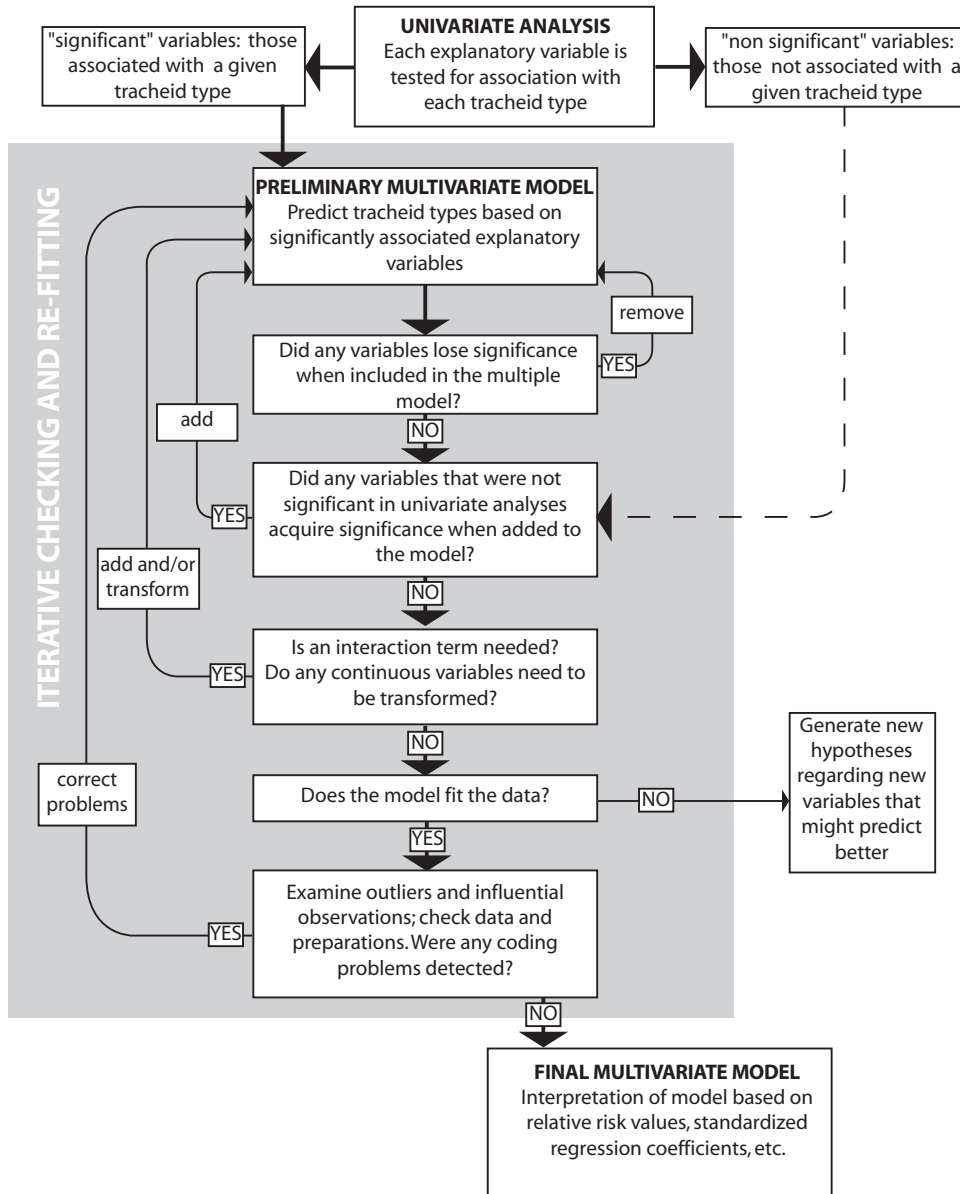


Figure 1. Flow chart illustrating the fitting process of logistic regression models, including the iterative checking and re-fitting procedure before arriving at the final multivariate logistic model.

tion, College Station, Texas, USA), is described in more detail below.

Initial steps in model construction: univariate analysis

The initial phase of model building used descriptive statistics, contingency tables, independence tests, and univariate logistic models to decide which variables should be included in the multiple logistic models and which should be excluded. To determine which variables were associated with the response variables, we applied tests of independence (or lack

of association). Two variables are said to be independent if the value of one of them cannot be used to predict the value of the other one. The variables that were found to be associated with a tracheid type were entered into the preliminary multivariate models (see Fig. 1). These initial analyses are frequently skipped when fitting a multivariate model. This is unfortunate because they provide valuable information regarding the association between variables, as we will show for the Carlquist and Hoekman data set.

When the explanatory variable was continuous, we used univariate (simple) logistic regression models to test for independence, whereas if it was categorical we used contingency tables. For continuous explanatory variables, the null hypothesis of independence between the response and the explanatory variable was not rejected when regression coefficients equalled zero. The significance of the regression coefficients was tested using the Wald statistic (Quinn & Keough, 2002). When the explanatory variable was categorical, a logistic model yielded the same results as the contingency table approach. We preferred contingency tables for cases with categorical explanatory variables because they allow the examination of how frequent each combination of characters in the data set is. This is important because small frequencies can produce unreliable estimates for the logistic model. Based on contingency table results, we tested for independence using one of two methods. If some frequencies in the contingency table were small, the Fisher exact test was computed; otherwise a Pearson chi-squared test was used (see Sokal & Rohlf, 1995).

Rejecting the null hypothesis of independence suggests an association between the response and categorical explanatory variables, but cannot quantify the degree of association. Toward this end, we computed the relative risk (RR). This statistic is defined as $RR = p_1/p_2$, where p_1 and p_2 are the proportions (or probabilities) of success of two groups classified in different categories of an explanatory variable. RR indicates how much more probable it is to find a given trait in group 1 as compared with group 2. The terminology of 'risk' is of relevance in medical applications, and may sound odd when applied to wood, but the idea of the relative probability of the presence of a given variable between two groups is useful for our purposes. For example, the percentage of species that had vasicentric tracheids when the wood was ring porous was $p_1 = 45\%$ (41/91), whereas it was $p_2 = 25.3\%$ (24/95) when the wood was semiring porous. In this case, RR equalled $45\%/25.3\% = 1.78$. Therefore, the percentage of species with vasicentric tracheids is almost doubled when the wood is ring porous instead of semiring porous. A RR close to unity would have suggested that the probabilities of the presence of vasicentric tracheids were independent of the growth ring type.

Preliminary multivariate logistic model

All the explanatory variables individually associated with the response were incorporated simultaneously into multiple (multivariate) models (Fig. 1). In cases in which two or more explanatory variables were associated with one another, some that were significant in the univariate analysis became unimportant. Including associated explanatory variables did not provide additional information in the model and could have

caused problems of collinearity in the estimation procedure, so variables that no longer appeared to be significant were removed from the multiple model. We also incorporated one by one the variables that were unrelated to the response in the univariate analyses to see if they would become significant in the presence of others. Next, we determined whether a continuous variable needed to be transformed or if interaction terms needed to be included in the model (Hosmer & Lemeshow, 2000). To test whether the effect of an explanatory variable, an interaction term, or a transformation was significantly different from zero, we used the Wald and likelihood ratio tests. The latter test was used when the significance of two or more regression coefficients was tested simultaneously, whereas the Wald statistic was used when the significance of a single regression coefficient was tested.

We examined how well our preliminary logistic models described the data using goodness-of-fit statistics and a detailed examination of individual data. Goodness-of-fit statistics are based on the discrepancies between the observed values of the response variable and its estimated values from the fitted model. Because our models included one or more continuous explanatory variables, we used Hosmer and Lemeshow's goodness-of-fit statistic (Hosmer & Lemeshow, 2000). We also examined each data point to detect unusual observations that deviated from the general trend described by the models or that exerted a strong influence on model fit. In the first case, we looked for standardized residuals greater than three, irrespective of the sign, to detect atypical or outlying observations. The model was not considered invalid if 5% or fewer of the standardized residuals were greater than three (Collett, 2003). In addition, we detected influential observations using Pregibon's index. Influential observations have an undue impact on the estimated regression coefficients because of their distance from the remaining data in the values of their explanatory variables. Pregibon's index (Pregibon, 1981) identifies these observations by measuring the overall change in the coefficients when an observation is omitted from the data set. We directed special attention to influential observations to determine whether the anatomical preparations required reinterpretation, the data were recorded correctly, or the samples represented previously unrecognized anatomical modes or features. In the first two situations, the data were corrected and the model was fitted again (Fig. 1).

Final multivariate logistic model and interpretation

The iterative process of checking and refitting the models ended when the fit of the model could not be improved (Fig. 1). The models thus obtained are referred to as the final multivariate logistic models, and it is upon these that our interpretations were

based. These interpretations employed standardized regression coefficients, estimated probabilities, and RR based on them.

Within a given model, it is important to identify which variables are most strongly associated with the response variable. For example, is vasicentric tracheid presence more strongly associated with vessel diameter or vessel grouping? Traditionally, a measurement of the degree of association, known as the odds ratio, is computed directly from the estimated regression coefficients in the model. However, because the odds ratio is difficult to interpret, we preferred to examine the sign and magnitude of the regression coefficients and to calculate the estimated probabilities of finding each tracheid type. Regression coefficients reflected the degree and direction of association between an explanatory variable and the response. The sign indicated whether the association was positive or negative between the explanatory variable and the probability of the presence of a particular tracheid type, whereas the magnitude indicated the strength of the association. However, it would have been misleading to compare the magnitude of two regression coefficients to determine which is more strongly associated with the probability of presence when the explanatory variables were measured in different units. To achieve valid comparisons, we standardized the regression coefficients by multiplying each by the standard deviation of its corresponding explanatory variable (see Agresti, 2002).

We also interpreted the model using the estimated probabilities of finding each tracheid type for different species. For example, the probability of having vasicentric tracheids can be computed for two species with helical sculpture in latewood but differing in vessel grouping. These two probabilities were compared graphically and using RR.

RESULTS

This section is arranged in three main parts. First we report descriptive statistics for continuous vessel characteristics, highlighting species with extreme

values. The second part reviews the occurrence and exclusive relationship between the three types of conductive imperforate tracheary elements. The final and main part of this section is devoted to the construction of the logistic regression models that predict the presence or absence of the different conductive imperforate tracheary elements based on the other variables. We have divided this last part into three subsections, one for each of the conductive imperforate tracheary element types. Each subsection is further subdivided into the three modelling steps described above.

DESCRIPTIVE STATISTICS FOR CONTINUOUS CHARACTERISTICS OF VESSELS

The histograms in Figure 2A–D show that all four continuous vessel characteristics had an asymmetrical distribution, with small values being more frequent than large ones. Vessel density for 75% of the species was less than 341 vessels mm^{-2} (Fig. 2A), and species such as *Romneya coulteri* and *Fremontodendron californicum* had an atypically large number of vessels mm^{-2} (1350 and 875 vessels mm^{-2} , respectively). The largest recorded average vessel diameter in the data set belonged to the liana *Vitis girdiana*, with 186 μm . The most highly asymmetrical distribution for vessel characters was found in vessel grouping (Fig. 2D). Nearly 77% of the species had between one and three vessels per group, with the largest value coming from *Romneya coulteri*, with 150 vessels per group. Additional summary statistics for continuous vessel characters are shown in Table 2.

Because of the non-normal distribution of the continuous vessel characteristics (Fig. 2A–D) and the presence of the extreme data mentioned, Spearman's rank correlation coefficient was used to measure the degree of association between each pair of continuous vessel characteristics (Table 3). Only the association between vessel diameter and vessel density was of noteworthy magnitude and statistically significant, showing that fewer vessels mm^{-2} are found when vessels are wider.

Table 2. Descriptive statistics for continuous vessel characteristics. The strong differences between medians and means were due to extreme values that influenced the means strongly

Vessel characteristic	Minimum	Maximum	Median	Mean	Standard deviation
Vessels mm^{-2}	10.8	1350	191	250.97	210.32
Vessel element length (μm)	53.1	643	208	233.17	110.3
Vessel diameter (μm)	12.5	186	29.4	35.19	20.22
Vessels per group	1	150	1.95	3.86	10.97

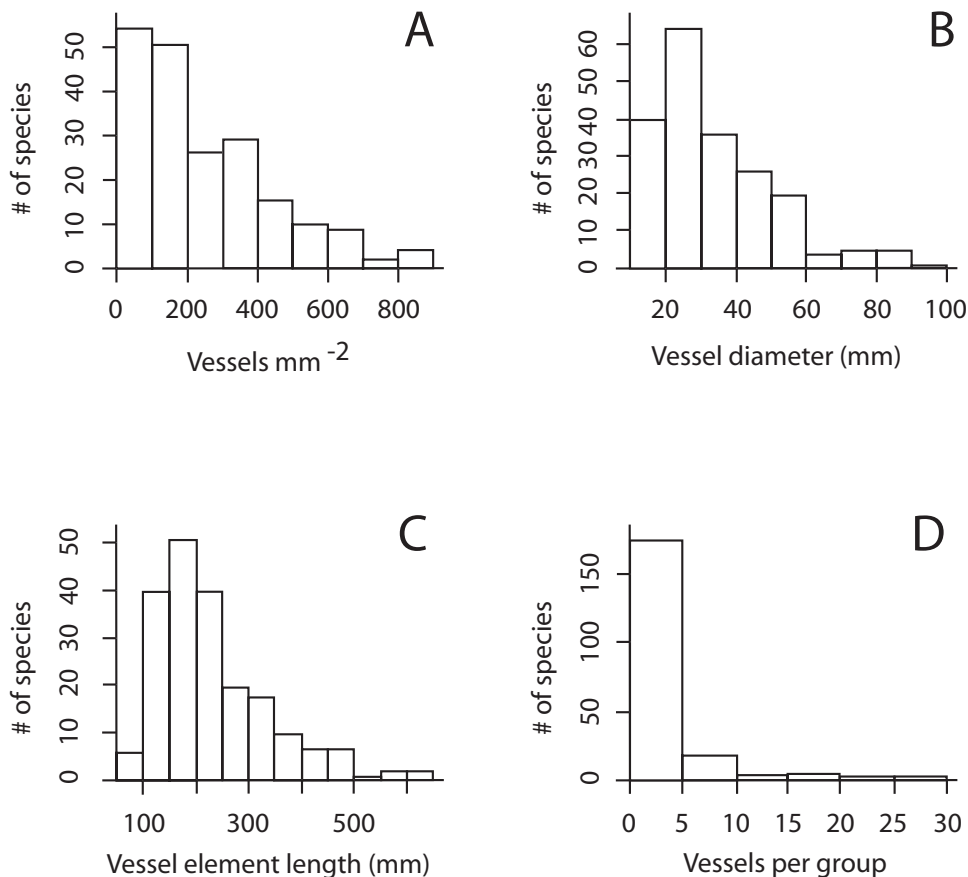


Figure 2. Histograms showing the strongly skewed distributions of continuous vessel characteristics. A, distribution of vessel density, with most species having relatively low density. B, distribution of vessel diameter, with most species having diameters smaller than 60 μm . C, distribution of vessel element length, showing that most species have vessel elements shorter than 300 μm . D, distribution of vessels per group, with its extremely skewed histogram in which the majority of species have fewer than five vessels per group. The following species with extreme values are not included in the histograms: for vessel density and vessels per group, *Romneya coulteri* (1350 vessels mm^{-2} and 150 vessels per group); for vessel diameter, *Vitis girdiana* (186 μm).

Table 3. Spearman's rank correlation coefficients between pairs of continuous vessel characteristics. All correlations were weak, except for that between vessel density and vessel element diameter

	Vessels mm^{-2}	Vessel element length (μm)	Vessel element diameter (μm)
Vessel element length (μm)	-0.13*		
Vessel element diameter (μm)	-0.75**	0.1	
Vessels per group	0.12*	-0.21**	-0.07

** $P < 0.005$; * $P < 0.10$.

OCCURRENCE AND RELATIONSHIPS BETWEEN IMPERFORATE TRACHEARY ELEMENT TYPES

Table 4 shows how the three types of conductive imperforate tracheary element were distributed among species. Vasicentric tracheids were the most common, with 33.3% (69/207) of the species, followed by true tracheids with 23.7% (49/207). Vascular tracheids were observed in 13% (27/207) of the species, but this was an underestimation caused by the coding problem mentioned earlier. Close to 30% (62/207) of the species examined had no subsidiary conduction system and rely exclusively on vessels. Because of the apparently small number of species in which vascular and vasicentric tracheids co-occur, even if vascular tracheids were correctly coded, the three types of cell would not be considered statistically independent,

because the presence of any tracheid type almost always implies the absence of the other two. We did not test for independence between the three tracheid types because several expected frequencies were lower than five, violating the assumptions of Pearson's chi-squared test. Therefore, we combined vasicentric and vascular tracheids, the first two columns of Table 4, into a single variable. We then tested for independence between this new variable and true tracheids. Pearson's test showed that the presence or absence of true tracheids depended strongly on the presence or absence of vascular–vasicentric tracheids ($\chi^2 = 55.10$, 2 d.f., $P < 0.001$).

LOGISTIC MODELS PREDICTING THE PRESENCE OR ABSENCE OF CONDUCTIVE IMPERFORATE TRACHEARY ELEMENT TYPES

The fitting of the logistic models for each type of conductive imperforate tracheary element is described in three subsections. Within each of these subsections,

Table 4. Distribution of conductive imperforate tracheary elements in the species of the data set. Vasicentric and vascular tracheids were combined into a single variable to yield a two-dimensional contingency table. The strong differences between observed and expected frequencies (shown in parentheses and calculated under the hypothesis of independence between variables) suggested a marked lack of independence between tracheid types

Vasicentric tracheids	Vascular tracheids	True tracheids		Total
		Absence	Presence	
Absence	Absence	62 (84.7)	49 (26.3)	111
Absence	Presence	27 (20.6)	0 (6.4)	27
Presence	Absent/ present	69 (52.7)	0 (16.3)	69
Total		158	49	207

Table 5. Univariate logistic models for each tracheid type (vasicentric, true, and vascular) as response variables and the continuous vessel characteristics as explanatory variables

Explanatory variable	Vasicentric tracheids		True tracheids		Vascular tracheids	
	Coefficient (SE)	<i>P</i> -value	Coefficient (SE)	<i>P</i> -value	Coefficient (SE)	<i>P</i> -value
Vessels per group	0.11 (0.04)	0.011	-3.07 (0.55)	< 0.001	0.002 (0.017)	0.885
Vessel diameter	-0.04 (0.01)	< 0.001	-0.05 (0.02)	< 0.001	0.02 (0.01)	0.057
Vessel element length	-0.003 (0.002)	0.057	0.01 (0.001)	0.001	-0.004 (0.002)	0.075
Vessels mm ⁻²	0.001 (0.001)	0.096	0.003 (0.001)	< 0.001	-0.002 (0.001)	0.184

SE, standard error of the logistic regression coefficient.

we first report the results of analyses of association between the response and explanatory variables, which guided decisions regarding which variables would be included in a preliminary multivariate logistic model. We start with the fitting of univariate logistic regression models for continuous variables and then report the results of contingency table analyses that detected association between the response and the categorical explanatory variables. In no case was it necessary to include interaction terms or to transform continuous variables. On the basis of the preliminary model, we calculated Pregibon's index, which permitted the identification of species with a strong influence on the estimated regression coefficients. In many cases we referred to the original preparations, and in some instances changed the coding of these species for the final analyses, which are described at the end of each subsection. These changes in interpretation of anatomical preparations guided by the logistic models represent one of the most noteworthy results from our analysis, and are treated further in the discussion section. The last subsection indicates how the final logistic multivariate model was interpreted.

Vasicentric tracheids as the response variable

Initial steps in model construction: univariate analysis:

The simple logistic regression models fitted with continuous vessel characteristics as explanatory variables showed that vasicentric tracheids were more likely to be found as the number of vessels per group or vessel density increased. Conversely, it was less likely to find them as vessel diameter or length increased (Table 5).

All of the categorical explanatory variables were strongly associated with vasicentric tracheids. First, with regard to perforation plate type, vasicentric tracheids were found in 35.2% (69/196) of the species with simple perforation plates, whereas they were absent in all of the 11 species with scalariform plates. The strong negative association between vasicentric trac-

heids and scalariform perforation plates was statistically significant (one-sided Fisher exact test with $P = 0.01$).

With regard to habit, trees, herbs, and vines were combined into a single habit group to avoid categories with small frequencies. Shrubby species were most abundant, accounting for 66.67% (138/207). Vasicentric tracheids were common in smaller life forms, being found in 39.13% of shrubs (54/138) and 31.25% of subshrubs (10/32). Only 13.51% (5/37) of the other types of habit had such cells. Thus, vasicentric tracheids were more probable in shrubs (RR = 2.89) and subshrubs (RR = 2.31) than in the rest of the habits. The association between habit and the presence of vasicentric tracheids was corroborated by Pearson's chi-squared test ($\chi^2 = 8.69$, 2 d.f., $P = 0.013$). Carlquist and Hoekman's data set contained two vines, 16 herbs, and 19 trees. They represented 18% of the studied habit types, but just 6% of them had conductive imperforate tracheary elements. Therefore, although these habits are obviously distinct, for the purposes of our analysis they are virtually indistinguishable. To avoid table cells with very low values, we thus decided to combine them into a single category before examining the association between habit type and the response variables.

Growth ring type was also closely associated with the presence or absence of vasicentric tracheids. These cells were present in 45% (41/91) of the species with ring porous wood, whereas only 25.3% (24/95) and 19.0% (4/21) of those with semiring porous or diffuse porous wood had them. Vasicentric tracheids were approximately twice as probable in species with ring porous wood than in species with semiring porous (RR = 1.78) or diffuse porous wood (RR = 2.36). The association between growth ring type and the presence or absence of vasicentric tracheids was supported by Pearson's chi-squared test ($\chi^2 = 10.34$, 2 d.f., $P = 0.006$).

A variable very strongly associated with vasicentric tracheids was the presence of helical sculpture, both in early- and latewood. In turn, helical sculpture in earlywood and latewood was also strongly associated with one another ($\chi^2 = 128.79$, 1 d.f., $P < 0.001$). There was no case in which helical sculpture was present in earlywood without being present in latewood. Vasicentric tracheids were present in 50% (41/82) of species with helical sculpture in latewood, whereas just 22.4% (28/125) of those without helical sculpture presented such cells. Thus, the percentage of species with vasicentric tracheids was doubled in the presence of helical sculpture (RR = 2.23). Pearson's chi-squared test was significant for the association between vasicentric tracheids and helical sculpture in latewood ($\chi^2 = 16.97$, 1 d.f., $P < 0.001$). Likewise, the 11 species with scalariform perforation plates lacked both helical sculpture

(except *Philadelphus microphyllus*, which had latewood sculpture) and vasicentric tracheids.

Preliminary multivariate logistic model: Because of the strong association between the two types of helical sculpture, little was gained when both were used to predict the presence or absence of vasicentric tracheids. In fact, the inclusion of both variables could have led to collinearity and the consequent unstable regression estimates, and therefore only one was included. We chose helical sculpture in latewood because all species with helical sculpture showed it in latewood, but not all had it in earlywood, thereby including all species with helical sculpture.

Growth ring type was not highly significant after helical sculpture in latewood was included as an explanatory variable (likelihood ratio test statistic = 5.80, 2 d.f., $P = 0.055$). When the average vessel diameter was added to the model, growth ring type lost all predictive contribution and was eliminated from the model (likelihood ratio test statistic = 3.87, 2 d.f., $P = 0.144$). Finally, the number of vessels per group was added to the model.

The preliminary multiple logistic model predicted the presence or absence of vasicentric tracheids based on helical sculpture in latewood, vessel diameter, and the number of vessels per group. Pregibon's index detected two species that strongly influenced the model fit, *Baccharis salicifolia* and *Fremontodendron californicum*. Both deviated from the general trend of the data in having very high vessel grouping but lacking vasicentric tracheids. All species with more than 11 vessels per group exhibited vasicentric tracheids, except for *Baccharis salicifolia* and *Fremontodendron californicum*, which despite having 29 and 26.7 vessels per group were reported as lacking them. Before continuing with the fit of the definitive model, we re-examined the preparations of these species, which revealed the presence of vasicentric tracheids in both. When we refitted the model with these species recoded as having vasicentric tracheids, a non-significant effect of vessel diameter on the response variable was reported (Wald statistic = -1.57, 1 d.f., $P = 0.116$), and this variable was therefore not included in the final model.

Final multivariate logistic model: The final model included vessels per group and helical sculpture in latewood as explanatory variables (Table 6), with updated coding for *Baccharis salicifolia* and *Fremontodendron californicum*. The Hosmer–Lemeshow test indicated that the model described the data well (Hosmer–Lemeshow statistic = 13.10, 8 d.f., $P = 0.11$), and just six of 207 species (3%) had a standardized residual greater than three in absolute value. The positive regression coefficients (Table 6) indicated that the

Table 6. Final multivariate logistic model predicting the presence or absence of vasicentric tracheids based on the number of vessels per group and the presence or absence of helical sculpture in latewood. Variables are listed in order of decreasing association with the response, according to the magnitude of their standardized coefficients

	Coefficient	SE	P-value	Stand coeff
Constant	-1.92	0.30	< 0.001	-0.49
Vessels per group	0.25	0.07	0.001	2.72
Helical sculpture in latewood	1.18	0.32	< 0.001	0.58

SE, standard error of the logistic regression coefficient; Stand coeff, standardized logistic regression coefficient, calculated as the original regression coefficient multiplied by the standard deviation of its corresponding explanatory variable.

probability of finding vasicentric tracheids is greater in woods with more vessels per group or with helical sculpture in latewood. Figure 3 presents the two curves showing how the estimated probability of finding vasicentric tracheids increases with the number of vessels per group. Species with helical sculpture in latewood, in the upper curve, have a higher probability of presenting vasicentric tracheids. The smaller the number of vessels per group, the greater the difference between the probabilities of finding vasicentric tracheids in species with and without helical sculpture in latewood.

The standardized regression coefficients (Table 6) implied that the number of vessels per group was the variable most strongly related to the presence of vasicentric tracheids. To give an idea of the magnitude of the effect of vessel grouping, consider a plant with helical sculpture in latewood. Based on the model, the probability of finding vasicentric tracheids is 62.3% if the plant has an average of five vessels per group and 38.05% if the average is one vessel per group (these cases are highlighted in Figure 3). Thus, an increase of four units in the average number of vessels per group produces an increase of 24.31% in the probability of finding vasicentric tracheids, and amounts to $RR = 1.64$.

True tracheids as the response variable

Initial steps in model construction: univariate analysis: Simple logistic regression models indicated that all the continuous characteristics of vessels were strongly associated with true tracheids (Table 5). They tended to be present in species with a large number of vessels mm^{-2} or with long vessel elements. On the contrary, the wider the vessels were or the greater the

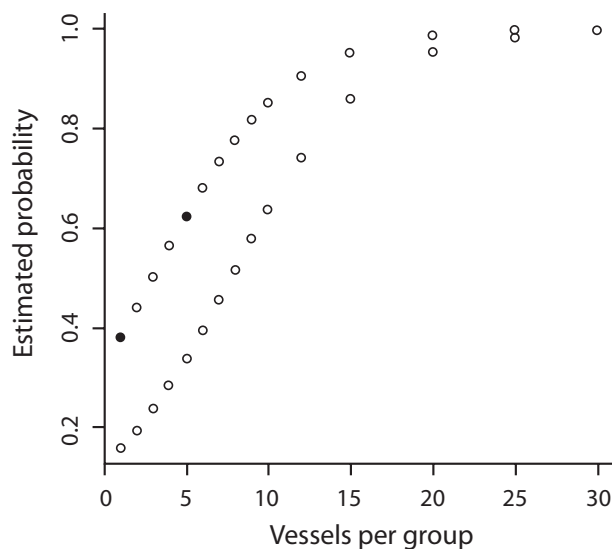


Figure 3. Estimated probability of the presence of vasicentric tracheids as vessel grouping is varied in the presence of helical sculpture in latewood (upper curve) and in the absence of helical sculpture in latewood (lower curve). The estimates are based on the final multivariate model predicting the presence or absence of vasicentric tracheids. Based on the model, the probability of finding vasicentric tracheids is 62.3% if a plant has an average of five vessels per group and 38.05% if the average is one vessel per group. These two cases are highlighted in the graph.

number of vessels per group, the less probable it became to find true tracheids.

The only categorical variable strongly associated with true tracheids was perforation plate type. Only 11 species in the data set had scalariform perforation plates, and all of them had true tracheids, except for *Alnus rhombifolia* and *Betula fontinalis*. Of the 196 remaining species that had simple plates, only 20.41% (40/196) had true tracheids. This clear association between the presence of scalariform perforation plates and the presence of true tracheids was confirmed by the Fisher exact test ($P < 0.0001$). The RR value indicated that the probability of finding true tracheids in species with scalariform perforation plates was four times that of species having simple plates ($RR = 4.01$).

Preliminary multivariate logistic model: A preliminary model was fitted to predict the presence of true tracheids using all the continuous vessel characters as explanatory variables. Vessel diameter was then excluded because, although it was associated with true tracheids, it was not significant in the presence of the other continuous variables (Wald statistic = -0.76 , 1 d.f., $P = 0.445$). Perforation plate type was not included in any multivariate model because the low number of species with scalariform perforation plates

and lacking true tracheids did not enable us to estimate some regression coefficients precisely.

As with vasicentric tracheids, Pregibon's index was calculated to detect influential observations, with *Symphoricarpos mollis* having the largest index. When this species was removed from the data and the model fitted again, the estimated coefficient for vessels per group changed considerably, corroborating the influence of *Symphoricarpos mollis*, which had unusually high vessel grouping for a species with true tracheids. Upon the examination of preparations of *Symphoricarpos mollis*, we found that nonconductive axial cells formed the ground tissue in earlywood, along with grouped vessels, and that vessels were nearly solitary when embedded in a matrix of latewood true tracheids. Therefore, we considered only the grouped earlywood vessels, where tracheids are absent, and recoded this species as lacking true tracheids rather than having them before proceeding with the final version of the model.

Final multivariate logistic model: The final model included vessel density and grouping, and vessel element length as explanatory variables (Table 7). The model fitted the data quite well (Hosmer–Lemeshow statistic = 2.31, 8 d.f., $P = 0.97$). Only three species had a standardized residual whose absolute value ranged between 3 and 3.5. Vessel density and vessel element length were positively associated with the presence of true tracheids, whereas vessel grouping reduced the probability of finding true tracheids (Table 7). The standardized regression coefficients of these variables in the multiple model (Table 7) indicated that vessel grouping and vessel density were the two variables most strongly related to the presence of true tracheids. For illustrative purposes, consider a plant with 200 vessels mm^{-2} and an average vessel element length of 200 μm . If the average number of vessels per group was one, the probability of finding true tracheids would be 66.8%, whereas this probability would be nearly zero (0.01%) if there were three per group.

Table 7. Final multivariate logistic model predicting the presence or absence of true tracheids based on vessels per group, vessel density, and vessel element length. Conventions as for Table 6

	Coefficient	SE	P-value	Stand coeff
Constant	1.71	1.320	0.195	-12.479
Vessels per group	-4.90	0.996	< 0.001	-53.763
Vessels mm^{-2}	0.011	0.002	< 0.001	2.387
Vessel element length	0.01	0.002	0.001	0.896

Thus, this difference of two vessels per group produces a drastic decrease in the probability of finding true tracheids.

Vascular tracheids as the response variable

Just 13% of the species in the data set had vascular tracheids. This percentage is underestimated because vascular and vasicentric tracheids were coded as mutually exclusive when they can actually be present in the same plant. Therefore, the results in this section should be interpreted with caution until they can be repeated with the correct coding.

Initial steps in model construction: univariate analysis: Univariate logistic models indicated that vessel diameter and vessel element length were associated with vascular tracheids, albeit weakly (Table 5). Neither vessel grouping nor vessel density were associated with the presence of vascular tracheids (Table 5). Likewise, none of the categorical variables was associated with vascular tracheids. *Betula fontinalis* was the only species with both vascular tracheids and scalariform perforation plates.

Preliminary multivariate logistic model: A multivariate logistic model with vessel diameter and vessel element length as explanatory variables was fitted to the data. *Sambucus mexicana* and *Betula fontinalis* were the two species with the largest influence on the model. These two species affected the estimated regression coefficient for vessel element length, because the 37 species with a vessel element length greater than 328 μm lacked vascular tracheids, except *Sambucus mexicana* and *Betula fontinalis* (vessel element length 438 and 426 μm , respectively).

Final multivariate logistic model: The final model included vessel element diameter and length as explanatory variables (Table 8), and fitted the data well (Hosmer–Lemeshow statistic = 10.41, 8 d.f., $P = 0.237$). Only five species had a standardized

Table 8. Final multivariate logistic model predicting the presence or absence of vascular tracheids based on vessel element length and vessel diameter. Conventions as for Table 6

	Coefficient	SE	P-value	Stand coeff
Constant	-1.588	0.607	0.009	-2.015
Vessel element length	-0.005	0.002	0.055	-0.512
Vessel diameter	0.019	0.009	0.050	0.377

residual with an absolute value between 3 and 5. Species with wide vessels had a higher probability of presenting vascular tracheids, but, as indicated by the Wald test (Table 8), the association was weak. Similarly, a weak association was observed between vessel element length and the presence of vascular tracheids. The low proportion of species with vascular tracheids and the problems with coding may be responsible for the low power of the tests to detect association.

DISCUSSION

In many cases, our results were congruent with well-established concepts in ecological wood anatomy, such as the negative relationship between vessel density and vessel diameter (e.g. Baas, Werker & Fahn, 1983; Carlquist & Hoekman, 1985; Carlquist, 2001). Nevertheless, the present study represents the first time that the magnitude of many of these 'well-known' associations has ever been documented and assigned a *P*-value. However, rather than focus on widely recognized associations, in this section we treat less commonly discussed aspects of ecological wood anatomy highlighted by our work, and novel directions for further research that our analysis suggested. Among these are compelling results regarding the functional interplay between vessel grouping and imperforate tracheary element type, the detection of unusual species for further study, and the identification of suites of character combinations that may be of functional significance. We also discuss lessons pointed to by our analyses regarding the limits of standard comparative wood anatomical sampling and data handling, and ways that statistical analyses could be used to evaluate schemes for classifying wood features.

VESSEL GROUPING, DROUGHT RESISTANCE, AND IMPERFORATE TRACHEARY ELEMENT TYPE

In a keenly insightful application of the comparative method, Carlquist (1984) proposed that, if vessel grouping is driven by selective pressure favouring redundancy of conductive streams and consequent drought resistance, then it should be lessened in the presence of subsidiary conductive cells such as true tracheids or vasicentric tracheids. Building on this notion, he suggested that the conductive nature of imperforate tracheary elements could be diagnosed by vessel grouping, with lowered grouping indicating conductive imperforate elements (Carlquist, 1984, 2001). The strong pressure differential between an embolized vessel and an adjacent water-filled one appears to put the non-embolized vessel at risk (Sperry & Hacke, 2004), so there may in fact be selection for decreased

vessel grouping in the presence of sufficient subsidiary conductive cells, rather than simply relaxed selection. Although this reasoning provides the anatomist with a comparative means of inferring the functional nature of the imperforate tracheary elements in a given taxon, it appears not to have been incorporated into functional comparative wood anatomical analyses generally. However, our findings strongly support Carlquist's interpretation.

True tracheids and vessel grouping

Vessel grouping showed a remarkable ability to predict true tracheid presence (Tables 5 and 7). Figure 4 shows that, as Carlquist (1984) noted, vessels are almost exclusively solitary when true tracheids are present, with no instances of substantial vessel grouping having been observed in the presence of true tracheids. Likewise, the differences in vessel grouping between woods with true tracheids and those without them suggested by Figure 4 were strongly statistically significant (Mann–Whitney $U = 757.5$, $P < 0.001$). That vessel grouping only occurs when true tracheids are absent implies that true tracheids are indeed conductive, and that they provide greater conductive safety than vessel grouping (cf. Carlquist, 2001).

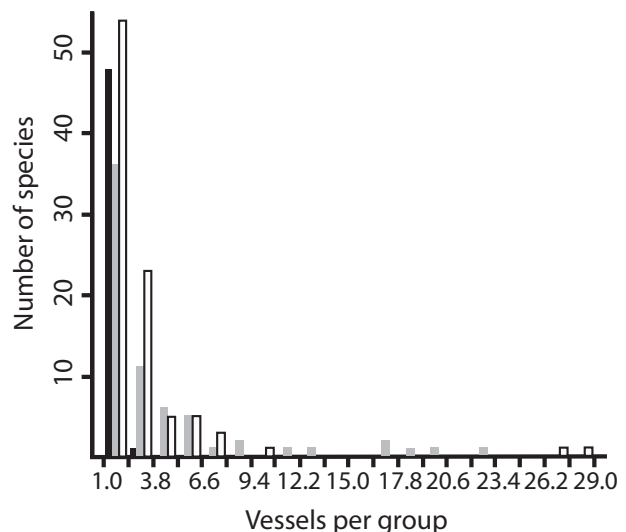


Figure 4. Difference in the distribution of vessel grouping in species with true tracheids (black bars), vasicentric tracheids (grey bars), and vascular tracheids or no conductive imperforate tracheary elements (white bars). There is a significant difference between vessel grouping in taxa with true tracheids and those with vasicentric tracheids ($P < 0.001$), and also between species with vasicentric tracheids and no conductive imperforate tracheary elements ($P < 0.001$).

Vasicentric tracheids and the functional significance of vessel grouping type

Vasicentric tracheids are thought to be subsidiary conductive cells of high safety. Just as true tracheid presence is associated with solitary vessels, lower vessel grouping could be predicted in a wood with vasicentric tracheids as compared with one with only nonconductive imperforate tracheary elements. In contrast to these expectations, our logistic regression model showed that vasicentric tracheid presence is actually *more* probable when vessels are grouped (Tables 5 and 6). Figure 4 illustrates this result graphically. If vasicentric tracheid presence lowered vessel grouping in a way analogous to that of true tracheids, then the distribution of vessel grouping in species with vasicentric tracheids should overlap that of species with true tracheids. To the contrary, the distribution of species with vasicentric tracheids appears distinct from that of species with true tracheids, a difference that is supported statistically (Mann–Whitney $U = 487.5$, $P < 0.001$).

Although some species with vasicentric tracheids do have very low vessel grouping (Table 9), Figure 4 shows that many species have remarkably large vessel groups. That this range of vessel grouping is observed in species with vasicentric tracheids suggests that plants with these cells employ an array of functional strategies, in contrast to the consistent lowering of vessel grouping observed when true tracheids are present (Fig. 4; Carlquist, 1984, 1985). Carlquist (1985, 2001) illustrated the radially extensive, often diagonal, aggregations of vessels that typify many species with vasicentric tracheids, and suggested that interconnection between these massive aggregations probably unites most of the vessels in a given stem into a single highly redundant conductive system. That large aggregations of vessels have evolved in a wide array of lineages, producing so strong a statistical association with vasicentric tracheids, suggests that they are one of the key strategies for conductive safety that arise in sclerophyllous plants of drylands. From a statistical point of view, questions that cannot be addressed in a given study might be accessible by examining additional variables. In the case of vessel grouping types and vasicentric tracheids, a study explicitly designed to identify association between qualitative and quantitative aspects of vessel grouping type, vasicentric tracheid distribution and abundance, and variables such as phenology and libriform fibre characteristics (cf. Jacobsen *et al.*, 2005), could help to identify the selective pressures associated with different vessel grouping phenomena in the presence of vasicentric tracheids.

Vasicentric tracheids are consistently associated with high vessel grouping to the point where the logistic regression singled out *Baccharis salicifolia* and *Fremontodendron californicum* because of their high

Table 9. Species in the data set with vasicentric tracheids and low vessel grouping (fewer than three vessels per group) to show that a wide range of vessel grouping is observed in groups with vasicentric tracheids. This range is probably associated with a range of vasicentric tracheid abundance. Family names are given to show that many families are involved

Species	Family	Vessels per group
<i>Lithocarpus densiflora</i>	Fagaceae	1
<i>Quercus chrysolepis</i>	Fagaceae	1
<i>Quercus dumosa</i>	Fagaceae	1
<i>Larrea tridentata</i>	Zygophyllaceae	1
<i>Comarostaphylis diversifolia</i>	Ericaceae	1.08
<i>Fagonia laevis</i>	Zygophyllaceae	1.08
<i>Chrysolepis sempervirens</i>	Fagaceae	1.12
<i>Frankenia grandifolia</i>	Frankeniaceae	1.12
<i>Thamnosma montanum</i>	Rutaceae	1.2
<i>Arctostaphylos patula</i>	Ericaceae	1.28
<i>Trichostema lanatum</i>	Lamiaceae	1.34
<i>Condalia globosa</i>	Rhamnaceae	1.36
<i>Ornithostaphylos oppositifolia</i>	Ericaceae	1.43
<i>Holodiscus microphyllus</i>	Rosaceae	1.44
<i>Cassia armata</i>	Leguminosae	1.45
<i>Ribes cereum</i>	Glossulariaceae	1.56
<i>Ferocactus acanthodes</i>	Cactaceae	1.6
<i>Lippia wrightii</i>	Verbenaceae	1.6
<i>Arctostaphylos glauca</i>	Ericaceae	1.64
<i>Holodiscus discolor</i>	Rosaceae	1.64
<i>Arctostaphylos glandulosa</i>	Ericaceae	1.65
<i>Buddleja utahensis</i>	Buddlejaceae	1.76
<i>Echinocactus polycephalus</i>	Cactaceae	1.8
<i>Xylococcus bicolor</i>	Ericaceae	1.8
<i>Solanum xantii</i>	Solanaceae	1.8
<i>Celtis reticulata</i>	Ulmaceae	1.8
<i>Colubrina californica</i>	Rhamnaceae	1.85
<i>Beloperone californica</i>	Acanthaceae	1.96
<i>Salazaria mexicana</i>	Lamiaceae	2
<i>Mammillaria dioica</i>	Cactaceae	2.01
<i>Bernardia incana</i>	Euphorbiaceae	2.07
<i>Arbutus menziesii</i>	Ericaceae	2.1
<i>Monardella linoides</i>	Lamiaceae	2.16
<i>Haplopappus squarrosus</i>	Asteraceae	2.17
<i>Ceratooides lanata</i>	Chenopodiaceae	2.24
<i>Adolphia californica</i>	Rhamnaceae	2.32
<i>Rhamnus crocea</i>	Rhamnaceae	2.55
<i>Zizyphus parryi</i>	Rhamnaceae	2.55
<i>Gutierrezia microcephala</i>	Asteraceae	2.7
<i>Asclepias albicans</i>	Apocynaceae	2.85
<i>Echinocereus englemannii</i>	Cactaceae	2.95
<i>Rhamnus californica</i>	Rhamnaceae	2.95

vessel grouping but lack of vasicentric tracheids. After *Romneya coulteri*, with its extreme value of 150 vessels per group, these two species had the highest values for vessel grouping. Above ten vessels per group, all species had vasicentric tracheids, until reaching values of 26.7 (*Fremontodendron californicum*) and 29 (*Baccharis salicifolia*). This result raised several questions. For example, did these two species represent a strategy otherwise unique in the data set that obviated the need for these subsidiary conductive cells? Alternatively, could vasicentric tracheids, which are often difficult to identify, actually have been present in these species but were not observed in the original study? A re-examination of the slides of *Baccharis salicifolia* and *Fremontodendron californicum* in preparation for the present paper revealed that in fact both of these species do have vasicentric tracheids. Thus, a simple statistical procedure helped guide, to a remarkable degree, our interpretation of these preparations, and led to a refined understanding of the association between vasicentric tracheids and vessel grouping.

Vessel grouping, vessel diameter, and vessel density

Many anatomists have noted that the number of vessels per unit of transection is clearly related to how wide the vessels are, which in turn affects how many could be expected to be found in groups (e.g. Sidiyasa & Baas, 1998; Carlquist, 2001). We present levels of statistical significance for these associations (Table 3). The significant negative correlation between vessel diameter and density (Spearman's correlation coefficient = -0.75 , $P < 0.001$) is an intuitively obvious result, because fewer larger vessels can fit into a given space than small ones.

Likewise, the positive correlation between vessel density and the average number of vessels per group is to be expected, given that the more abundant vessels are, the more probable it is that they will come into contact with one another. In contrast to the correlation between vessel diameter and density, this correlation is in fact a rather weak one (Table 3), although it is significant at the 10% level and is thus worth calculating in other studies. Figure 5 shows the scatter of species based on vessel diameter and vessels per group and shows that most species have low vessel grouping but are distributed across a wide range of vessel diameter. The region of the graph in which diameter is wide and grouping is low is predicted to be associated with areas of low water stress, and species in this part of the graph comply with this expectation, or have wood with an internally mesic environment (e.g. *Cornus nuttallii* from shady canyons or the succulent tree *Bursera microphylla*).

Understanding the functional significance of vessel grouping could be refined by generating predictions

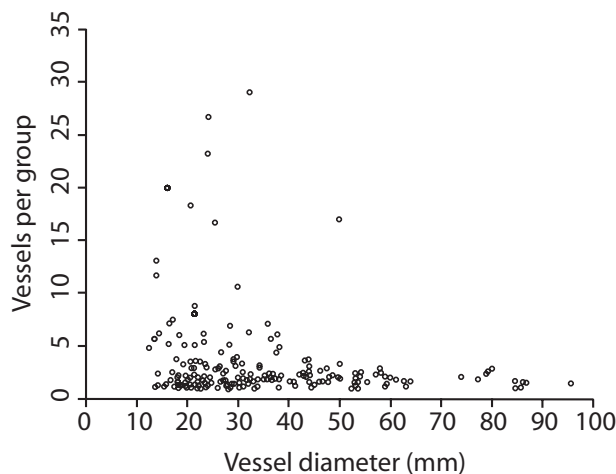


Figure 5. Scatterplot of the species in the data set according to their values of vessel diameter and vessel grouping. Species tend to have few vessels per group, but can vary their vessel diameter greatly.

regarding how many vessels should be found in groups if the probability of vessels being in contact in a given sample is random. Given the range of diameters and density of vessels in a given species, a certain number of vessels will be in contact if their distribution is determined at random. Vessel grouping that is lower than this figure for a given species would suggest selection for solitary vessels, whereas higher grouping could suggest selection favouring grouping of vessels.

IDENTIFICATION OF UNUSUAL SPECIES

One of the most fruitful results of the models we present was that they singled out certain species as being in some way unusual. 'Unusual' in this case refers to species with combinations of characteristics that differ from the rest of the species. One possibility for such a result is that subtleties in the original anatomical preparations remained undiscovered. As was the case for *Baccharis salicifolia* and *Fremontodendron californicum*, the models drew attention to readily overlooked details that might never have been noticed otherwise, leading to a refined understanding of the anatomy of these species. We detail an additional case here.

An example of a plant whose anatomical interpretation was refined as a result of our models is *Symphoricarpos mollis*, a finely branched evergreen caprifoliaceous understory shrub. The imperforate tracheary elements of this species were originally classed as true tracheids. However, vessels in this species were coded as grouped rather than having the solitary vessels that would be expected if true tracheids were present. Examination of the data showed that,

with the exception of *Symphoricarpos mollis*, true tracheids were only found in species with less than 2.36 vessels per group; all 75 species with more than 2.36 vessels per group lacked true tracheids except for *Symphoricarpos mollis*, which had true tracheids and 3.25 vessels per group. This raised several questions: Are the 'tracheids' of *Symphoricarpos mollis* truly conductive? What implications would this observation have for the notion that true tracheid presence should lower vessel grouping (Carlquist, 1984)? What features of the imperforate tracheary elements made them appear conductive if they were not? Resolution of this issue required the consultation of new preparations.

A re-examination of sections of *Symphoricarpos mollis* prepared from liquid-preserved material showed that true tracheids are indeed present, as are grouped vessels, but in distinct portions of growth rings. Earlywood vessels – but only for a short period of a season's growth – are grouped. They occur in a background of what could either be called living fibres (filled with starch in this case) or axial parenchyma that has not subdivided into strands. Using either designation, they are nonconductive cells, and thereby vessel grouping is an adaptive strategy for increasing conductive safety in earlywood. Most of each growth ring consists of latewood in which vessels are solitary, and the background tissue consists of true tracheids; the starch-filled living fibres (or fibriform parenchyma cells) are sparsely distributed among the tracheids. Thus, vessel grouping is not an adaptive strategy for increasing conductive safety in latewood. The example of *Symphoricarpos mollis* demonstrates the usefulness of the logistic models in highlighting taxa that require special consideration. In this case, vessel grouping and imperforate tracheary element type could be considered in early- and latewood separately.

UNUSUAL CHARACTER COMBINATIONS AND LACK OF CORRELATIONS

One of the keystones of the use of the comparative method for inferring the functional roles of wood anatomical features has been the detection of associations or the lack thereof between anatomical characters. In this approach, the functional nature of cells is inferred via examination of the association between characters of many species and not on the functional study of one or a few species. An approach such as the one we present is ideal for revealing such patterns of association. A special case of association would be represented by combinations of characters that are unusual or would be if they existed. *Philadelphus microphyllus* provides an example of a plant with such a combination, being the only species with true tracheids and helical vessel sculpture. Outside of the southern

California flora area, there is a small number of other genera in which true tracheids co-occur with vessels with helical thickening, such as *Buxus* (Carlquist, 1982) and *Ilex* (Baas, 1973). Both of these genera also have helical thickenings in tracheids (IAWA Committee, 1989). *Buxus*, *Ilex*, and *Philadelphus* may represent predominantly mesophytic clades in which a few genera (which have scalariform perforation plates as a symplesiomorphy) have been able to adapt to seasonal cold or drought (neither of a severe sort) with the aid of a few modifications, such as helical thickenings. Further reinforcing the idea that helical sculpture is somehow of value in drought survival, if helical thickenings are present in the vessels of woods from seasonal climates, they are always more pronounced in latewood, as in *Philadelphus*.

The absence of correlations is equally informative. For example, the lack of correlation between vessel element length and vessel diameter (Table 3) suggests that these characteristics can respond independently to selection. This was previously shown by Carlquist (1966) in a summary of woods of Asteraceae. Woods of Asteraceae are relatively uniform with respect to qualitative differences. Therefore, the family is like a template that reveals sensitively adaptive changes in quantitative vessel features to shifts in ecology. When subdivided into ecological categories ('mesic, dry, desert'), Asteraceae show a marked decrease in vessel diameter and vessel element length with increased xeromorphy accompanied by more numerous vessels per group. The absence of correlation among these three features strongly suggests that morphogenetically they are not related. Vessel element length is traditionally thought to represent about the same length as fusiform cambial initials in any given specimen, whereas vessel diameter is the result of radial and tangential cell enlargement during maturation. Finally, the number of vessels per group is a function of the number of vessels derived from the cambium in series or simultaneously, uninterrupted by other kinds of axial cell. The identification of which characters are correlated is a vital first step in understanding the types of evolutionary change that are possible (cf. Olson & Rosell, 2006).

STATISTICS AND WOOD ANATOMICAL TERMINOLOGY

All systems of classification to some extent gloss over biological realities. Although it is not our aim to advocate one set of wood anatomical terminology over another, our study does offer an example of how explicit statistical approaches can help to indicate terminological systems that are more closely aligned with biological realities than others. The terminology of imperforate tracheary elements has long been a subject of debate, much of which has consisted of

expressions of personal taste on the part of anatomists and little effort to identify biological discontinuities along which terminological lines could be drawn. For example, the distinction between vasicentric and vascular tracheids used here is not universally accepted by anatomists (e.g. IAWA Committee, 1989). If the distinction we used were truly arbitrary, then it would be unlikely that a statistical model could predict effectively the presence of either of these cell types. However, vasicentric tracheid presence was readily predicted by the model based on other variables (Table 6). If definitions are taken as hypotheses, then our results strongly support the hypothesis of vasicentric tracheids as conceived by Carlquist (1984, 1985, 2001).

The cell types conceived here thus do appear to have distinct biological functions, and their distinctness has been inferred by previous authors. Metcalfe & Chalk's (1950) list of families that have vasicentric tracheids was incomplete, although the concept of vasicentric tracheids in that work seems entirely consistent with our usage. An intensive search for vasicentric tracheid presence (Carlquist, 1985) greatly expanded the list of Metcalfe & Chalk (1950), but did not change the concept. The concept was changed in the IAWA Committee's (1989) listings. The IAWA Committee (1989) recognized vasicentric tracheids only in two families where they are abundant, Fagaceae and Myrtaceae. Although restriction of the concept of vasicentric tracheid to those two families may simplify identification work, it does not recognize the functional role evident in the earlier definition of the term as used by Metcalfe & Chalk (1950) and Carlquist (1985). Furthermore, by assigning the term vascular tracheid to imperforate tracheary elements with numerous bordered pits (in woods that also contain fibre-tracheids or libriform fibres), the IAWA Committee (1989) has blurred the distinction between vasicentric tracheids and vascular tracheids. The term vascular tracheid, as earlier used, applied only to last-formed latewood tracheary elements that lack perforation plates, as in *Sambucus* or *Betula*. In the traditional definition of vascular tracheids, by being embolism-resistant cells adjacent to the cambium when growth ceases, these cells protect the cambium but not the three-dimensional conductive pathways of a stem. Thus, vascular tracheids aid in protecting a stem (but not its leaves) in cold or dry periods when vessels in a stem may have embolized. Vascular tracheids are thus an adaptive mechanism in plants with drought-deciduous leaves (*Aesculus*, *Toxicodendron*) or winter-deciduous leaves (*Betula*). Vasicentric tracheids and true tracheids, by contrast, protect conductive pathways by remaining embolism free when nearby vessels embolize, and characterize the evergreen chaparral elements, such as *Adenostoma*,

Arctostaphylos, *Ceanothus*, etc. For the purposes of ecological wood anatomy, terminology reflecting cell function clearly influences the inferences that can be derived from a given data set.

The methods we suggest provide a way of comparing and choosing between classification systems. The 'true tracheids' of the present study are referred to as 'fibres with distinctly bordered pits' by many anatomists, following the wood identification guidelines of the IAWA Committee (1989), which does not distinguish based on cell function and thus includes both conductive and nonconductive cells in this category. However, the present study does suggest a very marked boundary between conductive tracheids and nonconductive imperforate tracheary elements, supporting the validity of the 'tracheid' category as conceived here. It would thus be possible to see how well the presence of 'fibres with distinctly bordered pits' is predicted by other variables in a data set constructed using the IAWA Committee's (1989) classification vs. a data set based on the same samples but classified using the definitions employed here. The classification system that results in better predictive power would be preferred as reflecting biological reality better than the other.

We must emphasize that our primary interest is not the classification of cell types or the invention of terminology. Indeed, this effort has to some extent hindered the progress of evolutionary comparative wood anatomy, because debate has at times focused more on what name to use to lump together superficially similar cells across dicots rather than the inference of their function or their status as homologies associated with individual clades. For studies of ecological wood anatomy, collecting quantitative data rather than classing cells should be considered, because the use of classes, e.g. 'vessels large, vessels small', etc., inevitably leads to a loss of statistical power vs. what can be achieved analytically with continuous data (e.g. Royston *et al.*, 2006). Moreover, these classes are often arbitrary divisions of continua, and all inferences based on them are subject to error to the extent that the classes are arbitrary (see Olson, 2005). For studies of ecological wood anatomy, effort is much better directed to gathering data that can be used to test a specific functional hypothesis than to gathering all of the traditional wood identification data typically collected by anatomists (e.g. IAWA Committee, 1989). Although terminology is not an end in itself, from the standpoint of ecological wood anatomy, terminology that reflects function is at the very least convenient. At best, and as our analysis shows, when classes apparently coincide with biological reality, they can be used to build models with excellent predictive ability, and consequently can be a rich source of biological information.

REACHING THE LIMITS OF THE DATA: LESSONS ON SAMPLING AND CODING

Every data set has its limits as a natural consequence of sampling. Identifying the limits imposed by the gathering and treatment of data in a given study can serve to widen the envelope of informativeness of future investigations. In this section we discuss specific examples of analyses that remained inaccessible due to such limitations. By identifying currently unanswerable questions, our models provide explicit directions for future work.

The coding of variables directly determines the inferences that can be drawn. In some cases, simplifying these codings can be a detriment to the conclusions that can be made. For example, Carlquist & Hoekman (1985) attempted to simplify the interpretation of the data by coding a single type of conductive imperforate tracheary cell per species. The species in which both vasicentric and vascular tracheids were found were coded as having exclusively vasicentric tracheids. Possibly as a result, the logistic regression model was unable to predict the presence or absence of vascular tracheids dependably based on the other variables (Table 8). Coding the presence of both vasicentric and vascular tracheids when they co-occur should increase the explanatory and predictive abilities of the model.

Anatomists often break continua into categories, thereby losing crucial information. One example of the use of categories instead of continuous variables includes recording presence/absence rather than abundance data. In the current study, we found that the probability of finding vasicentric tracheids increased with increasing numbers of vessels per group (Tables 5 and 6; Fig. 3). This finding is significant because the presence of subsidiary conductive cells could be expected to lower, rather than raise, vessel grouping (Carlquist, 1984). Carlquist & Hoekman (1985) mentioned that vessel grouping is lowered only in the presence of very abundant vasicentric tracheids. This would clearly appear to be the case in families such as Fagaceae and Myrtaceae, in which very abundant vasicentric tracheids are found in many species (Metcalf & Chalk, 1950). Consistent with expectations, vessels are solitary in species that appear to have abundant vasicentric tracheids (Table 9). At the other extreme, vasicentric tracheids are relatively sparse in other taxa, and a range of vessel grouping is observed. Between these extremes, a threshold of vasicentric tracheid abundance is probably crossed, below which selection for vessel grouping becomes a significant force. To identify this threshold, abundance data for vasicentric tracheids would be required. However, not only is vasicentric tracheid abundance not recorded in the Carlquist and Hoekman data set, but

it is doubtful that this information has ever been gathered. Yet without abundance data it is impossible to test the hypothesis that vessel grouping is lowered in the presence of abundant vasicentric tracheids quantitatively and to describe the nature and magnitude of the association.

Similarly, rather than categorizing imperforate tracheary elements (tracheid, fibre-tracheid, etc.), a better test of Carlquist's (1984) hypotheses would be to compare vessel grouping with quantitative features of imperforate tracheary elements, such as pit dimensions and density. Such an approach could help to identify the threshold range of continuous features of imperforate tracheary elements over which the change from solitary to grouped vessels occurs. The identification of a quantitative threshold of pit size and density below which imperforate tracheary elements are apparently nonconductive would be an invaluable aid to inferring the adaptive responses of woody plants to environmental challenges.

To make such inferences valid, analyses must simultaneously take into account biological and statistical considerations. It should go without saying that statistical models should never be used to make inferences without checking whether they adequately fit the data, yet such diagnostics are seldom performed in practice. However, some of the most important results of our study, such as the identification of unusual species, emerged in exactly this phase. Likewise, it is crucial to heed the need for a sufficient number of observations to obtain reliable estimates for the standard deviations of the estimated regression coefficients. Thus, although worthwhile, simply obtaining a large overall sample size does not guarantee that standard deviations can be precisely estimated. In our case, it was also necessary to examine how many species with and without each tracheid type were found for different values of the explanatory variables. For example, all species in the Carlquist and Hoekman data set with scalariform perforation plates lacked vasicentric tracheids. Thus, the presence of scalariform perforation plates perfectly predicted the absence of vasicentric tracheids. This would have resulted in a zero observed frequency in the contingency table defined by the two variables, yielding estimates of regression coefficients with standard deviations so large as to be practically meaningless. Similar data patterns are common in the Carlquist and Hoekman data (e.g. the presence of any tracheid type is generally associated with the absence of the other two; the presence of helical sculpture in earlywood implies the presence of helical sculpture in latewood, etc.). Such patterns may be expected in any ecological wood anatomy study and it is therefore crucial that their effect on the analysis be taken into account.

Finally, a large number of strong ecological wood anatomical correlations, some of which form the foundations of the current ecological wood anatomy paradigm, are almost certainly indirect, correlating with plant size rather than directly with environmental variables. The positive correlations between vessel diameter and water availability (e.g. Baas *et al.*, 1983) and between tracheary element length and latitude (Van der Graaff & Baas, 1974; Lens *et al.*, 2004) are probably in this category. Nevertheless, we are not aware of anatomical studies in which vessel diameter is corrected for stem size before seeking ecological correlations. Results that may be similarly indirect were also recovered in the present analysis. For example, vessel diameter tends to be smaller when vasicentric tracheids are present (Table 5). This finding is consistent with the common ecological wood anatomy assumptions that both narrow vessels and vasicentric tracheids are associated with dry habitats, and thus both could be interpreted as adaptations to drought. However, RR values show that vasicentric tracheids are more common in shrubs and subshrubs than in trees or other habit types. Likewise, a narrower vessel diameter is found in smaller stems (Gartner, 1995; Carlquist & Grant, 2005; Olson & Rosell, 2006). It is thus unclear whether both narrow vessels and vasicentric tracheids are directly associated with drought or indirectly via an association with plant size, which is in turn associated with dry conditions. Does natural selection act on vessel dimensions independently of plant size, or does selection act on plant size, with vessel size changing accordingly (or vice versa)? If smaller habits tend to have narrower vessels *and* have vasicentric tracheids, the association between vessel diameter and vasicentric tracheid presence could be an indirect one. Also, it is not clear why vasicentric tracheids are so rare in trees. Yet another example is the association between the presence of growth rings and the presence of vasicentric tracheids. RR values highlight that the association is most important in ring porous woods, and is also strong, although less so, in semiring porous woods. Are vasicentric tracheids related directly to growth rings, or do both represent independent responses to drought resistance? Many more examples could be cited, clearly seeming to belie the notion that these ecological wood anatomical associations are 'well known'. In fact, much work remains to disentangle the chain of causality leading to most such associations.

CONCLUSIONS

Comparative wood anatomy has succeeded in identifying patterns, despite employing practices that date from the founding of the field. Many of these results have been repeatedly confirmed, which may make it

seem that there is no reason to change these traditional methods. However, although the application of basic statistics has allowed the identification of strong patterns, more subtle associations and the identification of causality have clearly remained undiscovered. Also, it is possible that outright incorrect use of statistics (e.g. applying analyses of variance without checking assumptions) has led to erroneous conclusions. Very simple measures would substantially improve statistical practice in comparative wood anatomy. Specific recommendations stemming from our analysis naturally include the use of analytical techniques that take advantage of the considerable amounts of data locked away in comparative anatomical data sets, including the analysis of categorical data. Our analysis also points to situations in which gathering quantitative data (e.g. abundance of vasicentric tracheids, pit size, and density) would be preferable to traditional categorical data (e.g. the presence or absence of vasicentric tracheids, tracheids vs. fibre-tracheids). Gathering data regarding the abundance of cell types would likewise be extremely useful and, avoiding arbitrary or overly simplistic codings, is imperative.

Many associations between anatomical characters, and between characters and environmental variables, are restricted to certain taxonomic groups. For example, in this study, all instances of trees with vasicentric tracheids come from Fagaceae. Likewise, both species with scalariform perforation plates but lacking true tracheids are Betulaceae. A final example is the presence of helical sculpture on vessel walls in plants with diffuse porous wood, with the only two examples coming from Rosaceae. These within-family resemblances almost certainly do not represent independent occurrences, but instead characters inherited from a common ancestor. This tendency for closely related species to be more similar to one another than to distantly related ones is present in all comparative data. If the observed association arose only once in the evolutionary history of the group, all species should not be considered independent observations when describing the strength of the association in statistical terms. Nevertheless, although some anatomists may mention the apparent effect of phylogeny, all ecological wood anatomy studies to date have employed standard, nonphylogenetic statistical analyses. This practice is equivalent to considering data to be independent and translates into the implicit assumption that wood characters respond evolutionarily instantaneously to climatic conditions.

Statistical methods that deal with the non-independent nature of comparative data are available (e.g. Felsenstein, 1985; Harvey & Pagel, 1991; Martins & Hansen, 1997; Paradis & Claude, 2002), but have been applied in only a few anatomical studies (e.g.

Olson & Rosell, 2006; Preston, Cornwell & DeNoyer, 2006). Reanalysing the Carlquist and Hoekman data set with these methods would test whether the association patterns detected with the standard logistic models in this paper are maintained and would inform the degree of phylogenetic effect that is present in anatomical characters. It would thus provide a valuable guide as to just how much or how little neglecting of phylogeny distorts the inferences drawn by wood anatomists.

Carefully planned sampling and appropriate comparative methods complement functional studies because they can examine a greater number of species and ecological situations than could ever be studied using experimental approaches (e.g. Osborn, 1915; Bailey, 1920; Mayr, 1982). The analysis we present demonstrates that new information does remain even within a supposedly well-known data set. Furthermore, carrying out the suggestions for further work pointed to by this analysis would greatly refine the knowledge of wood cell function across families. We suggest that the future of comparative ecological wood anatomy would appear to depend on the eagerness of anatomists to abandon traditional methods that lead to a loss of analytical possibilities by refining sampling strategies and adopting more powerful analytical approaches designed to test specific functional hypotheses.

ACKNOWLEDGEMENTS

We thank Gerardo Rivas, Teresa Terrazas, José Luis Villaseñor, and Calixto León for helpful comments. Funding was provided by the Programa de Apoyo a Proyectos de Investigación e Innovación Tecnológica, DGAPA, UNAM, project #IN228207-3, and the Instituto de Biología, UNAM.

REFERENCES

- Agresti A. 2002.** *Categorical data analysis*, 2nd edn. New York: John Wiley & Sons.
- Alves ES, Angyalossy-Alfonso V. 2000.** Ecological trends in the wood anatomy of some Brazilian species. 1. Growth rings and vessels. *International Association of Wood Anatomists Journal* **21**: 3–30.
- Alves ES, Angyalossy-Alfonso V. 2002.** Ecological trends in the wood anatomy of some Brazilian species. 2. Axial parenchyma, rays and fibres. *International Association of Wood Anatomists Journal* **23**: 391–418.
- Arias S, Terrazas T. 2001.** Variación en la anatomía de la madera de *Pachycereus pecten-aboriginum* (Cactaceae). *Anales del Instituto de Biología, UNAM, Serie Botánica* **72**: 157–169.
- Baas P. 1973.** The wood anatomical range in *Ilex* (Aquifoliaceae) and its ecological and phylogenetic significance. *Blumea* **21**: 193–258.
- Baas P. 1986.** Terminology of imperforate tracheary elements—in defense of libriform fibres with minutely bordered pits. *International Association of Wood Anatomists Bulletin* **7**: 82–86.
- Baas P, Werker E, Fahn A. 1983.** Some ecological trends in vessel characters. *International Association of Wood Anatomists Bulletin* **4**: 141–159.
- Bailey IW. 1920.** The cambium and its derivative tissues II. Size variations of cambial initials in gymnosperms and angiosperms. *American Journal of Botany* **7**: 355–367.
- Bailey IW. 1936.** The problem of differentiation and classifying tracheids, fibre-tracheids, and libriform wood fibres. *Tropical Woods* **45**: 18–23.
- Burley J, Miller RB. 1982.** The application of statistics and computing in wood anatomy. In: Baas P, ed. *New perspectives in wood anatomy*. The Hague: Martinus-Nijhoff, 223–242.
- Carlquist S. 1966.** Wood anatomy of Compositae: a summary, with comments on factors controlling wood evolution. *Aliso* **6**: 25–44.
- Carlquist S. 1975.** *Ecological strategies of xylem evolution*. Berkeley, California: University of California Press.
- Carlquist S. 1982.** Wood anatomy of Buxaceae: correlations with ecology and phylogeny. *Flora* **172**: 463–491.
- Carlquist S. 1984.** Vessel grouping in dicotyledon wood: significance and relationship to imperforate tracheary elements. *Aliso* **10**: 505–525.
- Carlquist S. 1985.** Vasicentric tracheids as a drought survival mechanism in the woody flora of southern California and similar regions: review of vasicentric tracheids. *Aliso* **11**: 37–68.
- Carlquist S. 1986.** Terminology of imperforate tracheary elements. *International Association of Wood Anatomists Bulletin* **7**: 75–81.
- Carlquist S. 2001.** *Comparative wood anatomy. Systematic, ecological and evolutionary aspects of dicotyledon wood*, 2nd edn. Berlin: Springer.
- Carlquist S, Grant JR. 2005.** Wood anatomy of Gentianaceae, tribe Helieae, in relation to ecology, habit, systematics, and sample diameter. *Brittonia* **57**: 276–291.
- Carlquist S, Hoekman DA. 1985.** Ecological wood anatomy of the woody southern Californian flora. *International Association of Wood Anatomists Bulletin* **6**: 319–347.
- Collett D. 2003.** *Modelling binary data*. Boca Raton, Florida: Chapman & Hall.
- Feild TS, Brodribb T, Holbrook NM. 2002.** Hardly a relict: freezing and the evolution of vesselless wood in Winteraceae. *Evolution* **56**: 464–478.
- Felsenstein J. 1985.** Phylogenies and the comparative method. *American Naturalist* **125**: 1–15.
- Gartner BL. 1995.** Patterns of xylem variation within a tree and their hydraulic and mechanical consequences. In: Gartner BL, ed. *Plant stems: physiology and functional morphology*. San Diego, California: Academic Press, 125–149.
- Harvey PH, Pagel MD. 1991.** *The comparative method in evolutionary biology*. Oxford: Oxford University Press.
- Hosmer DW, Lemeshow S. 2000.** *Applied logistic regression*, 2nd edn. New York: John Wiley & Sons.

- IAWA Committee. 1989.** IAWA list of microscopic features for hardwood identification. *International Association of Wood Anatomists Bulletin* **10**: 219–332.
- Jacobsen AL, Ewers FW, Pratt RB, Paddock WA, III, Davis SD. 2005.** Do xylem fibres affect vessel cavitation resistance? *Plant Physiology* **139**: 546–556.
- Jansen S, Baas P, Gasson P, Lens F, Smets E. 2004.** Variation in xylem structure from tropics to tundra: evidence from vested pits. *Proceedings of the National Academy of Sciences of the USA* **101**: 8833–8837.
- Kleinbaum DG. 2002.** *Logistic regression: a self-learning text*. New York: Springer.
- Kutner MH, Nachtsheim CJ, Neter J, Li W. 2005.** *Applied linear statistical models*, 5th edn. New York: McGraw-Hill.
- Lens F, Luteyn JL, Smets E, Jansen S. 2004.** Ecological trends in the woody anatomy of Vaccinioideae (Ericaceae s.l.). *Flora* **199**: 309–319.
- Martins EP, Hansen T. 1997.** Phylogenies and the comparative method: a general approach to incorporating phylogenetic information into the analysis of interspecific data. *American Naturalist* **149**: 646–667.
- Mayr E. 1982.** *The growth of biology thought*. Harvard, Massachusetts: Harvard University Press.
- Metcalfe CR, Chalk L. 1950.** *Anatomy of the dicotyledons*. Oxford: Clarendon.
- Olson ME. 2005.** Homology, typology, and homoplasy in comparative wood anatomy. *International Association of Wood Anatomists Journal* **26**: 507–522.
- Olson ME, Rosell JA. 2006.** Using heterochrony to infer modularity in the evolution of stem diversity in *Moringa* (Moringaceae). *Evolution* **60**: 724–734.
- Osborn HF. 1915.** Origin of single characters as observed in fossil and living animals and plants. *American Naturalist* **49**: 193–239.
- Paradis E, Claude J. 2002.** Analysis of comparative data using generalized estimating equations. *Journal of Theoretical Biology* **218**: 175–185.
- Pregibon D. 1981.** Logistic regression diagnostics. *Annals of Statistics* **9**: 705–724.
- Preston KA, Cornwell WK, DeNoyer JR. 2006.** Wood density and vessel traits as distinct correlates of ecological strategy in 51 California Coast Range angiosperms. *New Phytologist* **170**: 807–818.
- Quinn GP, Keough MJ. 2002.** *Experimental design and data analysis for biologists*. Cambridge: Cambridge University Press.
- Royston P, Altman DG, Sauerbrei W. 2006.** Dichotomizing continuous predictors in multiple regression: a bad idea. *Statistics in Medicine* **25**: 127–141.
- Sidiyasa K, Baas P. 1998.** Ecological and systematic wood anatomy of *Alstonia* (Apocynaceae). *International Association of Wood Anatomists Journal* **19**: 207–229.
- Sokal RS, Rohlf FJ. 1995.** *Biometry. The principles and practice of statistics in biology research*, 3rd edn. New York: Freeman.
- Sperry JS, Hacke UG. 2004.** Analysis of circular bordered pit function I. Angiosperm vessels with homogenous pit membranes. *American Journal of Botany* **91**: 369–385.
- Van der Graaff NA, Baas P. 1974.** Wood anatomical variation in relation to latitude and altitude. *Blumea* **22**: 101–121.